Investigation of the Application of Polylactic Acid-Calcium Phosphate Composite Materials as Novel Periodontal Barrier Membranes

by

Ahmed Talal

Submitted in fulfilment of the requirements for the degree of
Doctor of Philosophy

Department of Mechanical Engineering
Faculty of Engineering
University of Glasgow

August 2009

Dedicated to my parents

Abstract

The ultimate aim of periodontal treatment is to regenerate the tissue lost during the disease process, thereby restoring the aesthetics and function of the periodontium. Guided tissue regeneration (GTR) is one technique that is used clinically to promote tissue regeneration. The technique employs a membrane to create space in the appropriate surgical site to produce periodontal regeneration. However there may be considerable potential to improve the outcomes of this technique by development of novel membrane materials.

The aim of the studies described in this thesis was to investigate the potential of polylactic acid-calcium phosphate (PLA-Ca P) composite materials to be developed into a GTR membrane with increased potential for producing periodontal regeneration. Ca P materials included nano-hydroxyapatite (n-HA) and ß tri-calcium phosphate (ß-TCP). PLA-Ca P composite films were produced by the solvent casting method. The Ca P powders and the PLA-Ca P composite films were characterized. The degradation of PLA-Ca P composites was analysed in phosphate buffer saline (PBS). The bioactive potential of the composite films was determined in simulated body fluid (SBF). The growth and differentiation of PDL cells and osteoblasts were assessed on PLA-nHA composite films and the ability of these films to carry platelet derived growth factor (PDGF) and its effect on osteoblast growth was investigated. Further, fibre reinforced PLA-HA composite membranes were fabricated and their mechanical strength and kinetics of protein interactions were investigated. Finally mandibular alveolar bone profiles were analyzed to define the possible shapes required for manufacture of GTR membranes.

Results showed that Ca P decreased the degradation and increased the bioactivity of the PLA-Ca P composite films. The cell proliferation on composite films containing 10 wt % nHA was high when compared to PLA films. However, cell proliferation decreased with increase in nHA concentration. The highest alkaline phosphate activity (ALP) was shown by cells on composite films containing 70 wt % nHA. The PDGF added to the PLA-nHA composite films retained its activity and increased the proliferation of osteoblasts. The flexural strength was high for the

fibre reinforced PLA-HA composite membranes, containing maximum number of PLA fibres laid at 0°. The fibre reinforced membranes containing HA showed gradual and sustained protein release compared to fibre reinforced membranes without HA. The analysis of alveolar bone profiles of different patients showed marked similarities between each other, suggesting that only a few membrane shapes may be required to fit most patients in clinical use.

These studies demonstrate the potential of fibre reinforced PLA-HA composite material to be used for the production of preshaped GTR membranes with favourable properties to increase periodontal regeneration.

Acknowledgements

I wish to express my utmost gratitude to my supervisors, Professor Liz Tanner and Professor Francis Hughes. Without their help and invaluable guidance, this project would not have been possible. I feel highly indebted to them for their special attention and generous help in meeting every challenge that I came across. I am truly privileged to have been associated with them.

Professor Liz Tanner was a source of great encouragement for me. Her knowledge, deep insight of the subject and thoughtfulness always led me to explore new dimensions of the subject. Professor Francis Hughes was the other person behind my effort. Though far (in London) yet so near, he was ever available to extend advice and help. Working with them has been indeed a great experience. I express my sincere thanks for whatever they have done for me, during my stay in UK.

I am grateful to Dr I.J. Mckay, Queen Mary University of London, for his invaluable advice on cell culturing; Dr. Zofia Luklinska, Queen Mary University of London and Peter Chung, University of Glasgow for helping me with the SEM and TEM.

My special thanks to all the lab staff. Their quite presence and participation has a huge role in this project. They are truly the people behind the scene.

My thanks go to my colleagues and friends especially Dr Samad, Dr Wojciech, Dr Nima and Dr Zeeshan for their cooperation and providing me the relaxing moments when needed.

I am also thankful to National University of Science and Technology, Pakistan, Queen Mary University of London and University of Glasgow for help and financial support.

Finally, I would like to thank my parents for their prayers, my brothers and sister for their encouragement, my wife for providing me comfort and my son (born during my studies here) for giving me all the joy.

Above all, I am thankful to Allah Almighty for His unlimited blessings.

Declaration

The contents of this thesis are entirely my own work, except where mentioned and acknowledged. This work has not been previously submitted for any other degree or qualification in any university.

Ahmed Talal August 2009

Table of Contents

List of Tables

List of Figures

List of Abbreviations

βTCP	Beta tricalcium phosphate
BMP	Bone morphogenic proteins
Ca	Calcium
CO	Carbon monoxide
Cl	Chlorine
c-fms	Colony-stimulating factor receptor
EDS	Energy dispersion Spectroscopy
FGF	Fibroblast growth factor
FTIR	Fourier Transform Infrared spectroscopy
GPa	Gigga Pascal
GTR	Guided Tissue Regeneration
HA	Hydroxyapatite
IGF	Insulin–like growth factor
K	Potassium
mg	Milligram
M-CSF	Macrophage colony-stimulating factor
MPa	Mega Pascal
Mg	Magnesium
Na	Sodium
nHA	Nanohydroxyapatite
nm	Nanometer
OH	Hydroxyl
P	Phosphorous
Pb	Lead
PBS	Phosphate Buffer saline
PDGF	Platelet derived growth factor
PCL	Poly-ε-caprolactone
PGA	Polyglycolic acid
PLA	Polylactic acid
PO_4	Phosphate

PTH	Parathyroid hormone
RANKL	Receptor Activator for Nuclear Factor κ B Ligand
SBF	Simulated body fluid
SD	Standard deviation
SEM	Scanning electron microscopy
Sr	Strontium
TEM	Transmission electron microscopy
T_g	Glass transition temperature
T_m	Melting temperature
vol	volume
XRD	X-ray diffraction
Zn	Zinc
μm	Micromete
wt	Weight
%	Percentage
°C	Degree Celsius
θ	Theta

Glossary

Osteoinduction: **"**This term means that primitive, undifferentiated and pluripotent cells are somehow stimulated to develop into the bone-forming cell lineage" [Albrektsson and Johansson, 2001].

Osteoconduction: **"**This term means that bone grows on a surface. An osteoconductive surface is one that permits bone growth on its surface" [Albrektsson and Johansson, 2001].

CHAPTER 1: LITERATURE REVIEW

1.1 INTRODUCTION

Periodontal diseases are common and in their advanced stages can lead to severe periodontal tissue loss, ultimately resulting in tooth loss. Different modes of treatments ranging from scaling the teeth to the use of advanced techniques such as bone grafts and guided tissue regeneration (GTR) have been employed for treatment of periodontal diseases depending on the severity of disease and amount of tissue loss. In the last two decades GTR has evolved as an effective mode of treatment for regeneration of periodontal tissues lost during the disease process. GTR has helped to overcome the limitations and disadvantages associated with other regeneration techniques. However there is still a need for research to optimise and improve the results possible with the use of GTR. GTR works on the principle of blocking the invasion of competing non-osteogenic soft tissue cells into the wound defect area by placement of a membrane over the bone defect. The membrane maintains a space between the defect and soft tissue and allows periodontal ligament and bone cells to repopulate the space.

Both resorbable and nonresorbable membranes have been used for GTR procedures, however the membranes used have limitations and the results with these membranes have been modest. Thus there is a need to develop a membrane with better mechanical properties with the ability to deliver growth factors and to facilitate tissue regeneration.

This study aims towards making a composite membrane for GTR procedures, with better mechanical and physical properties, and with the ability to release bioactive proteins at the defect site to facilitate and accelerate the regeneration process.

1.2 PERIODONTIUM

The periodontium consists of tissues that surround and anchor the tooth in the alveolar processes of maxilla and mandible. The periodontium includes: (a) Gingiva, (b) Periodontal ligament, (c) Cementum and (d) Alveolar bone (Figure 1.1).

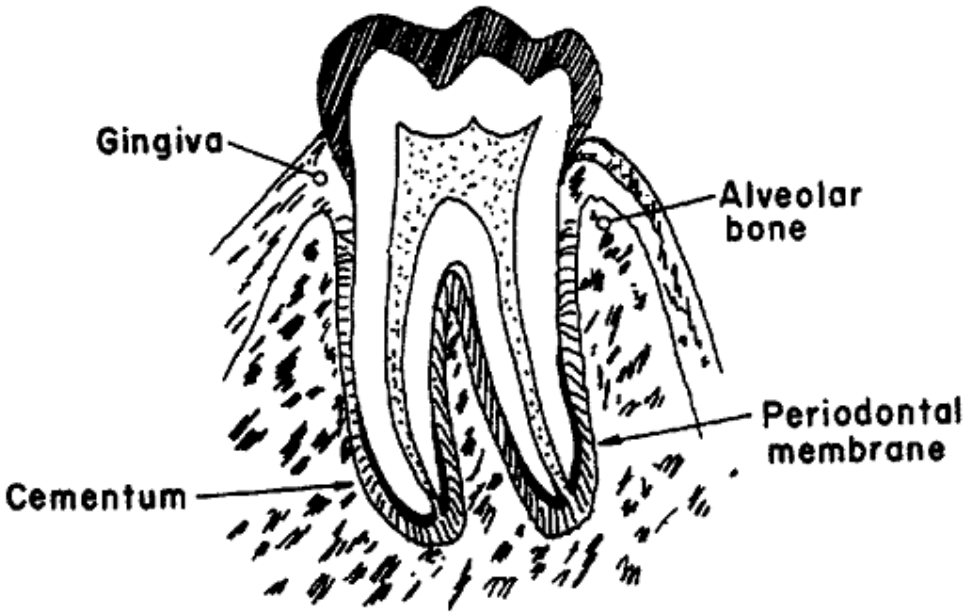

Figure 1.1: Schematic presentation of periodontium [adapted from Suchanek et al., 2002].

The characteristics of a healthy periodontium are shown in Figure 1.2.The functions of the periodontium include:

a) To provide a tissue seal at the cervical portion of the tooth.

b) To provide support to the teeth during mastication

c) To hold the tooth in the socket

d) To protect the dentine

e) Mechanoresponsive regulation of mastication

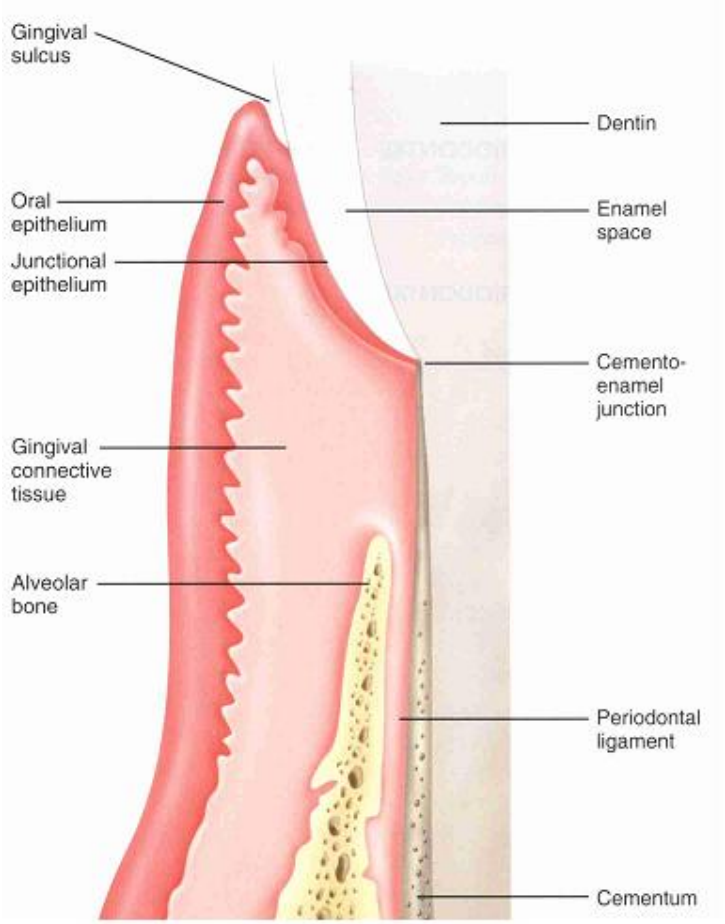

Figure 1.2 Schematic drawing of a healthy periodontium [from Rose, 2004].

1.2.1 Gingiva

Gingival tissue covers the alveolar processes of the jaws and cervical portions of the teeth and provides a seal around the cervical portions of the teeth. It is composed of an outer layer of epithelium and an inner core of connective tissue called the lamina propria. The healthy gingiva is pale pink, however, the colour may vary depending on epithelial thickness, keratinisation, vascularity and pigmentation. The gingiva consists of free and attached gingiva (Figure 1.3).

The free gingiva is also called the marginal or unattached gingiva. It surrounds the tooth at the region of the cemento-enamel junction (CEJ). It consists of the gingival tissue from the gingival margin to the free gingival groove. The space

between the free gingiva and tooth surface is called the gingival sulcus. It meets the tooth in a thin rounded margin called the gingival margin.

The attached gingiva is located between the free gingiva and the alveolar mucosa and is tightly attached to the cementum of the cervical third of the tooth and to the periosteum of the alveolar bone. Healthy attached gingiva is pink and has stippling which is caused by the presence of connective fibres that attach the gingival tissue to the cementum and the bone. Attached gingiva provides support to the gingival tissue during mastication, talking and tooth brushing [Rose, 2004].

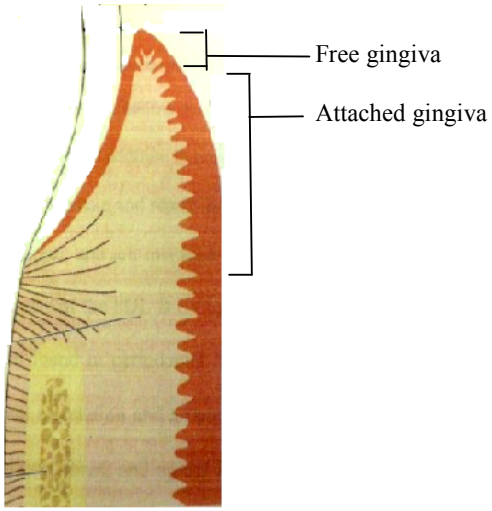

Figure 1.3: Schematic presentation of free and attached gingiva [dapted from Eley and Manson, 2004]

The epithelium of gingiva, which is a keratinized stratified squamous epithelium, is divided into four cell layers depending on the degree of keratin-producing cell differentiation. These layers are the basal cell layer, prickle cell layer, granular cell layer and keratinized cell layer. Keratin producing cells comprise 90% of the total cell population of the oral epithelium; other cells present in the oral epithelium are melanocytes, Langerhan's cells, Merkel's cells and inflammatory cells.

The connective tissue of gingiva consists of collagen fibres (60%), vessels and nerves (35%), fibroblasts and other cells (5%). The collagen fibres of gingival connective tissue are produced by fibroblasts, which are the main cells of

connective tissue and comprise 65% of total cell population. Other cells present are mast cells, macrophages and inflammatory cells. The cells, nerves and vessels are embedded in a matrix which is mainly produced by fibroblasts [Nanci and Ten Cate, 2003].

1.2.2 Periodontal Ligament

The periodontal ligament (PDL) is a soft connective tissue which is highly vascular and cellular. It covers the tooth root and attaches it to the bone of the tooth socket. The periodontal ligament is composed of fibre bundles which are attached to the cementum on one side and to the alveolar bone of the tooth socket on the other side. The length of periodontal ligament fibres is in the range of 0.2 - 0.4mm depending on their position around the tooth root.

PDL contains osteoblasts, osteoclasts, cementoblasts, fibroblasts and undifferentiated mesenchymal cells. Undifferentiated mesenchymal cells present in the PDL can differentiate into osteoblasts, cementoblasts and fibroblasts when a suitable trigger is applied. PDL cells can play an important role during alveolar bone regeneration and during normal alveolar bone formation [Hosoya et al., 2008; Zhou et al., 2008]. Studies have shown that regeneration of periodontal tissue can be achieved when epithelial and gingival connective tissue cells are blocked and cells from periodontal ligament are allowed to repopulate the healing area [Gottlow et al., 1984]. Progenitor PDL cells differentiate into cementoblasts on direct contact with root dentin [Hasegawa et al., 2005]. It is still not clear whether a single progenitor cell gives rise to daughter cells which then differentiate into different cell types, or whether separate progenitor cells are present for each cell type [Nanci and Ten Cate, 2003].

The fibres of periodontal ligament are divided into five groups depending on their location (Figure 1.4):

Alveolar crest: Extend from the cervical cementum to the alveolar crest. They resist lateral forces and retain the tooth in the alveolus.

Horizontal: Present just below the alveolar crest fibres and their orientation is perpendicular to the long axis of the tooth.

Oblique: Extend from the cementum and run diagonally towards the crown of the tooth inserting in the alveolus. These fibres provide resistance against axially directed forces.

Interradicular: Present between the roots of multi rooted teeth, they prevent tipping and extrusion of the teeth.

Apical: Present at the apex of the root. They prevent the extrusion of teeth and provide protection to the blood vessels and nerve supply of teeth.

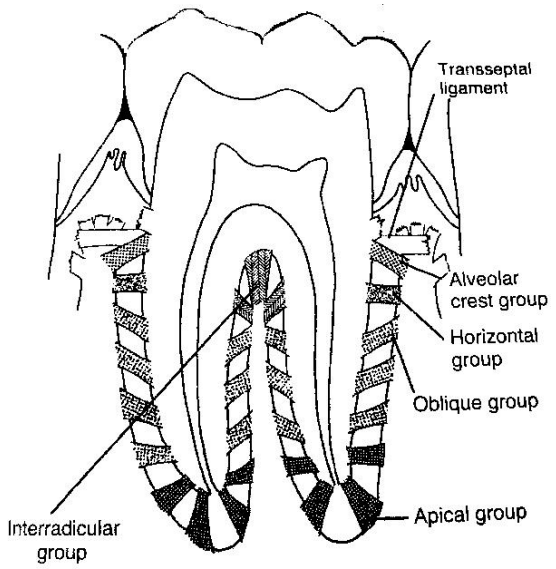

Figure 1.4: Schematic presentation of PDL fibres [adapted from Nanci and Ten Cate, 2003]

The PDL has the following functions:

Supportive function: PDL attaches and maintains the teeth in the alveolar sockets. PDL allows the transfer of forces generated during mastication and tooth contact to be transferred to and absorbed by the alveolar bone.

Nutritive function: It provides nutrition to the bone and the cementum.

Sensory function: Sensory feelings such as pain and pressure are provided to the tooth by the PDL.

***Formative function*:** It builds up and maintains cementum and alveolar bone of the *tooth socket*.

Resorptive function: In response to the pressure the PDL can remodel the alveolar bone, as occur during orthodontic procedures.

1.2.3 Alveolar Bone

Alveolar bone surrounds and supports the tooth root. The development of alveolar bone is dependent on the presence of teeth. Alveolar bone resorbs after the extraction of teeth and does not develop if teeth do not erupt. Alveolar bone constantly undergoes remodelling depending on its functional stimuli. The outer surfaces of alveolar processes consist of compact bone which overlies a trabecular bone structure. There are numerous small canals in the alveolar walls through which vessels and nerves enter the periodontal ligament space. The layer of the bone into which the fibres are inserted is sometimes referred to as "bundle bone" and it has many features similar to root cementum in respect of function and structure. The compact bone on the superficial/outer aspects of the alveolar processes varies in thickness. In the maxilla, the buccal cortical bone in the incisor, canine and premolar regions is thin, but thicker at the buccal and palatal aspect of the molars. In the mandible the cortical bone is thinner on the buccal aspect of the incisors and premolar, whereas in the molar region it is thinner on the lingual aspect than on the buccal aspect. Alveolar bone like other bones consists of bone matrix and bone cells [Rose, 2004].

1.2.3.1 Bone Matrix

Bone matrix consists of organic collagen fibres, ground substance and inorganic bone minerals (Table 1.1). Toughness and stiffness of bone is provided by its mineral content whereas collagen provides bone with tensile strength and flexibility [Murugan and Ramakrishna, 2005]. The organic matter consists of type I collagen and amorphous ground substance containing proteoglycans, glycoproteins, glycosaminoglycans, lipids and peptides [Triffitt and Owen, 1973].

The organic matter of bone is produced by osteogenic cells which are then surrounded by this organic matter. 90% of the organic matrix is collagenous and these collagen fibres in association with hydroxyapatite gives bone its stiffness and strength. Noncollagenous protein and ground substance act as a cementing agent for collagen fibres and crystals. They also play a role in mineralisation of the bone.

The inorganic matter makes up 50% of the dry weight of bone matrix and mainly consists of calcium and phosphorus in addition to bicarbonate, citrate, magnesium, potassium and sodium ions [Damien and Parsons, 1991]. Calcium and phosphorus form substituted hydroxyapatite crystals having the composition $Ca_{10}(PO_4)_6(OH)_2$ with the substances also including CO_3, Si and Fl.

Table 1.1: Composition of bone matrix [adapted from Murugan and Ramakrishna, 2005]

Inorganic components		*Organic components*	
	Wt%		***Wt%***
Hydroxyapatite	60	Collagen	20
Carbonate	4	Water	9
Citrate	0.9	Non-collagenous proteins	3
Sodium	0.7		
Magnesium	0.5		
Others: Cl^-, F^-, K^+, Sr^{2+}, Pb^{2+}, Zn^{2+}, Cu^{2+}, Fe^{2+}		Others: Polysaccharides, lipids, cytokines	

1.2.3.2 Bone Cells

The three main cells of bone are osteoblasts, osteocytes and osteoclasts. These cells are responsible for the production, maintenance and resorption of bone respectively. In addition to these cells, bone also contains mesenchymal stem cells which are present in the bone marrow and which act as a cell reservoir [Weiss, 1988]. These stem cells can differentiate into different cell types which include osteoblasts, chondrocytes, myocytes and adipocytes (Figure 1.5) [Aubin, 1998; Spagnoli et al., 2009].

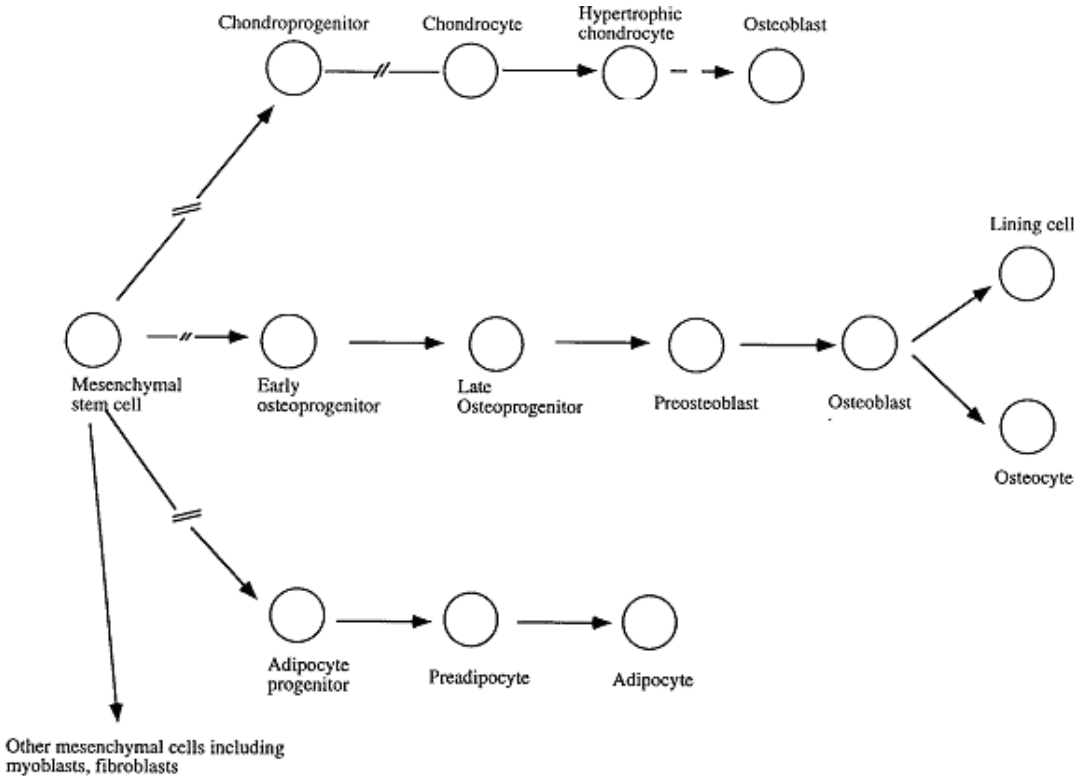

Figure 1.5: Schematic presentation of bone mesenchymal stem cells differentiation into different cells types showing the three major cell lines they can form [adapted from Aubin, 1998].

Osteoblasts: Osteoblasts are the bone producing cells which are derived from multipotent mesenchymal stem cells, and are present at the surface of the bone tissue. They synthesize and secrete the organic component of bone matrix including type I collagen, proteoglycans and glycoproteins between the cell and the mineralized matrix [Gorski, 1998]. During active production of bone matrix osteoblasts have cuboidal or columnar shape (Figure 1.6) and have high alkaline phosphatase activity, however as their activity declines they become flattened [Barrere et al., 2006]. Active osteoblasts produce a new layers of uncalcified matrix (osteoid), calcium salts are subsequently deposited into this newly formed matrix thus completing the process of bone apposition. When entrapped in newly formed matrix osteoblasts become *osteocytes*. As matrix is formed around the cell and cytoplasmic process, lacunae and canaliculi appear [Junqueira and Carneiro, 2005].

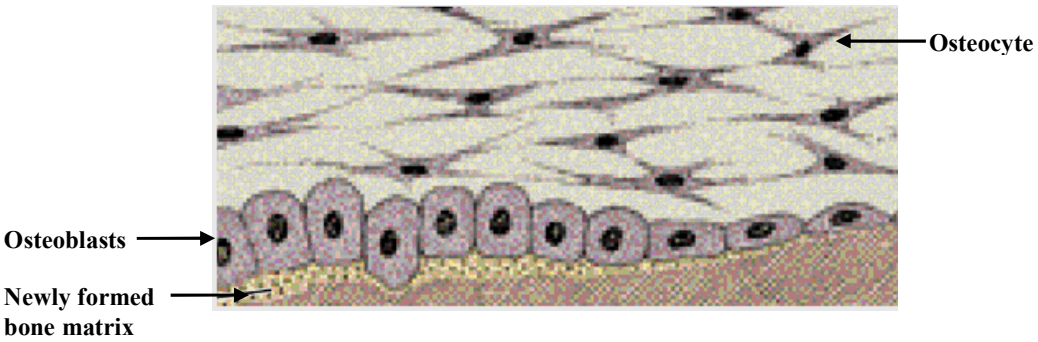

Figure 1.6: Bone forming osteoblasts depositing new bone [adapted from Junqueira and Carneiro, 2005].

Osteoblasts also play a part in the calcification of the bone by regulating the flow of calcium and phosphate through bone. It is believed that in bone remodelling the growth factors released during the bone matrix resorption by osteoclasts causes the preosteoblast cells to differentiate into osteoblasts [Martin, 2009]. Plasma membranes of active osteoblasts contain high amounts of alkaline phosphatase which is a marker for the osteoinductive nature of the cell. Alkaline phosphatase from osteoblasts tends to cause cleavage of organically bound phosphatase which in turn contributes to the initiation and growth of mineral crystal of bone. Osteoblasts also produce certain cytokines and growth factors in addition to matrix protein. These growth factors, which include bone morphogenic proteins-2 (BMP-2) and 7 (BMP-7), insulin-like growth factors (IGF), fibroblast growth factors (FGF) and platelet derived growth factors (PDGF) increase the process of bone formation and repair. Parathyroid hormone (PTH), which is the most important hormone affecting bone (high concentration=>bone resorption, low concentration= >bone formation), works by controlling the secretion of growth factors and cytokines. When bone is not being formed the inactive osteoblasts become flat and extend along the bone surface, these cells are termed as *bone lining cells*. These cells control the mineral homeostasis by forming the gap junctions with osteocytes [Weiss, 1988; Nanci and Ten Cate, 2003].

Osteocytes: During the process of bone deposition some of the osteoblasts become trapped inside the matrix. These osteoblasts are then called osteocytes. The number of osteoblasts being surrounded by matrix and converted into osteocytes is directly proportional to the speed of bone formation. Initially osteocytes resemble osteoblasts, however with time their size reduces and they become flat, almond shaped with reduced Golgi complex and rough endoplasmic reticulum. The spaces occupied by osteocytes inside the matrix are called *lacunae*. Lacunae for younger osteocytes are round, however as the osteocytes mature and their size reduces, the lacunae also become oval or lenticular. Lacunae have narrow extensions called canaliculi which house the cytoplasmic processes of osteocytes and are formed by deposition of matrix around these processes (Figure 1.7). The cells make contact and exchange of molecules takes place with the adjacent osteocytes and with the bone lining cells through these processes. Osteocytes are responsible for the maintenance of bone matrix and the matrix is resorbed following the death of these cells [Weiss, 1988; Nanci and Ten Cate, 2003].

Osteocytes play an important role in maintaining the integrity and vitality of the bone, especially in repairing micro fractures. Osteocytes detect the biochemical and mechanical changes and transmitting the signal through their processes to osteoblasts and osteoclasts or to bone lining cells [Lanyon, 1987].

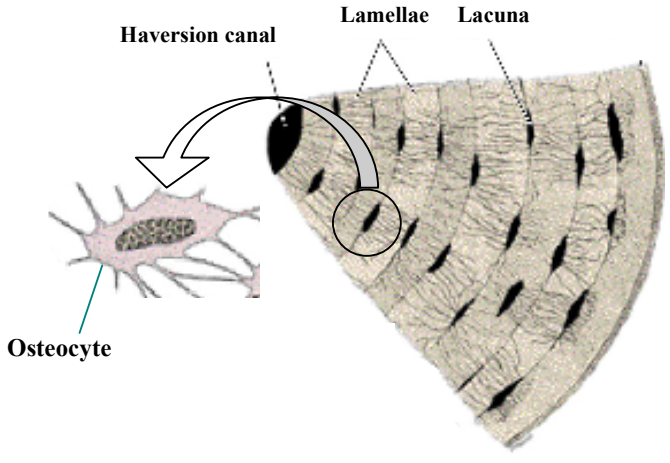

Figure 1.7: Schematic drawing of osteocytes present in lacunae arranged between lamellae [adapted from Junqueira and Carneiro, 2005].

Osteoclasts: Osteoclasts are bone resorbing cells and are of hematopoietic origin. They are large cells ranging from 20 μm to more than 100 μm in diameter and are multinucleated, containing from 5 to 50 nuclei. Osteoclasts contain abundant mitochondria which are scattered throughout the cytoplasm and Golgi complexes which are present around multiple nuclei. Osteoclasts can be cytochemically distinguished from the multinucleated giant cells by the presence of tartrate resistant acid phosphatase in their cytoplasmic vesicles and vacuoles. Acid, collagenase and other proteolytic enzymes secreted by osteoclasts attack the bone matrix thus liberating the calcified ground substance and also eliminate the debris produced during bone resorption. In the areas where active bone resorption is taking place they sit in enzymatically etched depressions in the matrix which are known as Howship's lacunae. When osteoclasts are active their bone facing surface is folded into irregular, subdivided projections, which are known as the ruffled borders. The importance of this ruffled border is seen in osteopetrosis, a genetic disease in which osteoclasts lack ruffled border formation, which renders them incapable of bone resorption. A cytoplasmic zone which is devoid of organelles and rich in actin, vinculin and talin surrounds the ruffled border. This zone creates a microenvironment between the cell and the bone matrix and provides cell adhesion to the site. Lysosomal enzymes which are synthesized in the rough endoplasmic reticulum are transported to Golgi complex from where these enzymes are transported to the ruffled border. A proton pump, which is associated with the ruffled border creates an acidic microenvironment and causes demineralisation of the bone thus exposing the organic matrix (Figure 1.8). The exposed organic matrix is then degraded by the released enzymes [Barrere et al., 2006].

The activity of osteoclasts is regulated by cytokines which are local proteins mediators and calcitonin which is a thyroid hormone. Although osteoclasts do not have receptors for parathyroid hormone, when osteoblasts are activated by parathyroid hormone they produce cytokines which in turn activate osteoclasts [Junqueira and Carneiro, 2005]. Osteoblasts play an important role in the regulation of osteoclasts as they produce M-CSF and RANKL which affect the proliferation and differentiation of osteoclast precursor cells. M-CSF stimulate the proliferation of osteoclast precursors cells by binding to c-Fms which is present on the cells surface. Whereas RANKL produced by osteoblasts triggers

osteoclast precursors differentiation into mature osteoclasts [Hughes et al., 2006].

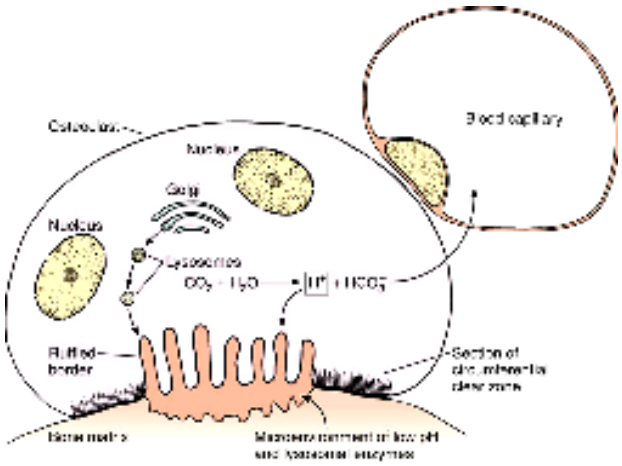

Figure 1.8: Schematic presentation of bone resorption process by an osteoclast [adapted from Junqueira and Carneiro, 2005].

In bone remodelling, osteoclasts resorb a certain amount of bone and die, leaving the space to be filled by mesenchymal cells that differentiate into osteoblasts and form bone [Martin, 2009].

1.2.4 Cementum

Cementum is a thin layer of hard and mineralized tissue which covers the root of the tooth, it is yellow in colour and covers the dentine. The matrix of cementum consists of calcified collagenous fibrils, mucopolysaccharides and glycoproteins, the mineral content is apatite. The main collagen fibres of cementum are of type I, however it also contains <5% of type III collagen fibres [Christner et al., 1977]. There are two main types of cementum, a*cellular* which covers the upper portion of the root and *cellular* which covers the lower portion of the root. Cellular cementum plays an adaptive role in response to tooth movement and wear. Cementum is produced by cells called cementoblasts which do not have a regular shape and are differentiated from PDL fibroblasts by their close proximity to cementum. Cementoblasts, like osteoblasts, have receptors for PTH [Zhang et al., 1992]. The origin of cementoblasts is considered to be from

Hertwig's epithelial root sheath (HERS) [Hammarstrom et al., 1996; Bosshardt, 2005]. Recent studies have shown that enamel matrix proteins (EMPs) can cause porcine bone marrow-derived stromal cells (BMSCs) to differentiate into cementoblasts [Song et al., 2007]. Cementum is more resistant to resorption than bone which makes it possible for teeth to be moved by orthodontic forces as they cause the resorption of alveolar bone for tooth movement without the resorption of the root. It is suggested that cementoblasts are generally nonresponsive to mechanical stimulation. Cementum does not resorb or remodel extensively. However it is deposited throughout life. Cementum lacks its own blood or nutrient supply and receives its nutrients from the PDL [Nanci and Ten Cate, 2003].

Cementum plays an important part of holding the tooth in the socket by providing anchorage to the ends of the PDL. PDL fibres are present between cementoblasts and are inserted into the cementum produced by these. Cementum protects the dentine and provides a seal for the open dentinal tubules. Toothwear at the occlusal or incisal surface of the teeth is compensated by the formation of cementum at the apical area of the tooth [Weiss, 1988].

1.3 DISEASES OF THE PERIODONTIUM

The primary aetiological factor associated with periodontal disease is the accumulation of dental plaque around the gingival margin and interdental gingiva on the tooth. The accumulation of plaque changes the microbial flora to pathogenic leading to mild to moderate gingivitis or severe periodontitis.

1.3.1 Gingivitis

Gingivitis is inflammation of the gingiva. It is characterised by changes in the color, contour and consistency of the gingival tissue (Figure 1.9). Gingivitis can be divided into plaque induced and nonplaque induced gingival inflammation. Plaque induced gingivitis can be further subdivided into plaque induced gingivitis with and without other local or systemic aggravating factors. These factors include pregnancy, diabetes mellitus and certain medications [Seymour et al., 2000]. In pregnancy the fluctuation of hormones causes enhanced growth of

certain plaque flora, whereas some drugs such as phenytoin and cyclosporin can cause the enlargement of gingiva in plaque induced gingivitis [de Oliveira Costa et al., 2006]. In diabetes mellitus the gingival inflammatory condition is aggravated as antibacterial host response is compromised. Nonplaque induced gingivitis can be caused by fungal, bacterial and viral infections [Scully et al., 1998]. Hypersensitivity to certain restorative materials and other oral care products can also produce gingival inflammation resembling plaque induced gingivitis [Holmstrup, 1999].

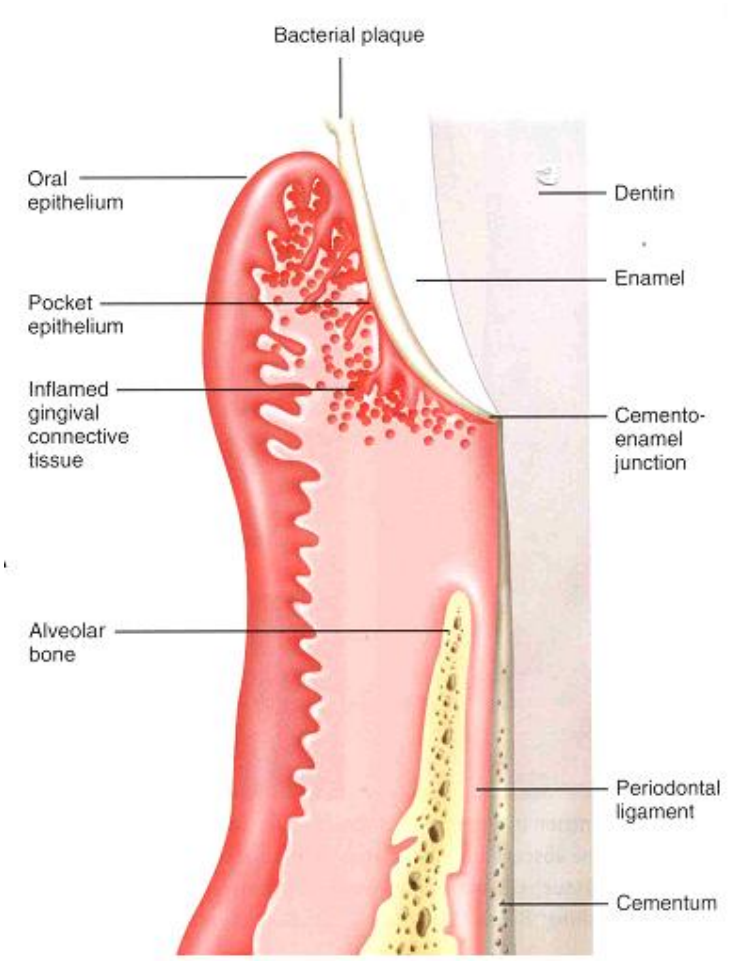

Figure 1.9: Schematic drawing of gingivitis [from Rose, 2004].

Gingivitis is a reversible condition with no permanent tissue damage and resolves when its aetiology is removed [Mariotti, 1999]. Blood flow to the gingiva increases, which gives the gingiva a red appearance. The gingiva becomes swollen as a result of the leaking of leukocytes and plasma proteins from the capillaries into the connective tissue. Gingival pockets are formed in gingivitis

due to gingival enlargement caused by swelling or fibrosis. At this stage there is no damage to PDL and alveolar bone. In most cases the body's immune system is adequate to counter bacterial infection and with patient self care and treatment gingivitis is resolved and the tissue returns to a healthy state.

In many untreated cases gingivitis may persist for years without ever progressing to the next stage of the disease. However in some cases (10-15% of population) it may aggravate to periodontitis.

1.3.2 Periodontitis

Initiation and sustainability of periodontitis is related to the accumulation of dental plaque. However the destruction of periodontal tissues depends on the host response to the plaque bacteria and the characteristics of the disease may also be affected by the individual's immune system [Kinane, 1999; Rose, 2004; Honda et al., 2006]. Periodontitis can be divided into chronic and aggressive periodontitis. Both forms of periodontitis can be further subdivided into localised and generalized periodontitis. However, in chronic periodontitis the two forms have the same aetiology and pathogenesis [Armitage, 2004], whereas in aggressive periodontitis the two forms may have differences in aetiology and pathogenesis [Lang et al., 1999]. In chronic periodontitis the tissue destruction process is not continuous. Short periods of tissue destruction are followed by extended periods of disease inactivity and the rate of tissue destruction may vary throughout the mouth [Socransky et al., 1984].

The severity of periodontal disease is judged by the amount of clinical attachment loss. 1-2mm attachment loss is described as slight, 3-4mm attachment loss is referred to as moderate and more than 5mm attachment loss is considered to be severe periodontal disease [Armitage, 1999]. Clinical attachment loss is measured by measuring the distance from cementoenamel junction to the base of the probable crevice. Periodontitis causes irreversible damage to the tissues and affects all parts of the peridontium including the gingiva, PDL, cementum and alveolar bone (Figure 1.10). Clinical characteristics of chronic and aggressive periodontitis are shown in Figure 1.11 and are listed in Table 1.2.

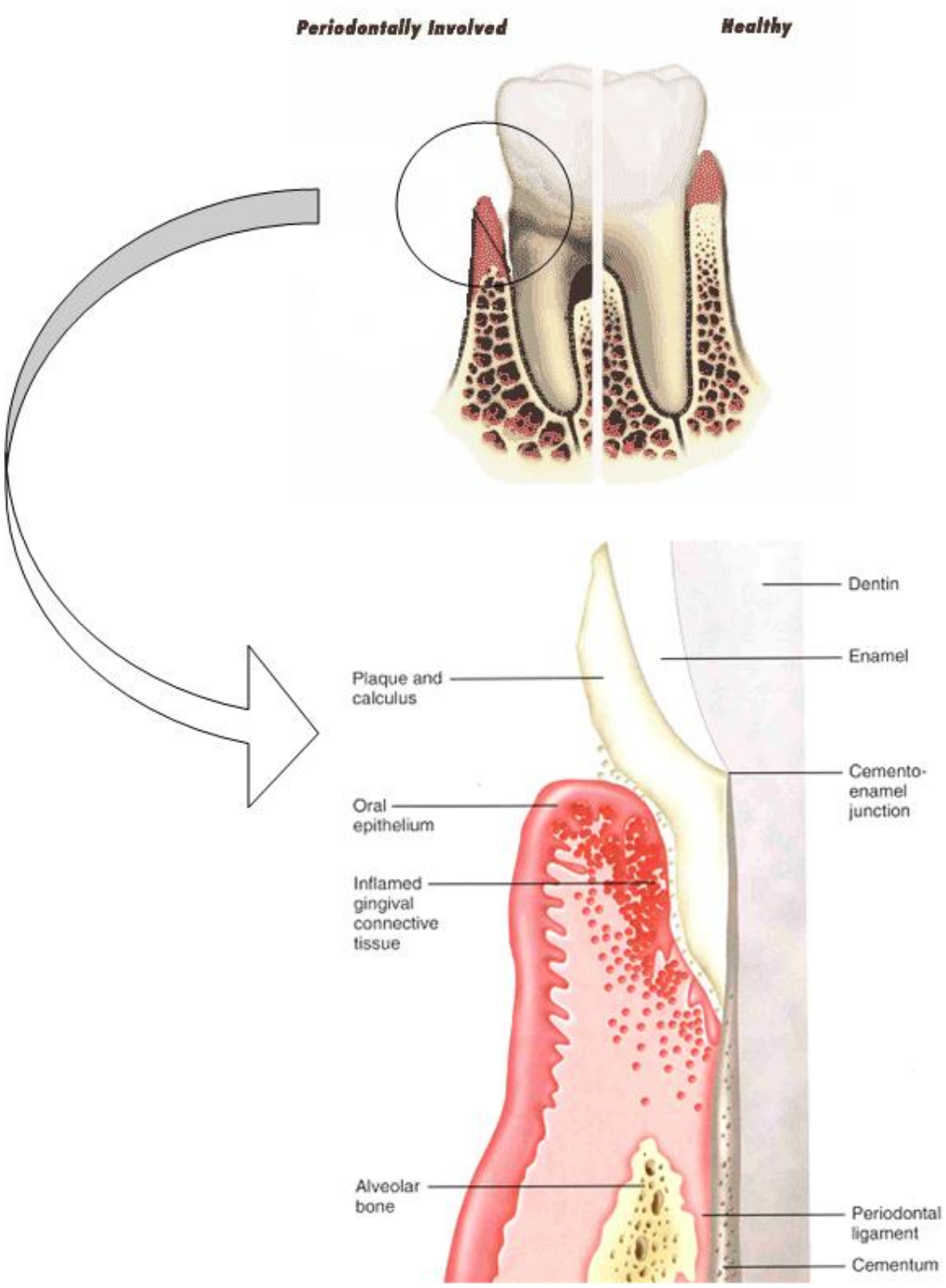

Figure 1.10: Schematic drawing of a periodontally involved tooth [from www.drfudge.com ;Rose, 2004].

Table 1.2: Clinical characteristics of chronic and aggresive periodontitis [from Lang et al., 1999; Lindhe et al., 1999; Armitage, 2004]

Chronic periodontitis

Mostly in adults, however can also occur in children and adolescents

Subgingival calculus

Apical migration of junctional epithelium and pocketing

Connective tissue attachment loss

Alveolar bone loss

Tooth mobility

Slow to moderate progression rate with periods of rapid progression

Can be associated and aggravated with systemic diseases

Local predisposing factors can be associated

Smoking and emotional stress can effect the disease characteristics

Aggressive periodontitis

Except for periodontitis the patient is healthy

Attachment loss and bone destruction is rapid

	Localized	***Generalized***
Onset:	*Circumpubertal*	*Usually under 30 years*
Subgingival calculus:	*Usually absent*	*May or may not be present*
Serum antibody response to infecting agents:	*Robust*	*Poor*
Involvement:	*First molar/incisor presentation Interproximal attachment loss on two permanent teeth one of which is first molar.*	*Interproximal loss is generalized affecting at least three permanent teeth other than first molar and incisor.*

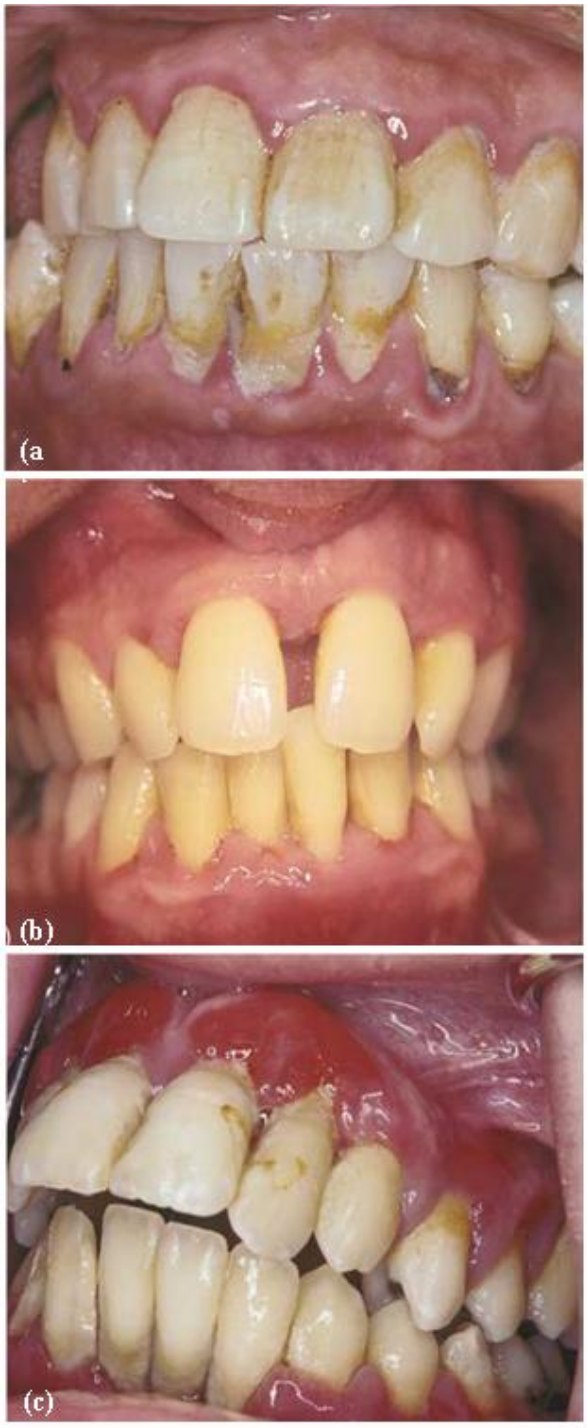

Figure 1.11 (a) Chronic periodontitis, gingival recession and bone loss is visible. (b) Localized periodontitis, bone loss of mandibular anterior teeth. (c) Generalized periodontitis, bone loss involving all teeth [from Armitage, 2004].

1.4 TREATMENT OF PERIODONTAL DISEASES

Treatment of periodontitis involves two components, elimination of bacterial plaque and correction of anatomical deformities produced by the periodontitis. There are two approaches to correct the anatomical defects: resective and regenerative. In resective treatment periodontal defects are eliminated by removal of gingival and bony walls; this includes gingivectomy, apically positioned flaps and apically positioned flaps with osseous resection. Regenerative treatment involves elimination of periodontal defects by the production of new bone and periodontal ligament and coronal displacement of gingival attachment.

1.4.1 Plaque removal and root planing

Elimination of bacterial plaque is essential for the treatment of periodontal diseases. Removal of supragingival and subgingival plaque and calculus using conventional methods of scaling and root planing with or without flap surgery is useful. With scaling a reduction in the probing depth can be gained and it can be effective in treating periodontal disease [Becker et al., 2001]. However studies have shown that nonsurgical subgingival root planing does not always produce good results in terms of complete removal of calculus deposits as produced with surgical subgingival root planing [Eaton et al., 1985; Sherman et al., 1990]. In root planing the cementum is removed along with calculus deposits and the root surface is made smooth and hard. These procedures improve gingival conditions and reduce gingivitis and bleeding.

1.4.2 Resective surgical procedures

Resective surgical procedures are done to eliminate the disease and to correct anatomical deformities. These procedures create the conditions which stop the recurrence of the disease and eliminate or reduce gingival pockets:

1.4.2.1 Gingivectomy

Gingivectomy involves removal of the soft tissue wall of pathological periodontal pocket. The development of flap techniques has limited the use of gingivectomy

to removal of enlarged gingiva and minor reshaping. Gingivectomy is indicated in cases where there is a need to eliminate the persistent gingival pockets after completion of scaling or root planing or to eliminate gingival enlargements due to any medication or genetic factors (Figure 1.12). Studies have shown that the regenerated gingiva following gingivectomy contains smaller lesions with lower densities of immunocompetent cells when compared to gingiva following non-resective open-flap debridement [Zitzmann et al., 2005]. For drug induced gingival overgrowth, gingivectomy remains the treatment of choice [Mavrogiannis et al., 2006]. However gingivectomy is contraindicated in cases of acutely inflamed gingiva and where there are infrabony defects and large exostoses [Rose, 2004].

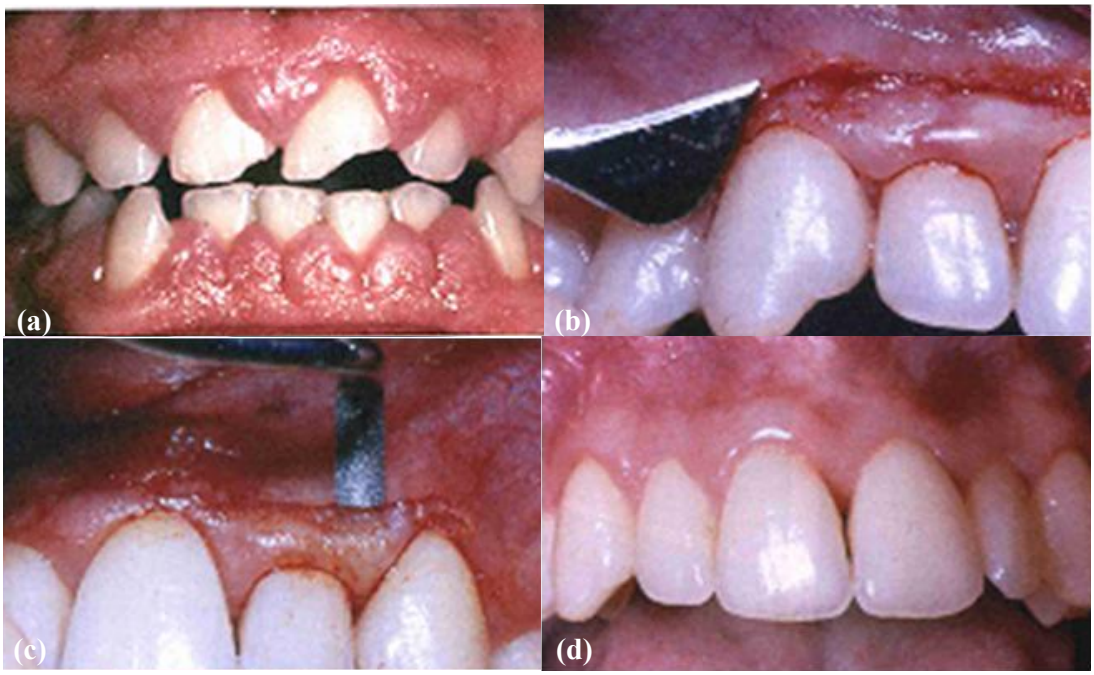

Figure 1.12(a) Gingival enlargement, a candidate for gingivectomy. (b) Gingival incision at the pocket depth(c) A sharp pointed periodontal knife to relieve interproximal area. (d) A normal gingiva after treatment [from Rose, 2004].

1.4.2.2 Apically repositioned flaps

This procedure eliminates the periodontal pocketing and increases the zone of attached gingiva by moving the flap in an apical direction [Carnio and Miller, 1999]. Carnio et al. [2007] described a modification of the apically repositioned flap which produced better results than the conventional method. After

repositioning the flap the alveolar crest is covered thus eliminating the pocket. A mucoperiosteal attached gingival zone is created on merging of connective tissue on the inner surface of the flap with the bone.

1.4.2.3 Apically positioned flap with osseous resection

This procedure is also used to reduce or eliminate periodontal pockets. This procedure involves (a) periodontal flap elevation, (b) granulation tissue removal (c) tooth root treatment and (d) bone contour correction. This results in positioning of the flap more apically than its original position. This procedure gives a stable dentogingival junction and is ideal for reducing periodontal pockets in patients with moderate periodontitis. However the main disadvantage associated with this technique is the root surface exposure which can result in hypersensivity and aesthetic problems [Rose, 2004].

1.4.3 Regenerative procedures

The resective procedures described above only arrest the disease process, but do not reverse or replace the tissue lost during the disease [Needleman et al., 2002]. Procedures such as bone grafting and guided tissue regeneration (GTR) are used to produce regeneration of tissues destroyed by periodontal disease. Architecture and function of the lost tissue can be restored by regeneration to a limited extent.

1.4.3.1 Bone grafts

Tissue loss in severe periodontal disease has been treated with bone grafts for many years. Bone grafts can play a part in the correction of the osseous aspects of periodontal defects either by the process of osteoinduction or osteoconduction [McAllister and Haghighat, 2007]. An osteoinductive material can induce bone formation by recruiting undifferentiated mesenchymal cells and causing them to differentiate into osteoblastic cells, whereas an osteoconductive material acts as a scaffolding material for new bone formation from existing bone.

Graft materials can be divided into following four general types;

Autograft: Autografts are obtained from the same individual. The bone is harvested from the patient's own jaw (intraoral) or from any other part of the patient's body (extraoral). Figure 1.13 shows a block autograft obtained from the patient's own ramus. Autograft bone eliminates the possibility of graft rejection and transfer of disease. In one study iliac autografts were shown to successfully fill 87% of Class II furcation defects and a bone fill from 2.6mm to 4.16mm was achieved [Schallhorn et al., 1970]. In another study where intraoral bone autografts were used, a bone gain of 2.88 to 3.44mm was achieved [Hiatt and Schallhorn, 1973]. However there are some studies in which autografts is shown not to produce good results [Carraro et al., 1976]. The factors on which the outcome of the treatment can depend include the morphology of the defect and the type of the bone used. In addition the availability of bone is limited and the patient has to undergo surgical procedures at two sites, which can increase pain and the potential for complications.

Figure 1.13 A block autograft fixed with screws [from McAllister and Haghighat, 2007].

Allograft: Allograft is the bone from another donor of the same species and provides a substitute for autograft (Figure 1.14). Allografts have the advantages of high availability as these are obtained from cadavers and eliminate need of a second surgical procedure on the patients. Iliac allografts were shown to produce bone gain of up to 3.6mm in periodontal defects [Hiatt et al., 1978]. Allografts used in periodontal regeneration are available in two forms: freeze-

dried bone allografts (FDBA) and demineralised freeze-dried bone allografts (DFDBA) [Rose, 2004]. FDBA and DFDBA both can be effective in correcting periodontal bone defects [Mellonig, 1992]. The osteogenic potential of DFDBA may depend on the age of the bone donor and recipient. Rat studies have shown that DFDBA obtained from middle age animals had more bone forming potential than younger animals and bone formation is better in younger recipients than older recipients [Jergesen et al., 1991]. Disease transfer, including HIV/AIDs and hepatitis, is one of the drawbacks of allografts.

Figure 1.14 A block allograft fixed with screws [from McAllister and Haghighat, 2007].

Xenograft: Xenograf*t* is bone obtained from different species. These bones are obtained from bovine or porcine sources and are thought to be osteoconductive and resorbed to be replaced by the host bone over time [McAllister and Haghighat, 2007]. A xenograft grafted at the defect site is shown in Figure 1.15. Bovine bone is treated with ethylene diamine which removes its organic and antigenic fractions, but retains its inorganic structure. In comparative studies anorganic bone showed better restoration of bone defects than bioactive glass ceramics [Schmitt et al., 1997], whereas there was no significant difference in the results produced by DFDBA and bovine derived xenograft [Richardson et al., 1999]. However risk of bovine or porcine virus or other infective agent transmission is associated with these grafts [Sogal and Tofe, 1999].

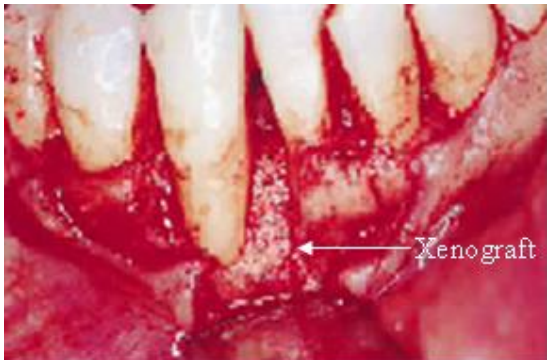

Figure 1.15 A bovine xenograft placed at the defect site [from Richardson et al., 1999].

Grafts of bone substitutes and synthetic materials (Alloplast): Alloplasts eliminate the problem of limited supply of autograft bone and risk of disease transmission from allograft or xenografts. However these materials only act as biocompatible space fillers. The following types of alloplastic synthetic grafts are available:

a) Porous hydroxyapatite

b) Non-porous hydroxyapatite

c) Beta tricalcium phosphate

d) HTR polymer

e) Bioactive glasses and ceramics

Bioactive glass produced similar clinical results and gain in attachment levels in comparison with expanded polytetrafluoroethylene (ePTFE) membranes for the treatment of mandibular Class II furcation [Yukna et al., 2001].

1.5 GUIDED TISSUE REGENERATION (GTR)

In modern periodontal disease treatment the aim is not only to stop the disease but also to regenerate lost periodontal and supporting bone tissues [Needleman et al., 2002]. Guided tissue regeneration (GTR) technique uses a membrane to cover the periodontal defect which isolates the defective area from overlying soft tissue, thus blocking fast growing soft tissue cells from invading the area and allowing mesenchymal cells from PDL or bone to repopulate the area.

It was proposed by Melcher [1976] that the nature of periodontal tissue healing depends on the type of cells which repopulate the root surface. Regeneration at the periodontal defect occurs if the root surface is populated by the undifferentiated mesenchymal cells from PDL or perivascular region of the bone which then differentiate into specific tissue forming cells, whereas if the surrounding tissues replace the lost periodontal tissues the healing of the periodontal defect occurs by repair. In repair, if the root surface is populated by the cells from gingival epithelium it results in formation of a long junctional epithelium and a connective tissue attachment is formed when the root surface is populated by the cells from gingival connective tissue which can also cause root resorption. If the cells from surrounding bone repopulate the root surface, then they will cause root resorption and ankylosis, which is fusion of the tooth to the bone.

The predictability of regenerating bone destroyed by periodontal diseases has been increased by use of guided tissue regeneration (GTR) techniques. For more than a decade GTR has been considered an effective method to regenerate the lost periodontal tissue [Caffesse et al., 1997]. Superiority of GTR over traditional techniques has been reported in a number of clinical studies [Nyman et al., 1982; Murphy and Gunsolley, 2003].

1.5.1 Principles of GTR

GTR is based on the *three principles* of wound healing.

First principle is that if the fast growing gingival epithelium and connective tissue are blocked from invading the periodontal wound, periodontal tissue can regenerate from multipotent cells of PDL and bone. Studies have shown that the gingival epithelium cells migrate more rapidly to the periodontal defect than the cells from PDL or bone [Caton et al., 1980]. GTR membranes are used to block the invasion of competing non-osteogenic soft tissue cells to the periodontal defect [Bunyaratavej and Wang, 2001; Ueyama et al., 2002].

Second principle is that if a GTR membrane maintains a space between the mucoperiosteal flap and the periodontal defect, which allows migrating and proliferating cells to reconstruct the defect.

Third principle is that GTR membranes stabilize and mechanically protect the newly formed clot in the wound [Koyama et al., 2003]. Protection of blood clot is important for the successful outcome. This clot acts as a scaffold for the regenerating osteogenic cells which regenerate bone [Koyama et al., 2003; McAllister and Haghighat, 2007].

1.5.2 Ideal requirements of GTR membranes

A GTR membrane should have the following properties to obtain the best results:

- Biocompatibility
- Mechanical stability
- Biodegradability
- Resorbability
- Adaptability
- Ability to release bioactive proteins
- Clinical manageability

1.5.3 Types of GTR membranes

GTR membranes can be divided into two types, resorbable and nonresorbable membranes. Nonresorbable membranes require a second surgical procedure for their removal. Resorbable membranes have the advantage over nonresorbable membranes as they do not require removal and are eliminated from the body by metabolic processes [Zellin et al., 1995; Mayfield et al., 1997].

1.5.3.1 Nonresorbable membranes

These membranes require a second surgical procedure for their removal which not only increase the cost and discomfort for the patient but the removal can also damage the newly formed tissue.

Expanded Polytetrafluoroethylene (ePTFE): These were the first commercially available membranes used for GTR. These membranes are removed approximately 1 to 3 months after placement [Pontoriero et al., 1988]. This membrane has two parts, a collar portion which has open pores which prevent migration of epithelium and allow ingrowth of connective tissue, and an occlusive portion which prevents the contact of flap tissue to the root surface [Scantlebury, 1993]. For larger defects ePTFE membranes are used with titanium reinforcement to improve space maintenance ability of the membrane (Figure 1.16).

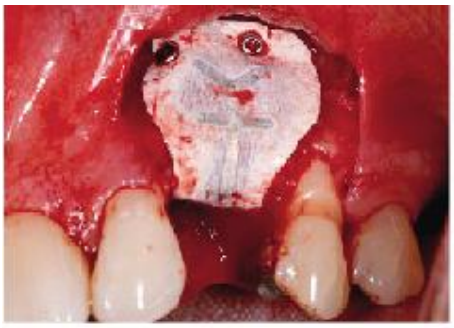

Figure 1.16 A titanium reinforced ePTFE membrane fixed with screws [from McAllister and Haghighat, 2007].

Although the use of ePTFE membranes in treatment of periodontal defects like class II furcation have shown improved clinical results, the regenerated tissue did not completely fill the defects [Pontoriero et al., 1988]. A comparative study

showed no significant difference between the results obtained from the defects treated by ePTFE and DFDBA [Guillemin et al., 1993]. Imbronito et al. [2002] have shown that the membranes made of ePTFE showed similar amounts of bone regeneration as compared to polylactic acid (PLA) membranes. In addition these membranes have the problem of exposure due to tissue dehiscence which may lead to their bacterial contamination which can negatively affect the outcome of GTR procedures [Tempro and Nalbandian, 1993; Nowzari et al., 1996; Machtei, 2001]. In a study carried out by Zitzmann et al. [1997], 44% of the ePTFE membranes had to be removed prematurely due to exposure. The use of ePTFE has now mostly been replaced by resorbable membranes [Dupoirieux et al., 2001].

1.5.3.2 Resorbable membranes

Due to the limitations associated with nonresorbable membranes, their use is mostly replaced by resorbable membranes which eliminate some of the drawbacks of nonresorbable membranes [McAllister and Haghighat, 2007]. These materials are resorbed and by products are eliminated by the body so do not require a second surgical removal procedure. Resorbable materials (Figure 1.17) have the advantage of less patient discomfort, cost and less chances of damage to newly formed tissues [Scantlebury, 1993; Caffesse et al., 1997]. The mechanical properties of resorbable membranes are generally not as good as those of nonresorbable membranes, however they can be equally osteopromotive and improve GTR if they can be designed to maintain the space for an adequate time [Zellin et al., 1995].

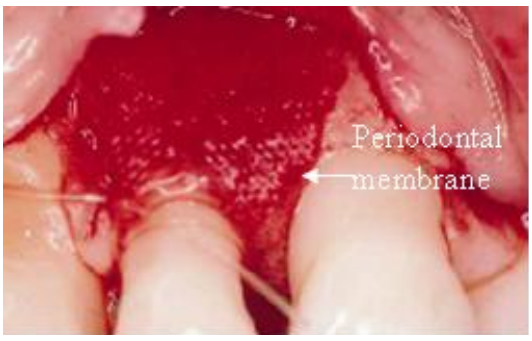

Figure 1.17: A PLA/PGA composite resorbable membrane placed over a periodontal defect [from Cortellini and Tonetti, 2000].

Resorbable membranes are divided into two groups: *synthetic* and *natural* [McAllister and Haghighat, 2007]. Synthetic and natural membranes have different degradation mechanisms. A study in which a synthetic membrane consisting of PLA/PGA copolymer and a natural type I collagen membrane was used showed equal clinical improvements from the use of either membrane [Jepsen et al., 2000].

Synthetic polymers: These polymers are eliminated out of the body through metabolic processes. Degradable polymers used for the production of GTR membranes include: *(a) Polylactic acid (b) Co-polymers of polylactic (PLA) and polyglycolic acid (PGA) (c) Polyurethane*.

Commercially available membranes made up of synthetic polymers includes Resolute®, Atrisorb®, Vicryl Periodontal Mesh®, Epi-Guide® and Mempol®.

Resolute®, which is a composite of PLA and PGA retains its structure for four weeks and then completely resorbs within 5 to 6 months [Hurzeler et al., 1997]. PLA and PGA copolymer membranes can promote regeneration when used for the treatment of intrabony defects and were easier to suture than collagen membranes, which tended to tear when tension is applied at the suture [Mattson et al., 1999]. Mayfield et al. [1997] used Resolute® in their clinical study and showed bone regeneration and complete bone coverage of implant threads in 14 cases out of 17 and partial coverage in 3 cases. Zellin et al. [1995] showed that polylactic/polyglycolic copolymer membranes produced a very low inflammatory response in the surrounding tissue and most of it was degraded after 6 weeks of healing. Resolute® produced equally good clinical improvements in a comparative study with ePTFE [Caffesse et al., 1997].

Atrisorb® consists of polylactic acid and is prepared at the chair side, is reported to be completely resorbed in six to twelve months after implantation [Bogle et al., 1997]. A study carried out by Stoller et al. [2001] showed regeneration of cementum, alveolar bone and periodontal ligament when they used polylactic acid membranes for the treatment of class II furcation defects.

Natural biomaterials: Natural biomaterials used for GTR include:

1). Collagen: These membranes are of porcine or bovine origin consisting of either type I or a combination of type I and type III collagen. A commercially available collagen membrane, Bio-Gide®, is produced from collagen of porcine origin. Studies have shown the ability of collagen membranes to promote regeneration in periodontal defects. Collagen membranes have been used in combination with other materials which include bone grafting material, fibronectin and heparan sulfate to enhance their regeneration potential [Mattson et al., 1999; Bunyaratavej and Wang, 2001]. When using these collagen membranes a space filling bone substitute should be used to avoid the collapse of these membranes into the defect and to improve GTR results [Strietzel et al., 2006]. Collagen membranes have a fast degradation rate which can affect their ability to act as a barrier, however studies have shown the ability of these membranes to inhibit apical migration of epithelium during early wound healing when epithelium actively migrates apically. It is reported that regenerative cells from bone and PDL reach the wound area in 3 to 4 weeks [Bunyaratavej and Wang, 2001]. On the whole, collagen membranes have limited potential to be used as GTR membranes because of their lack of ability to maintain space over the wound area [Tatakis et al., 1999a].

2). Dura mater: These are obtained from cadavers and consist of an irregular network of collagen fibres. They are processed and sterilized, but still pose a risk of transferring Creutzfeldt-Jakob disease to the patient and the operator as well [Martinez-Lage et al., 1994]. Their use as GTR membranes is limited [Yukna, 1992].

1.5.4 Limitations of GTR

The limitation with the currently used GTR membranes is that the nonresorbable materials need to be removed via a second surgical procedure which can adversely affect the newly formed periodontal tissues but they generally have suitable mechanical properties. Resorbable membranes on the other hand do not require removal but currently have too low mechanical properties. Resorbable membranes have shown variable results in term of their ability to produce GTR

mainly depending on their ability to maintain space and resist collapse. These membranes are prone to collapse because of their low mechanical properties.

Furthermore although GTR techniques have been shown to increase the regeneration of periodontal tissues, the increase has been modest [Needleman et al., 2002]. To improve the effectiveness of GTR, new research is focused on using the combination of different materials which can compliment each other to produce increased regeneration. One such combination can be the use of a bioactive composite membrane with the ability to deliver growth factors.

1.5.5 Growth factors and tissue regeneration

There is considerable interest in the potential therapeutic application of bioactive molecules such as growth factors to enhance healing outcomes, and GTR membrane materials might also be suitable as carriers for the sustained delivery of bioactive molecules [King, 2001; Hughes et al., 2006].

Different studies have shown the potential of growth factors to induce the regeneration of periodontal tissues [Cho et al., 1995; Park et al., 1995]. Growth factors are proteins or polypeptides which have the ability to initiate the proliferation or activity of cells. High concentrations of growth factors are present in bone and cementum which are released following an injury which effect the repair and regeneration of periodontal tissue [Giannobile, 1996]. Growth factors bind to specific receptors on target cells, generating a cascade of intracellular molecular signals, thus causing cells to proliferate and differentiate [Davidson et al., 1985; Giannobile, 1996; Rose, 2004]. Growth factors found in bone, cementum and other healing tissues include Platelet Derived Growth Factors (PDGF), Bone Morphogenic Proteins (BMPs), Enamel Matrix Derivatives (EMDs), Fibroblast Growth Factors (FGFs) and Insulin like Growth Factors (IGFs) [Giannobile, 1996]. These growth factors have the ability to induce and promote periodontal regeneration [King and Cochrant, 2002].

1.5.5.1 Platelet derived growth factors (PDGF)

PDGF is a heparin-binding polypeptide having a molecular weight of approx 30,000 Da [Antoniades, 1981]. Human platelet derived PDGF is a heterodimer of

A and B chains [Ross et al., 1986]. In addition to these chains, C and D chains have been recently discovered (AA, BB, AB, CC, DD). The principal source of PDGF is α-granules of platelets, however macrophages and fibroblasts when activated also produce PDGF. PDGF binds to the α and ß receptors on the surfaces of the cells. Both A and B chains bind to α receptors on the cell surface, however only the B chain of PDGF binds to the ß receptors of cells [Chong et al., 2006]. Each PDGF receptor contains five immunoglobulin-like domains extracellulary, and there is a tyrosine kinase domain intracellulrly. Autophosphorylation of PDGF receptors produce two affects; first, phosphorylation of tyrosine residue inside the kinase domains results in an increase in the catalytic efficiencies of the kinases. Secondly, phosphorylation of tyrosine residues located outside the kinase domain produce docking sites for SH2 domain protein such as phosphatidylinositol 3'-kinase (PI 3-kinase), phospholipase C (PLC)-γ. PI 3-kinase binds to and is activated by tyrosine kinase receptors, it plays a central role in the transduction of intracellular signals, many different cellular responses are mediated by it which includes, actin reorganization, chemotaxis and cell growth. PLC-γ acts on the same substrate as PI 3-kinase. On binding to PDGF receptor it phosphorylate on specific tyrosine residues and its catalytic activity increases. PLC-γ stimulates cell growth and motility in certain cell types [Heldin and Westermark, 1999].

PDGF is considered to play an important role in defining the activity of mesenchymal cells and an *in vitro* study showed that the proliferation of PDL was enhanced on addition of PDGF [Mumford et al., 2001]. Interestingly, Hsieh and Graves [1998] showed that although PDGF increases the proliferation and differentiation of bone forming cells, prolonged exposure of differentiated bone cells to PDGF inhibits their bone forming function. PDGF has been reported to have mitogenic and chemotactic effects on osteoblasts and it enhances the production of type I collagen by osteoblasts [Bolander, 1992].

During fracture healing PDGF is produced at the fracture site and PDGF receptors on the surfaces of cells also increase which suggests that it has a role during bone repair [Andrew et al., 1995; Fujii et al., 1999]. In a human clinical study enhanced periodontal regeneration was achieved when PDGF was used in combination with bone allografts for the treatment of Class II furcations and interproximal intrabony defects [Nevins et al., 2003]. In another clinical study

PDGF was shown to stimulate the cells involved in periodontal regeneration resulting in enhanced periodontal bone regeneration [Cooke et al., 2006]. An increased number of cell receptors for growth factors are found in regenerated tissues compared to normal gingival and periodontal ligament tissues [Parkar et al., 2001]. In a rat study PDGF loaded chitosan sponge produced enhanced bone regeneration in calvarial defects [Lee et al., 2000; Park et al., 2000b]. Sant'Ana et al. [2007a] showed increased proliferation of PDL cells in response to PDGF in an in vitro study. Howell et al. [1997] reported increased alveolar bone formation in human osseous defects with the use of PDGF as compared to bone formed by conventional flap surgery. PDGF absorbed to ß-TCP alloplast material produced increased proliferation of osteoblastic cells *in vitro* [Bateman et al., 2005].

1.5.5.2 Bone morphogenic proteins (BMPs)

Bone morphogenic proteins (BMPs) belong to the transforming growth factor ß (TGF-ß) family and their activity was first identified by Urist in 1965 when he showed that demineralised bone extracts contains substances which can induce bone formation at ectopic sites in rodents [Urist, 1965; Sigurdsson et al., 1997; Massague, 1998]. Later these substances were recognized as BMPs and BMP 1,2, 3 and 4 were successfully purified and cloned [Wozney et al., 1988]. BMPs can be isolated and purified from dentine, bone and osteosarcoma tissues, however demineralized bone matrix still is used extensively as their source [Urist et al., 1984; Granjeiro et al., 2005].

Since then more than 20 different types of BMPs have been identified with each having a different biological activity. BMPs play important roles both during embryonic growth and later throughout life in repair [Boden, 2005]. BMPs act by binding to transmembrane serine-threonine kinase receptors which are present on the cell membranes. BMPs form a complex by binding to type II receptors on the cell surface and then recruiting a type I receptor. The receptors phosphorylate after the formation of the BMP-receptor II-receptor-I complex and then phosphorylate SMAD proteins. These phosphorylated SMAD proteins then enter the nucleus of the cell and cause the transcription regulation of target genes [Massague, 1996; Sakou, 1998]. A schematic description of the possible mechanism of action of BMPs on a cell is shown in Figure 1.18.

BMPs regulate the processes of cell proliferation, differentiation and apoptosis and can induce different tissue formation [Granjeiro et al., 2005]. BMPs stimulate the differentiation of mesenchymal stem cells into osteoblasts and can induce the production of new bone, among BMPs differentiation of osteoblasts is specially regulated by BMP-2, BMP-4 and BMP-7 [Hughes et al., 2006] [Rose, 2004].

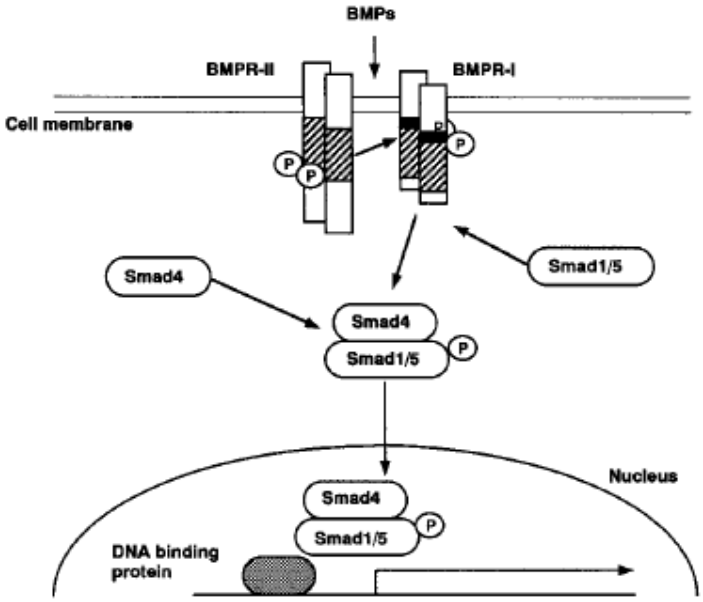

Figure 1.18: A schematic description of BMP action on cell. BMPs bind to the receptors in the cell and signals are transduced through Smad 1/4/5 to the cell nuclei [Adapted from Yamaguchi et al., 2000].

Interestingly, it was found *in vitro* that when mesenchymal cells were exposed to low concentrations of BMPs they differentiate into adipocytes, however, on exposure to high concentrations these mesenchymal cells differentiate into osteoblasts. This finding lays emphasis on the importance of specifying the dose for their clinical use [Granjeiro et al., 2005]. In different animal studies BMP-2 has been shown to induce bone formation [Murakami et al., 2002]. An animal study has shown that BMP-2 can also be used for the treatment of osteoporosis as it increases the activity of mesenchymal cells and can reverse the age related bone loss when administered systemically [Gadi et al., 2002]. Although BMPs can induce regeneration even without a carrier, a delivery system is needed to get a better and more localized effect. BMPs play a considerable role in

periodontal healing and have osteoinductive activity. Application of rhBMPs enclosed in collagen membrane sponges in Wistar rats has been shown to stimulate early cell proliferation and migration towards the periodontal wound area and subsequent differentiation occurs more rapidly than in a normal wound [Boyne et al., 1997; King et al., 1998; King and Hughes, 2001].

In a human clinical study recombinant human (rh) BMP-2 was used for maxillary floor sinus augmentation incorporated in an absorbable collagen sponge, the results showed significant increased bone growth with a mean gain of 8.51 mm. No serious adverse effects were observed in the patients, however facial edema, oral erythema and rhinitis were reported [Boyne et al., 1997]. In another human clinical trial, Howell et al. [1997] also used rhBMP-2 in a resorbable collagen sponge for the treatment of localised osseous defects and prevention of alveolar ridge after tooth extraction. They also found out that the rhBMP-2 was effective in regenerating bone after tooth extraction and rhBMP-2 was well tolerated by the patients with no serious side effects.

1.5.5.3 Enamel matrix derivatives (EMD)

Enamel matrix derivatives consist of proteins which are derived from Hertwig's root sheath of porcine origin. EMD contains different low molecular weight proteins which include amelogenins (90%), ameloblastins and enamelin. EMD can induce acellular cementum regeneration which is an important part of periodontal regeneration, based on the theory that a protein preparation present in the EMD resembles the matrix proteins which induce cementogenesis [Hammarstrom, 1997; Rose, 2004].

In vitro studies have shown that EMD enhances the proliferation, proteins and collagen production, differentiation and osteoprotegerin production of PDL cells and when myoblast cells were exposed to EDM they differentiated into osteoblasts or chondroblasts. EMD did not show a significant effect on the proliferation of epithelial cells *in vitro* [Gestrelius et al., 1997; Ohyama et al., 2002; Lossdorfer et al., 2007]. In another study, Lyngstadaas et al. [2001] showed that when PDL cells were exposed to EMD the attachment rate, growth rate and metabolism of these cells was increased and they subsequently produced more growth factors.

In a monkey study, buccal alveolar bone, periodontal ligament and corresponding cementum were removed and the defects were then treated with porcine enamel matrix with and without a carrier system, the results obtained showed that application of EMD produced complete regeneration of cementum and collagenous fibres which were embedded in newly formed alveolar bone [Hammarström, 1997].

In a clinical trial intrabony defects were treated with the application of EMD. The treatment with EMD produces regeneration of periodontium which was comparable with the regeneration produced using a GTR membrane. In addition no systemic adverse effects with the application of EMD were observed [Sculean et al., 1999]. In another human study EDM was used with xenografts for the treatment of osseous periodontal defects with favourable results [Scheyer et al., 2002].

1.5.5.4 Fibroblast growth factor (FGFs)

FGFs belong to heparin binding growth factor family. Basic FGF is found in gingiva, periodontal ligament and bone.

In an in vitro study FGF was shown to have a mitogenic effect on PDL cells, when used with allografts as carrier, which can be beneficial for periodontal regeneration [Dereka et al., 2006]. In an animal study FGF in a gelatin carrier was topically applied to the created class II bone defects. The application of FGF produced more periodontal ligament formation and cementum along with new bone formation as compared to controls, without producing any ankylosis or root resorption. FGF inhibits the differentiation of PDL cells and inhibit their ability to produce calcified nodules, however, it enhances the proliferation of PDL cells in the early stages of healing. These undifferentiated cells in the later stages of healing differentiate into osteoblasts and cementoblasts which increase periodontal regeneration [Murakami et al., 2003]. A schematic description of FGF effect on PDL cells is shown in Figure 1.19.

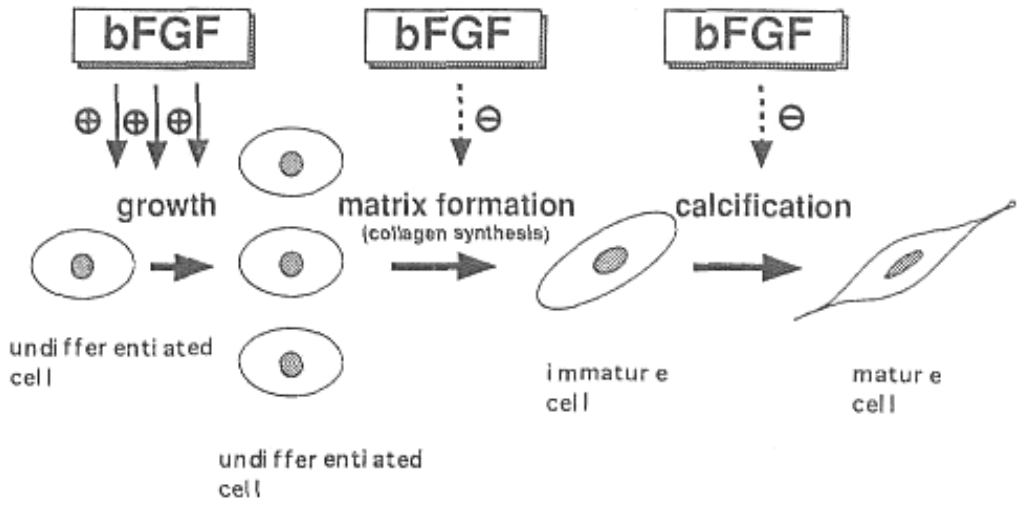

Figure 1.19: A schematic description of FGF effect on PDL cells. FGF has the positive effect on the mitosis of multipotent immature cells, whereas it downregulates the collagen synthesis and formation of calcified nodules by PDL cells [adapted from Takayama et al., 1997]

The proliferation effect of FGF on PDL proliferation is dose dependent and it decreases if the dose increases above an optimal level [Takayama et al., 1997].

1.5.5.5 Insulin like growth factors (IGFs)

IGFs are nonglycosylated polypeptides with a molecular weight of approx 7,500 Da. Their synthesis takes place in liver, smooth muscle, placenta and osteoblasts [Caffesse and Quinones, 1993].

In vivo studies have shown that application of IGF enclosed in dextran-co-gelatin hydrogel microspheres to denuded root surface in beagle dogs enhanced the regeneration of bone and cementum [Chen et al., 2006]. IGF application showed increased osteoblastic collagen synthesis and bone-matrix apposition and increased the regeneration of bone in an *in vitro* study [Hock et al., 1988]. In an animal study 100 µg IGF was delivered entrapped in biodegradable poly (lactide-co-glycolide) microspheres at 8-10mm defects in ovine long bones. The results showed that IGF application not only induced new bone formation but also reduced bone resorption and inflammation at the bone injury site [Meinel et al., 2003]. IGFs have also shown to increase the adhesion and proliferation of PDL cells in an *in vitro* study [Sant'Ana et al., 2007b]

1.6 BIODEGRADABLE POLYMERS AND CERAMICS

Biodegradable polymers are suitable for use in situations where an implant is only required to stay in the body for a limited period of time. They are currently used in sutures, drug delivery systems, fracture fixation devices and as scaffolds. Poly-ε-caprolactone (PCL), polyglycolic acid (PGA) and polylactic acid (PLA) are synthetic biodegradable polymers and belong to the family of aliphatic polyesters.

PCL is a semicrystalline polymer with a melting temperature between 59 to 64°C and glass transition temperature of -60°C. It has a slow degradation rate which makes it suitable for use in the long term drug delivery system. Many studies have reported use of PCL as a drug delivery system including antibiotics and antihypertensive drugs. Its degradation rate and mechanical properties can be tailored by copolymerizing it with PLA or PGA or blending it with ceramics. It has also been investigated as a scaffold material for bone [Marra et al., 1999; Wan-Ju et al., 2003; Sinha et al., 2004].

PGA is synthesised by ring opening polymerisation of cyclic dimer of glycolic acid. PGA has a melting point between 224 and 228°C and a glass transition temperature of 36°C. In the body PGA is degraded by a hydrolytic process and the degradation products are metabolized by the citric acid cycle which are subsequently eliminated out of the body in the form of carbon dioxide and water. It is mainly used as a suture material, however its is being expanded by using it as a copolymer with PLA [Athanasiou et al., 1996a; Liu et al., 2005].

PLA is synthesised by ring opening polymerisation of a cyclic dimer of lactic acid and is considered to be one of the most promising biodegradable polymers due to its processibility and ability to have tailored physical and biological properties and has been used in many biomedical applications [Rokkanen et al., 2000a; Lu et al., 2002; Georgiou et al., 2007; Gupta et al., 2007]. PLA is discussed in detail in section 1.6.1.

Drawbacks associated with biodegradable polymers such as low mechanical properties, low bioactivity and unpredictable degradation pattern can be improved by combining them with calcium phosphates and using them as a

composite material [Huang et al., 2008]. In bone contacting applications calcium phosphate are commonly used as coatings and composite fillers and are mainly hydroxyapatite ($Ca_{10}(PO_4)_6(OH)_2$) and tricalcium phosphate ($Ca_3(PO_4)_2$). Calcium phosphates are discussed in detail in section 1.6.2.

PLA is being used as sutures, scaffolds, fracture fixation devices, bone regeneration and in drug delivery systems due to its favourable properties. In the following section PLA is discussed in detail as it was selected for the production of polymer- Ca P composites due to its manipulable properties.

1.6.1 Polylactic acid (PLA)

Polylactic acid (PLA) is a degradable polymer which has been used in many biomedical applications and is still a subject of extensive research to expand its use due to its favourable properties. It belongs to the aliphatic polyesters family and is prepared by ring-opening polymerisation of the cyclic dimer of lactic acid ($HOCHCH_3COOH$) [Conn et al., 1995]. The chemical structure of PLA is shown in Figure 1.20.

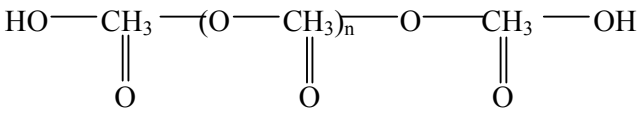

Figure 1.20: Chemical structure of PLA, where (n) denotes the central repeat unit [modified from Conn et al., 1995; Garlotta, 2001].

Lactic acid is converted into high molecular weight PLA by two methods. A solvent free route in which condensation of lactic acid produces a low molecular weight PLA, this is followed by controlled depolymerisation of this low molecular weight PLA which produces a cyclic dimer known as lactide. Lactide is purified by distillation. High molecular weight PLA is then produced by catalytic ring opening polymerisation. The second route is a solvent based azeotropic condensation in which lactic acid undergoes reduced pressure distillation for 2 to 3 hours at 130°C which removes most of the condensation water. Catalyst and diphenyl ether are then added and after passing through a molecular sieves the solvent is again kept at 130 °C for further 30 to 40 hours. This process also produces high molecular weight PLA Lunt, 1998; Garlotta, 2001]. A schematic description of these two processes is shown in Figure 1.21.

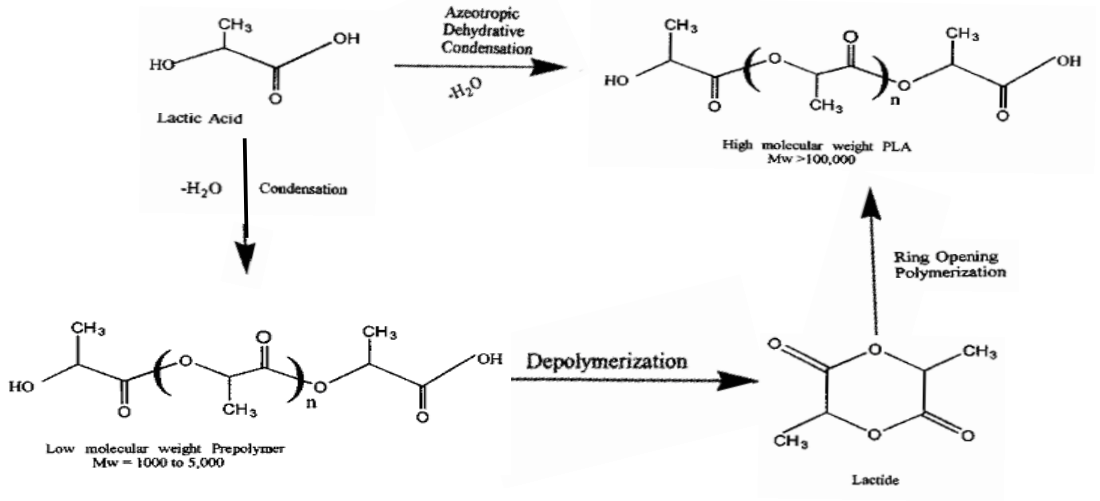

Figure 1.21: Schematic description of PLA synthesis [modified from Garlotta, 2001]

Lactic acid is a chiral molecule and exists in two stereoisomeric forms, L and D enantiomers (Figure 1.22) [Garlotta, 2001]. Mechanical properties, crystallinity and degradation of PLA depend and can be controlled by the ratio and type of the enantiomers used. L enantiomer provides PLA with higher mechanical strength and adding D enantiomers to PLLA reduces its melting temperature and crystallinity [Gupta et al., 2007].

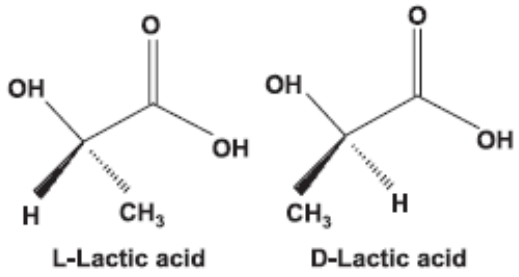

Figure 1.22: Structure of L and D enantiomers of PLA [adapted from Gupta et al., 2007]

A more amorphous material is generally obtained when the D content is above 20 %, whereas a highly crystalline material can be produced by keeping the D content below 2 % [Gupta et al., 2007]. Depending on the ratio of L to D a polymer with a molecular weight of thousands to millions can be produced. The

ratio and distribution of enantiomers play an important role in defining the thermal, mechanical and biological properties of PLA [Mehta et al., 2005].

Four different morphological types of polymers with different properties can be prepared depending on the enantiomers;

- *PDLA:* Semicrystalline and has good mechanical strength compared to PDLLA.
- *PLLA:* It is semicrystalline and has high mechanical strength, used for applications needing mechanical strength like sutures and fracture fixation. It has a melting point temperature of 170- 180 °C and a glass transition temperature of 57-67 °C.
- *PDLLA:* It is amorphous and racemix, used for applications such as drug delivery. Its properties depend on its L: D ratio. It is more susceptible to hydrolysis than to PLLA.
- *meso-PLA*: Obtained from L and D lactides, this type of PLA is rarely used.

A comparison of mechanical properties of PLAs containing different enantiomers is shown in Table 1.3.

Table 1.3: Effect of different enantiomers on the mechanical properties of poly lactic acid [modified from Garlotta, 2001].

	PLLA	PDLLA
Tensile strength (MPa)	59	44
Elongation at break (%)	7.0	5.4
Modulus of elasticity (MPa)	3750	3900
Yield strength (MPa)	70	53
Flexural strength (MPa)	106	88
Unnotched Izod impact (J/m)	195	150
Notched Izod impact (J/m)	26	18
Rockwell hardness	88	76
Heat deflection temperature (°C)	55	50
Vicat penetration (°C)	59	52

Degradation of PLA occurs by hydrolysis in which PLA is converted into lactic acid which is a metabolite present in the body. The degradation products are then eliminated out of the body after being converted into carbon dioxide and water. The mechanism of degradation involves hydrolytic cleavage of ester bonds on penetration of water inside the polymer, a new carboxyl end group is formed from the cleavage of each ester bond which in turn starts the process of autocatalysation [Zhang et al., 2005]. This autocatalysis speeds up the process of hydrolysis of the remaining ester bonds. In the beginning the degradation of PLA is a bulk degradation process and is homogeneous, however as oligomers are produced later in the process the pattern of degradation changes. The oligomers and carboxyl end groups produced inside the matrix cause an increase in acidity which in turn speeds up the degradation of the internal matrix, whereas the oligomers and carboxyl groups present close to the surface escape and become neutralised. Thus the outer surface does not degrade at the same rate as the internal matrix [Li, 1999]. PLA becomes more hydrophilic as the degradation proceeds which enhances water uptake and further accelerating degradation. Degradation of PLA depends on a number of factors such as its chemical composition, molecular weight, molecular weight distribution, processing condition, shape and implantation site and ranges from six months to two years. Degradation processes include reduction in the mass, molecular weight, configuration changes and reduction in the mechanical properties of an implant [Vert et al., 1992; Athanasiou et al., 1996b]. The ratio of L and D enantiomers plays an important role in determining the rate of degradation, the degradation rate of polymer is proportional to the D content. The degradation of high molecular weight polymers will be slower than that of polymers with low molecular weight [Li, 1999]. Glass transitional temperature (T_g) and melting temperature (T_m) both are directly proportional to the molecular weight, materials with high molecular weight have high T_g and T_m [Gupta et al., 2007]. The crystallinity and T_g of PLA also affect the degradation rate. PLA with high crystallinity has tightly packed and ordered polymer chains which make it more resistant to degradation and a polymer with a high T_g is more resistant to the penetration of water molecules which also makes it more resistant to degradation. In addition local pH, device morphology and size also affect the rate of PLA degradation [Place et al., 2009]. Factors which can play a role in the degradation of the biodegradable polymers are summarized in Table 1.4.

Table 1.4: Factors affecting the degradation of biodegradable polymers [from Vert et al., 1992].

- Structure of polymer
- Composition of polymer
- Ionic group presence
- Configurational structure
- Molecular weight and its distribution
- Presence of low molecular weight compounds like monomer, oligomers, solvents, initiators, drugs, etc
- Processing conditions
- Shape
- Sterilizing process
- Amorphous or semicrystalline
- Storage history
- Implantation site
- Adsorbed and absorbed compounds (water, lipids, ions, etc.)
- Shape and size
- Hydrolysis mechanism (enzymatic or hydrolytic)

1.6.1.1 Bone contacting applications of PLA

PLA is used in number of biomedical applications, however there are two major clinical areas where it comes in contact with bone. These two areas are orthopaedics and dentistry where PLA is used as fracture fixation devices and as membranes for GTR respectively.

The use of biodegradable PLA internal fixations devices such as pins, screws, plates etc (Figure 1.23) instead of metallic osteofixation devices not only eliminates the need of second removal surgery, but can also avoid the long term complications associated with metallic implants such as irritation and damage of soft tissue and disturbance of joint movement [Waris et al., 2004]. The use of biodegradable polymers in orthopaedics is also favourable as it eliminates the problems of stress shielding associated with metal implants. Studies have shown that the stress shielding effect associated with metallic implants results in a

weak, thin bone and an increase risk of fracture in mandible. Bone resorption is also reported in the cases of condylar fractures treated with metallic implants [Kennady et al., 1989; Iizuka et al., 1991].

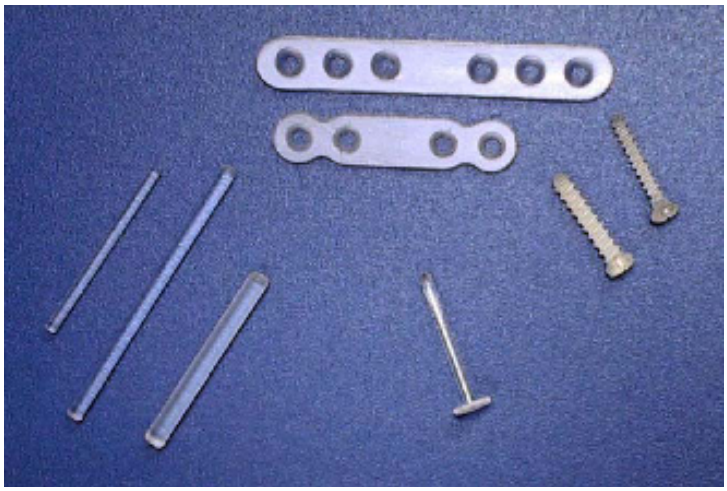

Figure 1.23: Pins, rods , screws and plates made of SR-PLLA [from Waris et al., 2004].

In the early 1970s, Kulkarni et al. [1971] successfully used polylactic acid pins for the treatment of mandibular fractures in dogs and 2mm thick polylactic acid films for the treatment of orbital floor fractures in monkeys. The results showed that the pins were completely degraded by 8 months and the healing was comparable to the controls where stainless steel pins were used. In an *in vivo* study PLLA pins implanted in the femur of the rats were shown to have osteostimulatory effect around their borders and did not produce a noticeable inflammatory response [Nordstrom et al., 1998].

In a clinical study self reinforced poly-L-lactide (SR-PLLA) screws were used for the fixation of subtalar extraarticular arthrodesis in children and the results showed that the cases treated with SR-PLLA screws had good fusion without any adverse response and that the screws maintained their strength for an adequate period [Partio et al., 1992]. Pihlajamaki et al. [1997] treated patients with displaced malleolar fractures by internal fixation using absorbable PLLA plugs and used magnetic resonance imaging (MRI) for postoperative assessment. The study showed that PLLA implants were visible in MRI and the implants did not produce any adverse response.

The use of biodegradable devices in craniofacial surgery was of great interest in the 1990s and extensive research is still being done to optimise the properties of such devices and maximise their use in order to avoid the risks and problems associated with metallic implants, especially in paediatric craniofacial surgery [Ashammakhi et al., 2001]. Moe et al. [2001] reported a study in which PLA implants were used for facial cosmetic and head and neck reconstructive surgery. PLA implants produced comparable results to metal implants with the advantages of ease of contouring the implants, less operative time and soft tissue reaction. In a clinical study a copolymer made of 82% L-lactide acid and 18% glycolic acid was used for the treatment of zygomatic fracture in 65 patients. The results showed good results for fracture fixation and there were no long term side effects associated with the degradation process of the polymers [Enislidis et al., 2005]. In another clinical study 80 patients with maxillary and mandibular fracture and reconstruction cases were treated with poly (L-lactide-co-glycolide) (PLGA) copolymer or poly (L-lactide- co-DL-lactide) implants. Only 6 % of the patients showed foreign body reactions, which was successfully controlled by conservative treatment and local curettage. All the devices were degraded within 24 months of implantation [Landes et al., 2006].

Another clinical area where, although poly-L-lactic acid (PLLA) does not come in direct contact with the bone, is its use for the treatment of facial asymmetry. When implanted in soft tissue PLA causes a foreign body reaction which results in fibrosis and collagen formation. This effect of PLLA is utilized for the treatment of facial asymmetry. In different studies the treatment has produced long lasting changes in dermal thickness which resulted in improved facial symmetry and appearance in patients. The treatment was well tolerated and the only adverse effect reported were non-bothersome subcutaneous papules [Barton et al., 2006; Burgess, 2008].

PLA or copolymers of PLA and PGA have been used and are commercially available as periodontal tissue regeneration membranes with varying success. In a clinical study 11 patients were treated with PLA membranes (Atrisorb® Free Flow™) in combination with bovine bone mineral (BBM) for intrabony defects. The results showed that the use of PLA-BBM produced a reduction of probing depth of 4.72 mm and a gain clinical attachment level of 3.71 mm in the patients which was better than in the patients which were treated with access

flap procedures which showed a reduction of 2.50 mm in the probing depth and a clinical attachment level gain of 2.43 mm [Ioannis et al., 2004].

In another clinical study, patients with Class II furcation defects in lower molars were treated with a polylactic acid membrane (Atrisorb). The results at the end of six weeks did not show significant difference in relative vertical clinical attachment level and relative horizontal clinical attachment level among the patients treated with Atrisorb or open flap debridement (control). However significant difference was found among the patients in probing depth reduction [Bremm et al., 2004].

Park et al. [1997] produced PLA membranes for guided tissue regeneration with the ability of controlled drug delivery and tested it *in vitro*. Lee et al. [2001b] reported the fabrication of PDGF loaded PLA-TCP membrane for GTR and have shown that these PLA-TCP membranes loaded with PDGF produced more bone formation when tested in rabbits.

With the advantages of PLA there are also some drawbacks which are associated with PLA, the most important being mechanical weakness and aseptic swellings due to accumulation of their acidic degradation products. However, this was mainly seen with the early implants where the method of manufacture leads to a high molecular weight outer layer which degraded more slowly than the core. After about two years the outer layer degraded enough to release the acidic central core degradation products producing a sudden release and consequently "sterile sinus" or inflammatory response. Other potential hazards, although not very common, associated with the use of biodegradable implants are toxicity, mutagenicity and infection [Bostman and Pihlajamaki, 2000].

The formation of sterile sinuses is more likely with crystalline poly (L-lactide) than amorphous poly (D-lactide) due to the formation of highly crystalline debris, however fast degradation rate of amorphous (D-lactide) can also be a cause of swelling as the low pH produced can cause inflammatory tissue reactions. Clinical use of amorphous polylactides can be more favourable than crystalline polylactides where mechanical strength is not a requirement [Tegnander et al., 1994; Ignatius et al., 2001; Ishii et al., 2003; Maquet et al., 2003]. In a clinical study by Bergsma et al. [1995], zygomatic bone fractures

were treated with high molecular weight poly lactic acid (PLLA) bone plates and screws. After three years of implantation swelling was reported at the implantation site which may be due to accumulation of degradation product and increase in osmotic pressure due to the degradation fragments. In *vitro* studies showed that amorphous PDLLA does not produce crystalline remnants on degradation [Heidemann et al., 2001].

A survey showed that only 1 out of 491 patients (0.2 %) treated with polylactic acid implants showed foreign body reaction and in other studies the reaction to poly lactic acid implants was also found to be lower than to polyglycolic acid implants [Bostman and Pihlajamaki, 2000]. No adverse response was observed in many clinical studies where polylactic acid implants were used [Partio et al., 1992; Pihlajamaki et al., 1997].

Optimised combinations of mechanical properties and degradation rates can be achieved by using appropriate ratios of D and L enantiomer, implant size, use of polymer as composite with ceramics or self reinforcement. The addition of ceramics such as HA and TCP can enhance the bioactivity and can improve the biological properties and mechanical properties of PLA [Rokkanen et al., 2000b; Kim et al., 2006; Jeong et al., 2008].

1.6.2 Bioactive calcium phosphate ceramics

Calcium phosphates (Ca P) have been used extensively in the field of biomaterials. Calcium phosphates of various kinds having different Ca/P ratio ranging from 0.5 to 2.0 can be synthesized by mixing calcium and phosphate solutions. However, the two calcium phosphates of major interest and which are widely used in biomaterials are HA and TCP. HA has a Ca/P ratio of 1.67 and its chemical formula is $Ca_{10}(PO_4)_6(OH)_2$. The Ca/P ratio of TCP is 1.50 and its chemical formula is $Ca_3(PO_4)_2$.

HA is a major component of bones and teeth and is one of the most important and widely used ceramic in biomaterials and tissue engineering due to its chemical and physical similarity to natural bone [Rossa, 1991; Kurashina et al., 1995]. In bones HA is present in the form of nanocrystals having dimensions of the order of 4 X 20 X 50 nm. Synthetic and natural HA are not identical but have

chemical and crystallographical similarities [Damien and Parsons, 1991]. Ca/P ratio of natural HA is less than the 1.67 Ca/P ratio of synthetic HA. HA present in the bones is not stoichiometric whereas synthetic HA is mostly stoichiometric [LeGeros et al., 1988; Murugan and Ramakrishna, 2005]. HA and TCP are considered bioactive, osteoconductive and non-immunogenic which makes them a material of choice for biomaterial applications [Frame, 1987; Damien and Parsons, 1991; Murugan and Ramakrishna, 2005]. General physiochemical, biological and mechanical properties of synthetic HA and TCP are listed in Table 1.5.

Table 1.5: General properties of HA [from Kitsugi et al., 1987; LeGeros, 1993; Larry, 1998; Murugan and Ramakrishna, 2005]

	HA	TCP
Chemical composition	$Ca_{10}(PO_4)_6(OH)_2$	$Ca_3(PO_4)_2$
Ca/P molar ratio	1.67	1.50
Crystal system	Hexagonal	
Young_s modulus (GPa)	80–110	
Compressive strength (MPa)	400–900	
Bending strength (MPa)	115–200	
Density (Mgm^{-3})	3.16	3.07
Fracture toughness (MPa $m^{1/2}$)	0.7–1.2	
Hardness (HV)	600	
Decomposition temperature (°C)	>1000	
Melting point (°C)	1614	
Thermal conductivity (Wcm^{-1} K^{-1})	0.013	
Biocompatibility	High	
Bioactivity	High	High
Biodegradation	Low	High
Cellular-compatibility	High	
Osteoinduction	Nil	Nil
Osteoconduction	High	High

Ceramics like HA and TCP degrade to varying degrees, the degradation tendency of HA and TCP depends on various factors which include synthesis method, crystallographic structure, particle size and site of implantation [Frame, 1987]. Biodegradation or bioresorbtion of ceramics is characterized by mechanical

strength loss, porosity changes, dissolution, formation of other CaP phases and transformation of these phases on the surface of the ceramic [LeGeros et al., 1988]. It is assumed that there are two mechanisms of ceramic bioresorption: the first mechanism involves dissolution of the ceramic implant by physiological solutions and second mechanism involves cell mediated processes such as phagocytosis, which result in the reduction of pH which increases the dissolution of the ceramic. In addition to these two mechanism physical abrasion, fracture and disintegration also contribute to the ceramic resorbtion [Jarcho, 1981; LeGeros et al., 1988]. Resorption of HA and TCP is affected by the site of implantation. The close proximity of implants to the cell systems, particularly osteoblasts and osteoclasts, plays an important role in the degradation of the implant. Studies have shown that the HA implanted in bone resorbs faster than implants implanted subcutaneously [Dubok, 2000]. Porosity of HA also play an important role in the degradation, more porous implants have higher degradation rate [Klein et al., 1983]. Factors which affect the biodegradation of HA and TCP are [LeGeros et al., 1988]:

- Porosity
- Crystal size
- Crystal imperfections
- Grain size
- pH level at the implantation site
- Implantation site
- Degree of bone contact

The size and shape of bioceramic particles is important for their application. Small particles and more uniform shape adjust better in a defect area than the particles with irregular shapes which also create large voids. HA with small particles have higher strength and lower porosity, as they have more contact points than larger particles [Ginebra et al., 2004]. Particles with nanosize and nanostructure provide a large surface area for adhesion which increases the interaction of particles with the surrounding environment [Ginebra et al., 2004]. Compared to micro HA, nano-HA promotes increased osteoblast adhesion, enhanced cell differentiation, proliferation and deposition of calcium containing

minerals by osteoblasts which can result in increased formation of new bone tissue [Webster et al., 2000].

1.6.2.1 Synthesis of Hydroxyapatite (HA)

HA powders having different morphology, stoichiometry and level of crystallinity can be produced by using different preparation techniques [Suchanek et al., 2002]. It is important to produce HA with controlled stoichiometry, crystal size, shape and agglomeration characteristics. All these factors play an important role in determining dissolution, bioactivity and mechanical properties of HA [Mostafa, 2005]. The different methods employed for the preparation of HA include a dry method, a wet-chemical method, a mechano-chemical hydrothermal method, a mechano-chemical method, spray pyrolysis, emulsion processing and microwave assisted synthesis [Feng et al., 2005; Murugan and Ramakrishna, 2005]. Some of the commonly used methods are described below:

- ***Wet-Chemical Method***

  - ***Precipitation***

Precipitation is the common method for the synthesis of HA. It involves a wet chemical reaction between calcium and phosphate precursors under controlled pH and temperature. Nano size crystals having shapes of plates, needles and rods can be prepared, crystallinity and Ca/P of the particles depend on the preparation conditions and are mostly lower than from well-crystallised stoichiometric HA [Suchanek et al., 2002]. This process involves a reaction between ammonium phosphate and calcium nitrate at 60°C and pH is maintained between 9 and 10 [Bezzi et al., 2003]. The precipitate after aging and drying is calcined at 400 °C to 600 °C and then sintered between 1000 °C and 1200 °C. This process however has some disadvantages such as it is important to maintain the pH value above 9, as reduction in the pH below 9 leads to formation of Ca deficient HA and the subsequent formation of tricalcium phosphate due to the decomposition of hydroxyapatite as a result of sintering at high temperature [Jillavenkatesa and Condrate, 1998].

- ***Sol-gel***

Highly pure HA powder can be produced by sol-gel method as it provides strict control on the process parameters. This process does not require maintenance of high pH values and high sintering temperatures unlike the precipitation technique [Feng et al., 2005]. Improved chemical homogeneity can be achieved by molecular mixing of calcium and phosphorous. High reactivity of the sol-gel powder results in the reduction of the processing temperature and degradation during sintering [Bezzi et al., 2003]. However possible hydrolysis of phosphates and expensive raw materials are two of drawbacks of this technique [Livage et al., 1992]. A variant of the sol gel method was developed by Deptula et al. [1992] in which repetitive emulsification of calcium acetate and phosphoric acid mixture followed by solidification by water extraction produces hydroxyapatite spheres. Calcination of these spheres produces HA particles.

Jillavenkatesa and Condrate [1998] also synthesized HA by the sol-gel method using relatively inexpensive calcium acetate and triethyl phosphate as precursors. This process also overcomes the difficulties associated with the slow hydrolysis of phosphate as the gel formed during the process is colloidal.

Feng et al. [2005] reported a simple sol gel method which eliminates the requirements of controlling pH value, vigorous stirring and long time for phosphate hydrolysis associated with conventional sol gel method. In the process the sintering temperature and aging time determine the crystallinity and morphology of the resulting HA powder. A flow chart of their process which produced 10-15 nm diameters HA powder is shown in Figure 1.24.

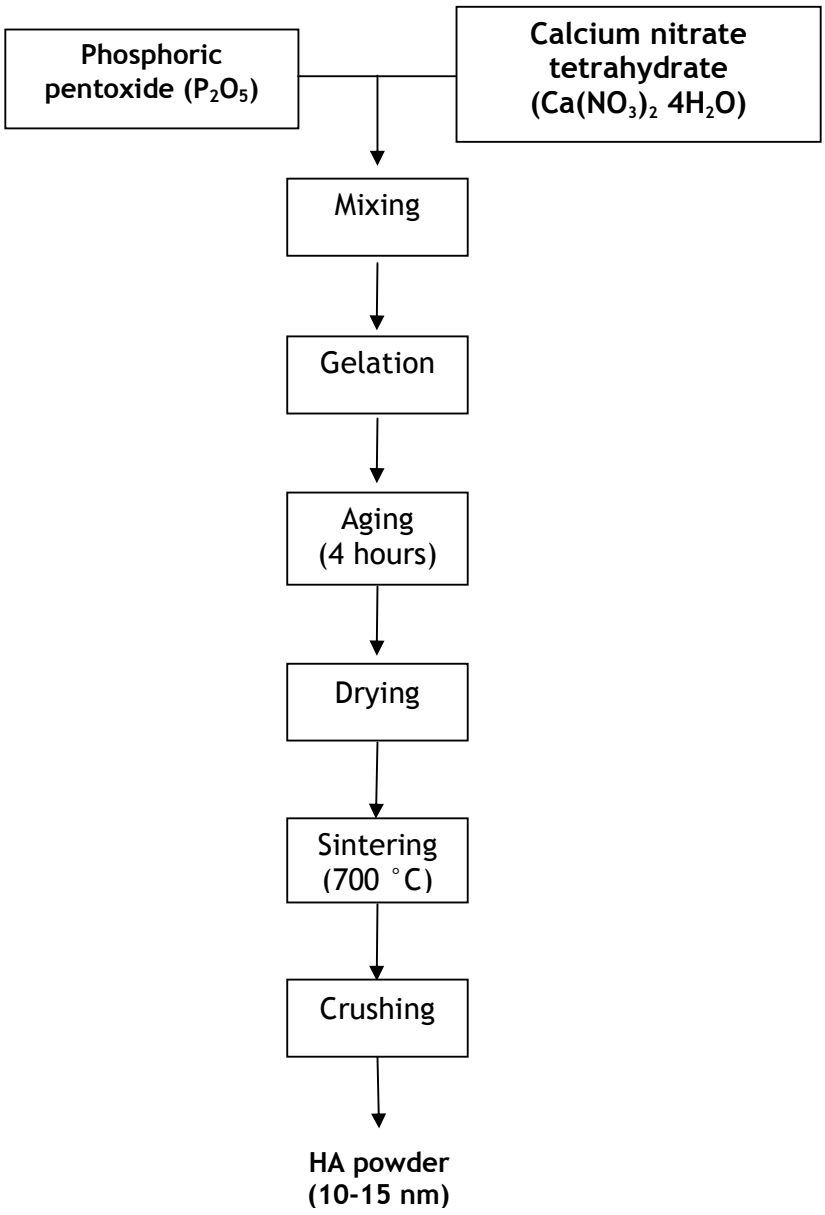

Figure 1.24: Synthesis of HA by a sol gel method reported by Feng et al. [2005]

- ***Hydrothermal***

Highly crystalline and pure HA can be obtained from this process. This process involves application of high temperatures to aqueous solutions which facilitate the precipitation of crystals of larger dimensions than obtained from ordinary wet methods. Crystals size in the range of nanometers to millimeters can be obtained [Narasaraju and Phebe, 1996].

- ***Hydrolysis***

Micron size HA particles of needle or blade shape can be obtained by hydrolysis of tricalcium phosphate, monetite, brushite and octacalcium phosphate at low temperature. However the calcium phosphate produced by this process is mostly nonstoichiometric HA [Suchanek et al., 2002].

- ***Mechanochemical Metho*d**

Mechanochemical synthesis describes a solid state method in which thermodynamic and kinetic reaction between solids is enhanced by pressure applied perturbation of surface bonded species [Suchanek et al., 2002]. This method of ceramic powder synthesis can be used in the industrial production of HA due to its simplicity and low cost. The mechanochemical method is different from mechanochemical hydrothermal method as it only involves solid-state reaction whereas the latter process also involves an aqueous phase. Simple equipment such as ball mills and vibratory mills are used for mechanochemical synthesis. In mechanochemical synthesis the overall temperature stays close to room temperature whereas local zones of high pressures and temperatures (up to 450-700°C) are produced due to friction of slurries and adiabatic heating of gas bubbles [Suchanek et al., 2002].

- ***Mechanochemical Hydrothermal Method***

The mechanochemical hydrothermal method is at the intersection of hydrothermal and mechanochemical processes. It incorporates an aqueous phase which accelerates the kinetic processes. The water participates actively in the processes by dissolving the reactant powders and serving as a reaction medium which produces highly crystalline and stoichiometric powder [Shuk et al., 2001]. Like the mechanochemical method this process can also be used to produce large quantities of HA as it requires simple equipment and is processed at room temperature, unlike hydrothermal method which requires high temperature. HA produced by mechanochemical hydrothermal method has better densification, uniform microstructure and mechanical properties as compared to HA produced by wet chemical precipitation method [Mostafa, 2005].

- ***Solid-state reaction***

Stoichiometric and well crystallized HA can be produced by solid-state reactions, however these reactions involve high temperatures and long duration of heat treatment [Lin et al., 2007].

- ***Emulsion Processing***

Well crystallized and pure nano HA can be synthesized by this process, the morphology and size of the particles strongly depends on the reaction temperature [Furuzono et al., 2001]. Water in oil emulsion method can be used to prevent the flocculation of HA particles during the synthesis as small micro or nano sized water spheres act like miniature reactors which prevent particle flocculation and limit particles growth [Phillips et al., 2003].

- ***Microwave Irradiation***

Microwave irradiation has been developed to eliminate the long sintering, time-consuming and tedious processes associated with synthesis of HA. It involves performing the precipitation method of producing HA but microwave energy is applied to accelerate the synthesis. This process has been shown to enhance the production of seed crystals of hydroxyapatite [Lerner et al., 1991]. Using microwave technique it is possible to obtain HA much faster than conventional methods [Teoreanu et al., 2008; Arami et al., 2009]. Siddharthan et al. [2004] successfully synthesized nanosized calcium deficient HA rapidly by microwave irradiation whilst reacting calcium nitrate hydrate and phosphoric acid. In another study HA nano-rods having a diameter from 60 to 80 nm and lengths of about 400 nm were prepared by a one-step microwave-assisted solid-state reaction at room temperature in much less time than using conventional heating [Cao et al., 2005].

1.6.2.2 Biomedical applications of HA

Owing to its biocompatibility, osteoconductivity and bioactivity HA is used in a wide of range of biomedical applications [Dubok, 2000]. Biomedical applications of HA include repair of alveolar bones through to long bones defects and fractures, middle ear prostheses, eye implants, spinal fusion, vertebral fusions, cranioplasty, craniofacial repairs, in dental restorative materials, drug and growth factor delivery [Damien and Parsons, 1991; Paul and Sharma, 2003; Murugan and Ramakrishna, 2005]. Particle size plays a key role in modifying the properties of HA. It is a useful parameter in order to adjust the behavior of the material to the specific clinical applications. The bioactivity of nanosize HA is higher than coarser crystals and it provides a formulation with improved osseointegration for use in orthopedic and dental implants [Han et al., 2004].

The first use of synthetic HA for treatment of bone defects was reported by Ray and Ward [1951] when they successfully synthesed and implanted HA in the short bones of cats and monkeys and long bones in dogs with positive outcomes. HA does not have the capacity to induce bone, however it is osteoconductive and provides a physical matrix which is suitable for deposition of new bone and allows bone growth. It is believed that the new bone formed bonds directly onto the implanted HA without any intermediate fibrous layer, this property is particularly important when used as bone graft substitute [Frame, 1987; Damien and Parsons, 1991]. Implantation of HA in the body is followed by an inflammatory process in which macrophages invade the implantation site and attack the surface of the HA in addition to clearing the area of dead cells and debris. This results in formation of a chemical apatite layer on the rough HA surfaces which is similar to biological apatite. Migrated osteoblasts then produce an osteoid layer in the surface of HA which is followed by mineralisation [Kitsugi et al., 1987].

Due to its high biocompatibility, sufficient mechanical strength and ease of use, HA is considered to be an ideal material for the augmentation of alveolar ridges [Dubok, 2000]. Treatment of alveolar bone defects such as defects created by periodontal diseases and surgical bone defects can be achieved by packing porous or dense hydroxyapatite granules in the defect area. For more than two decades HA has been successfully used for periodontal defect restoration and

correction of alveolar ridge defects. Figure 1.25 shows HA blocks and HA particles deposited by a syringe used for ridge augmentation. The use of HA eliminates the drawbacks associated with use of autologus and autogenous bone grafts for the treatment of these defects as discussed in section 1.4.3.1 [Rothstein et al., 1984].

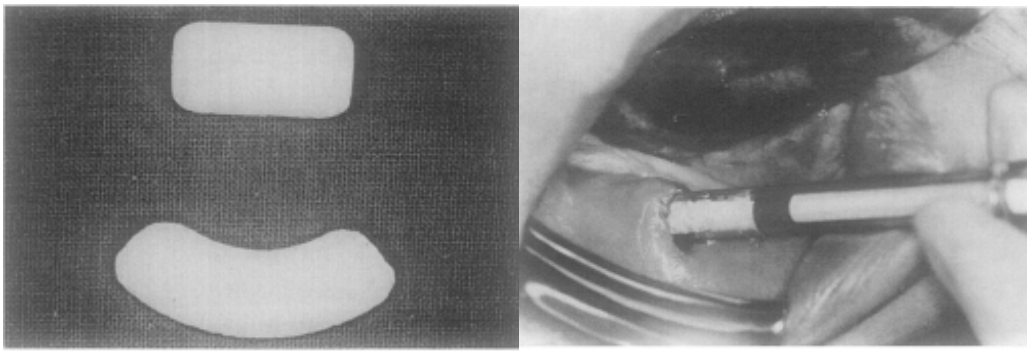

Figure 1.25: Hydroxyapatite blocks and particles deposited by syringe for alveolar ridge augmentation [adapted from Frame, 1987]

Kent et al. [1986] used HA and HA /autogenous bone grafts for alveolar ridge augmentations in more than 200 patients and followed the cases for five years. They found that all the cases either treated with HA alone or in combination with autogenous bone showed good alveolar ridge regeneration. In another study 110 patients with deficient alveolar ridges were treated with HA implants and followed for 33 months, all the cases showed improvement in the height, bulk, contour of the ridges without any major complications associated with the implants [Rothstein et al., 1984].

1.6.2.3 Use of hydroxyapatite for drug release

HA is considered to have the ability to act as a drug carrier and attempts have been made to exploit HA constructs for the delivery of growth factors and drugs [Paul and Sharma, 2003]. In an *in vitro* study enhanced proliferation and differentiation of human osteoblasts was observed when these were exposed to growth factors delivered by HA [Zambonin et al., 2000; Matsumoto et al., 2004b]. Ono et al. [1998] loaded porous HA rods (5 mm diameter, 10 mm length) with 1µg or 5µg rhBMP-2 and implanted them into the cranial bones of rabbits. They found that adding rhBMP-2 to the HA rods increased the bone formation.

The bone formation was higher with the higher dose of rhBMP-2. Adding rBMP-2 to HA rods also increased the strength of the rods in the initial stages of implantation. Porous blocks of HA have also been tested for sustained release of anticancer drugs in a rat model. The results showed a slow release profile of the drug sustained for 3 months which was more effective in inhibiting tumour growth than when administered intraperitoneally [Uchida et al., 1992]. Sustained and slow release of antibiotics from porous blocks of HA was evaluated by Shinto et al. [1992]. Gentamicin sulphate was placed in cylindrical cavity of HA blocks and implanted in rats. The release of gentamicin sulphate into the bone of rats was slow after maximum release within first week and sustained even at 12 weeks after implantation. In addition the antibacterial activity of the drug was not affected by the addition to HA.

1.6.3 Hydroxyapatite-polylactic acid composite

Drawbacks associated with degradable polymers such as low mechanical properties and unpredictable degradation pattern can be improved by combining them with other biomaterials and using them as a composite material [Huang et al., 2008]. The addition of stiff filler will increase the stiffness and may increase the strength of a polymer. In bone contacting applications calcium phosphates are commonly used. ß-tricalcium phosphate added to PLA was shown to slow the degradation rate of the polymer [Nazhat et al., 2001; Niemelä, 2005].

The use of ceramics such as HA in PLA, may confer a number of potential therapeutic advantages, including increasing mechanical properties, promoting cell attachment and osteoconduction, and the potential for use as a vehicle for slow delivery of bioactive proteins such as growth factors. HA may also provide mechanical reinforcement for the PLA, improving its stiffness and strength [Sui et al., 2007] which can enable it to maintain its shape during functional pressures *in situ*. Bleach et al. [2001] showed that adding HA increases the flexural modulus and yield strength of polymer composites. HA has regularly been proposed as a potential synthetic graft material with osteoconductive properties [Bonfield et al., 1981; Wang et al., 2003; Liao et al., 2005]. HA-containing composite membrane materials may increase osteoconductivity over PLA or other resorbable membrane materials as cell attachment to the mineral

will be dependent on protein absorption to the surface of the material. HA–PLA composite materials have been shown to be biocompatible, resorbable with good mechanical properties [Shikinami and Okuno, 1999]. HA-PLA composites have been proposed as a substitute for autologus bone powder [Ignjatovic et al., 2001].

In addition to other properties, HA also has the ability to both adsorb and release protein; protein adsorption increases with the increase in the surface area of HA [Matsumoto et al., 2004a; Nakamura et al., 2006]. A number of mineral-based carriers have been used experimentally for controlled release of growth factors in tissue regeneration experiments; for example collagen-hydroxyapatite microspheres have been successfully used as a carrier of bone morphogenic proteins (BMPs) for bone regeneration [Wang et al., 2003].

1.7 SUMMARY AND AIMS OF THESIS

Although GTR procedures are widely used for periodontal regeneration, their outcomes remain clinically modest on many occasions. There is thus the need to develop new ways of improving clinical outcomes. Currently used membranes for GTR are often limited by their relatively poor mechanical properties resulting in poor space maintenance during healing. In addition there is considerable research into the possible application of growth factors to wounds to improve the outcome of existing regenerative procedures.

One possible approach to address these issues is to consider using a resorbable composite material made from a PLA-HA composite. This material may be able to address issues of mechanical properties, whilst improving osteoconductivity and the possibility of using as an adjunctive delivery system for growth factors to promote regeneration further.

Thus the aims of these studies are to develop a degradable composite membrane for guided tissue regeneration and to investigate the physical, mechanical and biological properties of these membranes. Specific objective includes:

1). To develop a membrane with good mechanical properties which can maintain a space for periodontal regeneration without collapsing under occlusal pressure.

2). To investigate the possibility of incorporating growth factors in the membrane for their controlled release at the wound site to enhance tissue regeneration.

3). And to determine a membrane shape and size which can be can be used in most clinical situations/sites by analysing different bone resorption patterns.

CHAPTER 2: CHARACTERISATION OF CALCIUM PHOSPHATE POWDERS, POLYLACTIC ACID AND POLYLACTIC ACID-CALCIUM PHOSPHATE FILMS

2.1 INTRODUCTION

Calcium phosphates (Ca P) such as hydroxyapatite (HA) and tricalcium phosphate (TCP) have been extensively used as bone substitutes and in dental applications as their chemical composition closely resembles the mineral phase of bone and teeth [Soriano, 2000]. The drawbacks associated with Ca P such as brittleness, low impact resistance and low tensile strength limit their scope however these can be overcome by combining them with polymers such as PLA. The combination of Ca P and PLA enables easy fabrication of devices with good mechanical and biological properties [Sui et al., 2007; Jeong et al., 2008].

Polylactic acid (PLA) is a degradable polymer which has been used in many biomedical applications and is still a subject of extensive research to expand its use due to its biodegradability. With the advantages of PLA there are also some drawbacks, the most important being variable degradation rate in early devices and aseptic swellings due to accumulation and burst release of acidic degradation products.

The use of Ca P within PLA may confer a number of potential therapeutic advantages on this material, including increased mechanical properties, promotion of cell attachment and osteoconduction, and the potential for use as a vehicle for slow delivery of bioactive proteins such as growth factors. HA may also provide mechanical reinforcement for the PLA, thus improving its stiffness and strength. [Sui et al., 2007; Jeong et al., 2008]

In this study the fabrication of PLA-Ca P composite films and their characterisation is reported.

2.2 MATERIALS

2.2.1 Polylactic acid (PLA)

PLA with an L: DL ratio of 70/30 and an IV of ~ 3.0 dl/gr (MW 500,000-600,000) was obtained from PURAC Biochem, The Netherlands. It was supplied in the form of granules.

2.2.2 Nano-hydroxyapatite (nHA)

nHA with mean particle size less than 200nm was purchased from Sigma-Aldrich, UK.

2.2.3 Micro-hydroxyapatite

Two different types of micron size hydroxyapatite (HA) powders were used in the study. First, was spray dried HA (rHA) and the second was sintered HA (sHA), both having average particle size of 3.80 and 4.46 μm respectively, but with a factor of over 13 difference in the specific surface areas. Both the powders were purchased from Plasma Biotal Limited, UK. These two powders have been characterized previously by Zhang and Tanner [2008] and the particle size distribution and specific surface area are given in table 2.1.

Table 2.1: Physical properties of rHA and sHA [from Zhang and Tanner, 2008]

Powder	Particle size (μm) $d_{0.1}$	$d_{0.5}$	$d_{0.9}$	Specific surface Area ($m^2 g^{-1}$)
rHA	0.99	3.80	6.23	13.54
sHA	0.76	4.46	11.12	0.97

2.2.4 Beta tricalcium phosphate (ßTCP)

ßTCP was purchased from Plasma Biotal Limited, UK. The average particle size was 4μm.

2.3 METHODS

2.3.1 PLA and PLA-Ca P composite film fabrication

PLA and PLA-Ca P composite films were produced by a solvent casting method. To produce the PLA films 25 ml of chloroform was poured into spherical flasks and 0.5 g of PLA was added while stirring. The solution was then left on the stirrer for 24 hrs at room temperature. After 24 hrs of stirring the solution was spread in glass Petri dishes and then left overnight to allow slow evaporation of the chloroform. The same size of Petri dishes was used for all the films to get films of the same thickness.

For the production of PLA-Ca P composite films Ca P powders were added to the PLA solution dissolved in chloroform after 24 hrs of stirring in the required concentration to give 10, 40 and 70 weight % after the evaporation of the chloroform, while the same amount of PLA was used for each film. These weight contents are equivalent to 4.2, 20.9 and 48.0 volume % of HA using 1.250 Mgm^{-3} and 3.156 Mgm^{-3} for the densities of PLA and HA respectively and are equivalent to 4.3, 21.4 and 48.7 volume % of TCP using 3.07 Mgm^{-3} density for TCP. PLA-Ca P solutions were then stirred for a further 48 hrs. The solution was spread in 120mm glass Petri dishes which were covered to allow slow evaporation of chloroform. After evaporation of the chloroform, the films were peeled off the dishes and placed in a vacuum oven for one day. The films were then annealed by being pressed between the bases of two glass Petri dishes and were placed in the oven at 70 °C for one hour. The films were then allowed to cool gradually overnight. The heat treatment was done to relax any stresses produced in the films during the casting process and to prevent curling up of the films during the experiments.

2.3.2 Scanning Electron Microscopy (SEM)

The morphology and particle size of the Ca P powders and the morphology of the films were characterised by SEM (FEI Inspect F, EFI Company, The Netherlands) (Figure 2.1). For Ca P powders 20kV and for PLA and PLA-Ca P composite films 5kV were used. All the samples were gold coated.

Figure 2.1: Scanning Electron Microscope.

2.3.3 Transmission Electron Microscopy (TEM)

High Resolution TEM (JEOL JEM 2010) (Figure 2.2) operated at 200 keV was used to analyse the morphology and particle size of the Ca P powders. Powders were ultrasonically dispersed in methanol and then collected on copper grids coated with carbon (Holey Carbon Film, 300 mesh Cu, Agar Scientific) to be analysed by TEM.

Figure 2.2: Transmission Electron Microscope.

2.3.4 X- ray diffraction (XRD)

XRD is a non-destructive analytical technique which enables the analysis of chemical composition and crystallographic structure of a material.

Ca P powders were characterized using XRD, to find chemical composition, crystal state and the crystalline content. A Seimens/Bruker D5000 X-ray Diffractometer, with monochromatic Cu Ka radiation (k = 0.15418 nm) was used. Scans were obtained in the 2θ range = 20–60 and step size of 0.02° s^{-1}.

2.3.5 Fourier Transform Infra red spectroscopy (FTIR)

FTIR is an analytical technique which measures the infrared radiation absorption by a material versus wavelength, the molecular structure of the material is characterised by the wavelength of the light absorbed which causes vibration of the molecules. FTIR is also useful for the quantitative analysis as the band intensities which appear in the spectrum due to vibration of molecules of a material are directly proportional to the concentration of that molecule [Vlachos et al., 2006].

FTIR spectra of the Ca P powders and PLA and PLA-Ca P composite films were obtained by a Thermo-Electron Nicolet 8700 FTIR spectrometer. Dry helium gas was used to purge the sample chambers. The spectra were measured at 8cm^{-1} resolution and a total of 256 scans were obtained. A background spectrum of a carbon sample was obtained before obtaining sample spectra.

2.3.6 Raman Spectroscopy

Nicolet Almega XR dispersive Raman spectrometer was used to obtain Raman spectra of the Ca P powders and films, spectra were collected by taking 256 scans per sample and an exposure time of 2 sec was used at 8 cm^{-1} resolution. The spectra were collected between 4000-100cm^{-1}. A background spectrum was obtained before obtaining sample spectra.

2.4 RESULTS

2.4.1 Calcium phosphate powders

2.4.1.1 SEM and TEM

nHA powder

The morphology and size of nHA particles are shown in SEM and TEM images in Figure 2.3. The images show that the particles are spherical in shape with approximate size of 20-200 nm although agglomerated.

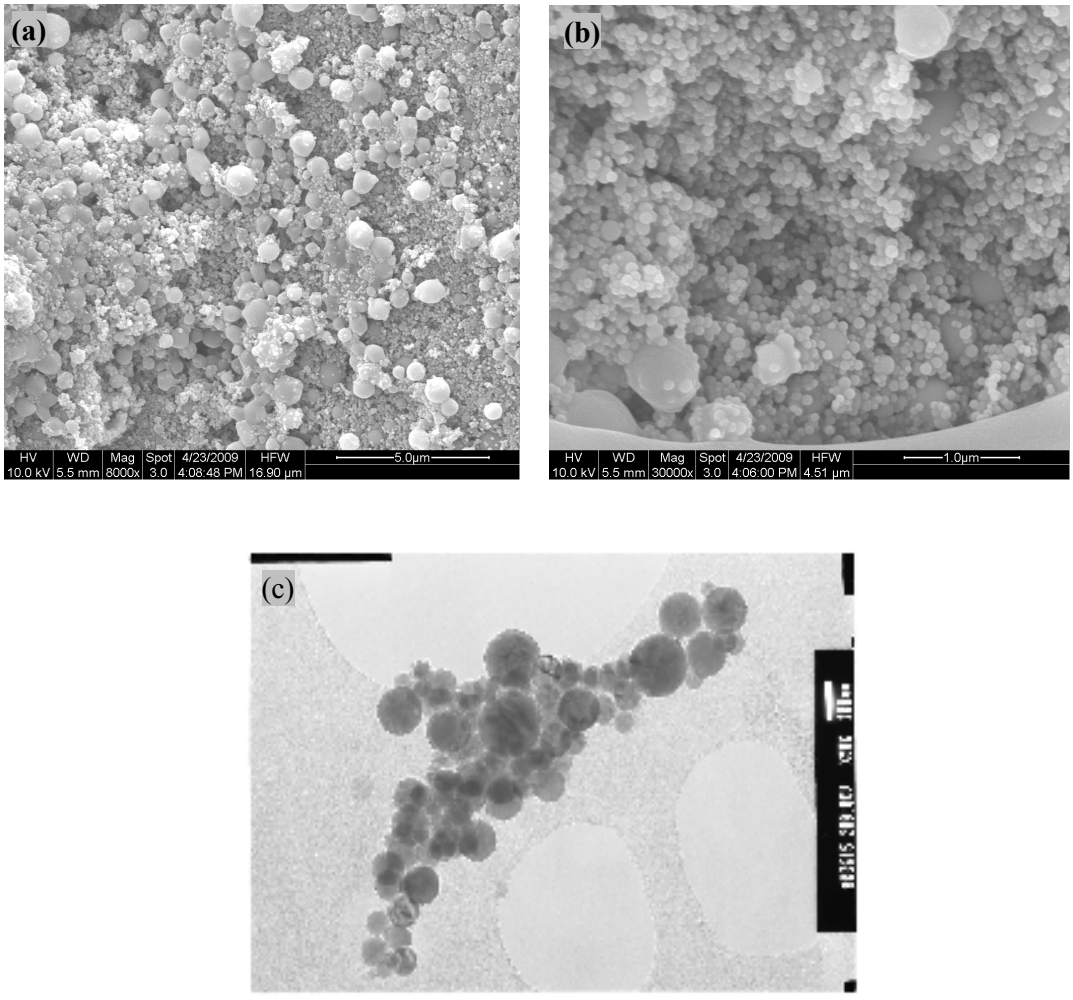

Figure 2.3: SEM images (a) lower magnification (scale bar= 5 µm) (b) higher magnification (scale bar= 1µm) and (c) TEM (scale bar= 100 nm) showing morphology and particle size of nHA.

sHA powder

The morphology and size of sHA particles are shown by SEM and TEM images in Figure 2.4. The images show that the particles have smooth surfaces and irregular shape with a mean particle size of approximately 4 µm.

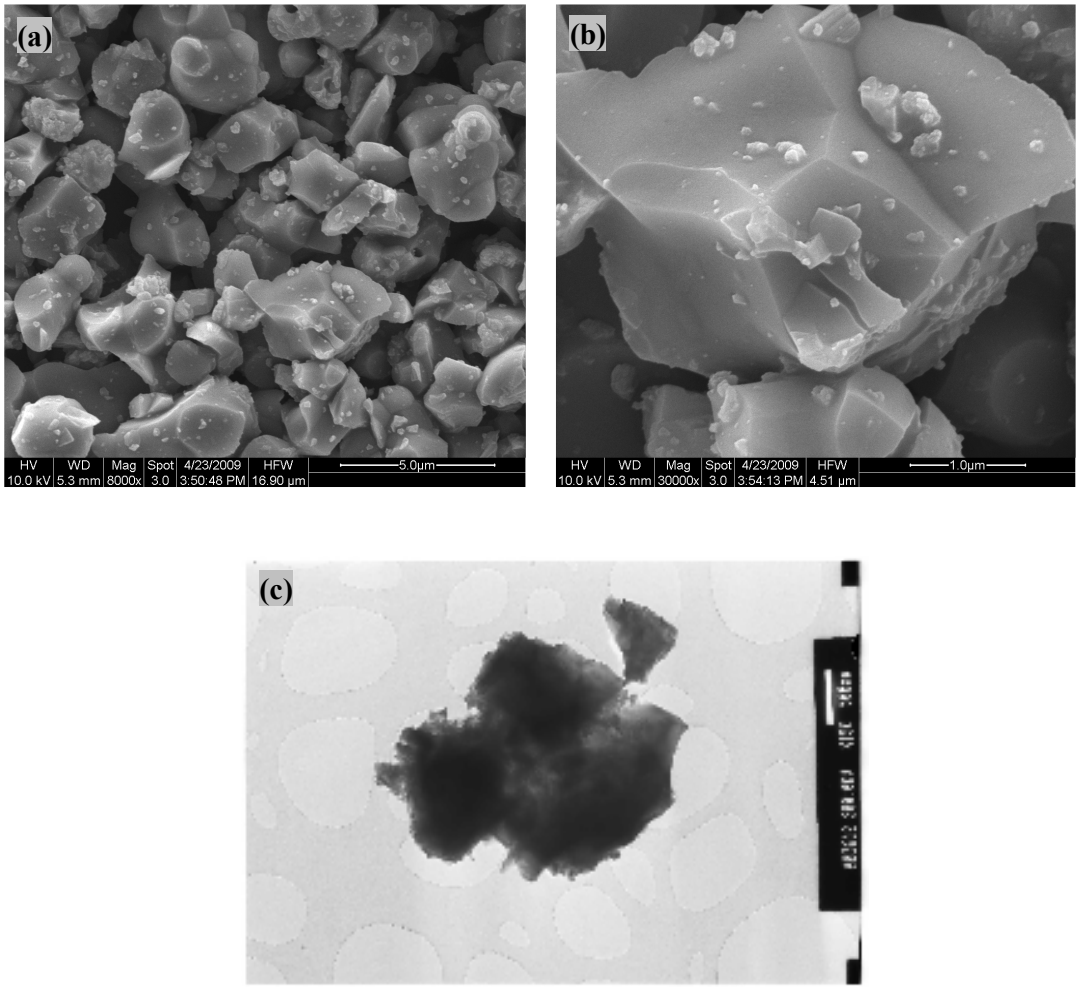

Figure 2.4: SEM images (a) lower magnification (scale bar= 5 µm) (b) higher magnification (scale bar= 1 µm) and (c) TEM (scale bar= 500 nm) showing morphology and particle size of sHA.

rHA powder

SEM and TEM images showing the size and morphology of rHA particles are shown in Figure 2.5. The images show that the particles have rough surfaces with a mean particle size of approximately 4 µm and are agglomerates of needle-like small particles.

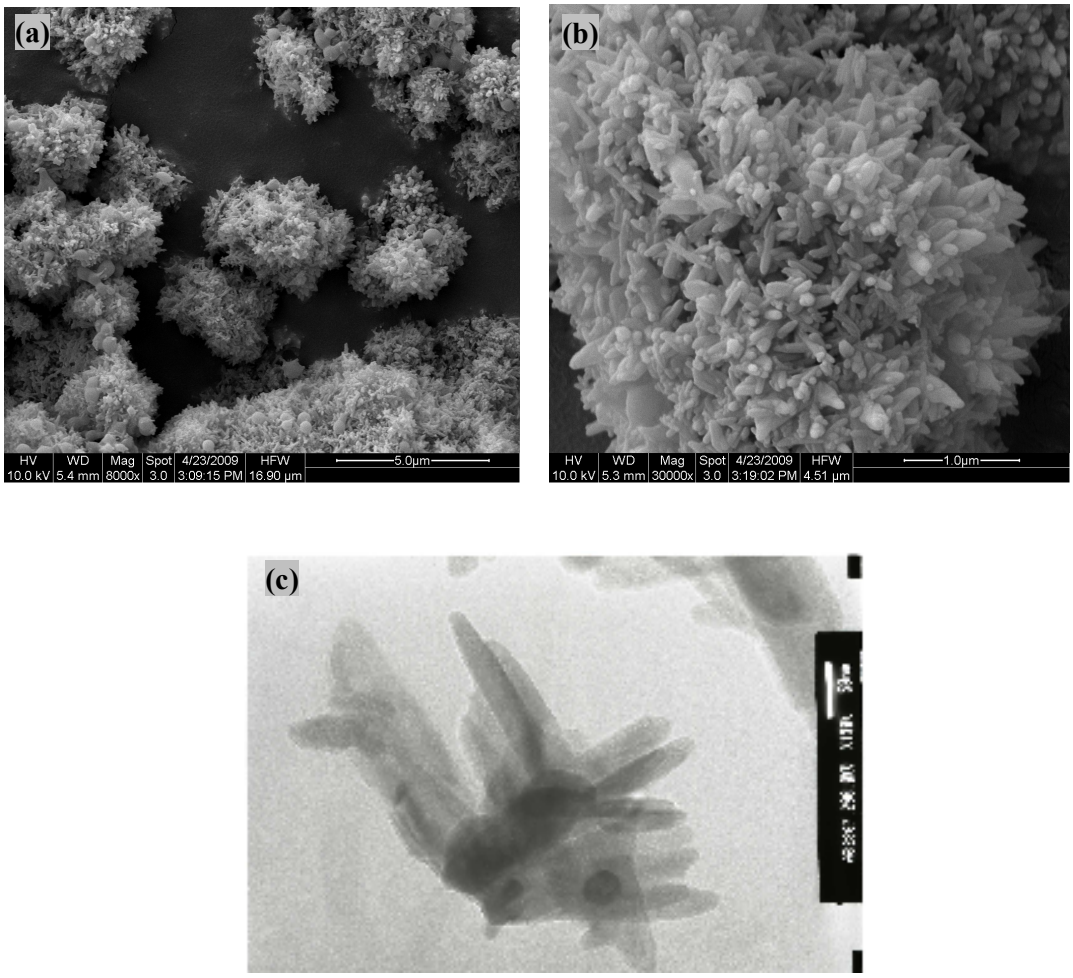

Figure 2.5: SEM images (a) lower magnification (scale bar= 5 µm) (b) higher magnification (scale bar= 1 µm) and (c) TEM (scale bar= 50 nm) showing morphology and particle size of rHA.

ßTCP powder

The morphology and size of ß-TCP particles are shown by SEM and TEM images in Figure 2.6. The images show that the particles have smooth surfaces, irregular shapes and consist of multiple particles which are fused together. The particle size ranges from 4 to 20 µm.

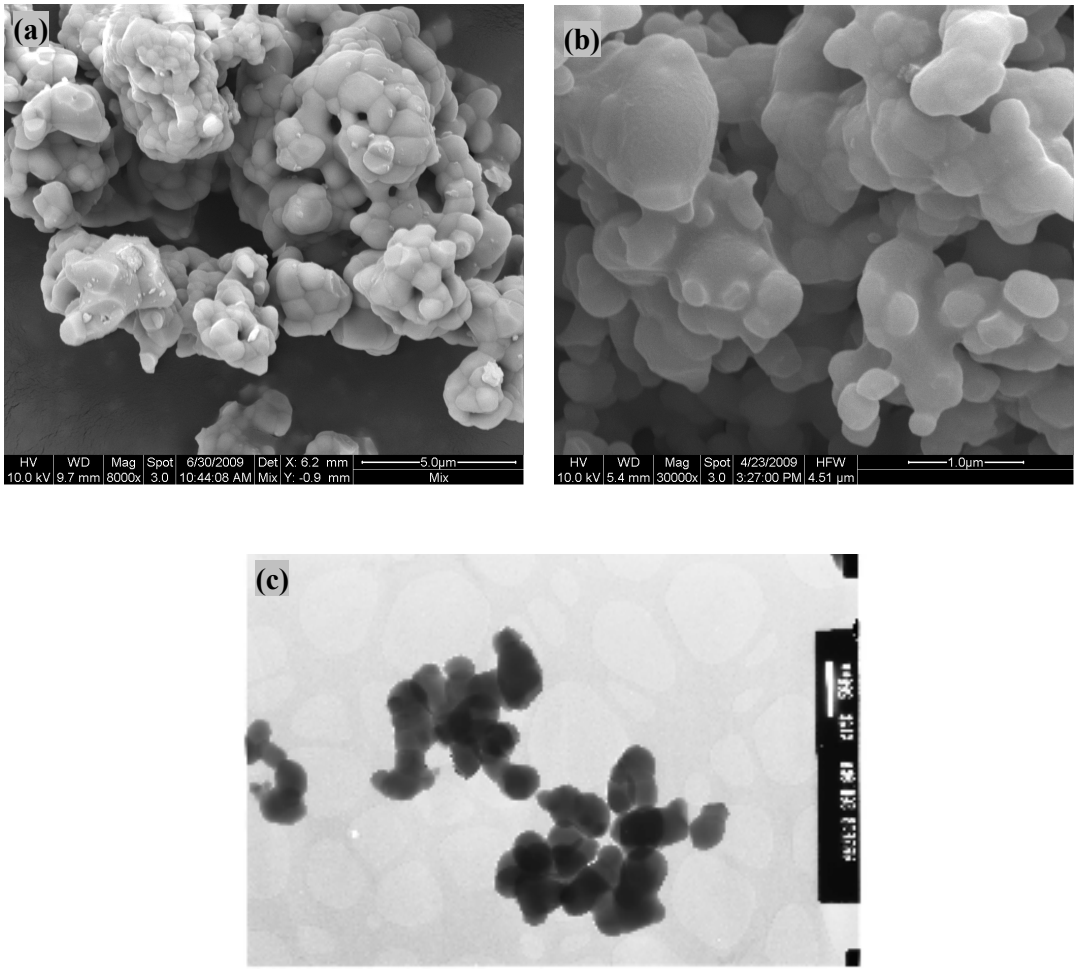

Figure 2.6: SEM images (a) lower magnification (scale bar= 5 µm) (b) higher magnification (scale bar= 1 µm) and (c) TEM (scale bar= 500 nm) showing morphology and particle size of ßTCP.

2.4.1.2 XRD

Figure 2.7 shows the XRD patterns for (a) nHA, (b) sHA (c) rHA and (d) ßTCP. All three HAs show diffraction peaks at 31.8° (211), 32.2° (112) and 32.9° (300) which are characteristic of HA XRD pattern and confirm the purity of all three HAs, however the crystallinity of three HAs was significantly different. sHA showed narrow and intense peak followed by rHA, whereas XRD of nHA showed broad and less intense peaks. The XRD peaks for ßTCP show the characteristic pattern with strong diffraction peaks at 27.8°, 31.0° and 34.4°.

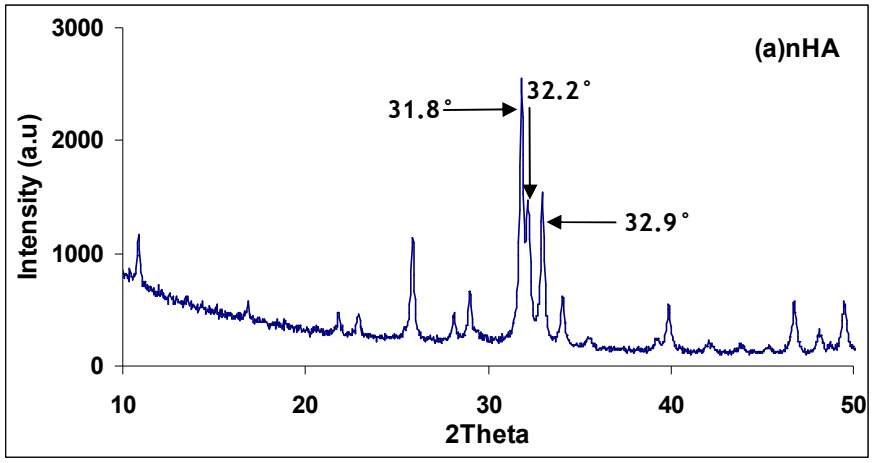

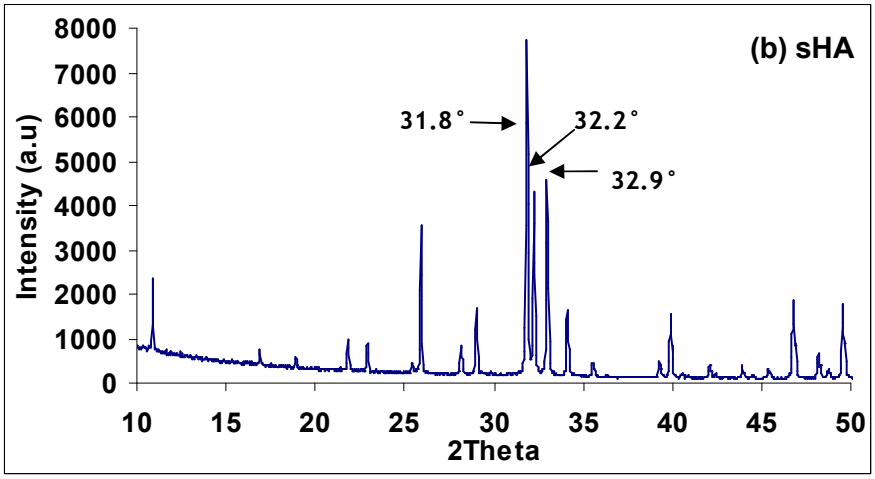

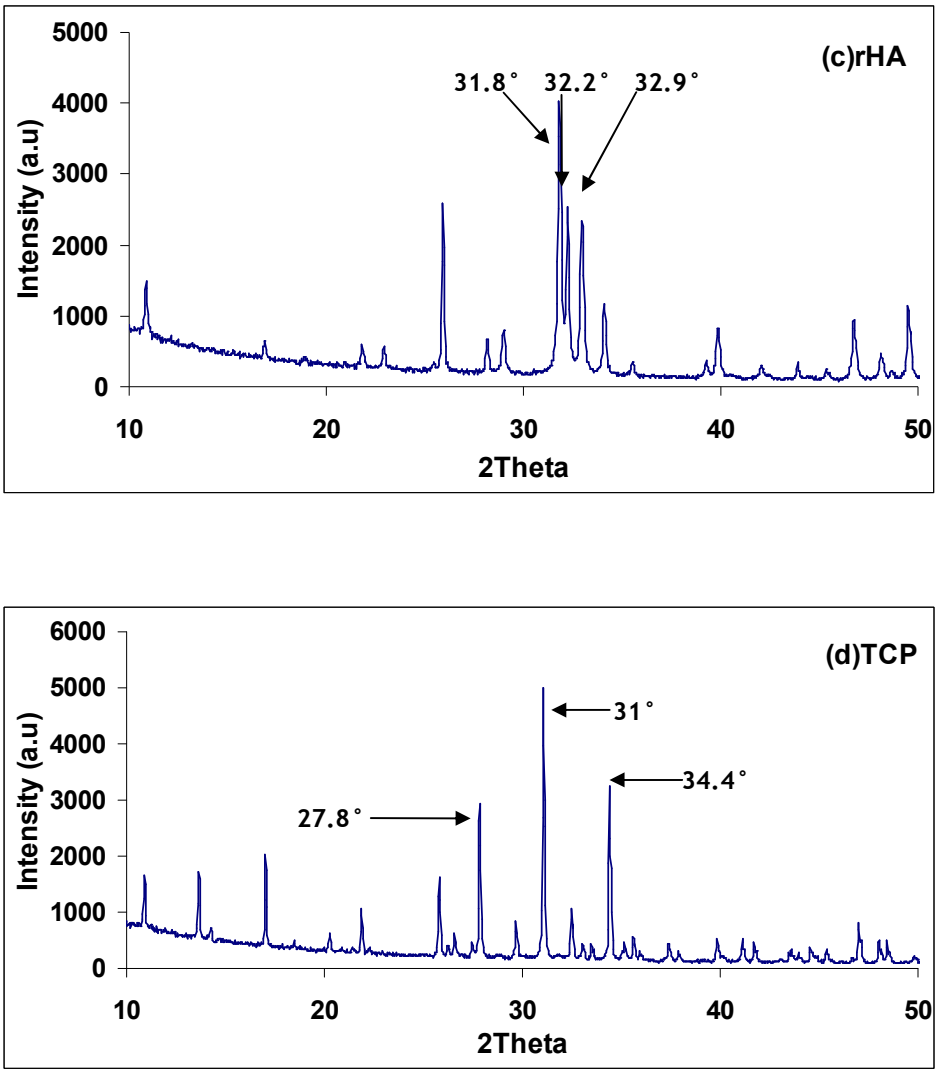

Figure 2.7: Comparative XRD pattern for (a) nHA (b) sHA (c) rHA and (d) ßTCP.

2.4.1.3 FTIR

Figure 2.8 (a), (b), (c) and (d) show the FTIR spectra of nHA, sHA, rHA and ßTCP powders respectively. The spectra of all three HA powders show the typical peaks associated with HA. The peaks at 3571 and 631 cm^{-1} were assigned to the hydroxyl group (-OH), while the peaks at 1473 and 875 cm^{-1} were attributed to stretching mode of carbonate groups (CO_3). The peaks at 1040, 946, 603 and 569 cm^{-1} were assigned to phosphate groups (PO_4) present in the HAs. Whereas the FTIR spectra of ßTCP show the characteristics phosphate peaks at 946, 603 and 569 cm^{-1} and there were no peaks observed associated with OH or CO_3.

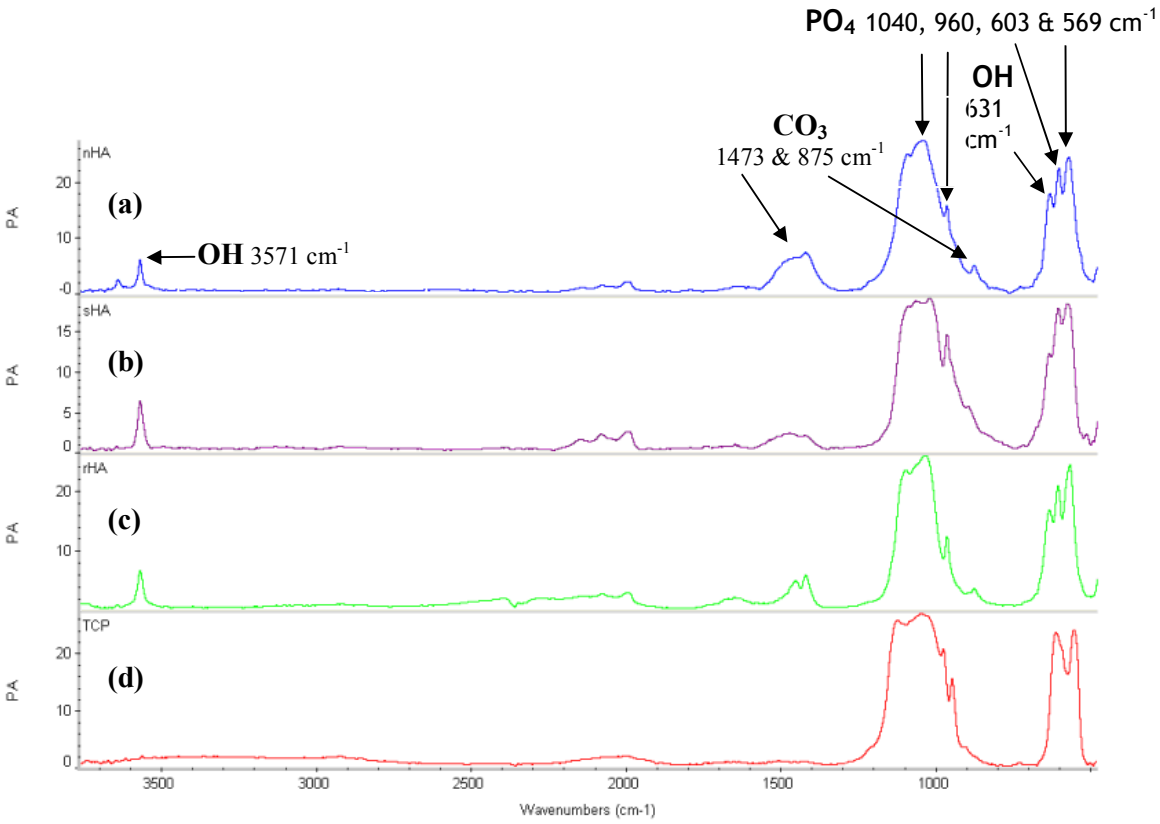

Figure 2.8: FTIR spectra of Ca P powders (a) nHA (b) sHA (c) rHA and (d) ßTCP.

2.4.1.4 Raman spectroscopy

Figure 2.9 shows the Raman spectra of (a) nHA, (b) sHA, (c) rHA and (d) ßTCP powders. For the three HAs the main peak was observed at 960 cm $^{-1}$ which is assigned to phosphate (PO_4) stretching. The intensity of this peak was highest for sHA followed by rHA and nHA respectively and represents the crystallinity of HA. In addition a less intense peak, which is assigned to PO_4 bending, was observed at 590 cm^{-1}.

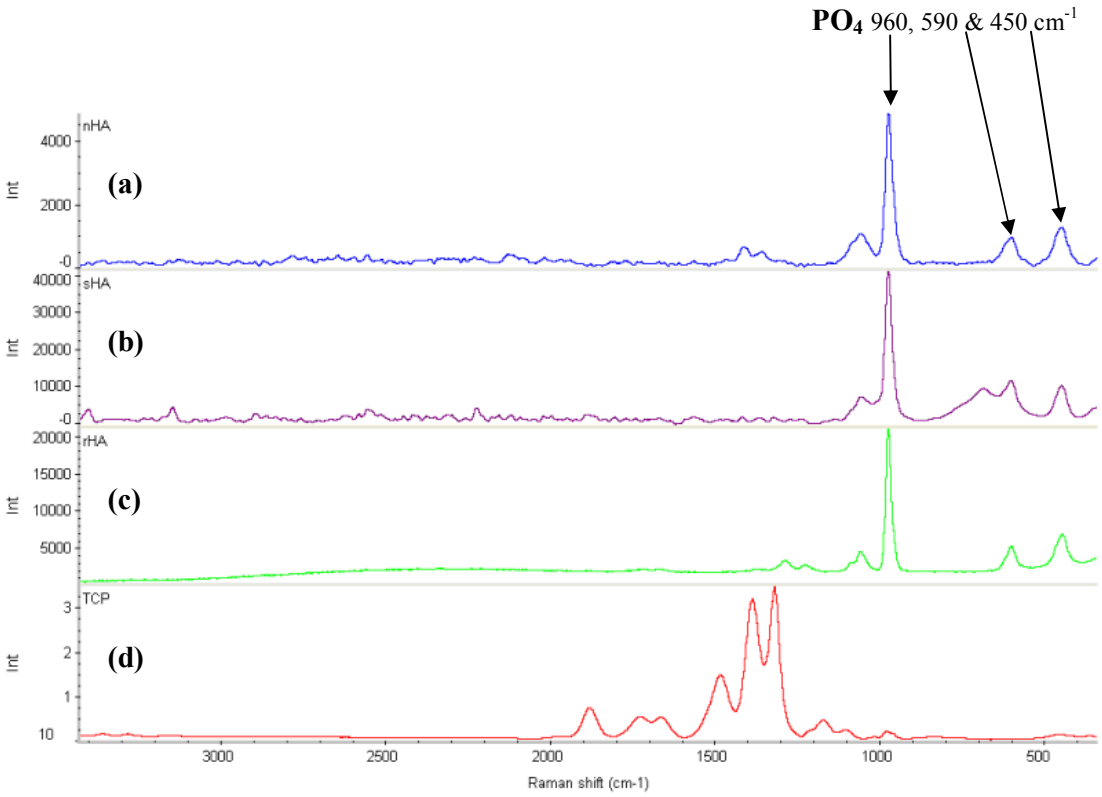

Figure 2.9: Raman spectra of Ca P powders (a) nHA (b) sHA (c) rHA and (d) ßTCP

2.4.2 PLA and PLA- Ca P composite films

2.4.2.1 SEM

PLA film

Figure 2.10 shows the SEM image of PLA films, the surface of the film appears very smooth.

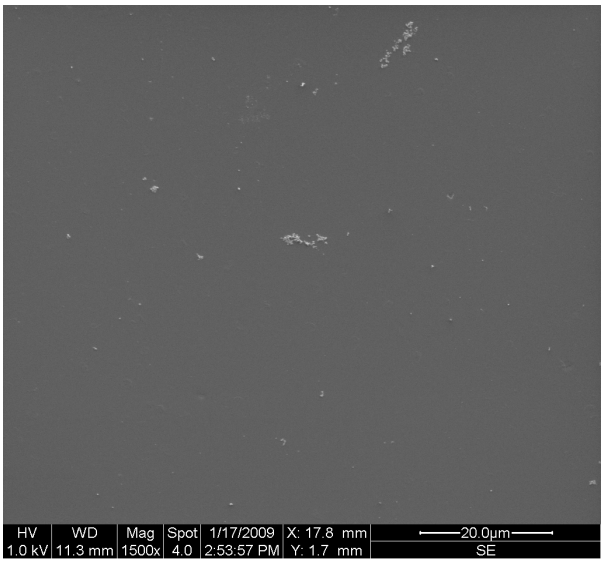

Figure 2.10: SEM image of PLA film. (Scale bar = 20 µm)

PLA-nHA composite films

Figure 2.11 shows the images of PLA-nHA composite film containing (a) 10 wt % nHA (PLA-nHA10), (b) 40 wt % nHA (PLA-nHA40) and (c) 70 wt % nHA (PLA-nHA70). PLA-nHA10 film appears relatively smooth and there was hardly any nHA present on the film surface and most of the nHA was covered by a layer of PLA. However as the nHA concentrations increased in PLA-nHA40 and PLA-nHA70 films the surfaces became rough and the films also had nHA present on the surfaces which was not covered by PLA.

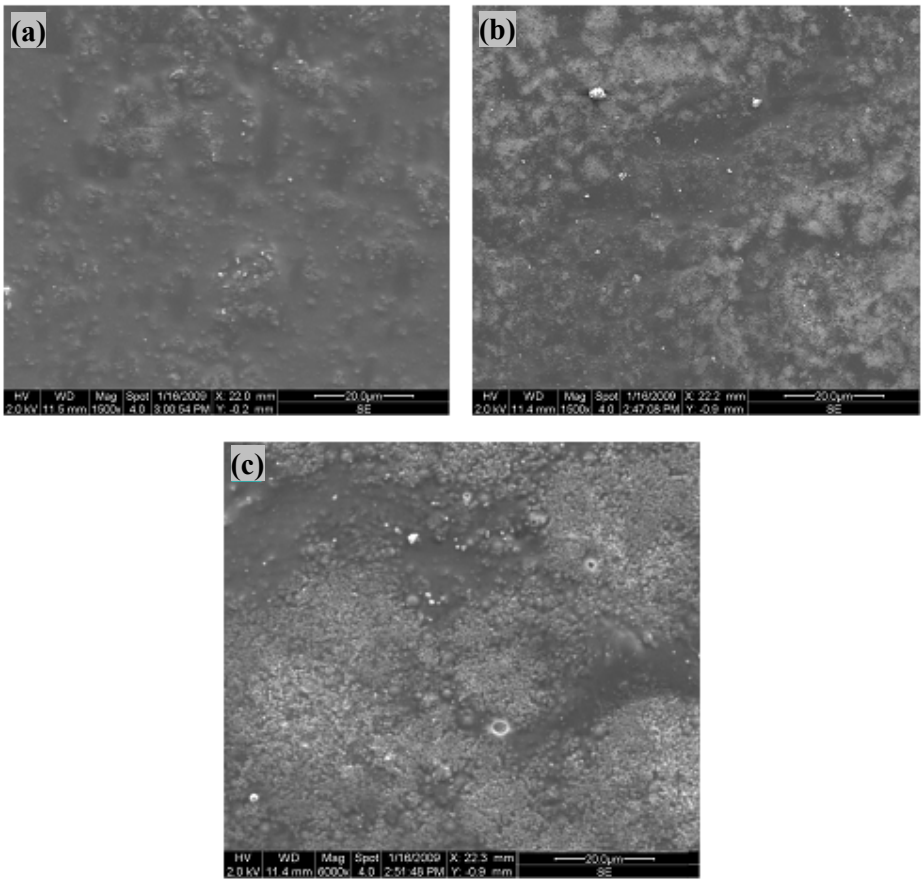

Figure 2.11: SEM images of (a) PLA-nHA10, (b) PLA-nHA40 and (c) PLA-nHA70 composite films. (Scale bar = 20 µm)

PLA-sHA composite films

Figure 2.12 shows the images of PLA-sHA composite film containing (a) 10 wt % sHA (PLA-sHA10), (b) 40 wt % sHA (PLA-sHA40) and (c) 70 wt % sHA (PLA-sHA70). The surfaces of all the films appeared rough, however most of the sHA present in the films appeared to be covered with PLA, except in PLA-sHA70 where some of the particles are visible partially out of the PLA layer.

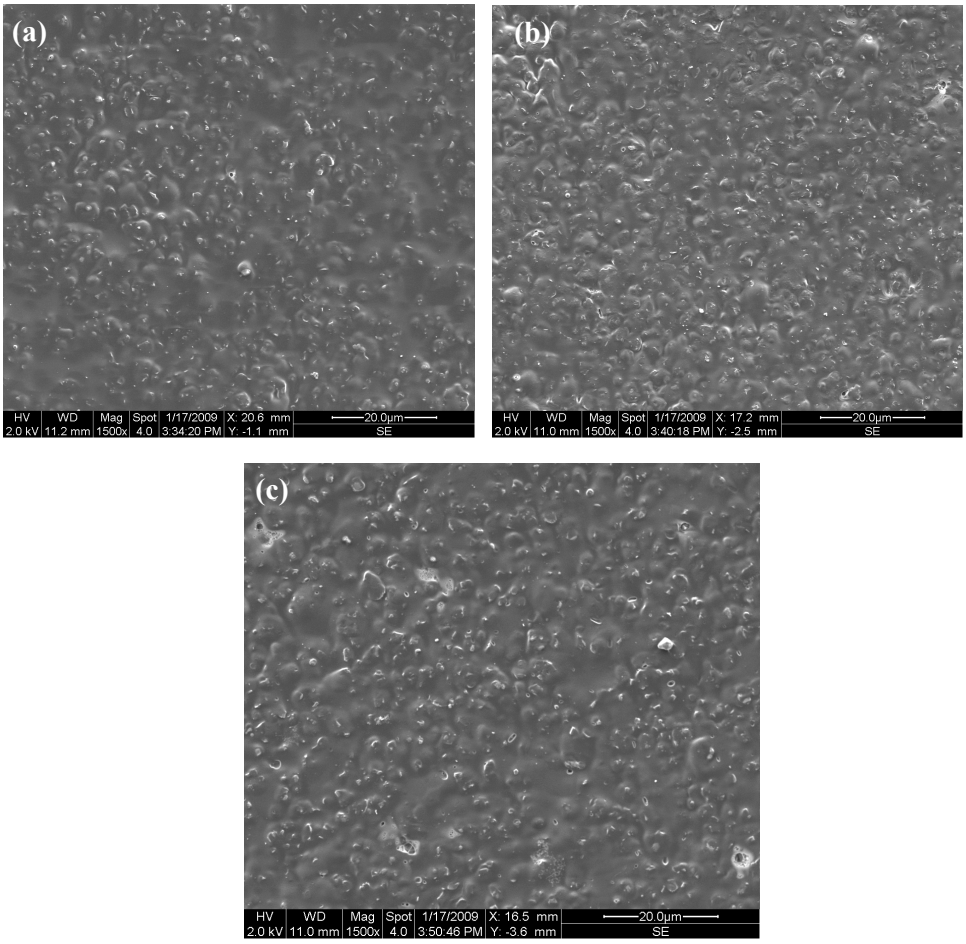

Figure 2.12: SEM images of (a) PLA-sHA10, (b) PLA-sHA40 and (c) PLA-sHA70 composite films. (Scale bar = 20 µm)

PLA-rHA composite films

Figure 2.13 shows the images of PLA-rHA composite film containing (a) 10 wt % rHA (PLA-rHA10), (b) 40 wt % rHA (PLA-rHA40) and (c) 70 wt % rHA (PLA-rHA70). The surface of PLA-rHA10 was smoother than the surfaces of the PLA-rHA40 and PLA-rHA70 films. In addition the PLA-rHA40 and PLA-rHA70 films also showed some micropores.

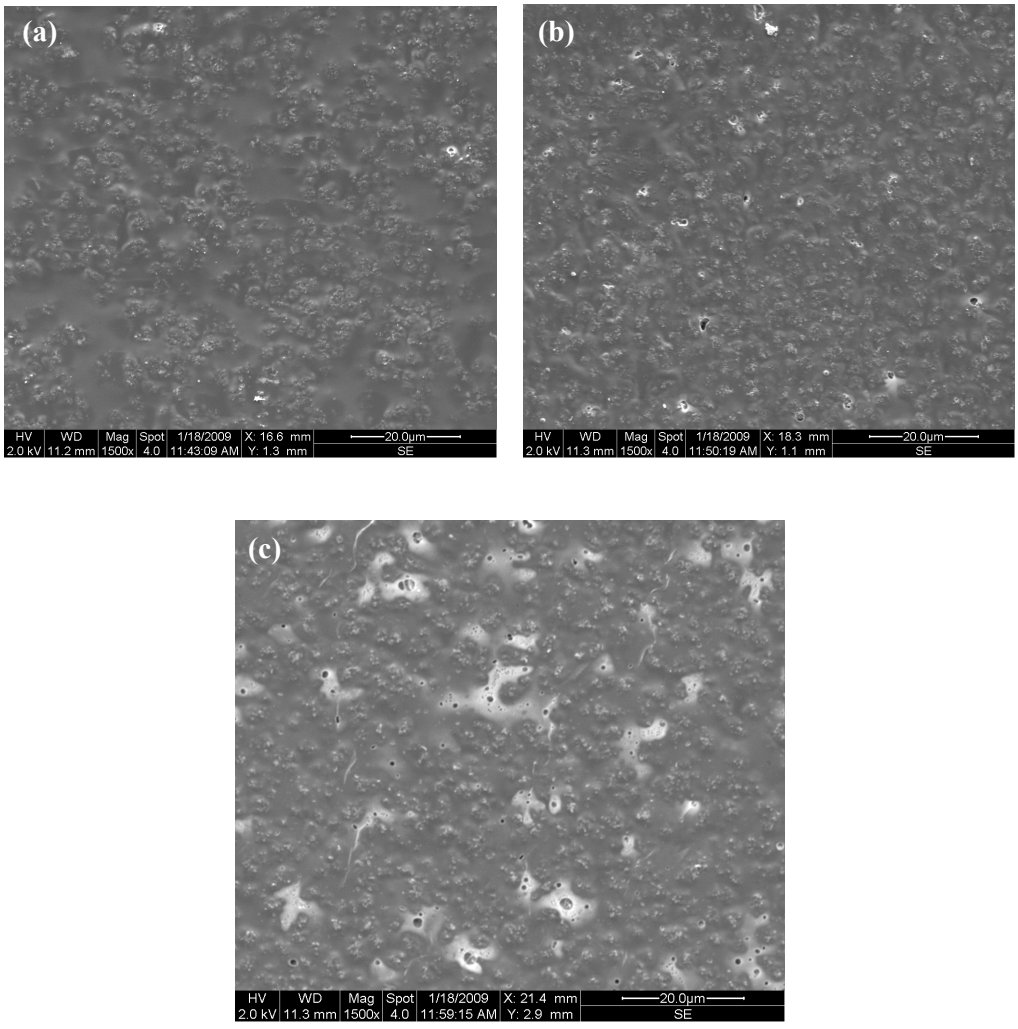

Figure 2.13: SEM images of (a) PLA-rHA10, (b) PLA-rHA40 and (c) PLA-rHA70 composite films. (Scale bar = 20 µm)

PLA- ßTCP composite films

Figure 2.14 shows the images of PLA-ßTCP composite film containing (a) 10 wt % ßTCP (PLA-ßTCP10), (b) 40 wt % ßTCP (PLA- ßTCP40) and (c) 70 wt % ßTCP (PLA-ßTCP70). In PLA-ßTCP10 films the ßTCP appeared to be homogenously dispersed, whereas PLA-ßTCP40 and PLA-ßTCP70 films with higher concentrations of ßTCP showed some agglomeration of the particles.

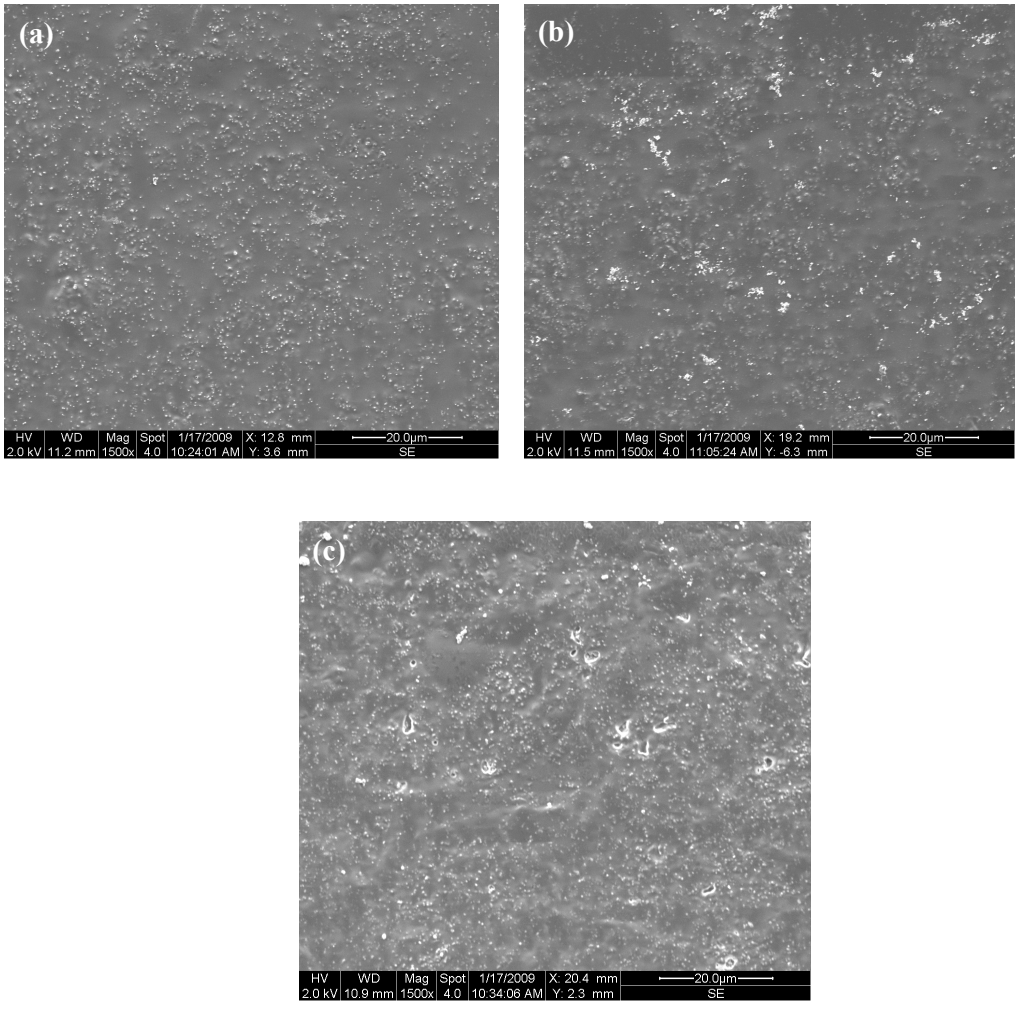

Figure 2.14: SEM images of (a) PLA-ßTCP 10, (b) PLA-ßTCP40 and (c) PLA-ßTCP70 composite films. (Scale bar = 20 µm)

2.4.2.2 FTIR

PLA film

Figure 2.15 shows the characteristic PLA FTIR peaks. The peaks at 2995 and 2945 cm^{-1} are assigned to C-H stretching of the methyl group (CH_3). The intense peak at 1760 cm^{-1} was assigned to C=O (carbonyl) stretching, while the peaks at 1130,1382 and 1453 cm^{-1} were assigned to C-H bending of CH_3.

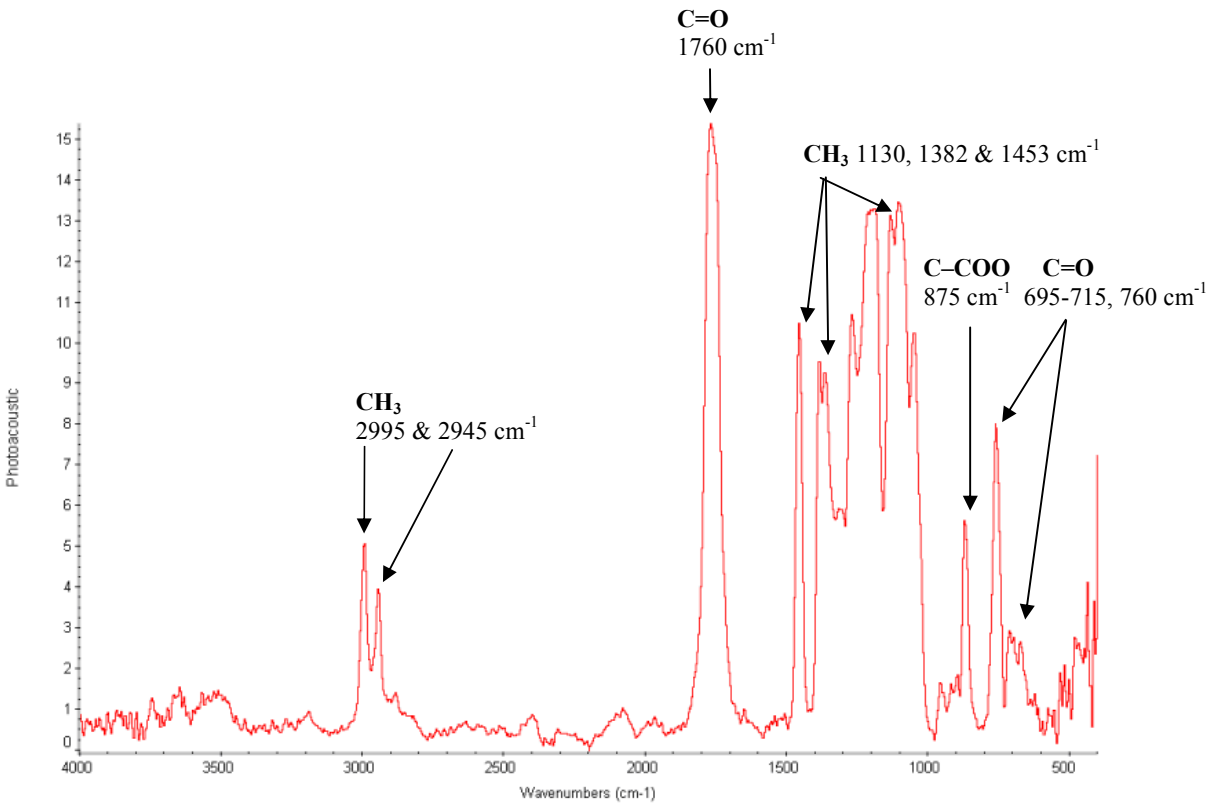

Figure 2.15: FTIR spectrum of PLA.

PLA-nHA composite films

Figure 2.16 shows the comparative FTIR spectra of (a) PLA, (b) nHA, (c) PLA-nHA10, (d) PLA-nHA40 and (e) PLA-nHA70. The spectra of PLA-nHA10, PLA-nHA40 and PLA-nHA70 composites films show the characteristic peaks of both HA and PLA. As the concentration of nHA increased the intensities of PO_4 peaks at 603 and 569 cm^{-1}, which were attributed to phosphate from HA, increased relative to the intensities of PLA characteristic peaks at 1760, 870 and 756 cm^{-1}.

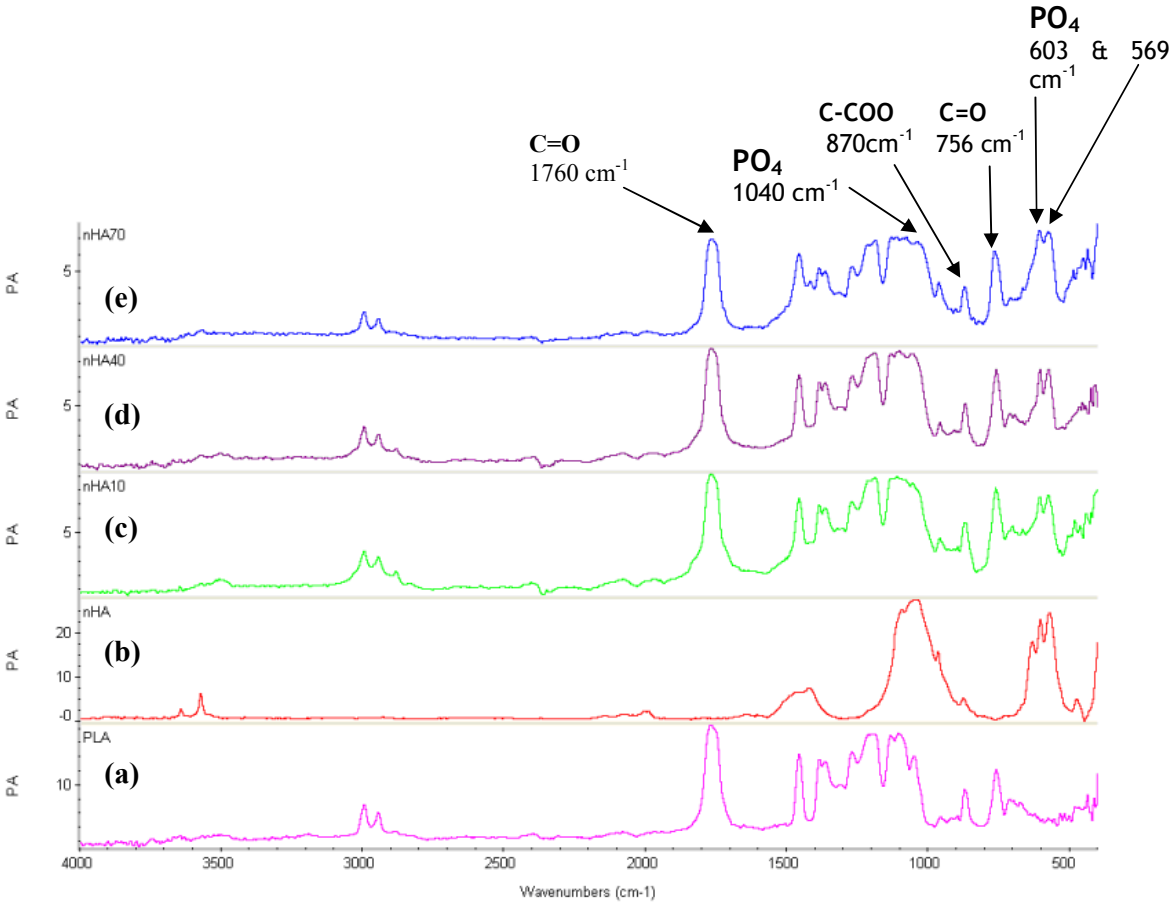

Figure 2.16: Comparative FTIR spectra of (a) PLA, (b) nHA, (c) PLA-nHA10, (d) PLA-nHA40 and (e) PLA-nHA70.

PLA-sHA composite films

Figure 2.17 shows the comparative FTIR spectra of (a) PLA, (b) sHA, (c) PLA-sHA10, (d) PLA-sHA40 and (e) PLA-sHA70. The spectra of PLA-sHA10, PLA-sHA40 and PLA-sHA70 composites films show the characteristic peaks of both HA and PLA. As the concentration of sHA increased the intensities of PO_4 peaks at 603 and 569 cm^{-1} which were attributed to phosphate from HA increased relative to the intensities of PLA characteristic peaks at 1760, 870 and 756 cm^{-1}.

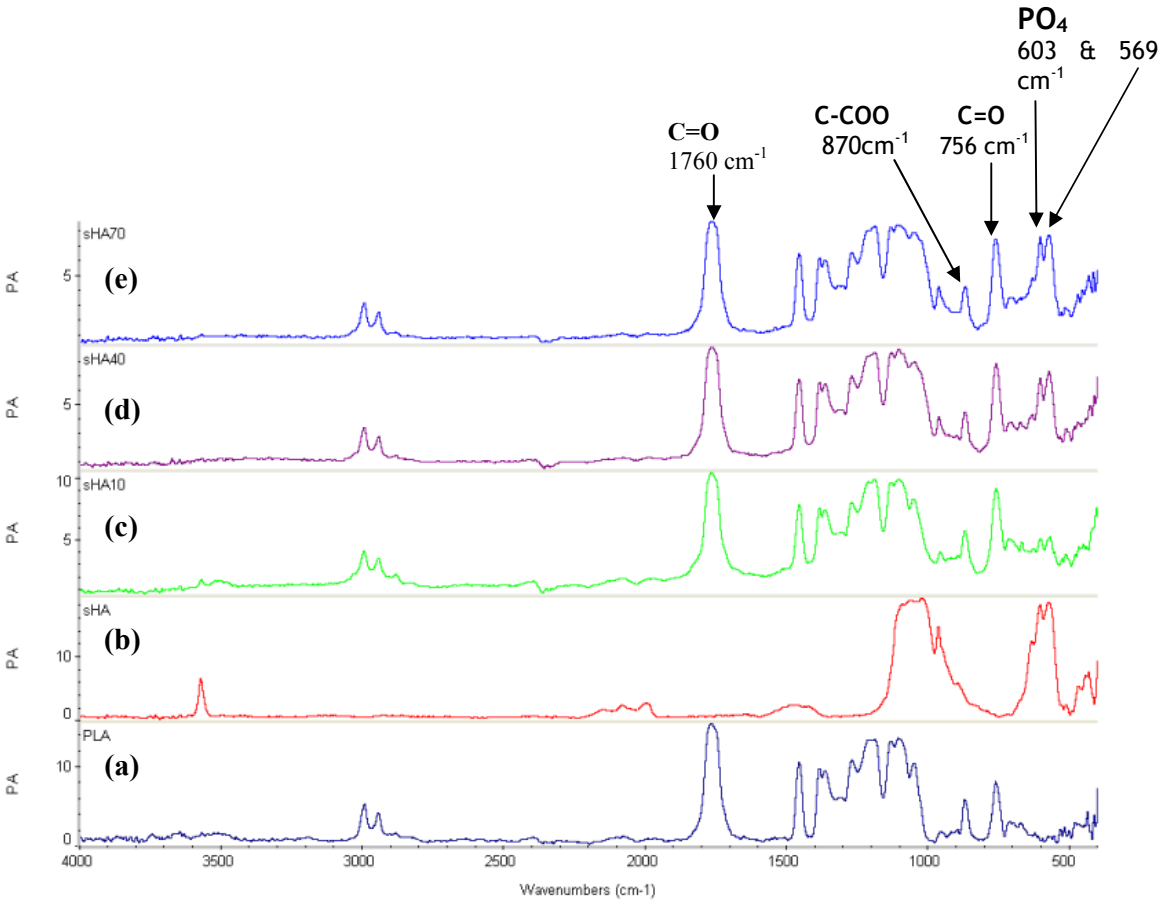

Figure 2.17: Comparative FTIR spectra of (a) PLA, (b) sHA, (c) PLA-sHA10, (d) PLA-sHA40 and (e) PLA-sHA70.

PLA-rHA composite films

Figure 2.18 shows the comparative FTIR spectra of (a) PLA, (b) rHA, (c) PLA-rHA10, (d) PLA-rHA40 and (e) PLA-rHA70. The spectra of PLA-rHA10, PLA-rHA40 and PLA-rHA70 composites films show the characteristic peaks of both HA and PLA. As the concentration of rHA increased the intensities of PO_4 peaks at 603 and 569 cm^{-1}, which were attributed to phosphate from HA, increased relative to the intensities of PLA characteristic peaks at 1760, 870 and 756 cm^{-1}.

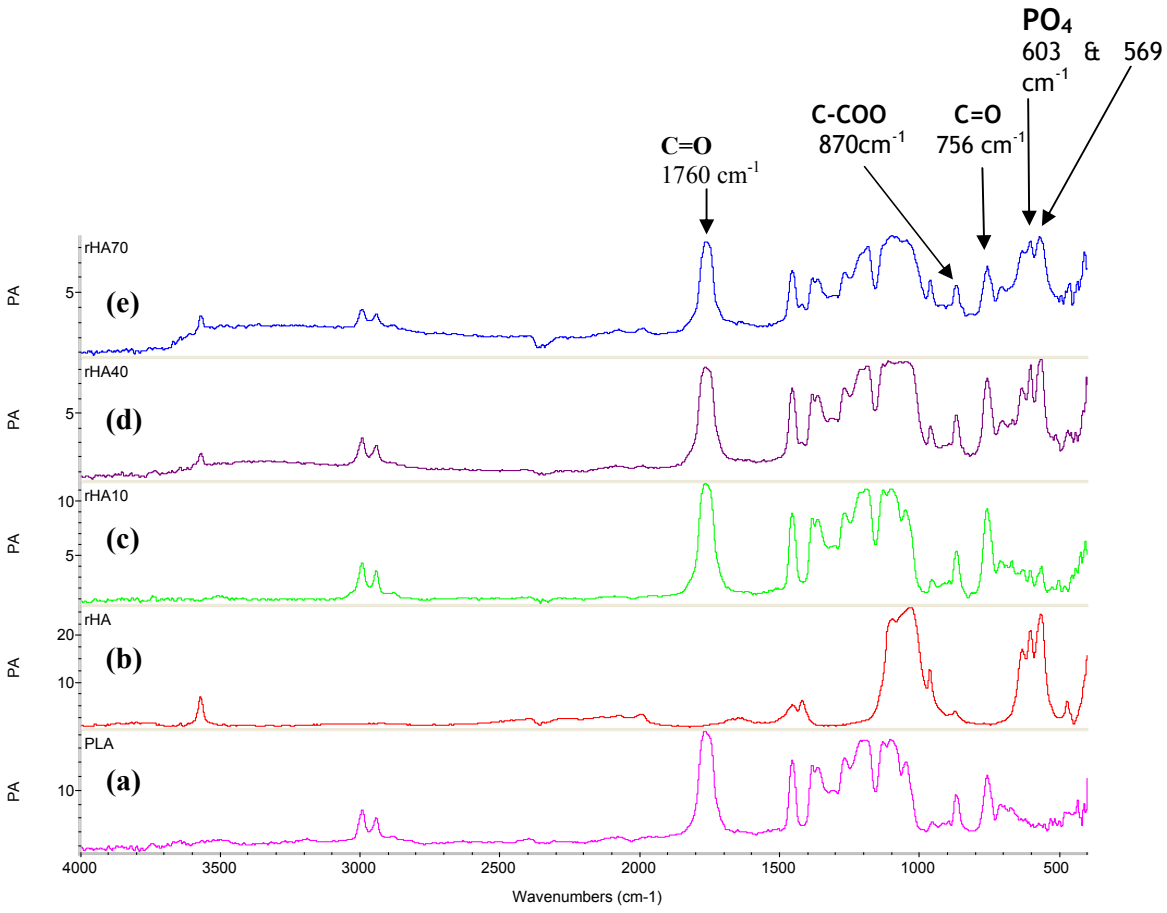

Figure 2.18: Comparative FTIR spectra of (a) PLA, (b) rHA, (c) PLA-rHA10, (d) PLA-rHA40 and (e) PLA-rHA70.

PLA- ßTCP composite films

Figure 2.19 shows the comparative FTIR spectra of (a) PLA, (b) ßTCP, (c) PLA-ßTCP10, (d) PLA-ßTCP40 and (e) PLA-ßTCP70. The spectra of PLA-ßTCP10, PLA-ßTCP40 and PLA-ßTCP70 composites films show the characteristic peaks of both HA and PLA. As the concentration of ßTCP increased the intensities of PO_4 peaks at 603 and 569 cm^{-1}, which were attributed to phosphate from HA, increased relative to the intensities of PLA characteristic peaks at 1760, 870 and 756 cm^{-1}.

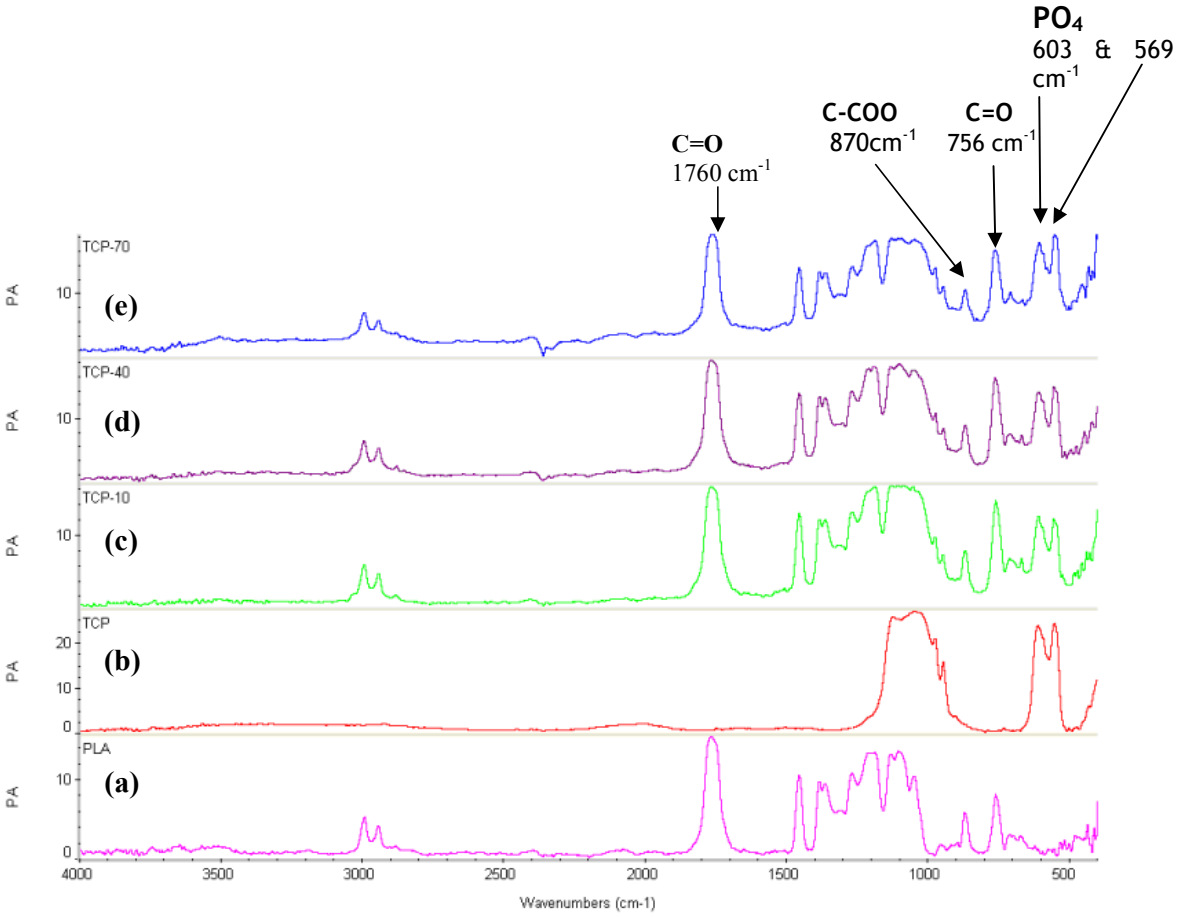

Figure 2.19: Comparative FTIR spectra of (a) PLA, (b) ßTCP, (c) PLA-ßTCP10, (d) PLA-ßTCP40 and (e) PLA-ßTCP70.

2.4.2.3 Raman spectroscopy

PLA film

Figure 2.20 shows the Raman spectra of PLA film. The spectra show characteristic peaks for PLA, the peak at 875 cm^{-1} is characteristic of carbon, carbonyl bond (C-COO) stretching. The peak at 1040 cm^{-1} corresponds to C-CH_3 stretching while the peak at 1766 cm^{-1} corresponds to C=O stretching. The peak at 1452 cm^{-1} corresponds to methyl group (CH_3) symmetric bending and at 1315 cm^{-1} to CH bending.

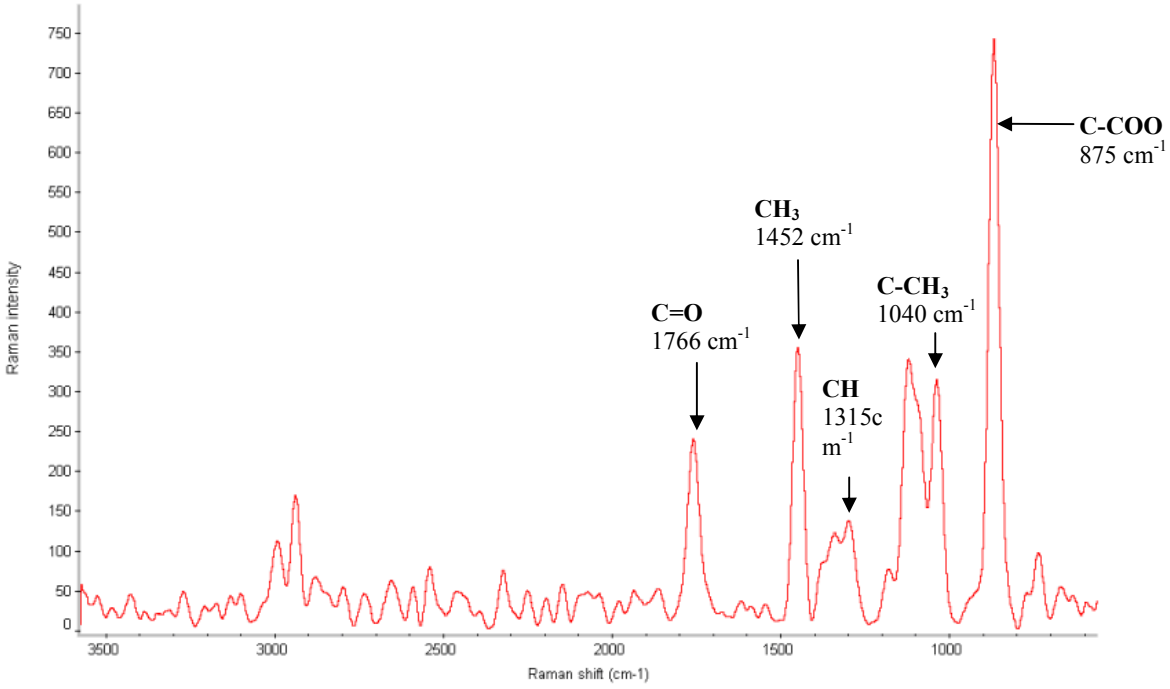

Figure 2.20: Raman spectra of PLA film.

PLA-nHA composite films

Figure 2.21 shows the comparative Raman spectra of (a) PLA, (b) nHA, (c) PLA-nHA10, (d) PLA-nHA40 and (e) PLA-nHA70. The spectra of PLA-nHA10, PLA-nHA40 and PLA-nHA70 composites films show the characteristic peaks of both HA and PLA. The PO_4 peak corresponding to nHA is low in PLA-nHA10, however as the concentration of nHA increased in the films from 10 wt % to 70 wt % the PO_4 peak became more intense and its height relative to the C-COO (PLA) peak increased.

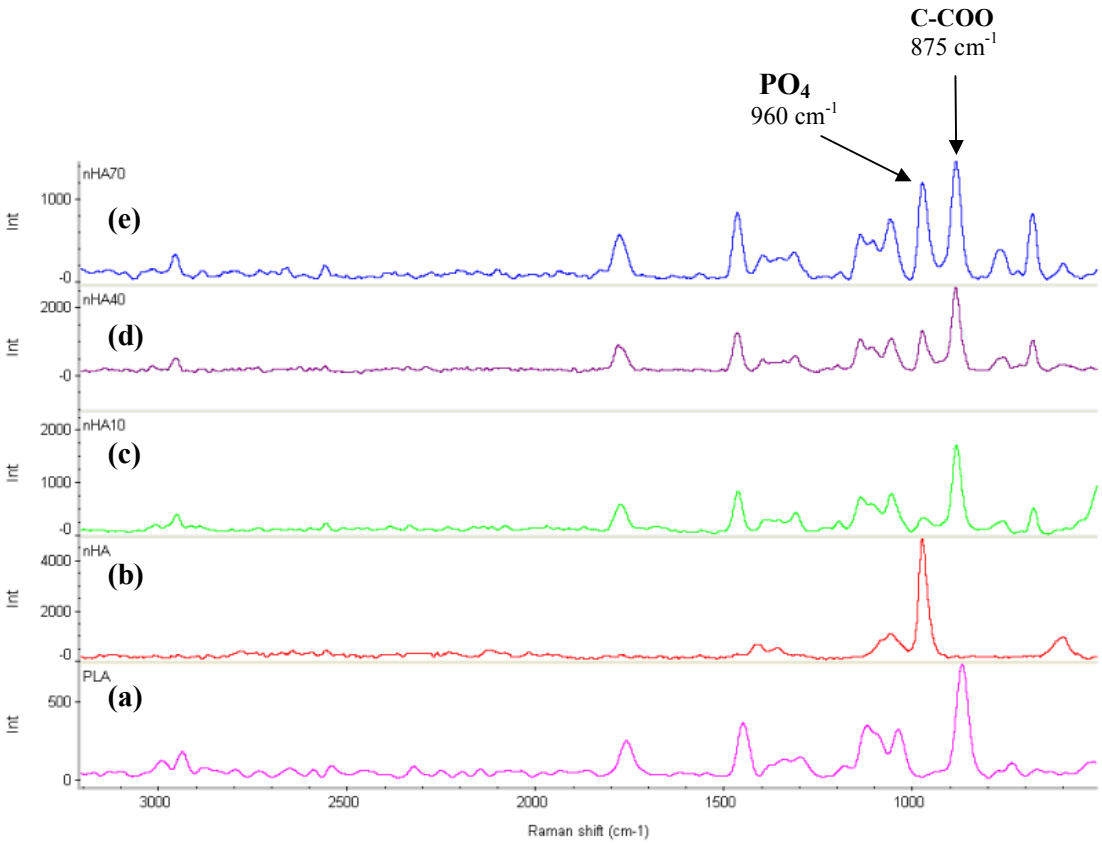

Figure 2.21: Comparative Raman spectra of (a) PLA, (b) nHA, (c) PLA-nHA10, (d) PLA-nHA40 and (e) PLA-nHA70.

PLA-sHA composite films

Figure 2.22 shows the comparative Raman spectra of (a) PLA, (b) sHA, (c) PLA-sHA10, (d) PLA-sHA40 and (e) PLA-sHA70. The spectra of PLA-sHA10, PLA-sHA40 and PLA-sHA70 composites films show the characteristic peaks of both HA and PLA. The PO_4 peak corresponding to sHA is low in PLA-sHA10, however as the concentration of sHA increased in the films from 10 wt % to 70 wt % the PO_4 peak became more intense and its height relative to the C-COO (PLA) peak increased.

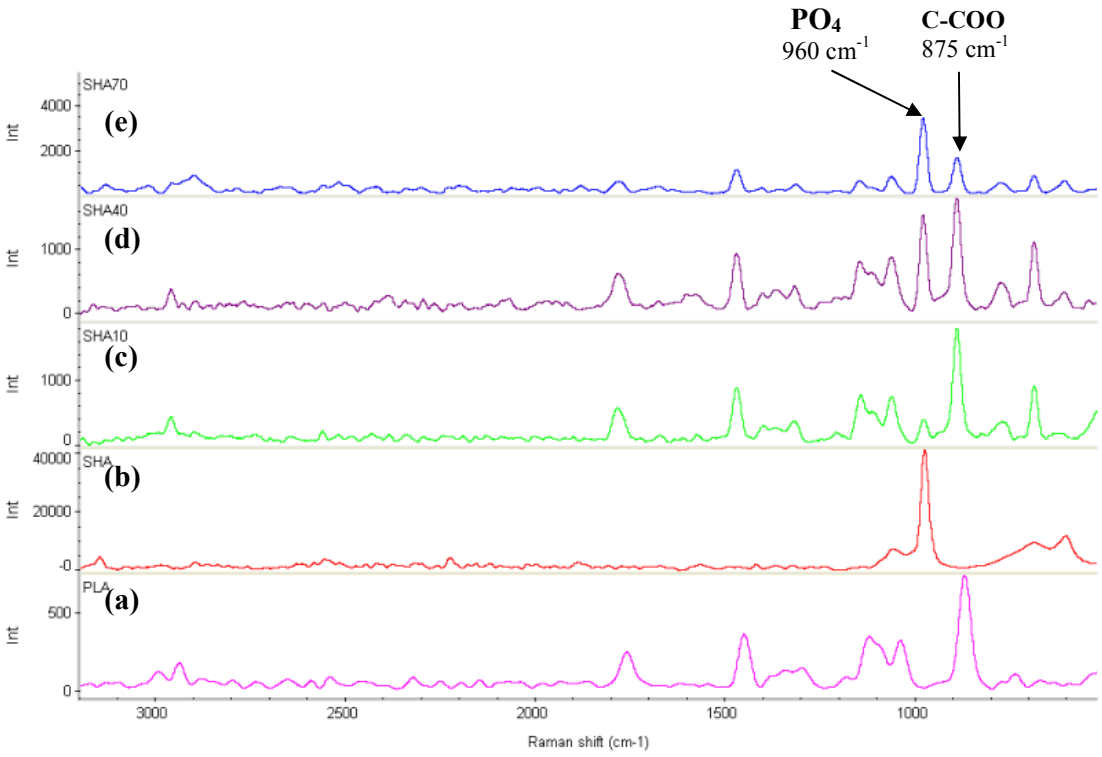

Figure 2.22: Comparative Raman spectra of (a) PLA, (b) sHA, (c) PLA-sHA10, (d) PLA-sHA40 and (e) PLA-sHA70.

PLA-rHA composite films

Figure 2.23 shows the comparative Raman spectra of (a) PLA, (b) rHA, (c) PLA-rHA10, (d) PLA-rHA40 and (e) PLA-rHA70. The spectra of PLA-rHA10, PLA-rHA40 and PLA-rHA70 composite films show the characteristic peaks of both HA and PLA. The PO_4 peak corresponding to sHA is low in PLA-rHA10, however as the concentration of rHA increased in the films from 10 wt % to 70 wt % the PO_4 peak became more intense and its height relative to the C-COO (PLA) peak increased.

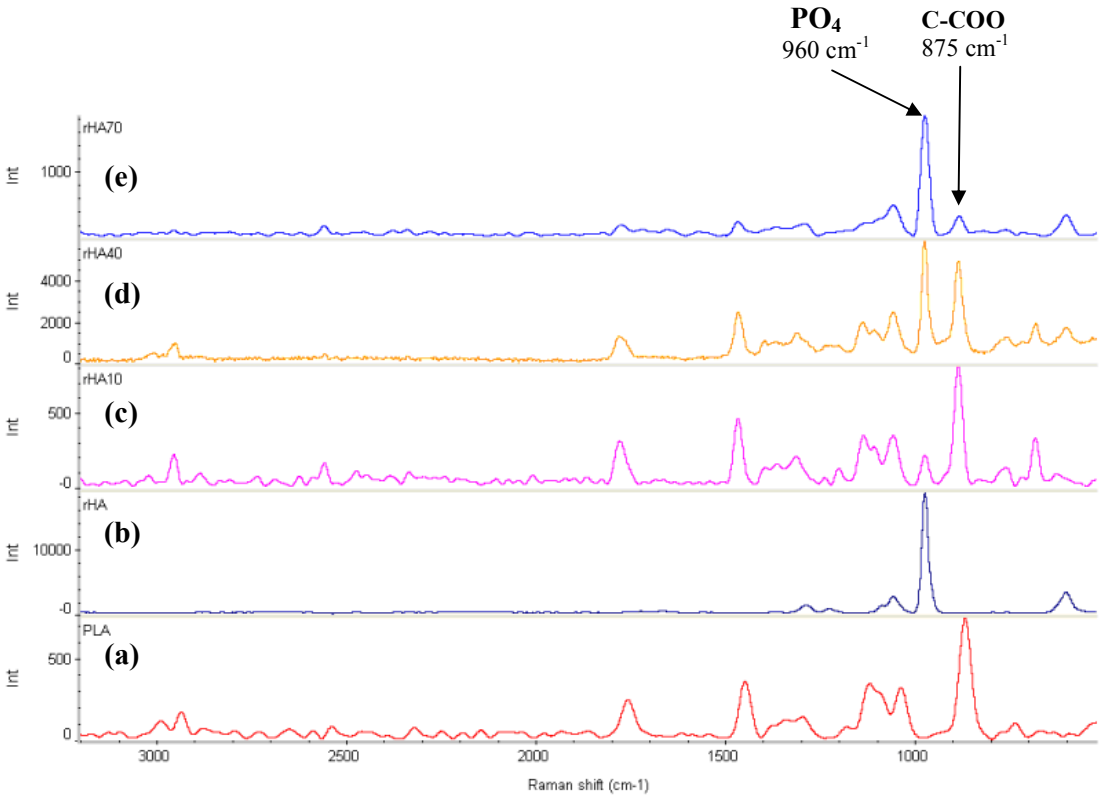

Figure 2.23: Comparative Raman spectra of (a) PLA, (b) rHA, (c) PLA-rHA10, (d) PLA-rHA40 and (e) PLA-rHA70.

PLA- ßTCP composite films

Figure 2.24 shows the comparative Raman spectra of (a) PLA, (b) ßTCP, (c) PLA-ßTCP10, (d) PLA-ßTCP40 and (e) PLA-ßTCP70. The spectra of PLA-ßTCP10, PLA-ßTCP40 and PLA-ßTCP70 composites films show the characteristic peaks of both ßTCP and PLA. The PO_4 peak corresponding to ßTCP is low in PLA- ßTCP10 whereas the intensity of C-COO (PLA) peaks is high, however as the concentration of ßTCP increased in the films from 10 wt % to 70 wt % the PO_4 peak became more intense and its height relative to the C-COO (PLA) peak increased.

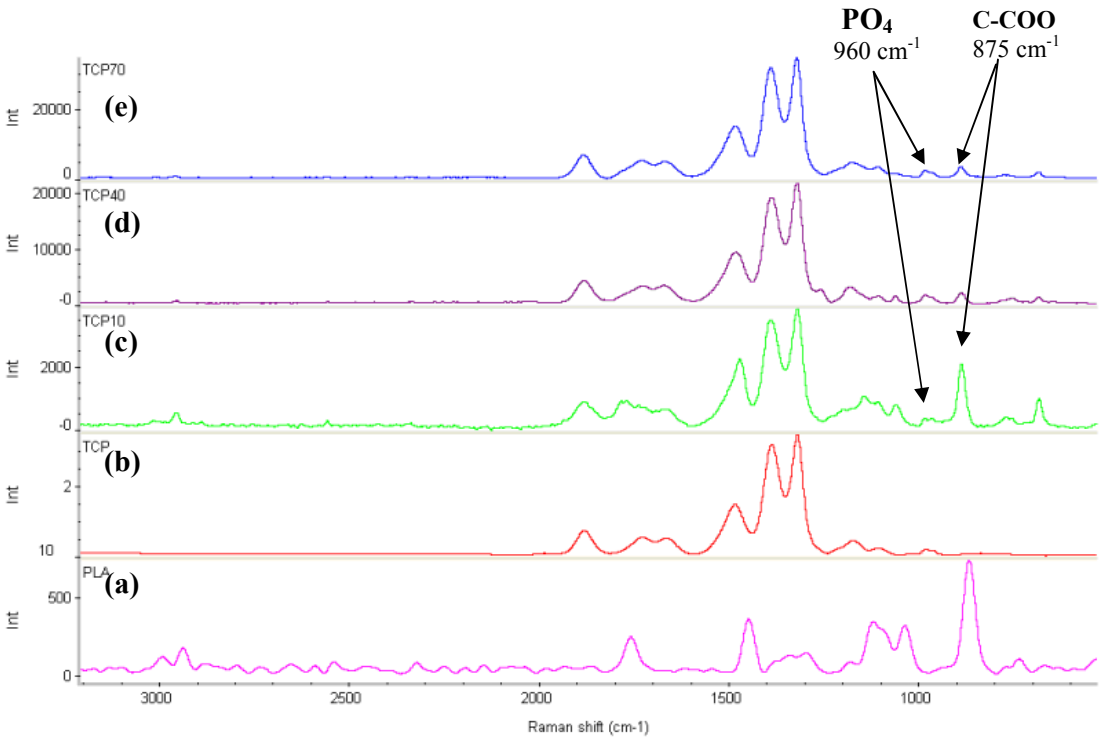

Figure 2.24: Comparative Raman spectra of (a) PLA, (b) ßTCP, (c) PLA-ßTCP10, (d) PLA-ßTCP40 and (e) PLA-ßTCP70.

2.5 DISCUSSION

The use of composites in biomedical applications has attracted a huge interest over the last few decades as the properties of composites can be tailored to suit a specific application. Addition of a Ca P such as HA and TCP to the polymer improves its bioactivity, osteoconductivity and mechanical properties. Crystalline HA is stable and non soluble, but can be resorbed by osteoclasts, whereas TCP is soluble. The rate of dissolution of different Ca P decreases as follows [Niemelä, 2005; Velayudhan et al., 2005; Rezwan et al., 2006]:

Amorphous HA > α – TCP > ß – TCP > crystalline HA.

In this study PLA Ca P composite films containing nHA, sHA, rHA and TCP at 10, 40 and 70 wt % concentrations were produced. The concentration, size and shape of the Ca P particles play an important role in determining the properties of the composite. It is reported that composites with higher HA contents have higher bioactivity and that nano size HA as compared to micro HA has shown to have better biological properties and promote attachment, proliferation and differentiation of cells [Di Silvio et al., 2002; Murugan and Ramakrishna, 2005; Sun et al., 2007]. The solvent casting technique used in this study enabled the production of films where HA or TCP particles were present on the surface without or with a thin coating of PLA with different degrees of surface roughness, this is beneficial as osteogenic cells or body fluid will make contact with the bioactive Ca P particles on implantation and it is also suggested that the cells adhesion and differentiation is more pronounced on rough surfaces [Ball et al., 2008].

SEM and TEM images of the Ca P powders showed that the HAs and TCP had different shapes and sizes. Images showed that nHA was spherical in shape with size in the range between 20 to 200nm. sHA has irregular shapes with smooth surfaces and an average particle size of 4 μm. Images of rHA showed that although the average particle size was 4 μm, each particle consisted of agglomerate of small needle like particles and had a rough surface agreeing with observation of Zhang and Tanner [2008]. TCP particles were fused together and had irregular, but smooth surfaces.

XRD of HA powders showed the purity of these powders as all showed the major characteristics HA diffraction peaks corresponding to (211), (112) and (300) planes at 31.8°, 32.2° and 32.9° respectively and did not show a peak at 31.0° (0210) which confirms that there was no secondary TCP phase present [Huang et al., 2007]. The XRD pattern of nHA powder showed that its crystallinity was lower than the other two HAs used in the study as the nHA peaks were broader and less intense. Sintered sHA showed very intense and narrow peaks, indicative of high crystallinity as would be expected after sintering. The crystallinity of HA is dependent on the temperature at which it is synthesised, HAs which are synthesised at higher temperature have higher crystallinity. The crystallinity of HA in turn affects the solubility of HA, HA with lower crystallinity have higher solubility [Matsumoto et al., 2004a; Zhu et al., 2006]. The XRD pattern of ßTCP also showed its purity as it showed the characteristics peaks corresponding to (214), (0210) and (220) planes at 27.8°, 31.0° and 34.4° respectively and did not show any peak at 30.7°(034), which is attributed to α-TCP [dos Santos et al., 2008].

FTIR of all the three HAs used in the study showed the OH peaks at 3571 and 631 cm^{-1}, the peak at 3571 cm^{-1} is assigned to stretching mode (v_s) while at 631 cm^{-1} is assigned to the librational mode (v_L) of OH group. The peak at 1040 cm^{-1} is assigned to P-O bond vibration of the PO_4 while the peak at 960 cm^{-1} is attributed to symmetric stretching of P-O bond of PO_4. The peaks at 603 and 569 cm^{-1} are assigned to bending mode of O-P-O bond of phosphate group [Rey et al., 1991; Koutsopoulos, 2002]. The absence of OH group in the spectra of TCP can be used to establish the difference between HA and TCP [de Aza et al., 1997]. Raman spectra of HAs showed a characteristic very strong peak at 960 cm^{-1} which is assigned to the P-O bond symmetric stretching of PO_4. Two peaks of medium intensities were also found at 590 and 450 cm^{-1} which are assigned to O-P-O bending mode of PO_4 [de Aza et al., 1997; Koutsopoulos, 2002].

SEM images of PLA and PLA/Ca P composite films showed the surface texture of these films. PLA films appeared smooth, whereas the composite films showed different degrees of surface roughness. Among the PLA-nHA films the films containing 10 wt % nHA appeared smooth as compared to films containing 40 and 70 wt % nHA. Additionally the films containing 40 and 70 wt % nHA had more nHA present on the film surfaces, whereas in films containing 10 wt % nHA most of

the nHA was embedded within the PLA matrix. Similarly in PLA-sHA composite films the surface roughness of films which had 40 and 70 wt% sHA was more than films with 10 wt % sHA content. The difference of roughness among the films containing 40 and 70 wt% sHA was not very pronounced, this can be due to more particle agglomeration in films containing 70 wt % sHA which resulted in less spread of particles in the matrix. The same roughness pattern was observed in PLA-rHA films, however the PLA-rHA films surface appear rougher as compared to PLA-sHA films which can be attributed to rougher rHA particles used in PLA-rHA films. With the greater specific surface area for the rHA more of the PLA will be involved. Among the PLA-TCP composite films, the films containing 10 wt % TCP had the most homogenous particle spread, while the films containing 40 and 70 wt % TCP showed some agglomeration of powders on their surfaces.

FTIR spectra of PLA-HA and PLA-TCP composite films showed the presence of characteristic PLA, TCP and HA peaks. The intensities of the peaks associated with PO_4 at 1040, 603 and 569 cm^{-1} increased with increase in the concentration of HA or TCP in the films from 10 to 70 wt %. This finding is in confirmation with the SEM images that more HA or TCP particles were present on the surfaces of the films containing higher concentrations of HA or TCP.

Raman spectra for PLA show the characteristic peaks. The peak at 875 cm^{-1} is characteristic of carbon-carbonyl bond (C-COO) stretching, while the peak at 1040 cm^{-1} corresponds to C-CH_3 stretching and the peak at 1766 cm^{-1} corresponds to C=O stretching. The peak at 1452 cm^{-1} corresponds to methyl group (CH_3) symmetric bending and at 1315 cm^{-1} to CH bending. The Raman spectra of PLA-HA and PLA-TCP composite films showed the characteristic strong peak PO_4 peak at 960 cm^{-1} in addition to PLA characteristics peaks. As the concentration of HA increased in the films the ratio of PO_4 peak also increased relative to PLA carbonyl bond (C-COO) peak at 875 cm^{-1}. As the spectra of composite films show the presence of both PLA and HA peak, it suggests that no chemical reaction took place during the mixing and the mixing was physical.

The presence of HA or TCP particles in higher quantities on the surface of the composite films may affect the biological and physical properties of the films.

2.6 CONCLUSIONS

Ca P powders and PLA-Ca P composite films were analysed using SEM, TEM, XRD, FTIR and Raman. The powders had different sizes and shapes. XRD, FTIR and Raman of Ca P confirmed the purity of these powders. The surface roughness of the films were influenced by the concentration and type of the powder used.

CHAPTER 3: BIOACTIVITY OF POLYLACTIC ACID-CALCIUM PHOSPHATE COMPOSITES

3.1 INTRODUCTION

Biodegradable polymers such as PLA are increasingly used in the treatment and fixation of skeletal defects due to their degradability in the body [Rokkanen et al., 2000a]. The advantages of using biodegradable polymers over non-resorbable implants are that they do not need a second surgical procedure for their removal and stress shielding effects can also be avoided. However one drawback associated with most of these polymers is their lack of bioactivity. Calcium phosphates such as HA and TCP, because of their osteoconductive and osteoinductive properties, are extensively studied and are widely used in various dental and orthopaedic application as they can accelerate the healing of bone tissue [Xin et al., 2005].

By using PLA with HA or TCP in a composite, the biodegradability and bioactivity of these materials can be combined to produce a material with enhanced properties. The bioactivity of materials is usually analysed by the ability of bone-like apatite to form on these materials when soaked in simulated body fluid (SBF). Ion concentrations in SBF closely match those present in human blood plasma (Table 3.1) [Kokubo et al., 1990].

Table 3.1: Comparison of ion concentrations in human blood plasma and SBF [adapted from Kokubo and Takadama, 2006].

	Ion concentrations (mM)							
	Na^+	K^+	Mg^{2+}	Ca^{2+}	Cl^-	HCO^-_3	$HPO^2_4^-$	SO_4^{2-}
Blood plasma	142.0	5.0	1.5	2.5	103.0	27.0	1.0	0.5
SBF	142.0	5.0	1.5	2.5	147.8	4.2	1.0	0.5

The aim of this study is to investigate the bioactivity of PLA-HA and PLA-TCP composite films by assessing the ability of an apatite layer to form on their surface when immersed in SBF.

3.2 MATERIALS

The materials used were PLA (PURAC Biochem, The Netherlands), nHA (Sigma-Aldrich, UK), sHA and rHA (Plasma Biotal Limited, UK) and TCP (Plasma Biotal Limited, UK) as described in detail in section 2.2.

3.3 METHODS

3.3.1 Preparation of Simulated Body Fluid

Simulated body fluid (SBF) was prepared as described by [Kokubo and Takadama, 2006] by dissolving reagents in deionised water. The reagents, their quantities and the order in which they were dissolved in the deionised water for the preparation of 1000 ml SBF are shown in Table 3.2. All the reagents were purchased from Sigma Aldrich, UK.

Table 3.2: Order, reagents and their quantities used for the preparation of 1000 ml SBF solution [adapted from Kokubo and Takadama, 2006].

Order	Reagent	Quantity
1	NaCl	8.035g
2	$NaHCO_3$	0.355g
3	KCl	0.225g
4	$K_2HPO_4.3H_2O$	0.231g
5	$MgCl_2.6H_2O$	0.311g
6	1.0_M-HCl	39ml
7	$CaCl_2$	0.292g
8	Na_2SO_4	0.072g
9	Tris	6.118g
10	1.0_M-HCl	0-5ml

For the preparation of 1000ml SBF initially 700ml of deionised water was placed in a glass beaker with a stirring bar and was heated up to 36.5 $\pm$ 1.5 °C on a magnetic stirrer. The reagents were dissolved in the water one by one at 36.5 $\pm$ 1.5 °C in the order of 1 to 8 as listed in Table 1. The next reagent was only added after the previous reagent was completely dissolved. Before the addition of 9^{th} and 10^{th} reagent, the solution volume was adjusted to 900ml. After volume

adjustment Tris was added to the solution little by little to gradually raise the pH of the solution to 7.45±0.01. Addition of Tris was stopped once the pH of the solution reached 7.45±0.01, as a next step HCl was added to the solution to lower the pH to 7.42±0.01 taking care not to lower the pH below 7.40. Again, the remaining Tris was added until the pH of the solution reached 7.45±0.01. The procedure of alternate addition of Tris and HCl was repeated to maintain the pH between 7.42 and 7.45 until all the Tris had dissolved. Finally after dissolving the total Tris the pH of the solution was adjusted to 7.40 by adding a small amount of HCl at 36.5°C. After cooling the solution to 20°C, deionised water was added to the solution to adjust the solution volume to 1000ml.

3.3.2 Sample Preparation

The films were prepared as described in section 2.3.1. The resultant films were then cut into 12 mm diameter discs and 5 samples for each time point and composite were used. The samples were sterilised by soaking in 70% ethanol for 1 minute and then dried at 50°C. The samples were immersed into 20 ml SBF in polystyrene bottles for 1, 7, 14, 21 and 28 days at 37 °C. The SBF in bottles was replaced by fresh SBF after 14 days. At given time points the samples were removed from the solution and rinsed with distilled water and dried at 50°C.

3.3.3 Sample characterisation

The samples were characterised by scanning electron microscopy (SEM) with energy dispersive spectroscopy (EDS) and Raman Spectroscopy.

3.3.3.1 SEM

The samples were carbon coated for SEM. SEM images and EDS spectra were obtained by using FEI Inspect F, EFI Company, The Netherlands.

3.3.3.2 Raman Spectroscopy

Nicolet Almega XR dispersive Raman spectrometer was used to obtain Raman spectra of the samples, spectra were collected by taking 128 numbers of scans/

sample and an exposure time of 2 sec was used at 8 cm^{-1} resolution. The spectra were collected between 4000-100cm^{-1}.

3.4 RESULTS

3.4.1 SEM

3.4.1.1 PLA

SEM images of PLA samples at 1, 7, 14, 21 and 28 days after immersion in SBF are shown in Figure 3.1. There was no apatite formation observed on PLA films immersed in SBF, even after 28 days.

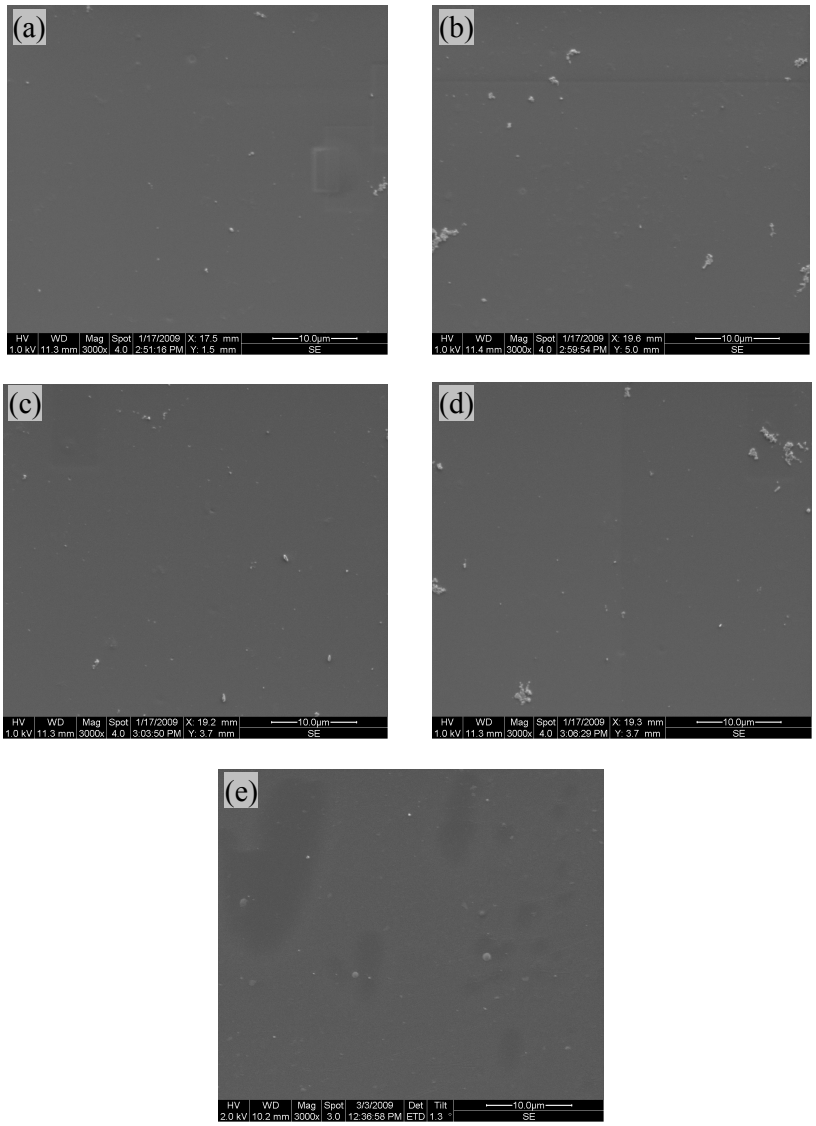

Figure 3.1: SEM images of PLA at day (a) 1, (b) 7, (c) 14, (d) 21 and (e) 28 days after immersion in SBF. (Scale bar=10 μm)

EDS analysis of PLA samples in SBF are showed in Figure 3.2. The spectra showed C and O peaks corresponding to carbon and oxygen present in the polymer and there were no Ca or P peaks corresponding to an apatite layer. However, at 28th day of immersion in SBF the spectra of the PLA sample showed small Na and Cl peaks which are probably due to deposition of these elements from SBF.

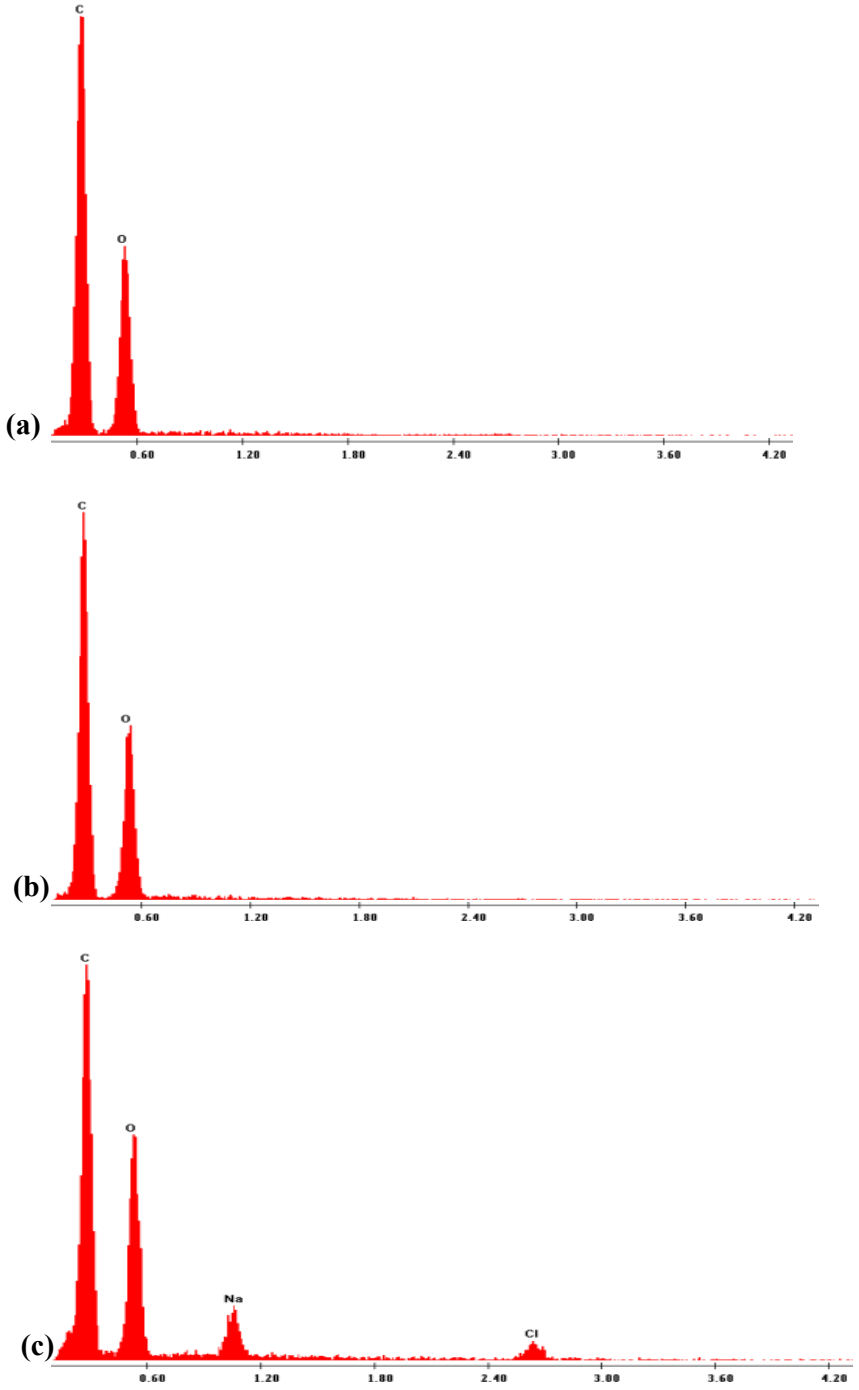

Figure 3.2: EDS spectra of PLA films at (a) 1, (b) 14 and (c) 28 days after immersion in SBF.

3.4.1.2 PLA-nHA composite films

Figures 3.3, 3.4 and 3.5 shows the SEM images of PLA-nHA10, PLA-nHA40 and PLA-nHA70 samples respectively at (a) 1, (b) 7, (c) 14, (d) 21 and (e) 28 days after immersion in SBF. As the figure shows, there was no apatite formation on day 1 on PLA-nHA10 and PLA-nHA40 films, however apatite formation was observed on these films on day 7. Whereas PLA-nHA70 film showed apatite formation on day 1 and by day 7 the sample was fully covered with the apatite layer. The apatite layer subsequently increased with time on PLA-nHA10 and PLA-nHA40 samples and by 21 days, it had started to become dense and packed. The apatite layers produced on the films containing 40 and 70 wt% nHA present finer microstructure as compared to the layer on film containing 10 wt% HA which has a globular appearance, this difference in morphology of the apatite layer is probably due to the presence of more crystallisation nuclei. By 28 days, the apatite layer was covering most of the samples surface. Whereas PLA-nHA70 film was fully covered by apatite layer on 7^{th} day and at 28^{th} day the apatite layer had considerably increased in thickness and had become very dense.

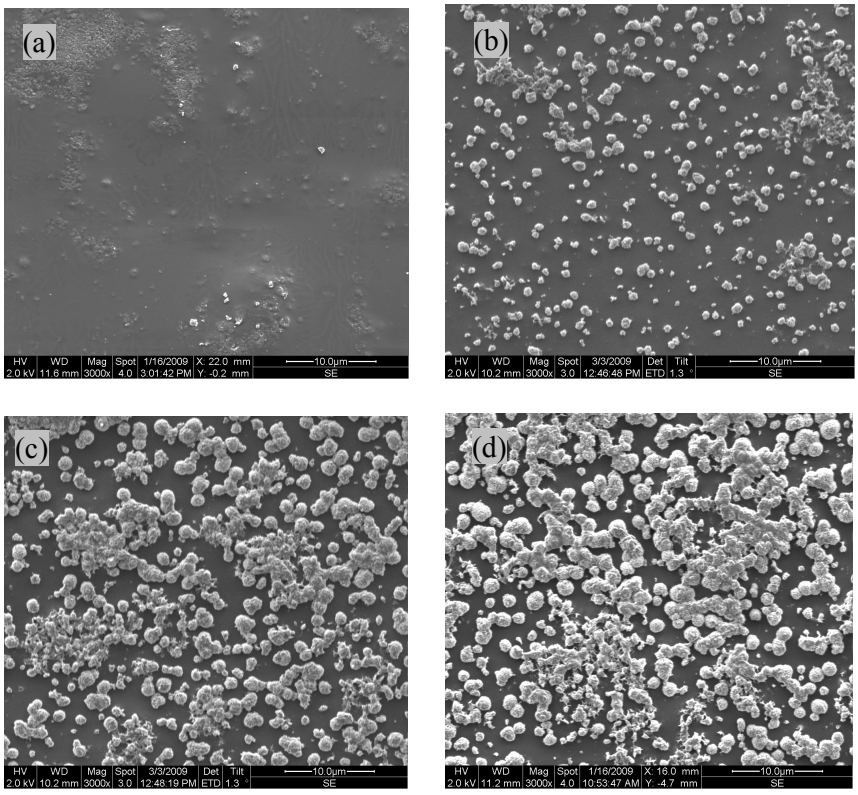

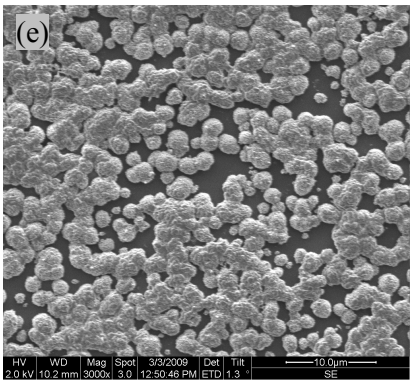

Figure 3.3: SEM images of PLA-nHA10 at day (a) 1, (b) 7, (c) 14, (d) 21 and (e) 28 days after immersion in SBF (all scale bars =10 µm).

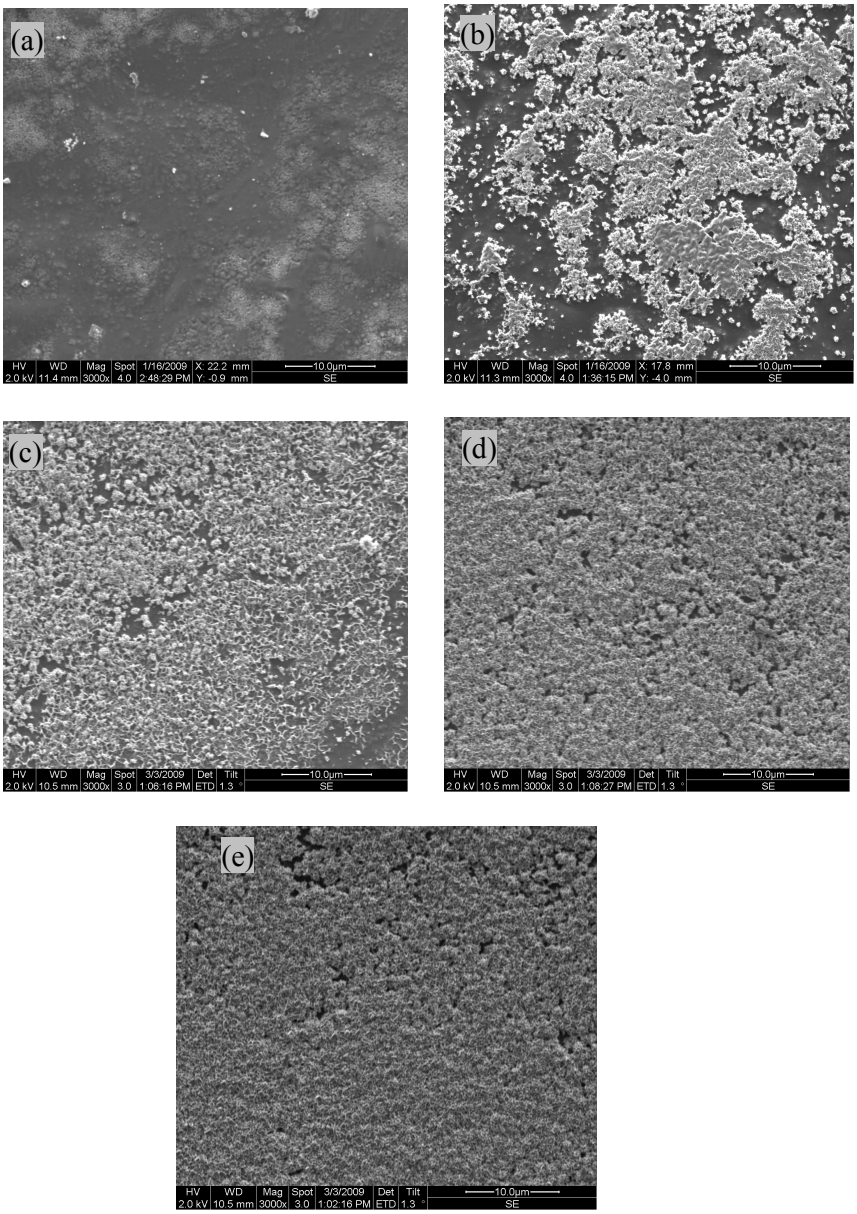

Figure 3.4: SEM images of PLA-nHA40 at day (a) 1, (b) 7, (c) 14, (d) 21 and (e) 28 days after immersion in SBF (all scale bars =10 µm).

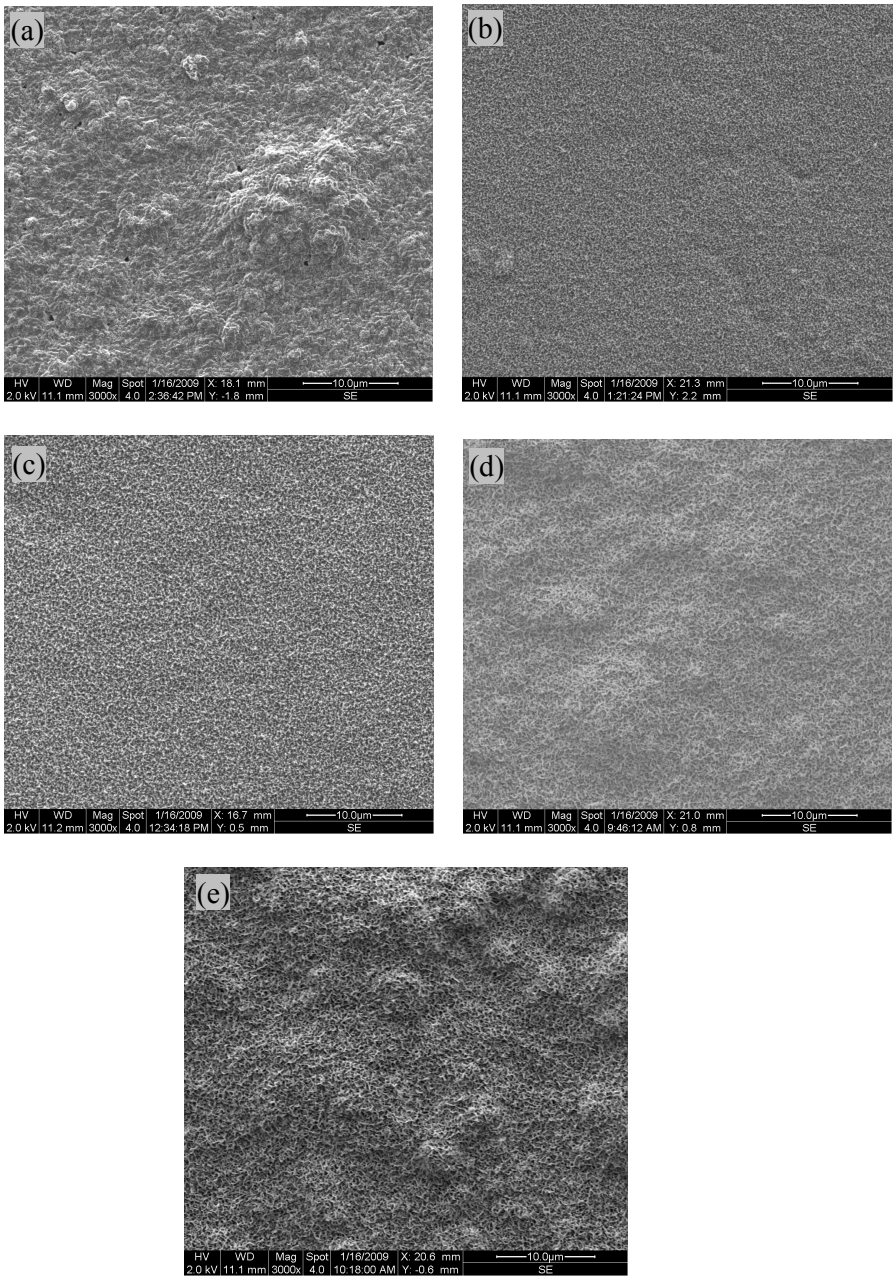

Figure 3.5: SEM images of PLA-nHA70 at day (a) 1, (b) 7, (c) 14, (d) 21 and (e) 28 days after immersion in SBF (all scale bars =10 µm) .

Figures 3.6, 3.7 and 3.8 shows the respective EDS spectra for PLA-nHA10, PLA-nHA40 and PLA-nHA70 samples at (a) 1, (b) 14 and (c) 28 days after immersion in SBF. Although the spectra for PLA-nHA10 and PLA-nHA40 shows the presence of Ca and P peaks even at day 1, these peaks do not correspond to apatite layer formation but to HA present in the films. However, the intensity of Ca and P peaks increased with the increase of immersion time in SBF that represent the formation of apatite layer. The EDS spectra for PLA-nHA70 showed high Ca and P peaks even on day 1 and the intensity of these peaks did not change much over time especially after day 14th.

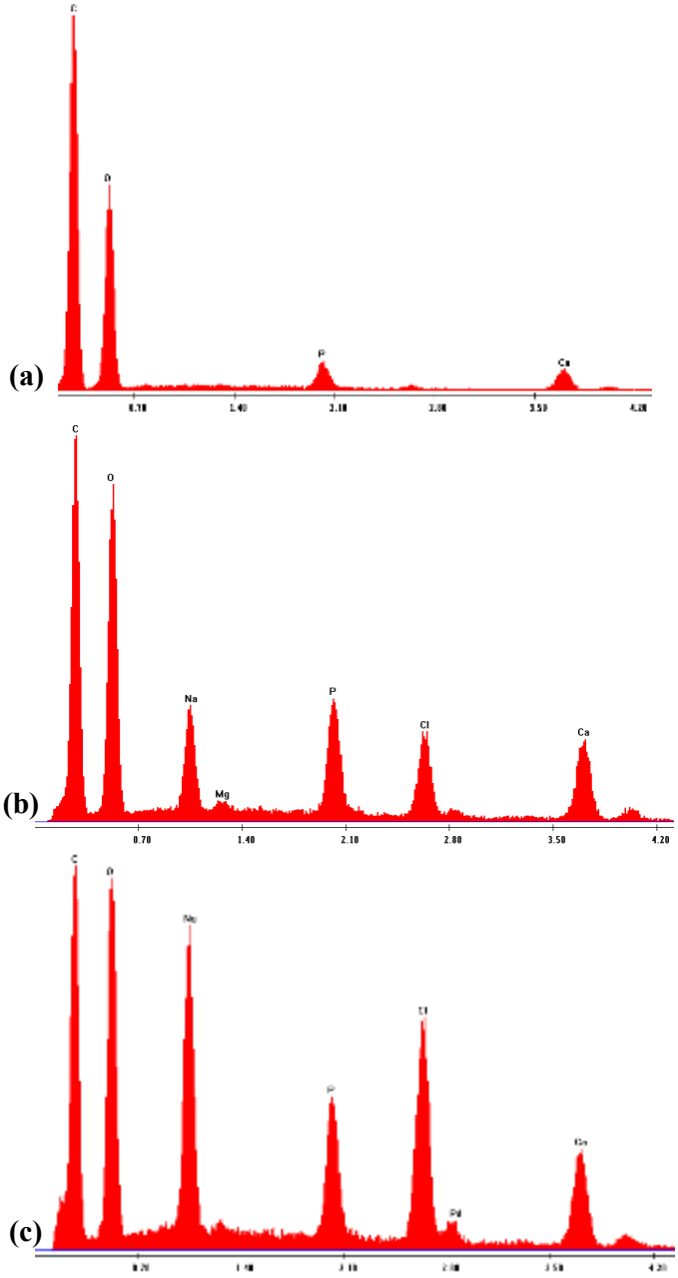

Figure 3.6: EDS spectra of PLA-nHA10 at (a) 1, (b) 14 and (c) 28 days after immersion in SBF

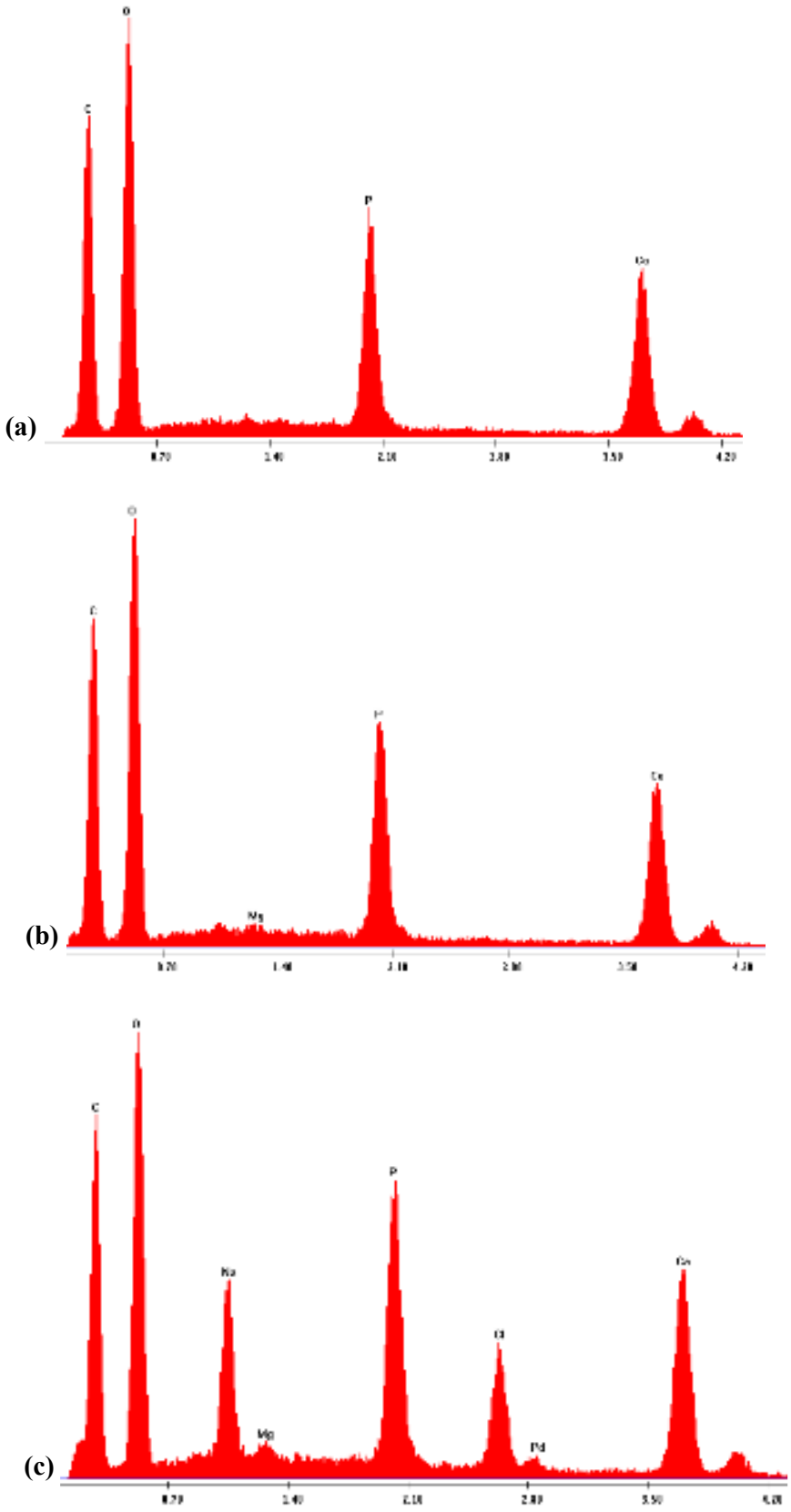

Figure 3.7: EDS spectra of PLA-nHA40 at (a) 1, (b) 14 (c) 28 days after immersion in SBF.

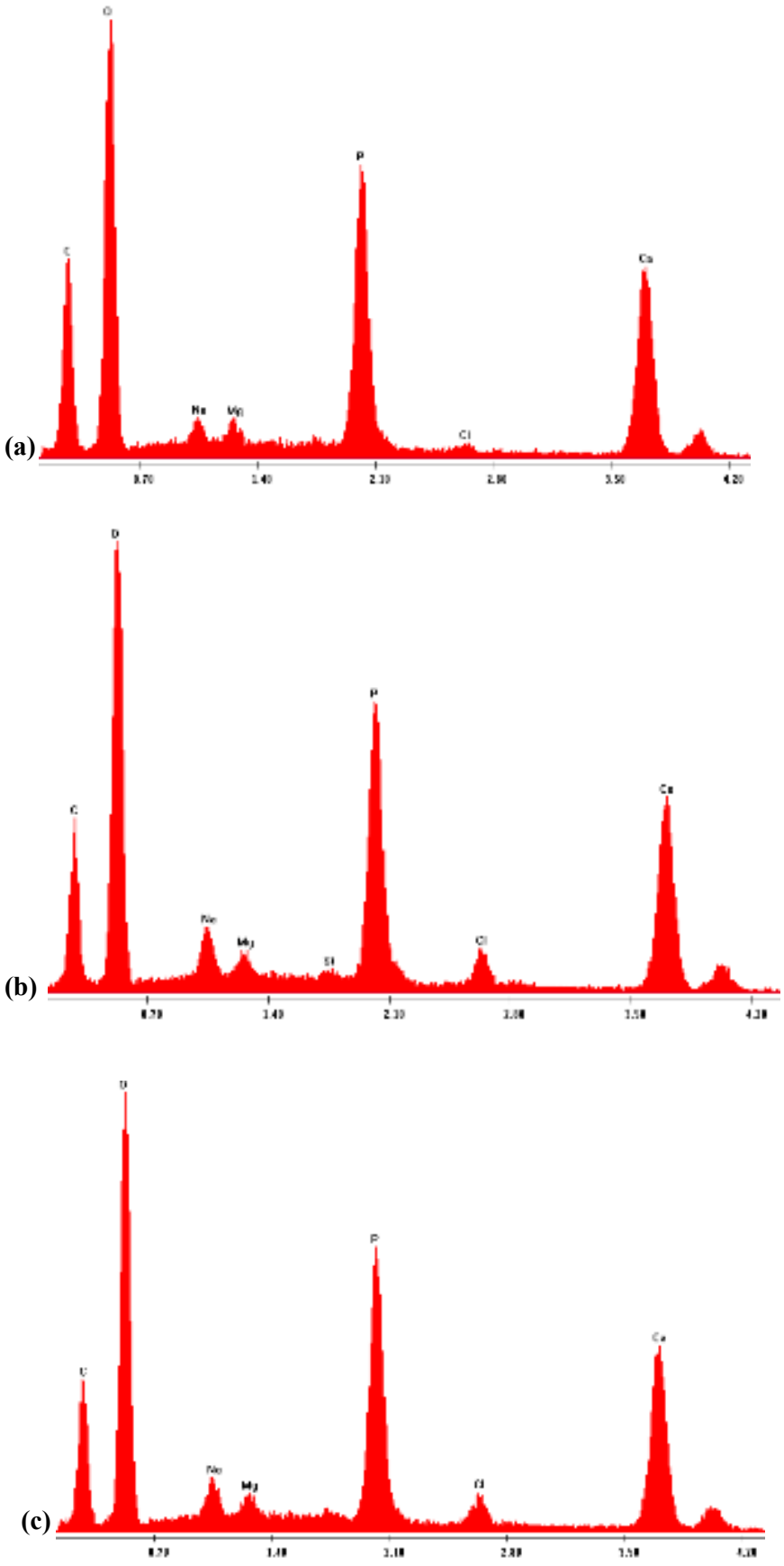

Figure 3.8: EDS spectra of PLA-nHA70 at (a) 1, (b) 14 (c) 28 days after immersion in SBF.

3.4.1.3 PLA-rHA composite films

Figures 3.9, 3.10 and 3.11 show the surface morphologies of PLA-rHA10, PLA-rHA40 and PLA-rHA70 samples respectively at (a) 1, (b) 7, (c) 14, (d) 21 and (e) 28 days after immersion in SBF. There was no apatite formation on any film at day 1. However all the films have apatite crystals formed at day 7. With increases in the soaking time the quantity and size of these crystals increased. More nucleation centres were present on films containing higher amounts of HA and these films showed increased apatite layer formation. Although by 21 days all the films were fully covered with the apatite layer, this layer was dense and more tightly packed on the film containing 70 wt% HA.

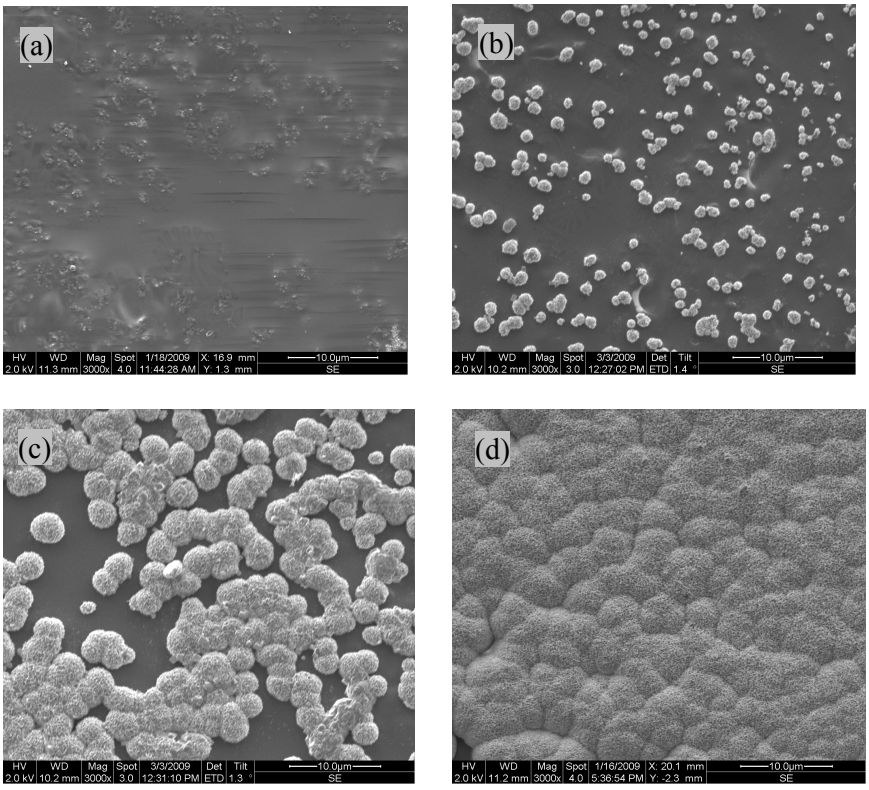

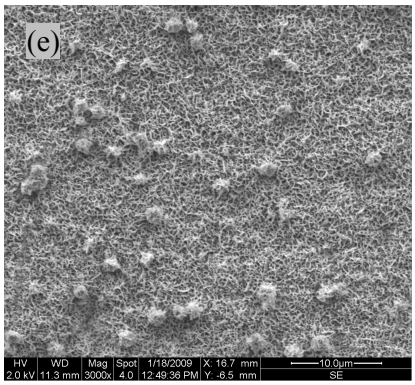

Figure 3.9: SEM images of PLA-rHA10 at day (a) 1, (b) 7, (c) 14, (d) 21 and (e) 28 days after immersion in SBF (all scale bars =10 µm).

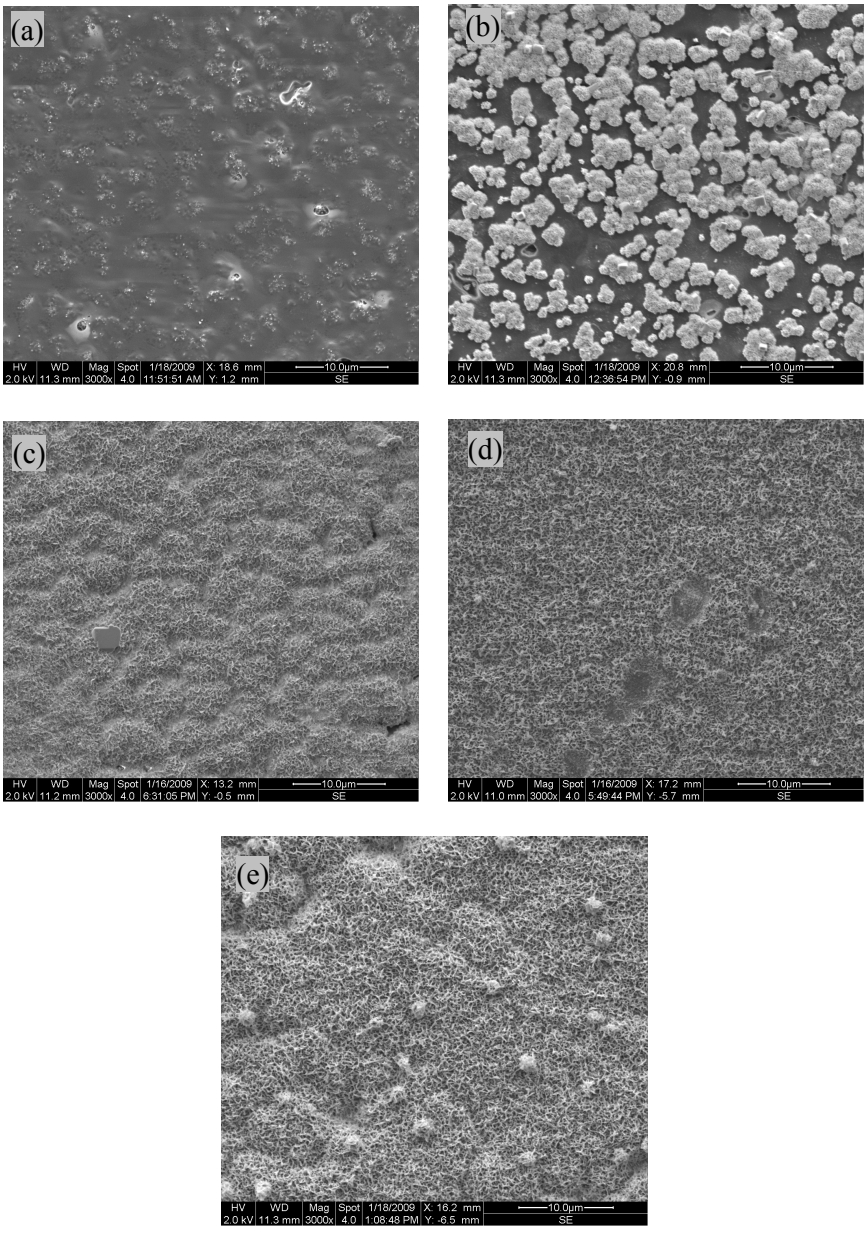

Figure 3.10: SEM images of PLA-rHA40 at day (a) 1, (b) 7, (c) 14, (d) 21 and (e) 28 days after immersion in SBF (all scale bars =10 µm) .

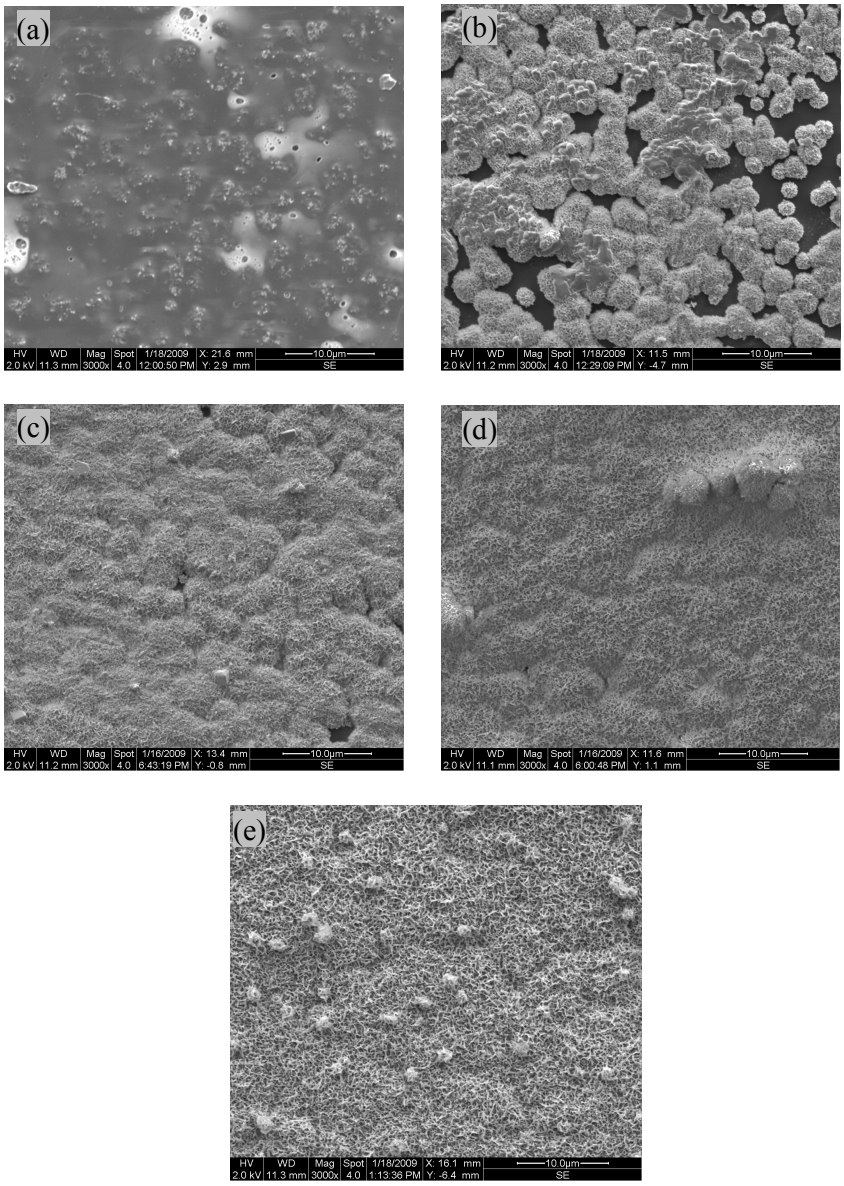

Figure 3.11: SEM images of PLA-rHA70 at day (a) 1, (b) 7, (c) 14, (d) 21 and (e) 28 days after immersion in SBF (all scale bars =10 µm) .

Figures 3.12, 3.13 and 3.14 show the EDS spectra for PLA-rHA10, PLA-rHA40 and PLA-rHA70 samples respectively at (a) 1, (b) 14 and (c) 28 days after immersion in SBF. At day 1 the spectra of all the films showed Ca and P peaks which are due to the presence of HA in the films and the intensity of these peaks were high in film containing higher amounts of HA.

However, the intensity of these peaks subsequently increased for all the films after immersion in the SBF due to the formation of apatite layer.

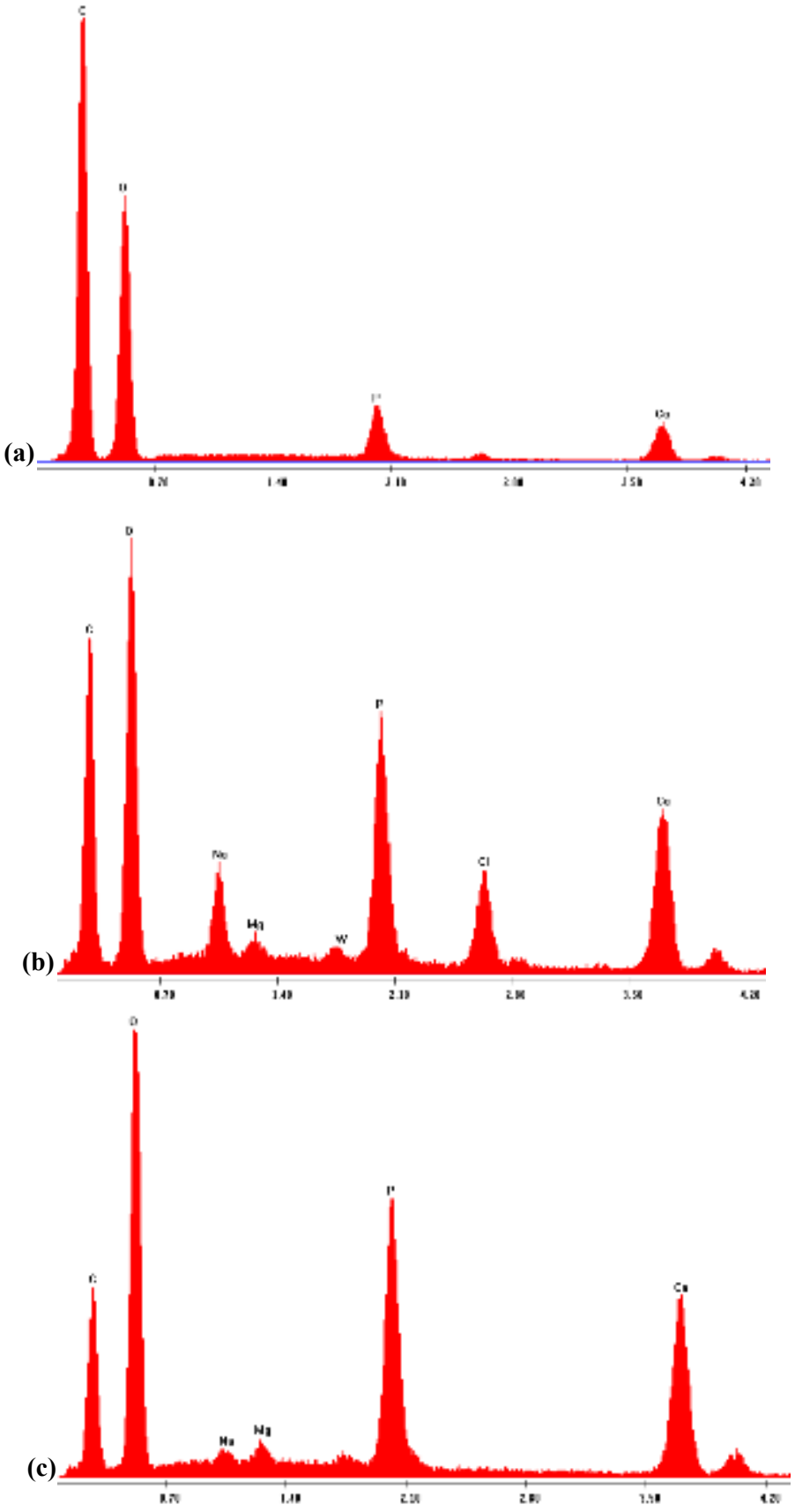

Figure 3.12: EDS spectra for PLA-rHA10 at (a) 1, (b) 14 and (c) 28 days after immersion in SBF.

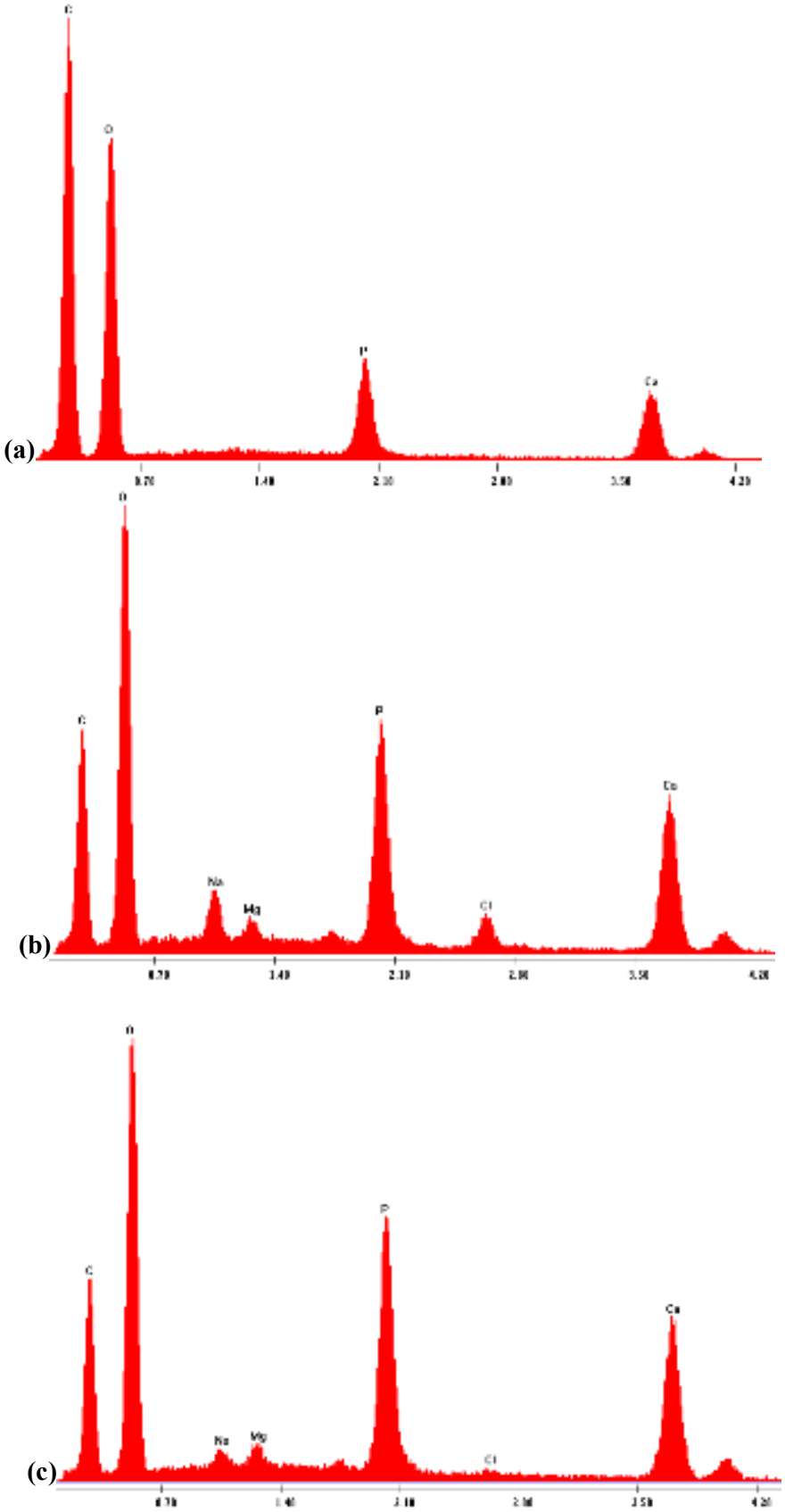

Figure 3.13: EDS spectra for PLA-rHA40 at (a) 1, (b) 14 and (c) 28 days after immersion in SBF.

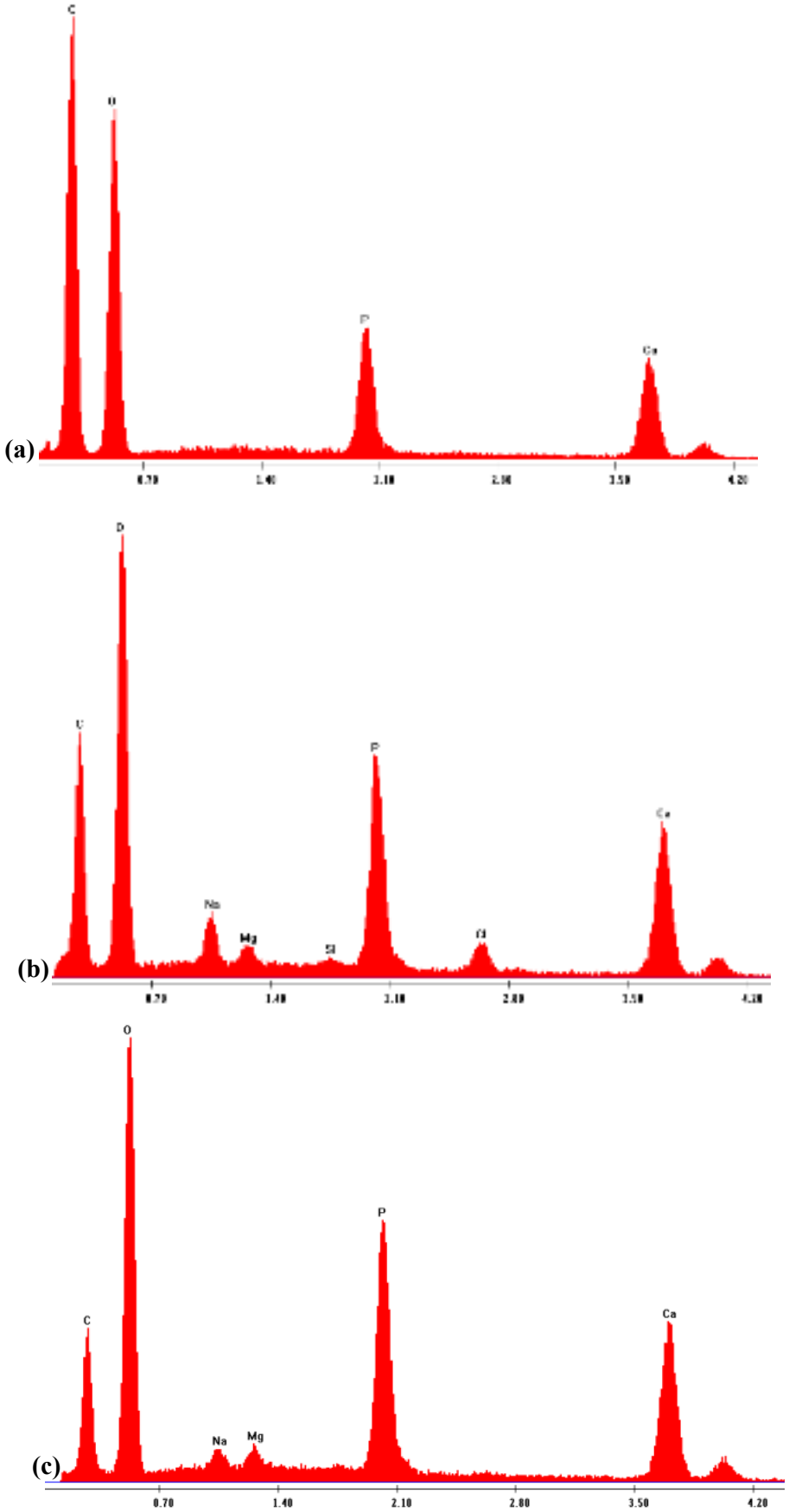

Figure 3.14: EDS spectra of PLA-rHA70 at (a) 1, (b) 14 and (c) 28 days after immersion in SBF.

3.4.1.4 PLA-sHA composite films

Figures 3.15, 3.16 and 3.17 show the SEM images of PLA-sHA10, PLA-sHA40 and PLA-sHA70 samples respectively at (a) 1, (b) 7, (c) 14, (d) 21 and (e) 28 days after immersion in SBF. There was no apatite formation on any film at day 1. At day 7 apatite formation has already started on all the films, with the highest amount formed on films containing 70 wt% sHA. Apatite formation started at individual sites and then grew in size and subsequently united to form a layer. The apatite layer subsequently increases with increase in immersion time on all films and by 21 days the all the films were fully covered with the apatite layer.

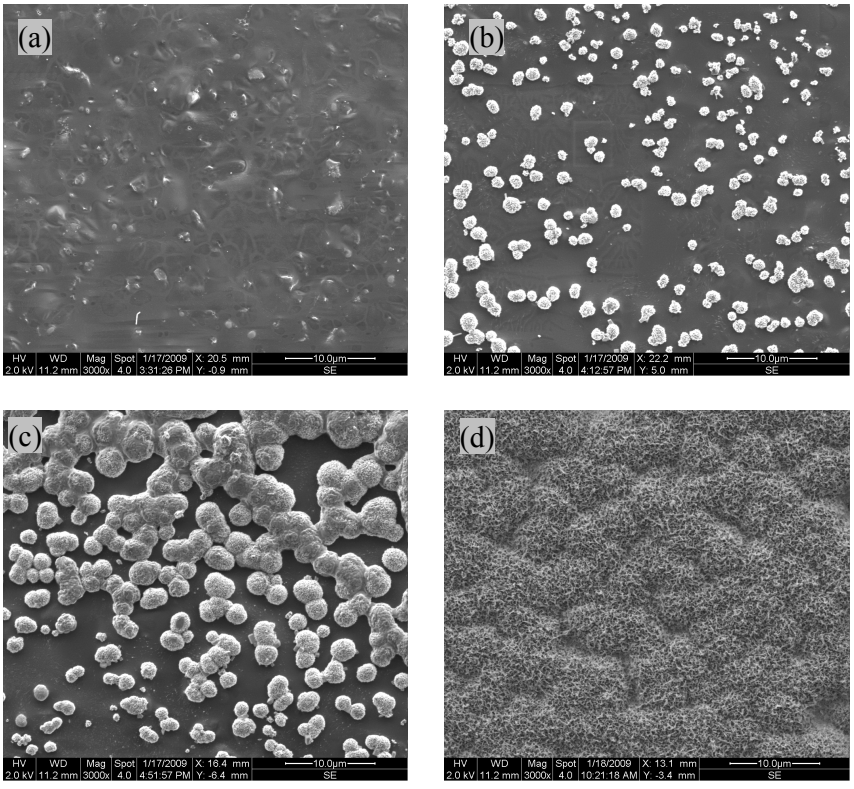

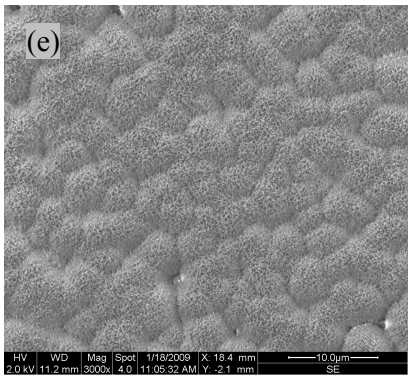

Figure 3.15: SEM images of PLA-sHA10 at day (a) 1, (b) 7, (c) 14, (d) 21 and (e) 28 days after immersion in SBF (all scale bars =10 µm).

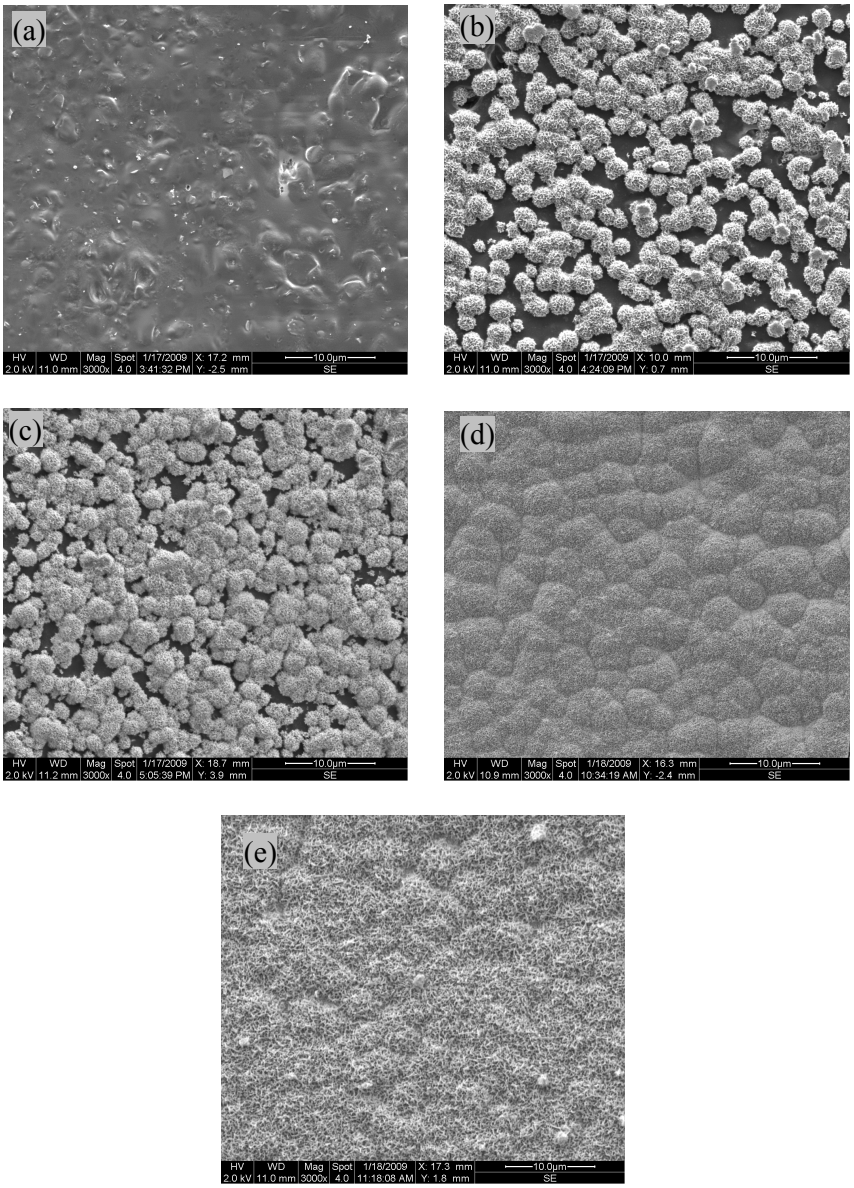

Figure 3.16: SEM images of PLA-sHA40 at day (a) 1, (b) 7, (c) 14, (d) 21 and (e) 28 days after immersion in SBF (all scale bars =10 µm).

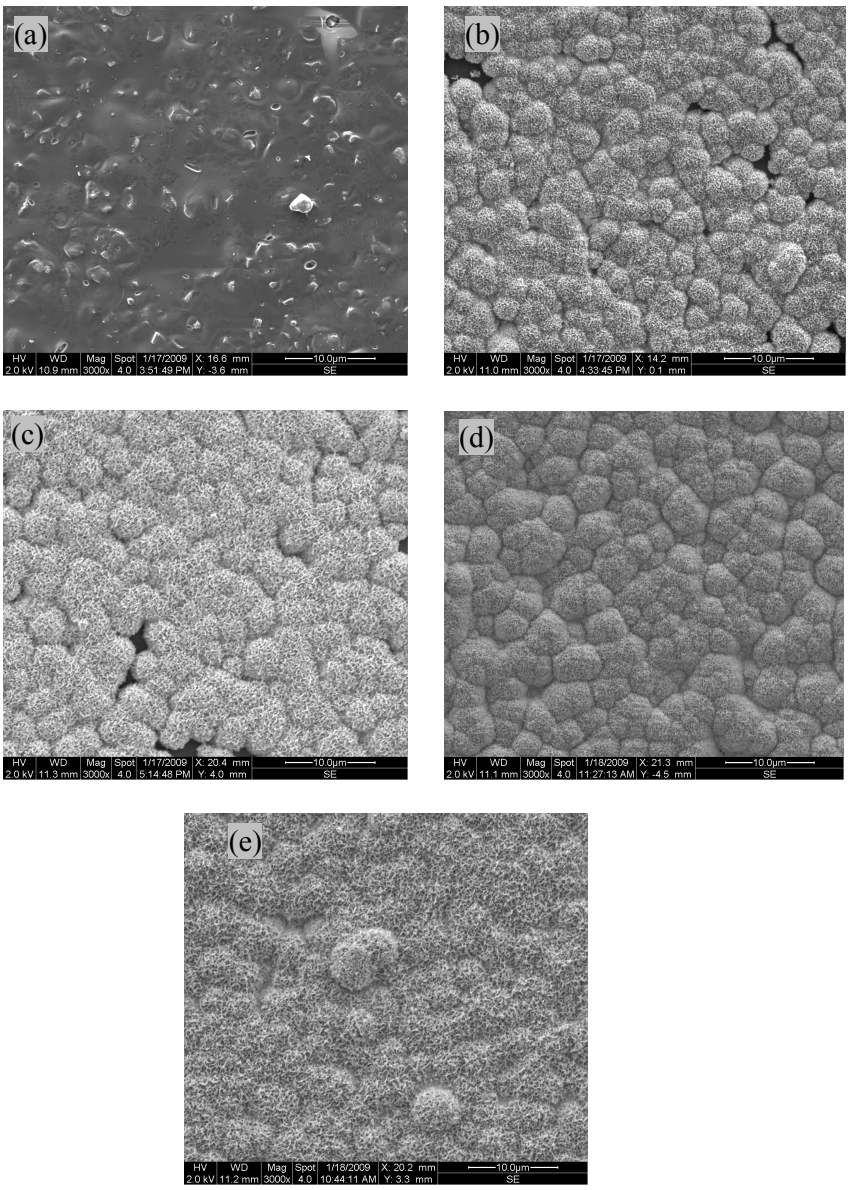

Figure 3.17: SEM images of PLA-sHA70 at day (a) 1, (b) 7, (c) 14, (d) 21 and (e) 28 days after immersion in SBF (all scale bars =10 µm).

Figures 3.18, 3.19 and 3.20 show the EDS spectra for PLA-sHA10, PLA-sHA40 and PLA-sHA70 samples respectively at (a) 1, (b) 14, and (c) 28 days after immersion in SBF. Ca and P peaks present at day 1 correspond to the sHA present in the films and the intensity of these peaks is directly proportional to the amount of sHA present.

The intensity of these peaks subsequently increased for all the films after immersion in the SBF, which representing formation of an apatite layer on these films.

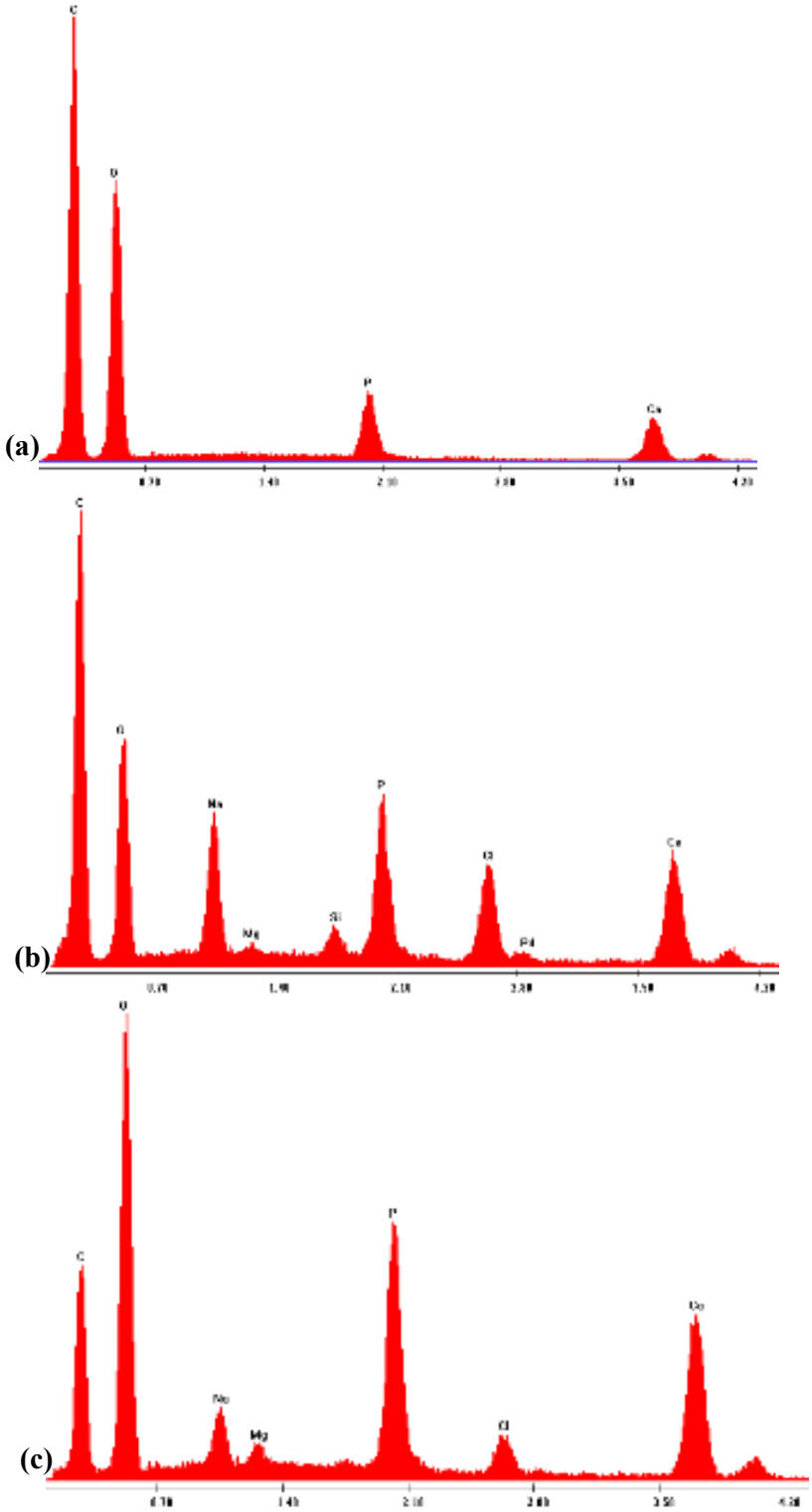

Figure 3.18: EDS spectra of PLA-sHA10 at (a) 1, (b) 14 and (c) 28 days after immersion in SBF.

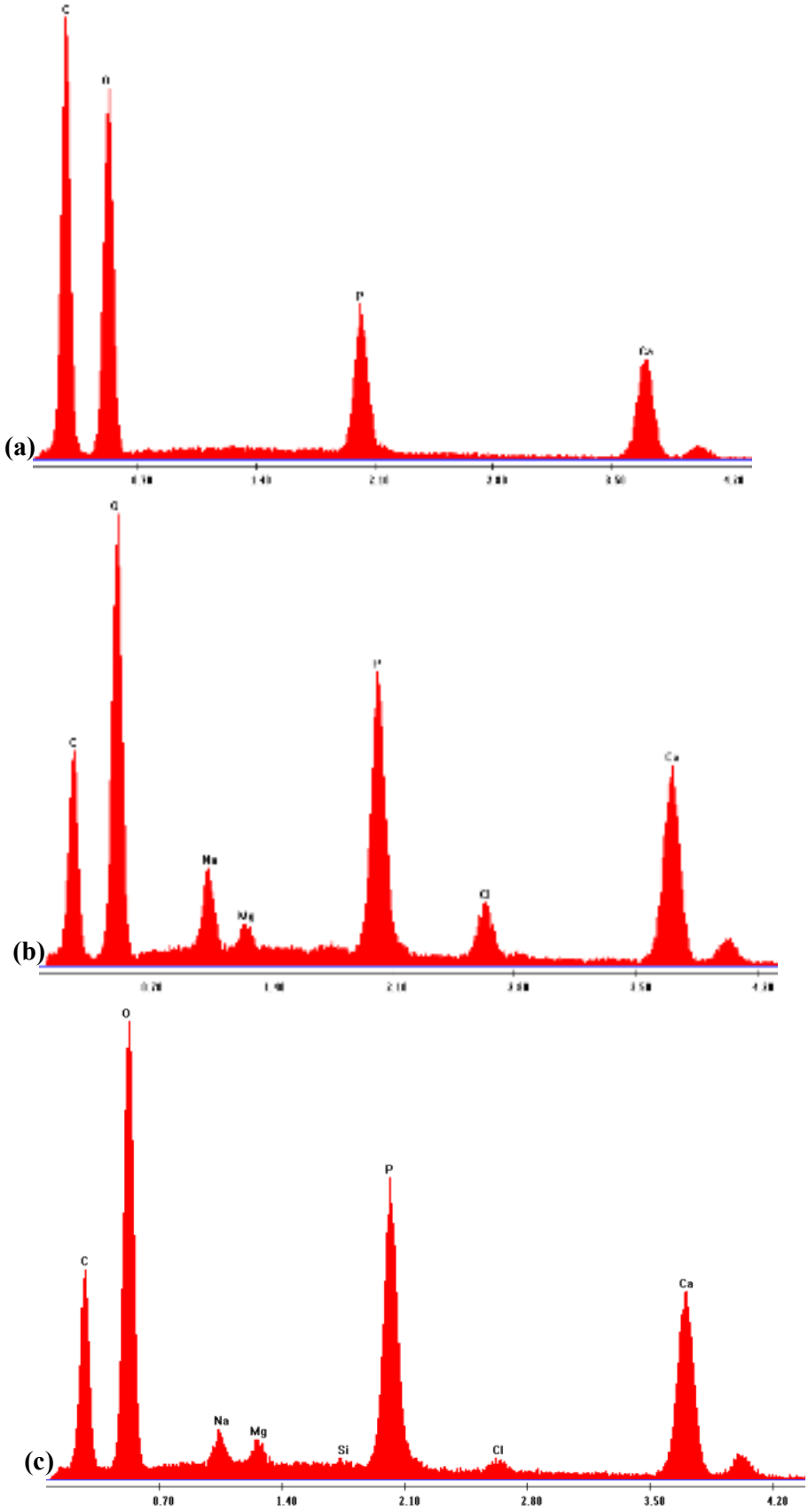

Figure 3.19: EDS spectra of PLA-sHA40 at (a) 1, (b) 14 and (c) 28 days after immersion in SBF.

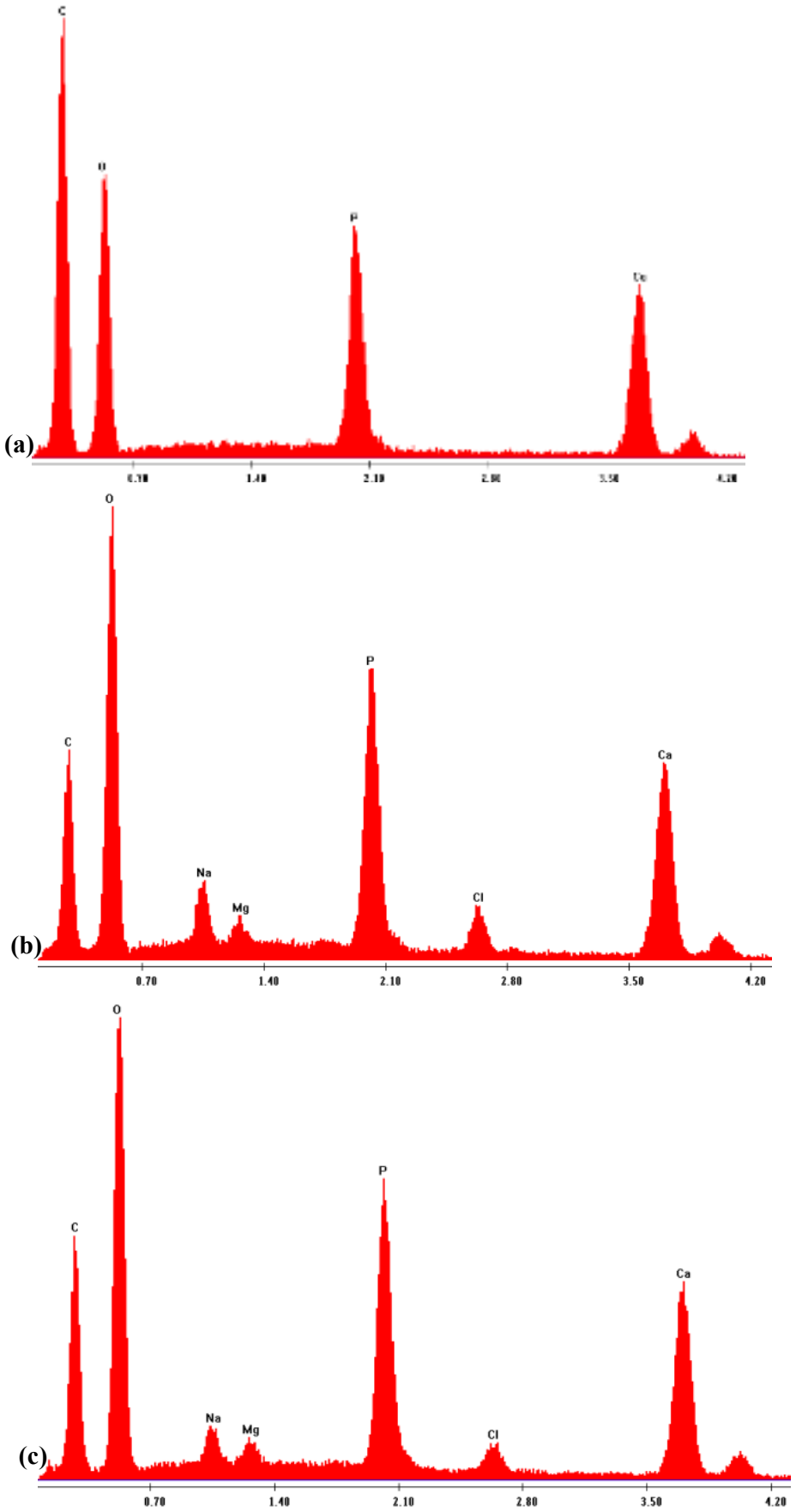

Figure 3.20: EDS spectra of PLA-sHA70 at (a) 1, (b) 14 and (c) 28 days after immersion in SBF.

3.4.1.5 PLA-TCP composite films

Figures 3.21, 3.22 and 3.23 show the SEM images of PLA-TCP10, PLA-TCP40 and PLA-TCP 70 samples respectively at (a) 1, (b) 7, (c) 14, (d) 21 and (e) 28 days after immersion in SBF. There was no apatite formation on films containing 10 and 40% TCP at day 1, however the film containing 70% TCP had apatite particles on its surface. All the films have apatite layer formation at day 7. The number of apatite particles increased on the films with increases in soaking time and the number of apatite crystals were directly proportional to the amount TCP present in the films. The apatite layer subsequently increases with time on all films, however, the film containing 70% TCP showed highest apatite formation.

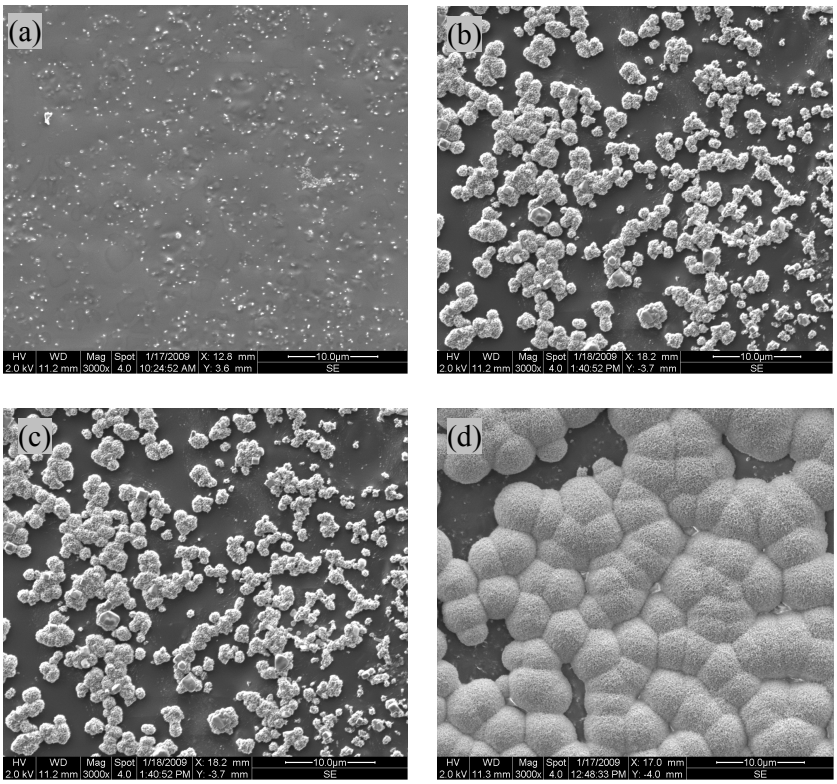

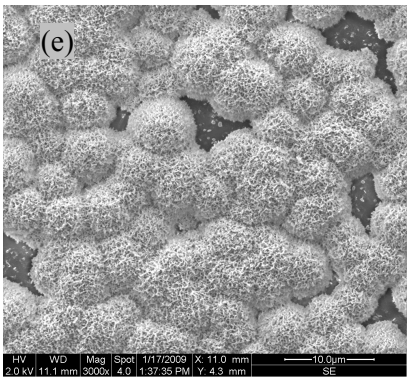

Figure 3.21: SEM images of PLA-TCP10 at day (a) 1, (b) 7, (c) 14, (d) 21 and (e) 28 days after immersion in SBF (all scale bars =10 μm).

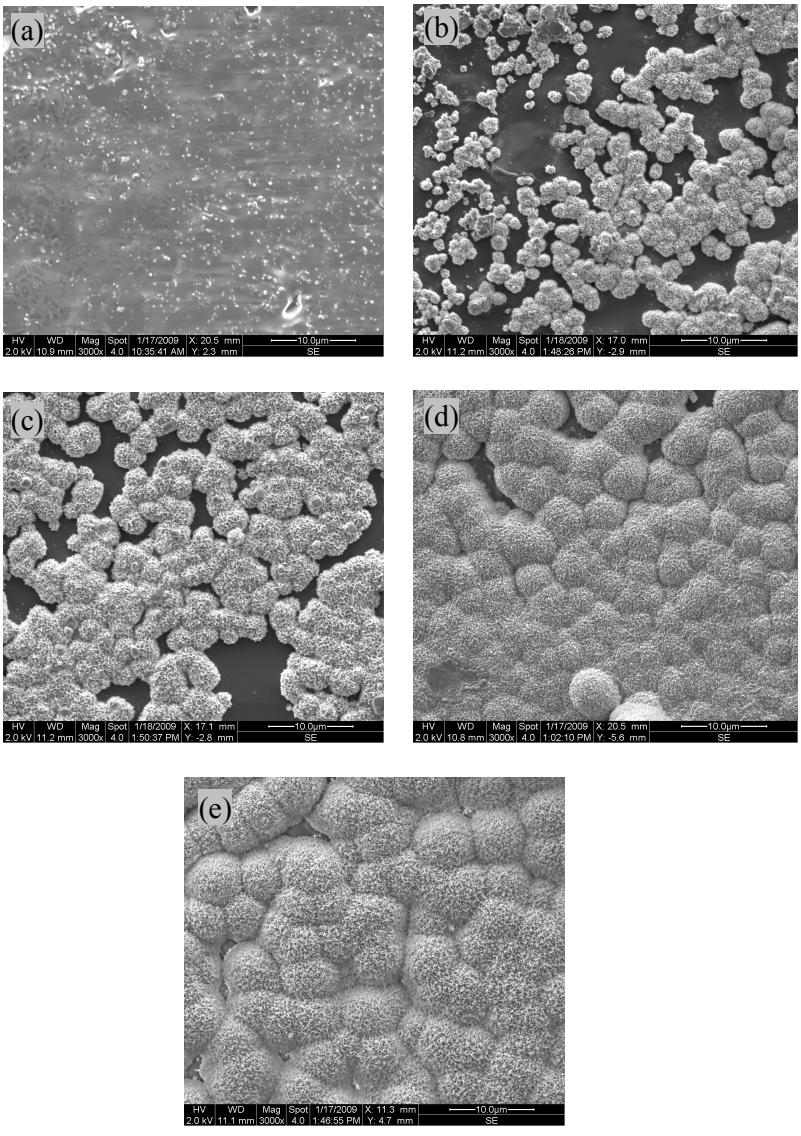

Figure 3.22: SEM images of PLA-TCP40 at day (a) 1, (b) 7, (c) 14, (d) 21 and (e) 28 days after immersion in SBF (all scale bars =10 μm).

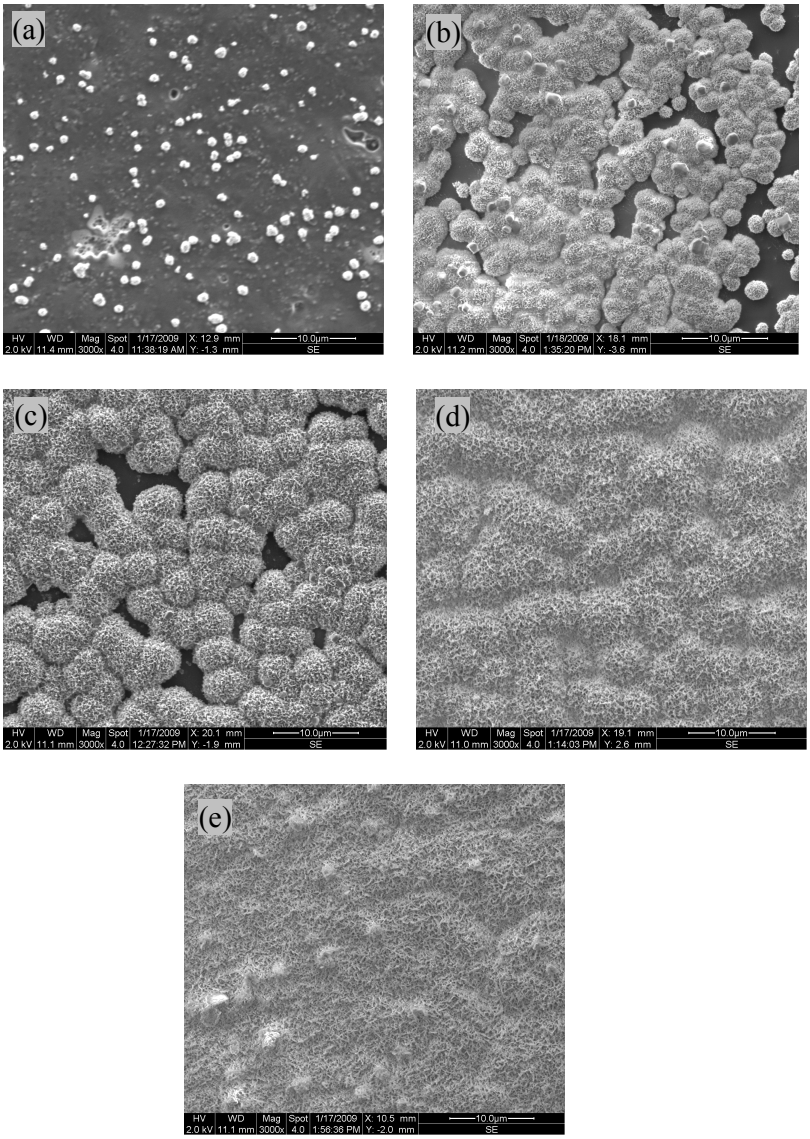

Figure 3.23: SEM images of PLA-TCP70 at day (a) 1, (b) 7, (c) 14, (d) 21 and (e) 28 days after immersion in SBF (all scale bars =10 µm).

Figures 3.24, 3.25 and 3.26 show the EDS spectra for PLA-TCP10, PLA-TCP40 and PLA-TCP70 samples respectively at (a) 1, (b) 14, and (c) 28 days after immersion in SBF. At day 1 the spectra of all the films showed Ca and P peaks which are due to the presence of TCP in the films and the intensity of these peaks were high in film containing higher amounts of TCP.

The intensity of these peaks subsequently increased for all the films with the formation of apatite layer after immersion in the SBF.

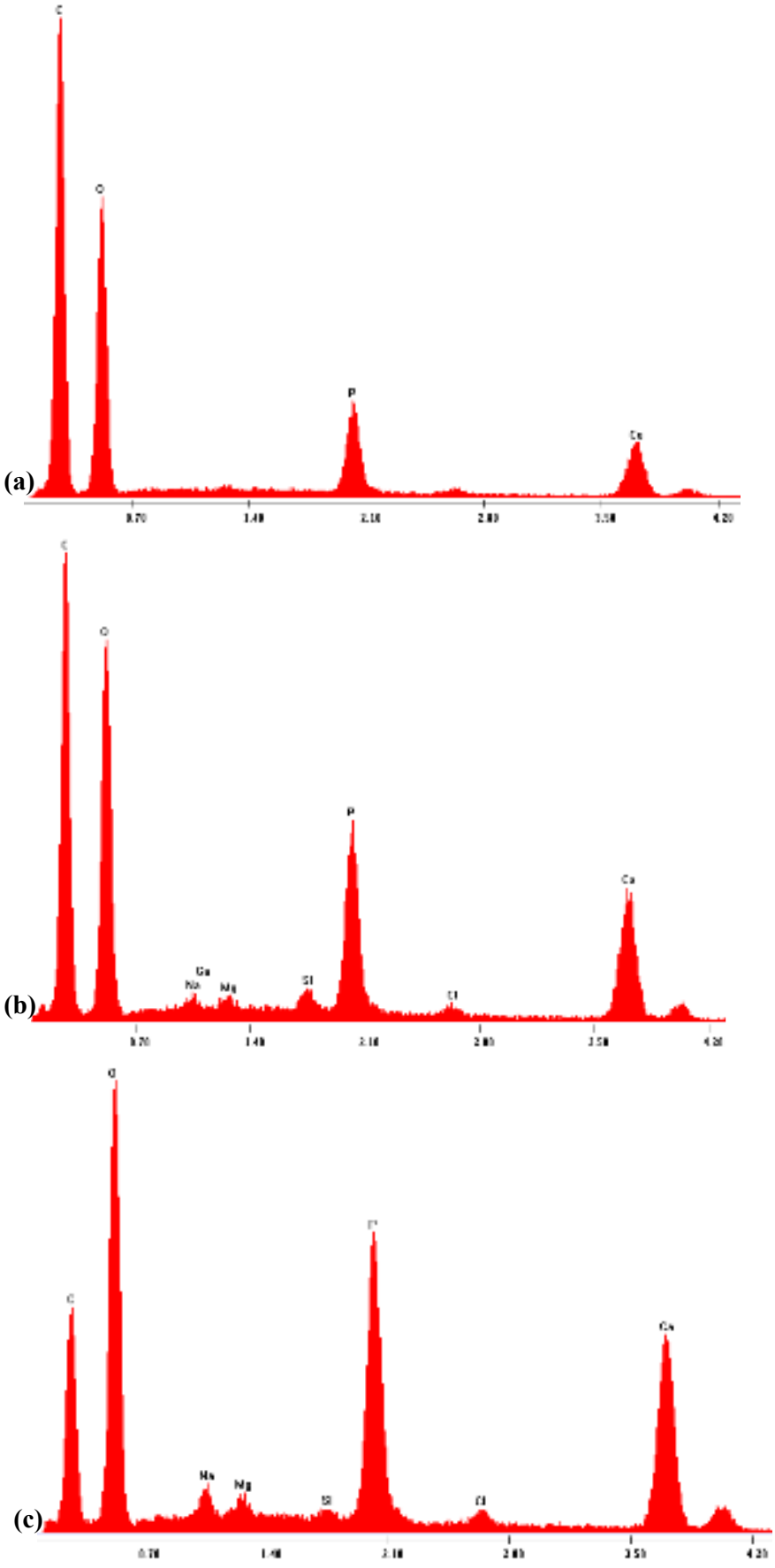

Figure 3.24: EDS spectra of PLA-TCP10 at (a) 1, (b) 14 and (c) 28 days after immersion in SBF

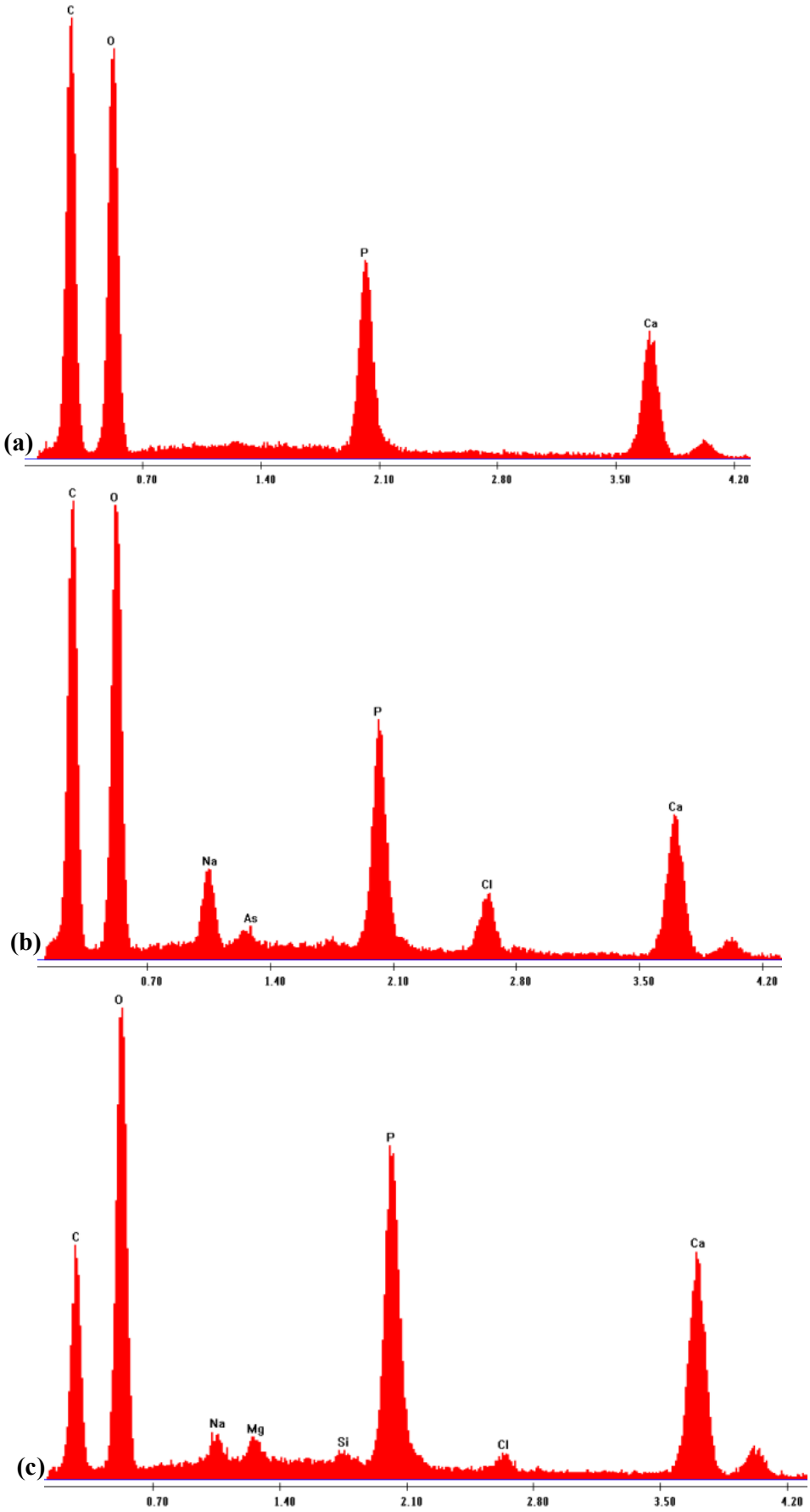

Figure 3.25: EDS spectra of PLA-TCP40 at (a) 1, (b) 14 and (c) 28 days after immersion in SBF.

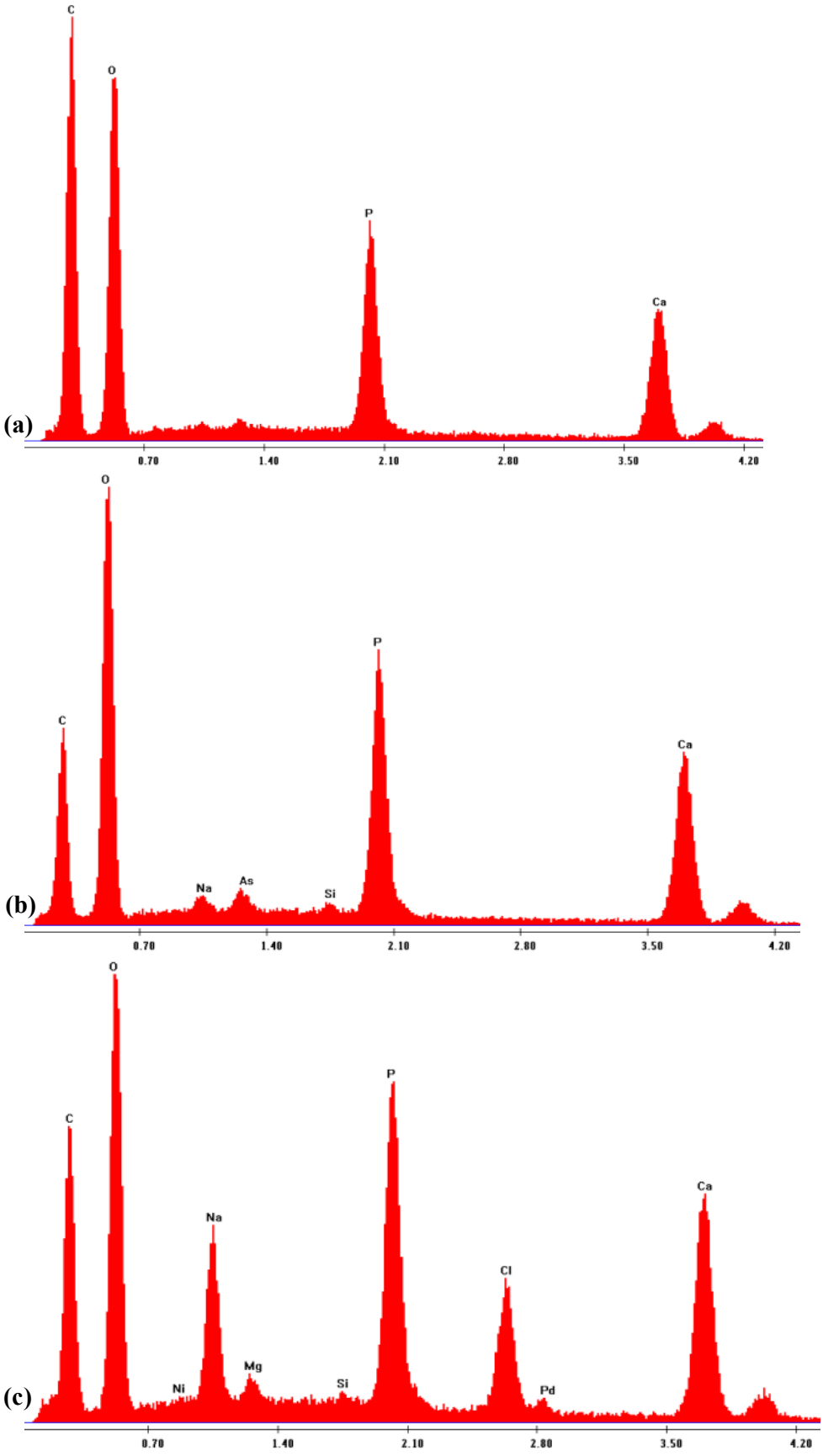

Figure 3.26: EDS spectra of PLA-TCP70 at (a) 1, (b) 14 and (c) 28 days after immersion in SBF

3.4.2 Raman spectroscopy

3.4.2.1 PLA

Figure 3.27 shows the Raman spectra of PLA films before immersion in SBF (a) and after immersion in SBF at day 1 (b), 14th (c) and 28th (d). The spectra show characteristic peaks for PLA and no phosphate peaks are visible even at 28 days. The peak at 1040 cm^{-1} corresponds to C-CH_3 stretching while the peak at 1766 cm^{-1} corresponds to C=O stretching. The peak at 1452 cm^{-1} corresponds to methyl group (CH_3) symmetric bending and at 1315 cm^{-1} to CH bending.

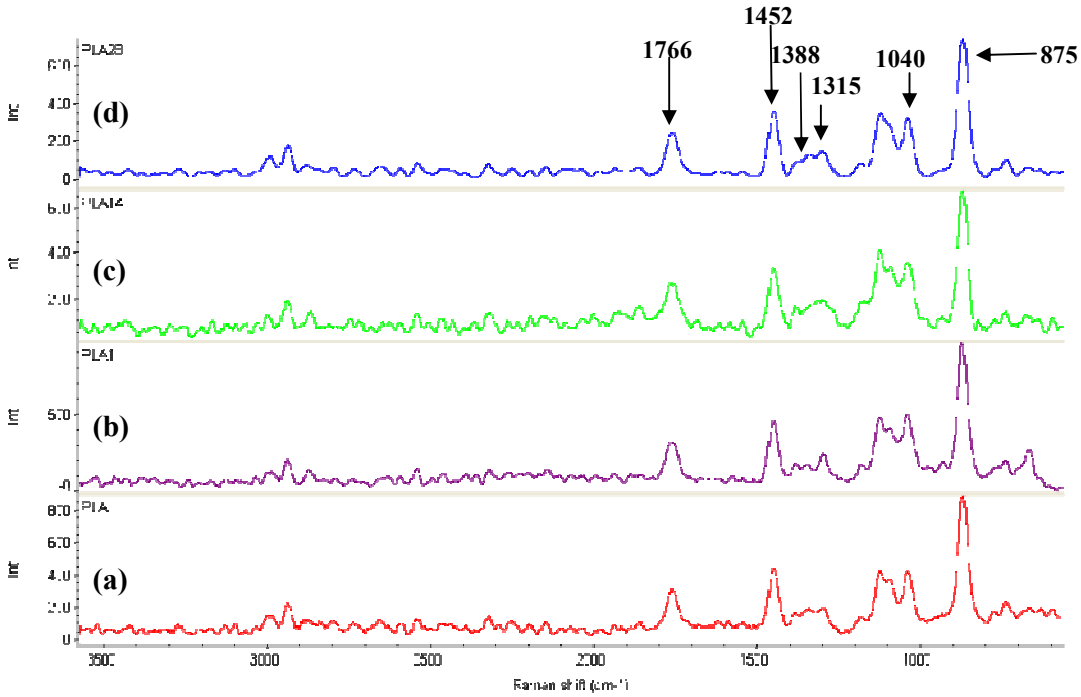

Figure 3.27: Comparative Raman spectra of PLA films at (a) 0 (b) 1, (c) 14 and (d) 28 days after soaking in SBF showing that the peaks do not change with soaking time.

3.4.2.2 PLA-HA composite films

Raman spectra of PLA-nHA, PLA-rHA and PLA-sHA composite films are shown in Figures 3.27-3.29, 3.30-3.32 and 3.33-3.35 respectively. The figures show Raman spectra of films before immersion in SBF (a) and after immersion in SBF at day 1 (b) day 14th (c) and at day 28th (d). The peak at 960 cm^{-1} is attributed to phosphate (P-O stretching). The presence of this peak at 960 cm^{-1} in the samples before immersion in the SBF can be attributed to phosphate present in the HA and after immersion in the SBF to phosphate present in the apatite layer formed. The intensity of this peak increased for all the samples with increase in immersion time in the SBF which can be ascribed to apatite layer formation. The increase was more prominent in PLA-HA samples containing 40 and 70 wt % HA than samples containing 10 % HA. This is due to greater apatite layer formation on samples containing higher quantity of nHA in PLA-HA samples. Characteristic peaks of PLA are also present. The peak at 1766 cm^{-1} corresponds to C=O stretching and the peak at 875 cm^{-1} which is characteristic of carbon, carbonyl bond (C-COO) stretching. The peak at 1040 cm^{-1} is assigned to C-CH_3 stretching. The peaks at 1388 cm^{-1} and 1452 cm^{-1} correspond to methyl group (CH_3) symmetric bending and at 1315 cm^{-1} to CH bending.

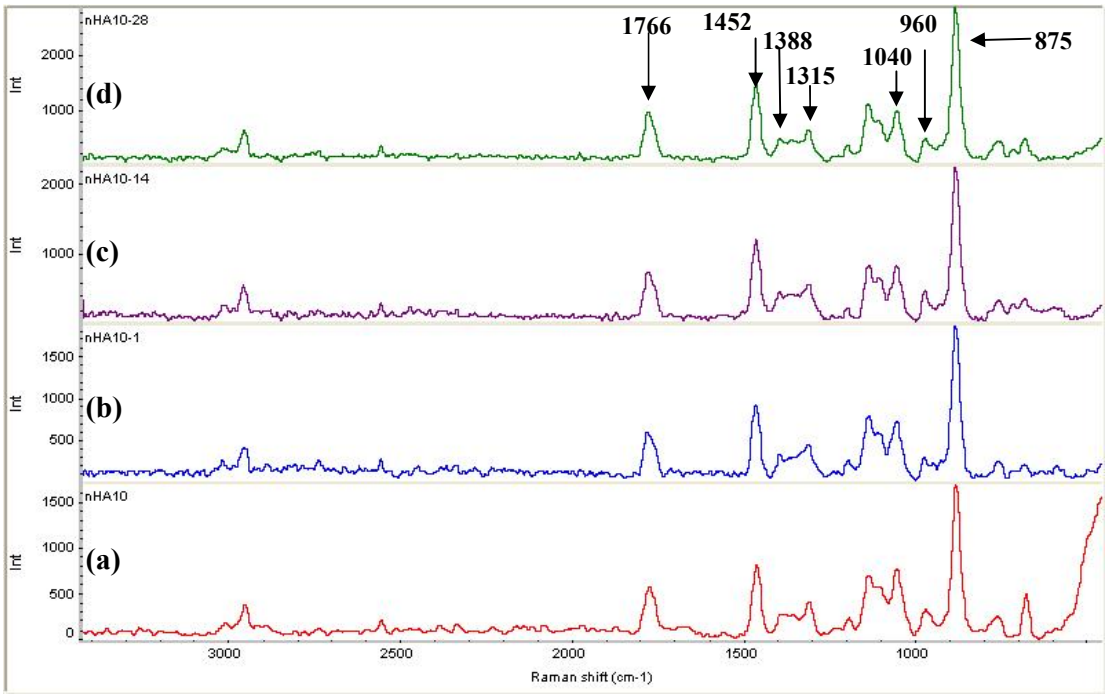

Figure 3.28: Comparative Raman spectra of PLA-nHA 10 at (a) 0 (b) 1, (c) 14 and (d) 28 days after soaking in SBF

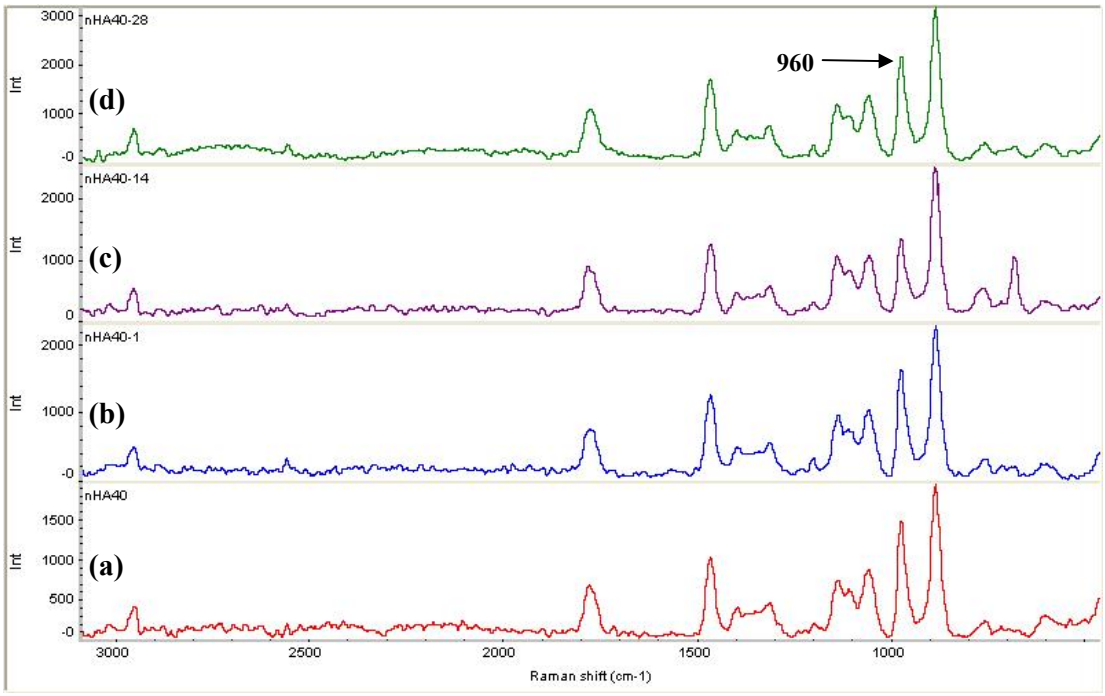

Figure 3.29: Comparative Raman spectra of PLA-nHA 40 at (a) 0 (b) 1, (c) 14 and (d) 28 days after soaking in SBF.

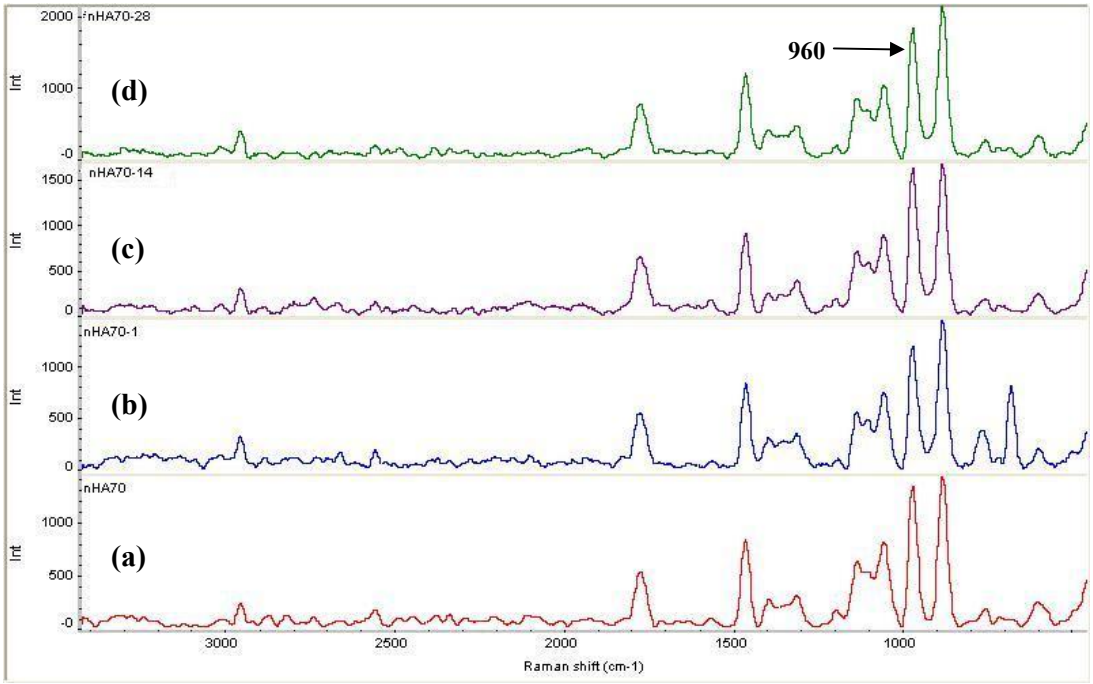

Figure 3.30: Comparative Raman spectra of PLA-nHA 70 at (a) 0 (b) 1, (c) 14 and (d) 28 days after soaking in SBF.

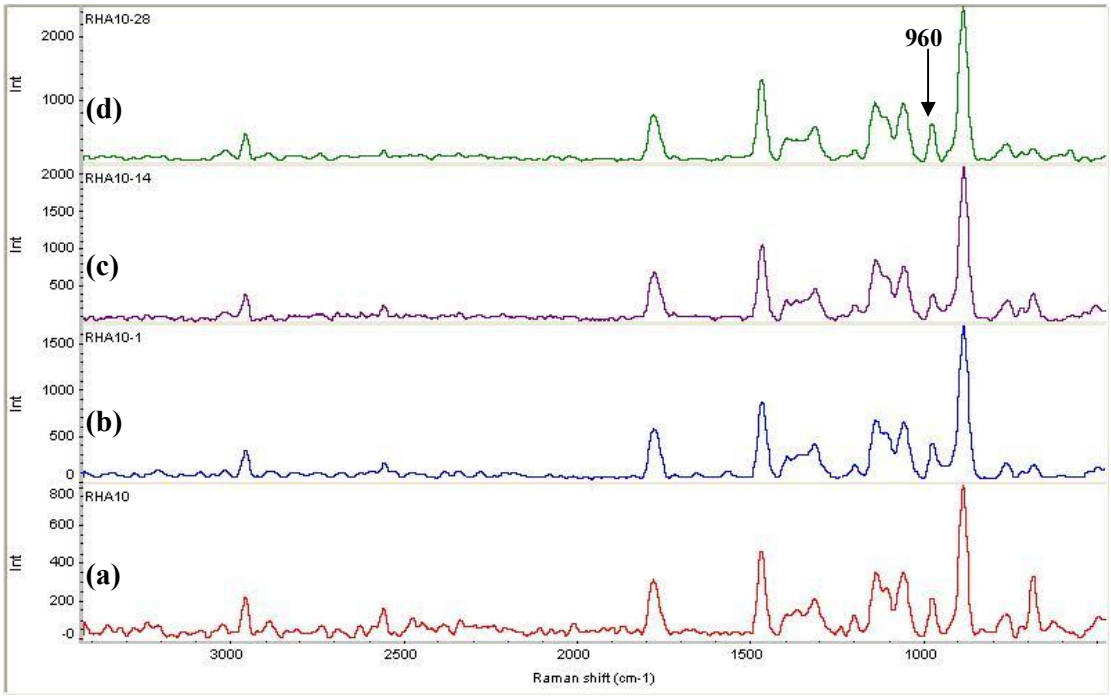

Figure 3.31: Comparative Raman spectra of PLA-rHA 10 at (a) 0 (b) 1, (c) 14 and (d) 28 days after soaking in SBF

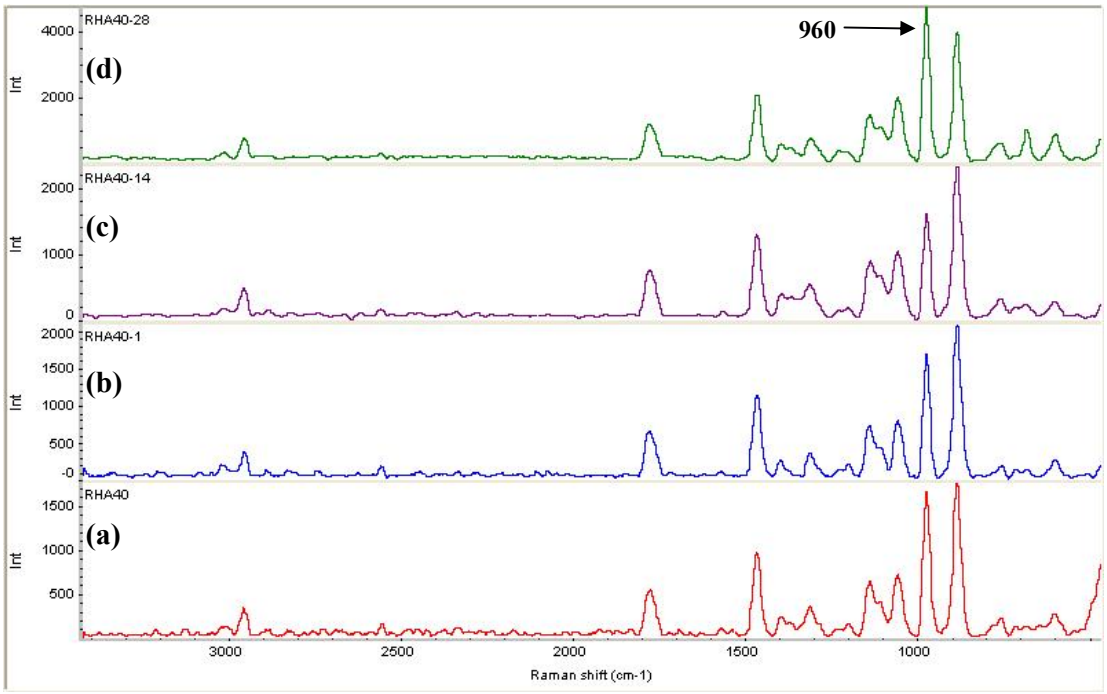

Figure 3.32: Comparative Raman spectra of PLA-rHA 10 at (a) 0 (b) 1, (c) 14 and (d) 28 days after soaking in SBF

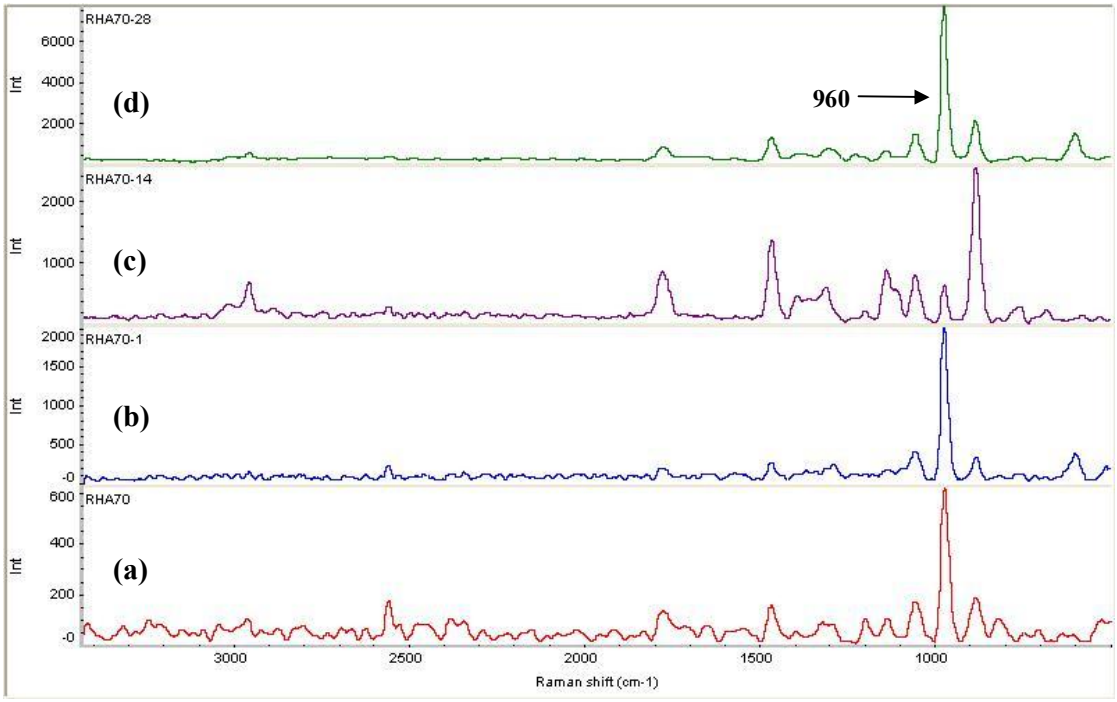

Figure 3.33: Comparative Raman spectra of PLA-rHA 70 at (a) 0 (b) 1, (c) 14 and (d) 28 days after soaking in SBF

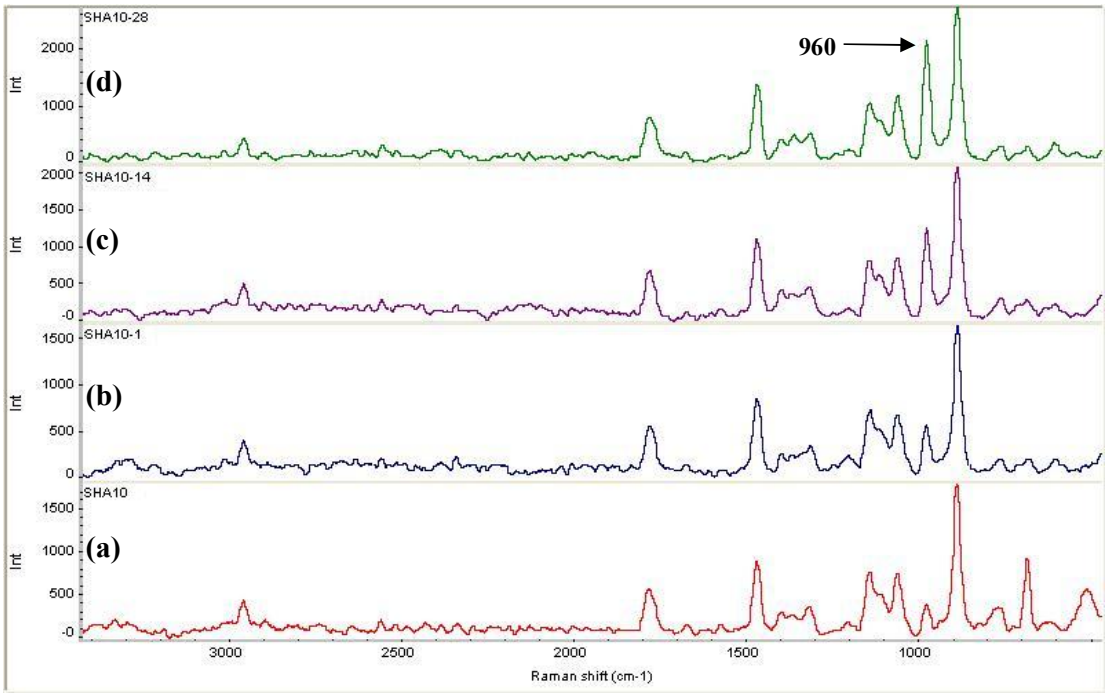

Figure 3.34: Comparative Raman spectra of PLA-sHA 10 at (a) 0 (b) 1, (c) 14 and (d) 28 days after soaking in SBF

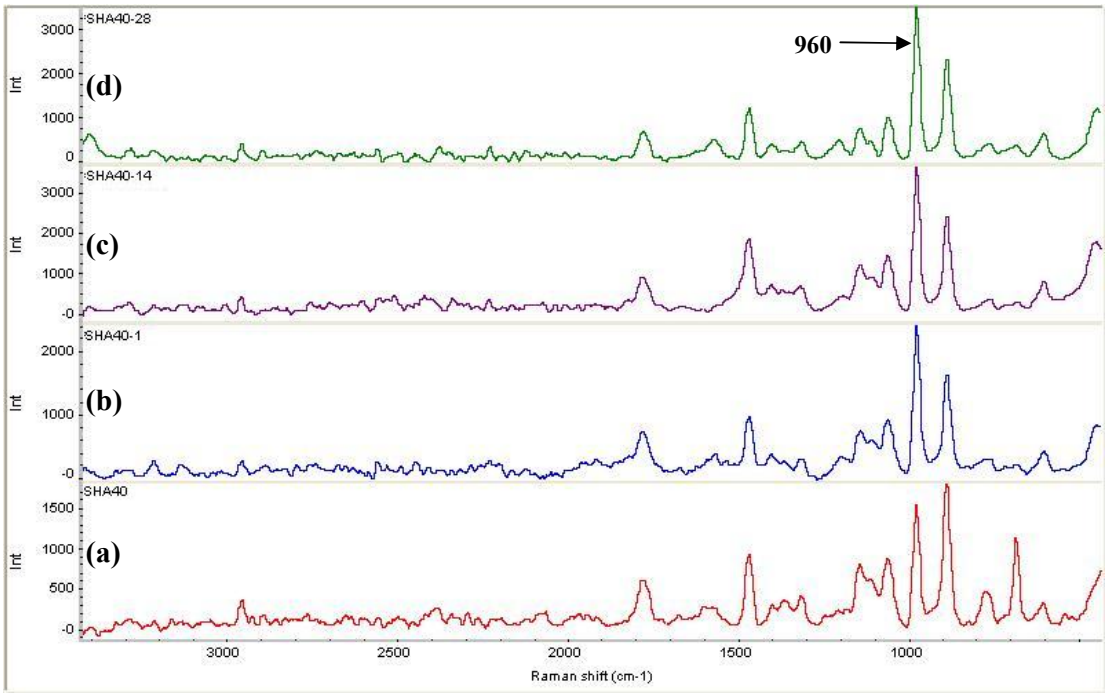

Figure 3.35: Comparative Raman spectra of PLA-sHA 40 at (a) 0 (b) 1, (c) 14 and (d) 28 days after soaking in SBF

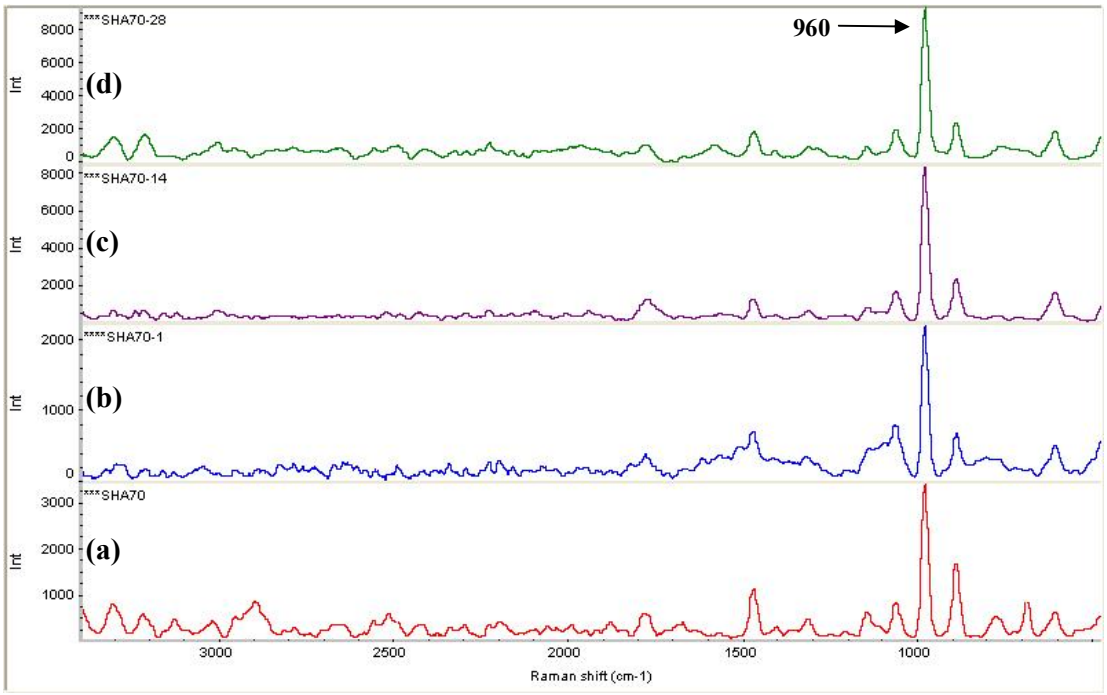

Figure 3.36: Comparative Raman spectra of PLA-sHA 70 at (a) 0 (b) 1, (c) 14 and (d) 28 days after soaking in SBF

3.4.2.3 PLA-TCP composite films

Raman spectra of PLA-TCP10, PLA-TCP40 and PLA-TCP70 composite films are shown in Figures 3.36, 3.37 and 3.38 respectively. The peak intensity of peak at 1388 cm^{-1} and 1315 cm^{-1} is very high as compared to intensities of the peaks at 960 cm^{-1} which is attributed to phosphate (P-O stretching) and at 875 cm^{-1} which is characteristic of carbon, carbonyl bond (C-COO) stretching. To make the changes in the intensities of these two peaks at 960 cm^{-1} and 875 cm^{-1} more appreciable, the selected area for these two peaks in the spectrum is shown in the box above the figures. The intensity of PO_4^{3-} peak at 960 cm^{-1} for all films increased with increase in the SBF immersion time, however the maximum change was observed in film containing 70 wt% TCP.

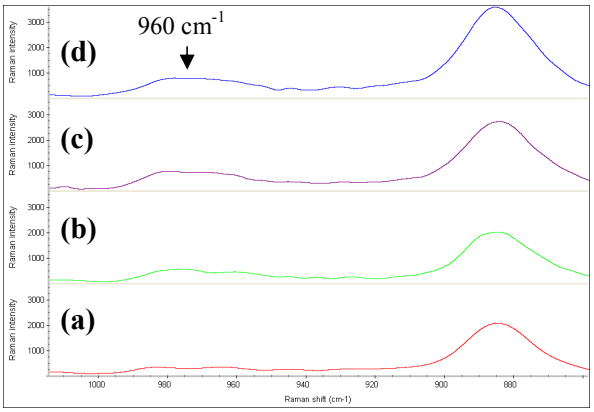

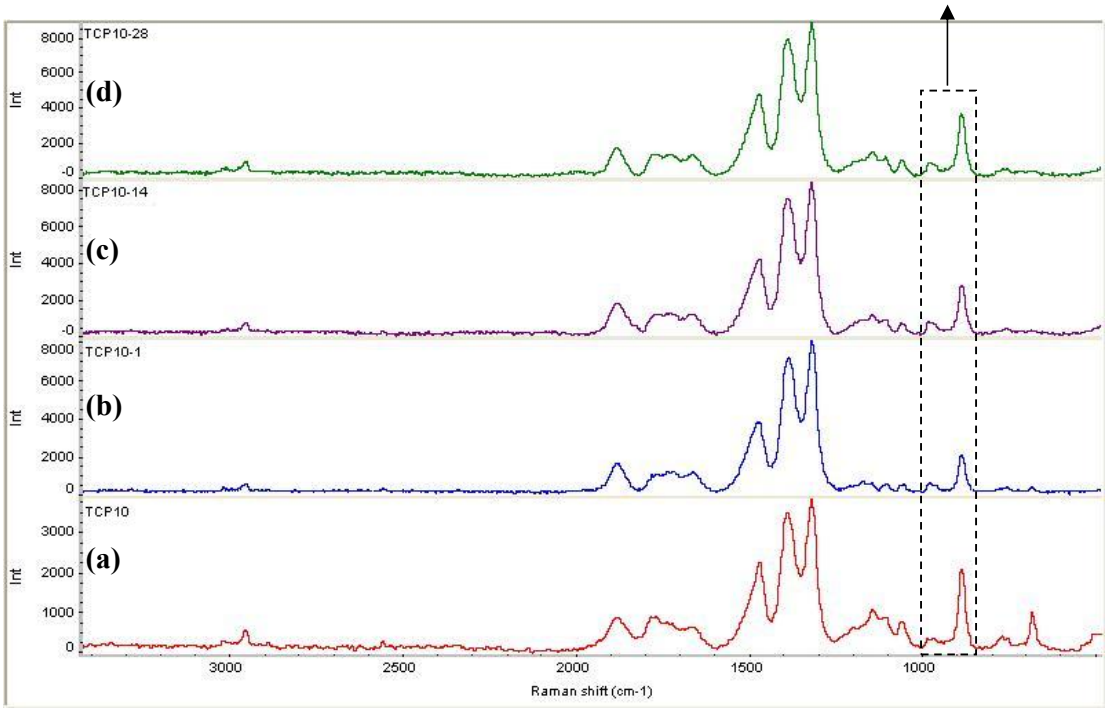

Figure 3.37: Comparative Raman spectra of PLA-TCP 10 at (a) 0 (b) 1, (c) 14 and (d) 28 days after soaking in SBF

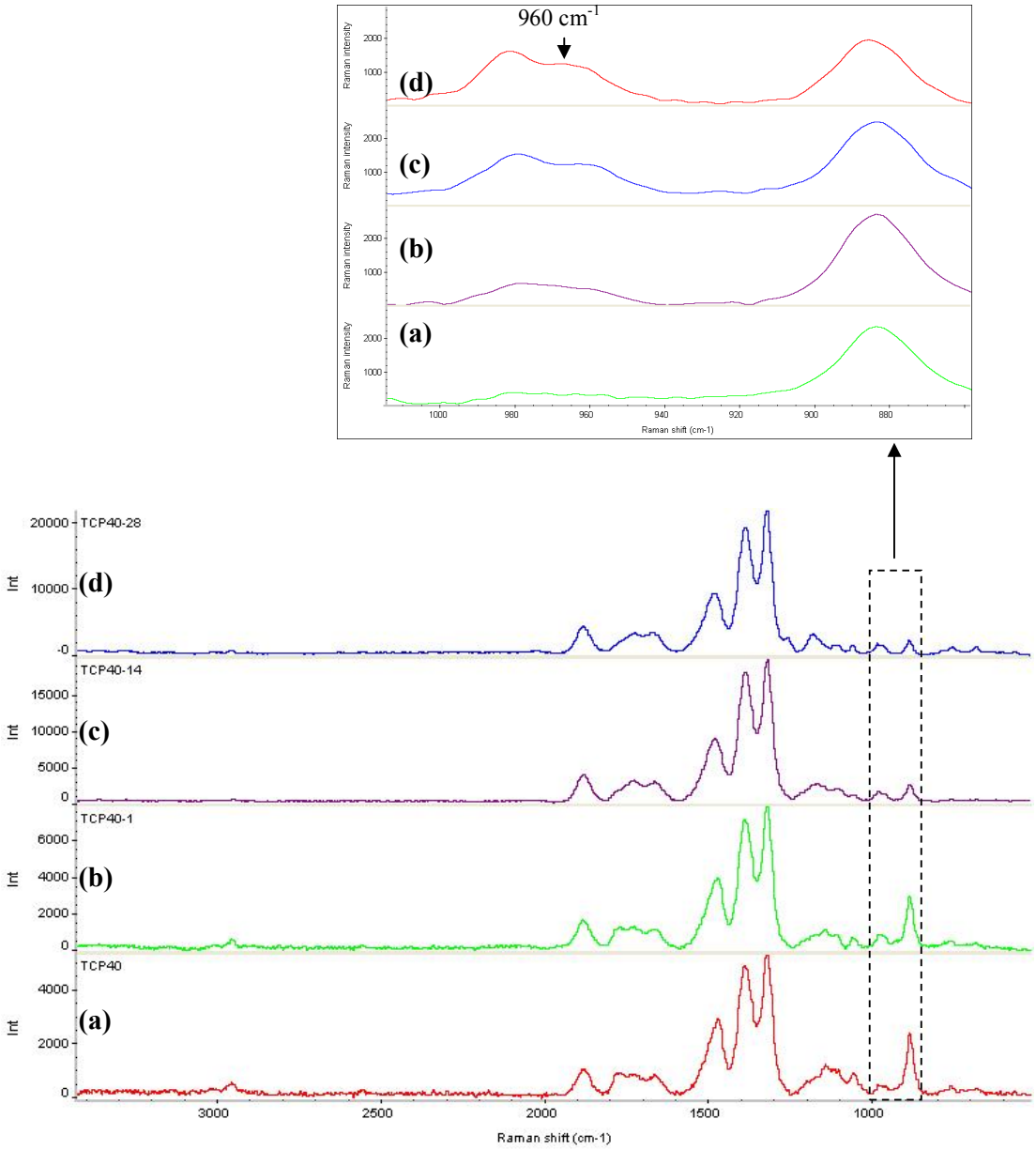

Figure 3.38: Comparative Raman spectra of PLA-TCP 40 at (a) 0 (b) 1, (c) 14 and (d) 28 days after soaking in SBF

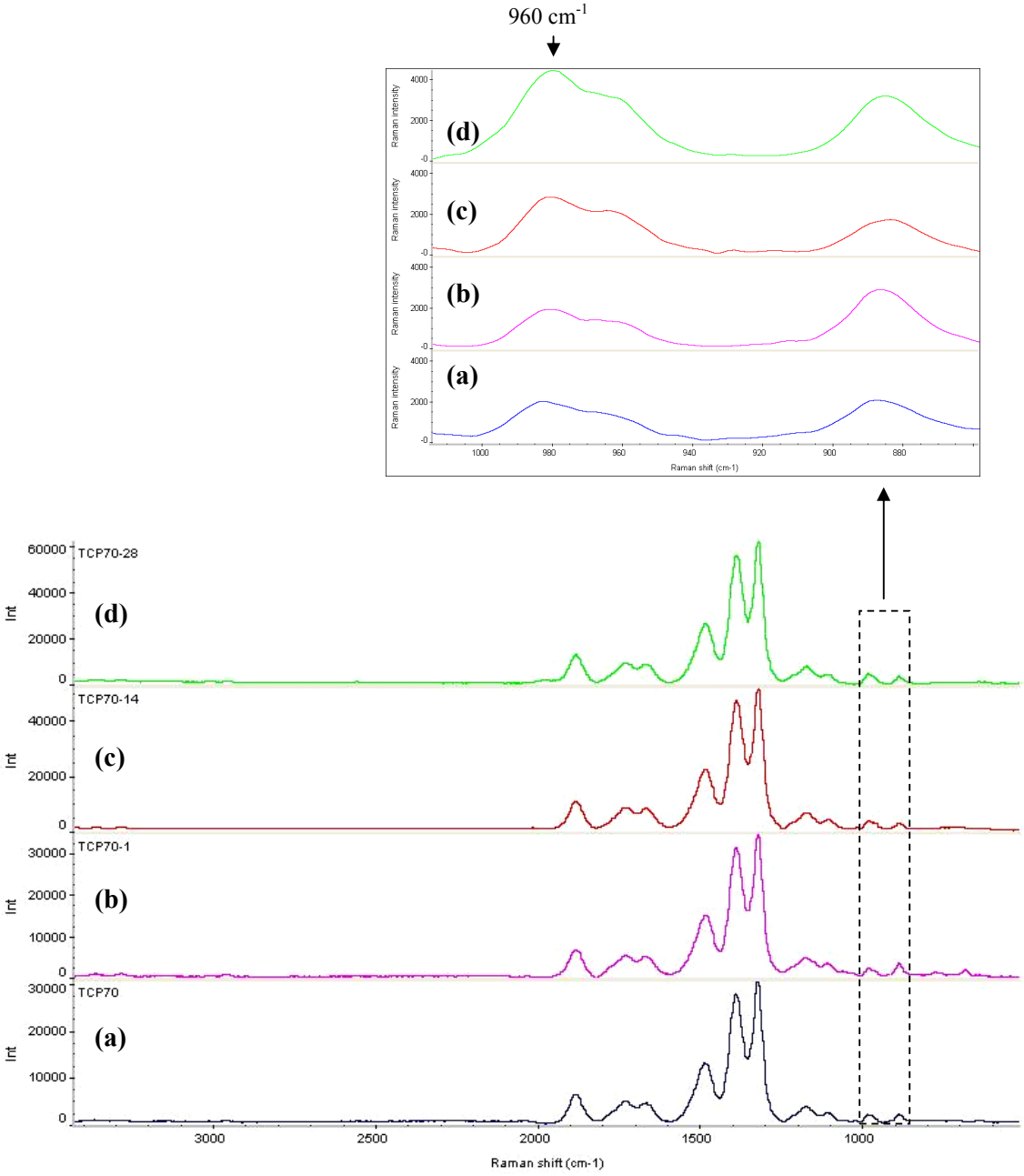

Figure 3.39: Comparative Raman spectra of PLA-TCP 70 at (a) 0 (b) 1, (c) 14 and (d) 28 days after soaking in SBF

3.5 DISCUSSION

When implanted a bioactive material produces a specific biological response and a biologically active apatite layer is formed on its surface. Bone bioactive implant materials are proposed to be categorised as; Class A, *osteoinductive materials* and class B, *osteoconductive materials*. Osteoinductive materials elicit both extracellular and intracellular responses in the host environment, whereas, osteoconductive materials only elicit an extracellular response [Hench, 1994; Cao and Hench, 1996]. The formation of an apatite layer on the implant surface also affects the topographic configuration of the material which in turn affects the cellular behaviour and tissue response to the implant. Bioactive material surfaces favour the proliferation of osteoblasts over fibroblast proliferation [Seitz, 1982]. The apatite which is formed on the surface of the bioactive material is carbonate-containing hydroxyapatite with small crystallites and resembles the bone apatite in composition and structure. These properties enable bone producing cells (osteoblasts) to proliferate and differentiate preferentially on this apatite layer and produce apatite and collagen [Kokubo, 1998].

Kokubo et al. [1990] proposed that the "essential requirement for an artificial material to bond to living bone is the formation of bonelike apatite on its surface when implanted in the living body, and that this in vivo apatite formation can be reproduced in a simulated body fluid (SBF) with ion concentrations nearly equal to those of human blood plasma". The process of apatite layer deposition on the surface of the material involves formation of apatite nuclei which subsequently grow, consuming calcium and phosphate ions from the SBF. Various studies have shown that as the apatite layer deposition increases the concentrations of calcium and phosphorous in SBF decreases [Jaakkola et al., 2004; Me et al., 2006]. SBF is supersaturated with calcium and phosphate ions and becomes stable by apatite crystal formation and the rate of formation of apatite nuclei is affected by the number of calcium ions released from the material. It is also proposed that the rate of formation of apatite on a material surface when soaked in SBF is predictive of the degree of in vivo bioactivity of that material [Kokubo, 1998; Kokubo and Takadama, 2006]. Thus

the bioactivity of a material can be evaluated by soaking it in SBF and analysing the rate of apatite formation.

Calcium phosphates are well documented bioactive materials and form bonelike apatite on their surface in SBF [Gu et al., 2004; Sun et al., 2006]. The formation of an apatite layer is thought to involve surface structural changes when soaked in SBF. The first structural change involves formation of a Ca rich amorphous calcium phosphate (ACP) as a result of specific interaction of HA surface with calcium ions in the SBF. The second surface structural change is the formation of a Ca poor ACP due the interaction of Ca rich ACP with the phosphate ions in the SBF. The third change is the gradual crystallisation of Ca poor ACP into bonelike apatite. Subsequently this apatite grows by consuming calcium and phosphate ions from SBF. HA has negative surface charge when immersed into SBF due to exposure of its hydroxyl and phosphate units. This negative charge HA interacts specifically with positive Ca ions in SBF thus forming a Ca rich ACP. Formation of Ca rich ACP changes the surface charge to positive which then facilitates the interaction of Ca rich ACP specifically with negative phosphate ions in the SBF and to form a Ca poor ACP which in turn crystallizes into bonelike apatite. The apatite which is formed then acts as nucleation centres for apatite deposition [Bell et al., 1972; Neo et al., 1993; Duan et al., 2004; Kim et al., 2005; Me et al., 2006].

In this study the bioactivity of PLA/Ca P composite films containing different types of HA and TCP in different concentration was evaluated by assessing the ability of an apatite layer to form on their surfaces in SBF. Among the PLA/HA and PLA/TCP composite films the formation of an apatite layer was highest and most rapid on films containing 70 wt % nHA followed by film containing 70 wt % TCP. In contrast there was no apatite layer formation on plain PLA films even after 28 days of immersion in SBF. Increased apatite formation on PLA-nHA films can be attributed to more nucleation centres present on the film in addition to its larger surface area. Previous studies have also shown that materials with large specific surface area produce earlier apatite formation as compared to materials with lower surface area [Jaakkola et al., 2004; Murugan and Ramakrishna, 2005; Bohner and Lemaitre, 2009]. PLA-TCP composite film which has similar sized particles as PLA-sHA and PLA-rHA composite films showed increased and faster formation of the apatite on its surface as compared to PLA-

sHA and PLA-rHA composite films. Among the PLA-TCP films the maximum apatite formation was on films containing the highest concentration i.e. 70 wt % TCP. This increased apatite formation can be attributed to the fact that the dissolution rate of TCP is higher than HA [Ducheyne et al., 1993] and the dissolution increases the Ca^{2+} concentration in the SBF around the area of dissolution. This increased Ca^{2+} concentration causes more ion attachment to the material surface, which then act as nucleation centres and an apatite layer is produced [Khor et al., 2003].

The morphology of the apatite layer formed on PLA-nHA films containing 40 and 70 wt % nHA showed a fine needle like structure as compared to globular morphology of apatite formed on the films containing 10 wt% nHA. This difference can be attributed to the presence of more nucleation centres which are more closely present on the films with a higher nHA concentration. The morphology of the apatite layers formed on composite films containing sHA, rHA and TCP is globular and the SEM images show individual globules at the site of nucleation. The apatite formation increased with the passage of time and the globules became tightly packed and gave the apatite layer a cauliflower like morphology.

Raman spectra of all the PLA-HA and PLA-TCP composite films show a $960cm^{-1}$ peak which corresponds to symmetric stretching vibration of P-O [Zhou et al., 2007] in apatite crystals, the intensity of this peak increased with increasing SBF immersion time which is indicative of apatite formation. In addition the change in the intensity of this peak was high in films containing higher amount of HA or TCP which is due to formation of more apatite on these films. The strong peak in PLA-HA films at 875 cm^{-1} is characteristic of carbon, carbonyl bond (C-COO) stretching in the polymer chain [Patrick, 2001; Taddei et al., 2002]. Raman spectra of plain PLA films did not show emergence of phosphate peak at $960cm^{-1}$.

3.6 CONCLUSIONS

Higher calcium phosphates content in the composite results in a higher rate of apatite formation. Additionally particle sizes of the calcium phosphates used in

the composite also play an important role in determining the rate of apatite layer formation. Increased apatite formation was observed with nano particles used in this study. The formation of an apatite layer on TCP was more compared to HA of the same content.

CHAPTER 4: DEGRADATION OF POLYLACTIC ACID-CALCIUM PHOSPHATE COMPOSITES

4.1 INTRODUCTION

Polylactic acid (PLA) has been used in many biomedical applications such as tissue engineering, drug delivery, orthopaedics and maxillofacial reconstruction due to its biocompatibility and biodegradability. The ability of PLA to be used in many different applications is due to the possibility of tailoring its physical, chemical and degradation properties to individual needs. The rate at which PLA degrades is very important and should match the rate at which the new tissue forms at its implantation site. Degradability of PLA depends on various factors which include its molecular weight, crystallinity, $_{L}$ and $_{D}$ isomer ratio, configuration, implant size and implant site [Grizzi et al., 1995; Middleton and Tipton, 2000; Ural et al., 2000].

Combining calcium phosphates such as hydroxyapatite (HA) and tri-calcium phosphate (TCP) with PLA not only improves bioactivity and mechanical properties of PLA but also affects its degradation rate [Takayama et al., 2009].

The aim of this study is to investigate the effect of HA and TCP addition on the degradation of PLA and also to examine the effect of different HA and TCP concentrations used.

4.2 MATERIALS

The materials used were PLA (PURAC Biochem, The Netherlands), nHA (Sigma-Aldrich, UK), sHA and rHA (Plasma Biotal Limited, UK) and TCP (Plasma Biotal Limited, UK) as described in detail in section 2.2.

4.3 METHODS

4.3.1 Composite films preparation

PLA-HA and PLA-TCP composite films were prepared as described in detail in section 2.3.1, namely dissolving the PLA in chloroform and once dissolved adding the Ca P powder, continue to stir and finally cast the film.

4.3.2 Degradation protocol

Degradation of the composite films *in vitro* was analysed by incubating composite film samples in phosphate buffered saline (PBS) at 37°C. Circular samples 12 mm diameter were cut using a hole puncher and sterilized by soaking in 70% ethanol for a 5 minutes and then dried at 50°C. Three samples for each composite film and time point were weighted (W_o) before immersion in the PBS and were placed in polypropylene bottles for 1 day, 1, 3, 6, 9 and 12 weeks. Each bottle containing a single sample was filled with 20 ml PBS which was replaced with fresh 20 ml PBS after every 3 weeks. At each time point the samples were removed from the bottles and weighted after gently wiping the sample surface with a tissue to give wet weight (W_w). The samples were then washed with deionised water to remove any soluble salt from their surfaces. After washing the samples were dried in an oven at 37 °C for 24 hours and then in a vacuum oven for 2 hours before weighing to give dry weight (W_d). The difference between W_o and W_w was taken as wet weight gain (WG) and the difference between W_o and W_d was taken as weight loss (WL). These two were calculated according to Equations 4.1 and 4.2 respectively.

WG (%) = $100\ (W_w-W_o)/\ W_o$ **Equation 4. 1**

WL (%) = $100\ (W_o-W_d)/\ W_o$ **Equation 4. 2**

4.3.3 Data Analysis

Statistical analyses were done by 1- way ANOVA with Bonferroni's post-test with $P < 0.05$.

4.4 RESULTS

4.4.1 PLA

Figure 4.1 shows the percentage wet weight gain by PLA films after immersion in PBS for up to 12 weeks. PLA films gained weight for up to 6 weeks, which increased gradually from day 1 up to the 6th week and reached a maximum of 0.59 %. After the 6th week the weight decreased and dropped until the end of testing.

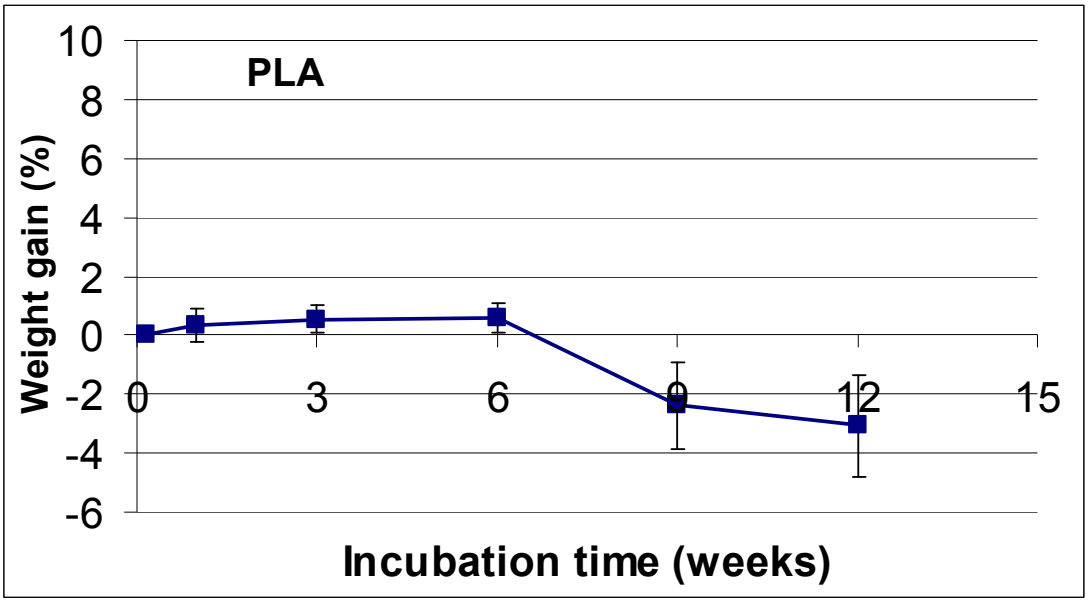

Figure 4.1: Percentage wet weight gain by PLA films versus incubation time in PBS at 37 °C. The first data point is at day 1 showing weight gain in the 1st 24 hours. Mean ± SD, n=3 for each time point.

Figure 4.2 shows the percentage dry weight loss by PLA films after immersion in PBS for up to 12 weeks. PLA films lost weight over the entire duration of immersion in SBF and reached 5 % at the end of the 12th week.

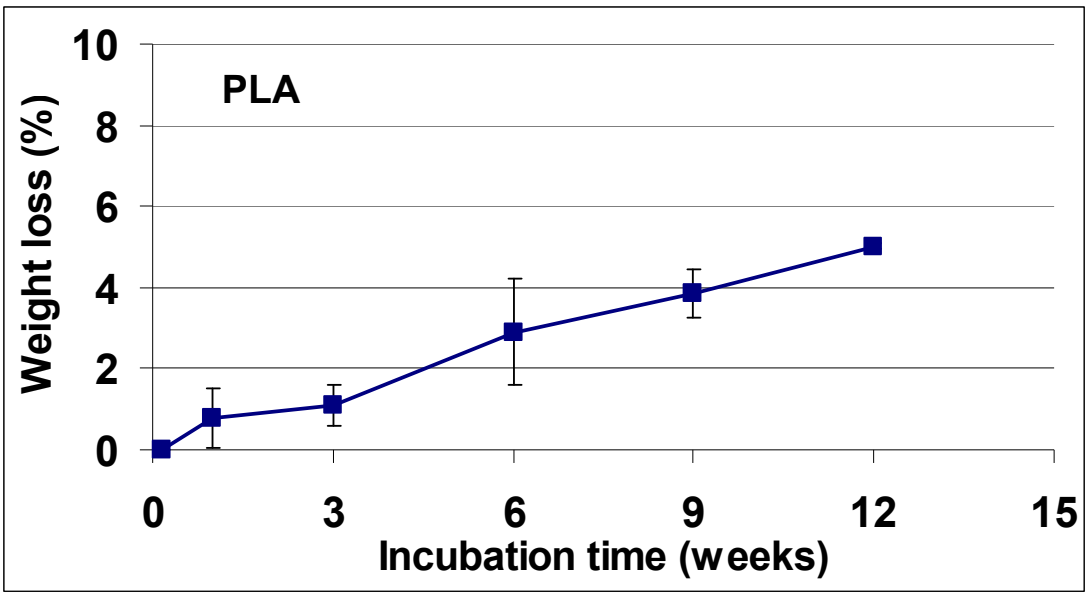

Figure 4.2: Percentage dry weight loss of PLA films versus incubation time in PBS at 37 °C. The first data point is at day 1 showing weight loss in the 1st 24 hours. Mean ± SD, n=3 at each time point.

4.4.2 PLA-nHA composite films

Figure 4.3 shows the percentage wet weight gain by PLA-nHA composite films containing 10, 40 and 70 wt % nHA after immersion in PBS for up to 12 weeks in comparison with the non-filled PLA film (results shown in figure 4.1.). PLA-nHA composite film containing 40 wt % nHA showed more weight gain than films containing 10 and 70 wt % nHA. At day 1 PLA-nHA70 films showed more weight gain than PLA-nHA10 films, however after the first day the weight gain by PLA-nHA70 film decreased and remained less than PLA-nHA10 throughout the incubation period. Weight gain by PLA-nHA70 films was 4 % on day 1 which decreased to 1.19 % at the 12th week. PLA-nHA40 films showed 4.3 % weight gain on day 1 which reached maximum at the 12th week i.e. 8.33 %. PLA-nHA10 films showed minimum weight gain among all the films on day 1 i.e. 1.89 %, the weight gain reached its maximum at 1 week and than gradually decreased to reach 3.33 % at the 12th week. All the composite films showed more weight gain than the non-filled PLA.

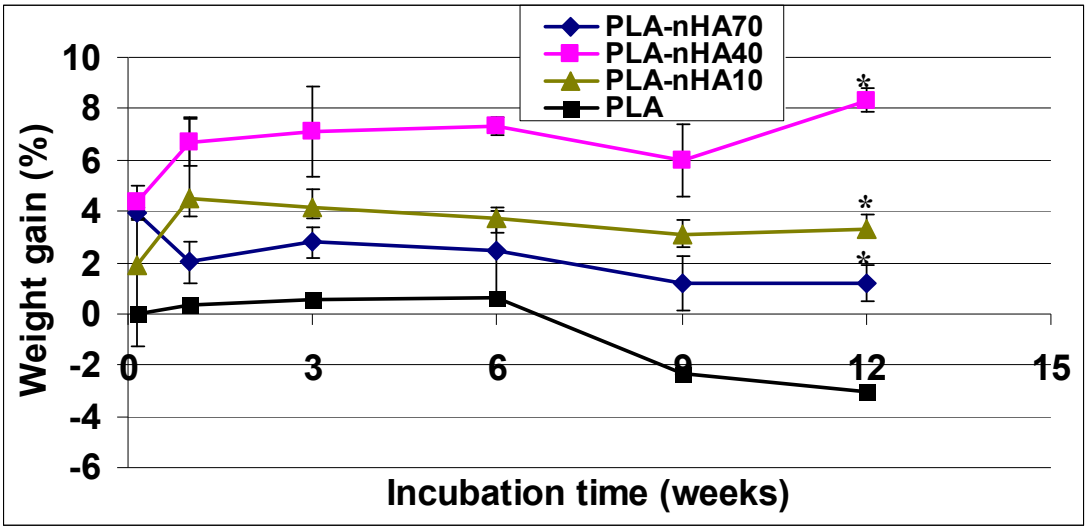

Figure 4.3: Percentage wet weight gain by PLA-nHA composite films versus incubation time in PBS at 37 °C. The first data points are at day 1 showing weight gain in the 1st 24 hours. Mean ± SD, n=3 at each time point. * Significantly greater than PLA, p<0.05, one way ANOVA and Bonferroni post test.

Figure 4.4 shows the percentage dry weight loss by PLA-nHA composite films containing 10, 40 and 70 wt % nHA after immersion in PBS for up to 12 weeks in comparison with the non-filled PLA film (result shown in figure 4.2). For all the films the weight loss increased with PBS immersion time and the maximum weight loss was shown by films containing maximum nHA i.e. 70 wt % nHA followed by films containing 40 and 10 wt % nHA respectively. Film containing 40 and 70 wt % nHA showed a sharp weight loss between day 1 and the 1st week which was followed by a plateau until the 3rd week. The weight for these two types of films then again decreased until the 12th week reaching 5.6 and 4.5 % for films containing 70 and 40 wt % nHA respectively. The films containing 10 wt % nHA lost weight gradually and reached 3 % at the end of 12 weeks. Only the 70 wt % nHA film lost more weight than the non-filled PLA film.

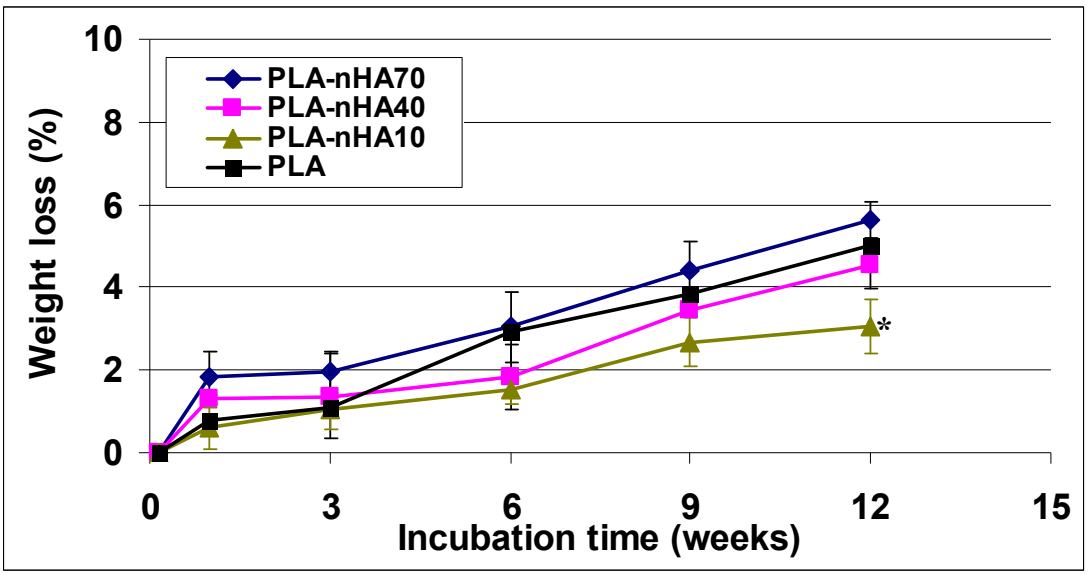

Figure 4.4: Percentage dry weight loss of PLA-nHA composite films versus incubation time in PBS at 37 °C. The first data point is at day 1 showing weight loss in the 1st 24 hours. Mean ± SD, n=3 at each time point. * Significantly less than PLA, p<0.05, one way ANOVA and Bonferroni post test.

4.4.3 PLA-rHA composite films

Figure 4.5 shows the percentage wet weight gain by PLA-rHA composite films containing 10, 40 and 70 wt % rHA after immersion in PBS for up to 12 weeks in comparison with non-filled PLA film (results shown in figure 4.1). On day 1 films containing 70 wt % rHA showed slight weight gain i.e. 0.48 %, the remaining two types of films containing 40 and 10 wt % did not show any weight gain. However after day 1 all PLA-rHA composite films showed negative values for weight gain up to the 12th week, except PLA-rHA composite film containing 70 wt % rHA which showed slight weight gain at the 12th week i.e. 0.67 %. Unlike PLA all composite films showed a reduction in weight.

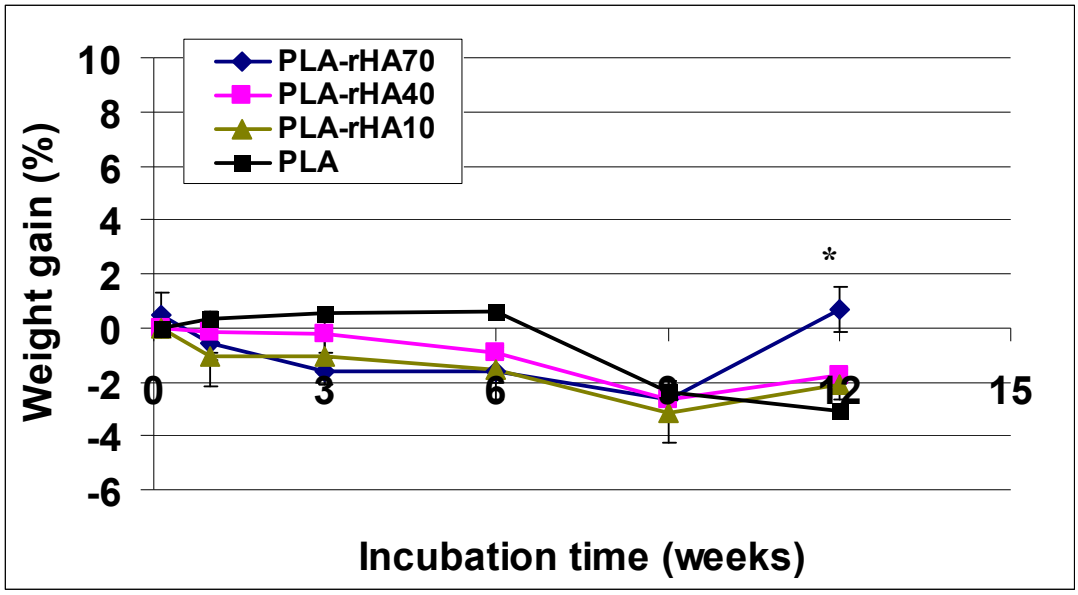

Figure 4.5: Percentage wet weight gain of PLA-rHA composite films versus incubation time in PBS at 37 °C. The first data points are at day 1 showing weight gain in the 1st 24 hours. Mean ± SD, n=3 at each time point. * Significantly greater than PLA, p<0.05, one way ANOVA and Bonferroni post test.

Figure 4.6 shows the percentage dry weight loss by PLA-rHA composite films containing 10, 40 and 70 wt % rHA after immersion in PBS for up to the 12 weeks in comparison with the non-filled PLA film (results shown in figure 4.2). All the composite films showed weight loss throughout immersion in the PBS up to 12th week. The greatest weight lost was shown by films containing 10 wt % rHA followed by films containing 70 and 40 wt % rHA respectively. The final weight loss at the end of the 12th week was 6.3, 3.8 and 5 % for films containing 10, 40 and 70 wt % rHA. The weight loss of film containing 10 wt % rHA was greater and of film containing 40 wt % rHA was less than non-filled PLA film.

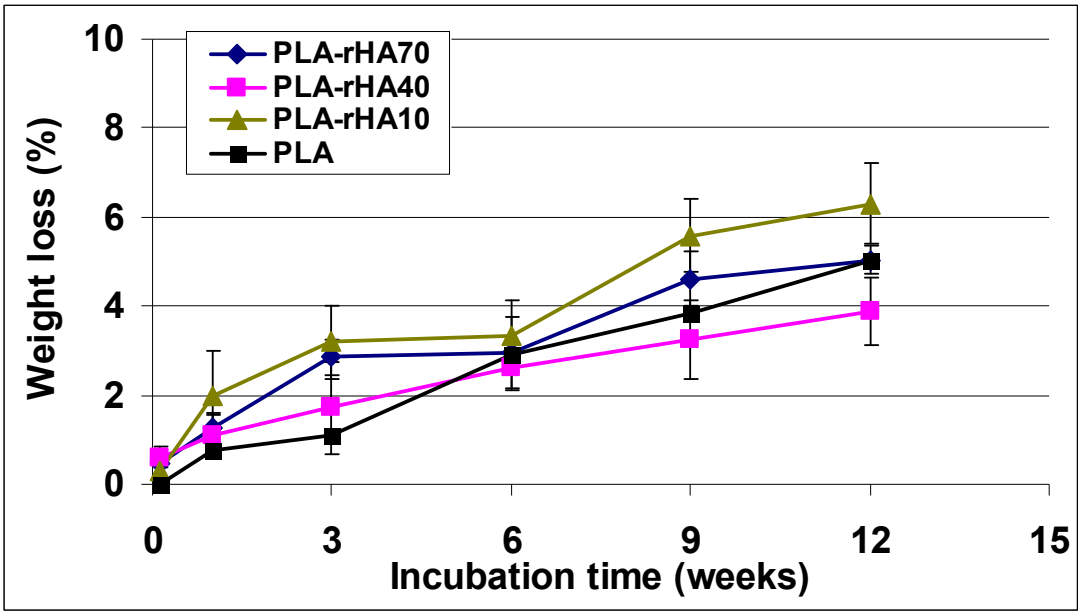

Figure 4.6: Percentage dry weight loss of PLA-rHA composite films versus incubation time in PBS at 37 °C. The first data points are at day 1 showing weight loss in the 1st 24 hours. Mean ± SD, n=3 at each time point.

4.4.4 PLA-sHA composite films

Figure 4.7 shows the percentage wet weight gain by PLA-sHA composite films containing 10, 40 and 70 wt % sHA after immersion in PBS for up to 12 weeks in comparison with non-filled PLA film (results showed in figure 4.1). At day 1 highest weight gain was shown by film containing 70 wt % sHA. After the 1st day the weight gain by film containing 70 wt % sHA decreased sharply and at week 1 it was less than weight gain by films containing 10 and 40 wt % sHA. However after the 1st week the weight gain by film containing 70 wt % sHA again increased upto 6th weeks, before again decreasing up to the 12th week. After increased weight gain at week 1 by both PLA-sHA10 and PLA-sHA40 films showed decrease in weight gain. At the end of the 12th week the weight gains were -1.3, -1.29, 0 % for PLA-sHA10, PLA-sHA40 and PLA-sHA70 composite films respectively.

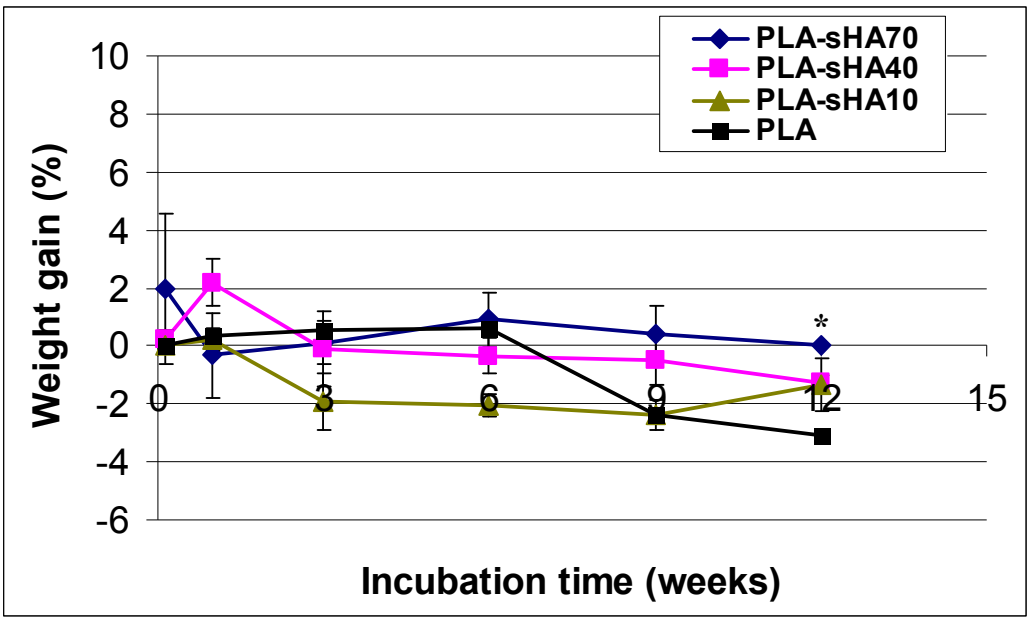

Figure 4.7: Percentage wet weight gain by PLA-sHA composite films versus incubation time in PBS at 37 °C. The first data points are at day 1 showing weight gain in the 1st 24 hours. Mean ± SD, n=3 at each time point. * Significantly greater than PLA, p<0.05, one way ANOVA and Bonferroni post test.

Figure 4.8 shows the percentage dry weight loss by PLA-sHA composite films containing 10, 40 and 70 wt % sHA after immersion in PBS for up to 12 weeks in comparison with non-filled PLA film (results shown in figure 4.2). All PLA-sHA composite films showed increasing weight loss with PBS immersion time. Until week 1 the maximum weight loss was shown by films containing 10 wt % sHA followed by films containing 40 and 70 wt % sHA respectively. However at week 3 the films containing 70 wt % sHA showed more weight loss compared to films containing 40 wt % sHA. At the end of the 12th week the weight losses were 5.4, 3.8 and 4.4 % for PLA-sHA10, PLA-sHA40 and PLA-sHA70 films respectively.

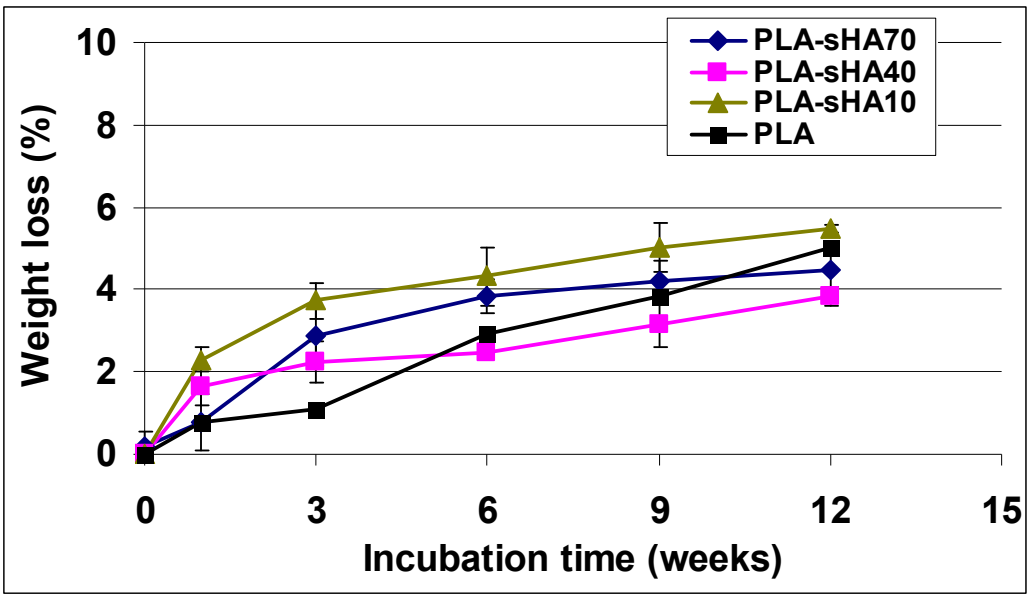

Figure 4.8: Percentage dry weight loss of PLA-sHA composite films versus incubation time in PBS at 37 °C. The first data points are at day 1 showing weight loss in the 1st 24 hours. Mean ± SD, n=3 at each time point.

4.4.5 PLA-TCP composite films

Figure 4.9 shows the percentage wet weight gain by PLA-TCP composite films containing 10, 40 and 70 wt % TCP after immersion in PBS for up to 12 weeks in comparison with non-filled PLA film (results shown in figure 4.1). On day 1 the maximum weight gain was shown by films containing 70 wt % TCP i.e. 1.6 %, whereas the films containing 10 and 40 wt % did not show any weight gain. However the weight gain by films containing 70 wt % TCP went negative after day 1. The films containing 10 and 40 wt % TCP showed an increase in weight gain between day 1 and 1st week after which the weight gain for these two types of films also decreased and went into weight loss.

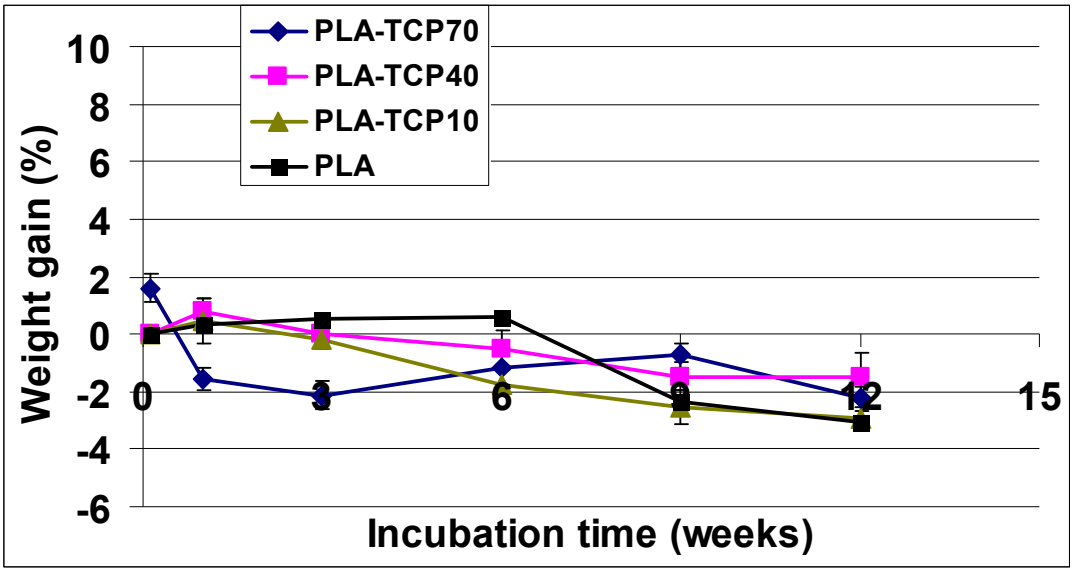

Figure 4.9: Percentage wet weight gain by PLA-TCP composite films versus incubation time in PBS at 37 °C. The first data points are at day 1 showing weight gain in the 1st 24 hours. Mean ± SD, n=3 at each time point.

Figure 4.10 shows the percentage dry weight loss by PLA-TCP composite films containing 10, 40 and 70 wt % TCP after immersion in PBS for up to 12 weeks in comparison with non-filled PLA film (results shown in figure 4.2). All PLA-TCP composite films showed an increasing weight loss with PBS immersion time. Until week 1 the maximum weight loss was shown by films containing 10 wt % TCP followed by films containing 40 and 70 wt % TCP respectively. However after week 1 the weight loss was more for films containing 70 wt % TCP as compared to films containing 40 wt % TCP. At the end of the 12th week the weight losses were 6.9, 5.3 and 6 % for films containing 10, 40 and 70 wt % TCP respectively. The weight loss by all composite films was greater than non-filled PLA film.

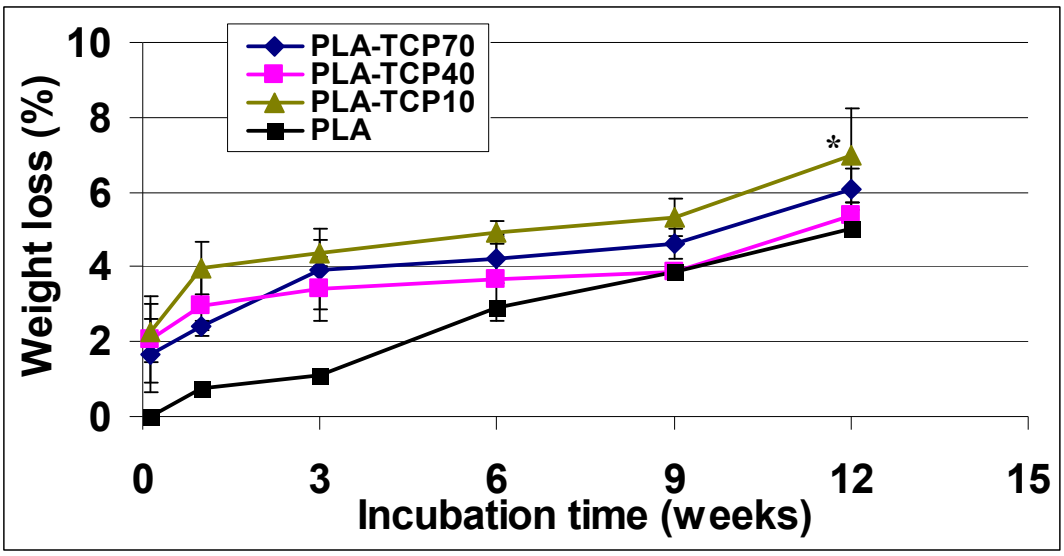

Figure 4.10: Percentage dry weight loss of PLA-TCP composite films versus incubation time in PBS at 37 °C. The first data points are at day 1 showing weight loss in the 1st 24 hours. Mean ± SD, n=3 at each time point. * Significantly greater than PLA, p<0.05, one way ANOVA and Bonferroni post test.

4.5 DISCUSSION

The degradation rate of an implant plays an important role in defining the success or failure of a resorbable implant. The rate at which an implant degrades affects its mechanical properties, cell growth and the body's response. Ideally an implant should maintain its strength until the strength of new bone is adequate and then should degrade at the same rate as the new bone regenerates [Liao and Cui, 2004].

Hydrolytic degradation of PLA is heterogeneous and involves surface and bulk erosion mechanisms. Surface erosion occurs at the polymer-liquid interface, whereas bulk erosion involves uniform degradation throughout the polymer. Depending on the manufacturing process the degradation of PLA devices can be faster in the centre than on the surface. The first event which takes place on immersion of a PLA device in the aqueous solution or when implanted is water uptake. These water molecules then produce hydrolytic decomposition of the polymer chain. During the degradation, oligomers are produced; the oligomers which are present close to the surface escape the matrix into the surrounding

medium. However those which are present inside the matrix diffuse out very slowly and mainly remain entrapped thus contributing to the autocatalytic effect and increasing the degradation rate in the centre of the device [Vasanthan and Ly, ; Grizzi et al., 1995].

The PLA degradation produces lactic acid and burst release of this lactic acid can produce tissue inflammation. Addition of TCP or HA can help in lowering the acidity thus controlling the degradation rate. However, in PLA-Ca P composites the acid breakdown is chemically buffered by the Ca P. Water absorption increases as the degradation progresses due to accumulation of hydrophilic degradation products inside the polymer matrix. However on reaching a certain level, it reduces due to release of degradation products [Yang et al., 2008].

In the present study, the *in vitro* degradation kinetics of PLA/Ca P composite films containing HA or TCP in different concentrations was analysed by incubating samples in PBS at 37 °C. To understand the results obtained in this study it should be considered that in composite films two mechanisms are occurring simultaneously, i.e. degradation of PLA and dissolution of particles from the surface and the matrix, while the presence of the interface between the PLA and Ca P filler allows liquid to accumulate at this interface.

Among the non-filled PLA and PLA/Ca P films the least weight gain was shown by non-filled PLA and PLA-TCP films containing 40 wt % TCP at the end of 12 weeks. However, in the case of PLA-TCP40 films the possible reason for this low value is the dissolution of TCP particles from the sample in addition to polymer degradation. Whereas the low liquid absorption by non-filled PLA is expected as PLA is hydrophobic and the non-filled PLA samples also lack any interfaces which are present in the composite films and liquid can ingress the matrix through these interfaces in the composite films. One thing to note is that at day 1 in all the composite films, maximum liquid absorption was observed with samples which had the highest filler concentrations i.e. 70 wt %, so it can be seen that the water absorption increases with increase in the filler content. Similar results of of more liquid absorption with increase filler content were shown by Suwanprateeb et al. [1997] who investigated 0, 20 and 40 vol % of a spray dried HA, similar to the rHA used in this study, in a high density polyethylene. However, after the first day the values for liquid absorption decreased for

samples which had 70 wt % filler which can be attributed to the dissolution of particles from the samples. As the incubation proceeded, the liquid absorption by the films did not follow a set pattern which can be due to multiple factors that were occurring simultaneously. These factors include dissolution of the particles from the films, degradation of PLA and exposure of the particle surfaces which were embedded in the matrix due to the degradation of PLA matrix and which then caused increase in liquid absorption.

The degradation of non-filled PLA and PLA composite films used in this study was slow and the maximum weight loss was 7% in 12 weeks observed with PLA-TCP films containing 10 wt % TCP. As the thickness of the samples used in the study was between 0.04 to 0.07 mm, it is expected that the oligomers produced in the matrix were able to escape in the surrounding aqueous medium easily thus their effect of contributing to the autocatalysis is lost and did not increase the degradation rate. A study by Grizzi et al. [1995] also showed similar results, in that the PLA films lost only 5-7 % weight in 25 weeks.

Among the composite films which contained rHA, sHA and TCP the maximum weight lost was observed in films containing lower filler content i.e. 10 wt % filler. This result is in keeping with other studies that HA and TCP incorporation into the composite slows the degradation rate by hindering the autocatalytic degradation of polymer [Agrawal and Kyriacos, 1997; Imai et al., 1999; Ara et al., 2002]. The reason for higher degradation of some composite films than non-filled PLA films can be due to the dissolution of particles from the composite films which also added to the total degradation. Initially films containing 40 wt % filler showed more weight loss than from the films containing 70 wt % filler, however after 3rd week of incubation more weight loss was shown by films containing 70 wt % filler. This is probably due to more filler dissolution from the films containing 70 wt % filler which resulted in increased overall weight loss. Ural et al. [2000] has also suggested that the addition of HA in a polymer composite reduces the degradation rate and further that the composites with higher filler content degrade at a slower rate compared to those with lower filler contents. This may be due to the ability of HA or TCP particles present in the composite to absorb water molecules which penetrate the polymer matrix and are responsible for the hydrolytic decomposition of polymer chains.

Interestingly among PLA-nHA composite films the maximum weight loss was observed in films containing 70 wt % nHA followed by films containing 40 and 10 wt % nHA respectively. The degradation of composite films containing 10 and 40 % nHA was less than neat PLA films, which is in agreement with a study conducted by Ural et al. [2000] which showed that adding HA to the polymer composite reduces the degradation rate. Higher weight loss in films containing 70 wt % filler can be attributed to faster dissolution of filler particles from the surface of the samples and as the PLA-nHA70 had more particles present on the surface than PLA-nHA40 and PLA-nHA10 the weight loss was more pronounced.

The maximum weight loss at day 1 and at the end of 12 weeks was shown by PLA-TCP composite films which is also in agreement with other studies, that TCP dissolves faster than HA [Paul et al., 1993; Kwon et al., 2003].

4.6 CONCLUSIONS

Water absorption increases with the filler content in the composite. Dissolution of TCP particles from PLA-TCP composite was higher than the dissolution of HA particles from PLA-HA composite. Incorporation of Ca P in the composite slows the degradation rate. Although in this study, the degradation of composite films was not always lower than neat PLA films, however in samples where it was higher this can be attributed to dissolution of particles from the composite. Thus by varying the concentration of Ca P the degradation rate of PLA can be tailored to suit individual need of clinical applications.

CHAPTER 5: EFFECTS OF nHA AND PDGF CONCENTRATIONS ON OSTEOBLAST AND PDL CELLS GROWTH IN PLA-nHA COMPOSITE

5.1 INTRODUCTION

The use of a ceramic such as HA within a degradable PLA may confer a number of potential therapeutic advantages on this material, including increased mechanical properties, promotion of cell attachment and osteoconduction and the potential for use as a vehicle for slow delivery of bioactive proteins such as growth factors. PLA-HA composite material has been shown to be biocompatible, resorbable and have good mechanical properties [Shikinami and Okuno, 1999].

The incorporation of a suitable growth factor into a GTR membrane could enhance significantly the outcome of GTR procedures.

The aim of the study reported here was to investigate the proliferation and differentiation of osteoblast cells on PLA-nHA composite with different concentrations of nHA and assessing the potential of this material to act as a carrier system for growth factors delivery. In addition the nHA and the PLA-nHA composite films produced for the experiments were characterized by Scanning Electron Microscopy (SEM), Fourier Transform Infra Red spectroscopy (FTIR) and X- Ray Diffraction (XRD).

5.2 MATERIALS

5.2.1 Polylactic acid

PLA (PURAC Biochem, The Netherlands) as described in section 2.2 was used for the fabrication of the films.

5.2.2 Nano-Hydroxyapatite

nHA was produced in the lab for this experiment. For nHA production, calcium nitrate tetrahydrate [$Ca(NO_3)_2.4H_2O$] was used as the calcium precursor dissolved in ethanol, both obtained from Sigma Aldrich (UK). Sodium hydrogen phosphate [$(NH_4)_2HPO_4$] also purchased from Sigma Aldrich (UK) was used as a phosphate precursor in the reactions dissolved in deionised water. The production method is described in section 5.3.2.

5.2.3 Cells

Primary rat calvarial osteoblasts isolated by collagenase digestion and rat periodontal ligament (PDL) cells isolated by explant culture were used in the experiments. Osteoblasts and PDL cells were donated by Dr C Wellman and Dr M Al-Masri respectively (Barts & The London School of Medicine & Dentistry). The cells were cultured and maintained in Minimal Essential Medium (MEM) Alpha medium (Invitrogen, UK) which was supplemented with 10% fetal calf serum (FCS) (Sigma Aldrich, UK), 0.3µg/ml fungizone (Invitrogen, UK) and 50u/ml penicillin- 50ug/ml streptomycin (Invitrogen, UK). The cells were grown in a humidified incubator at 37°C with 5% CO_2. The medium was replaced twice a week.

5.2.4 Platelet Derived Growth Factor

Recombinant rat Platelet Derived Growth Factor – BB (PDGF-BB) purchased from Sigma Aldrich (UK) was used in the experiments.

5.2.5 CASY cell counter

Cells cultured on the films were counted using a CASY electronic cell counter (Model TTC, Sedna Scientific Ltd). CASY measures the cells suspended in the solution by aspirating through a precision measuring pore. On passing through the aperture these cells are scanned at a frequency of 1 MHz in a low voltage field (Figure 5.1). The signal data is then accumulated to give the total number of cells.

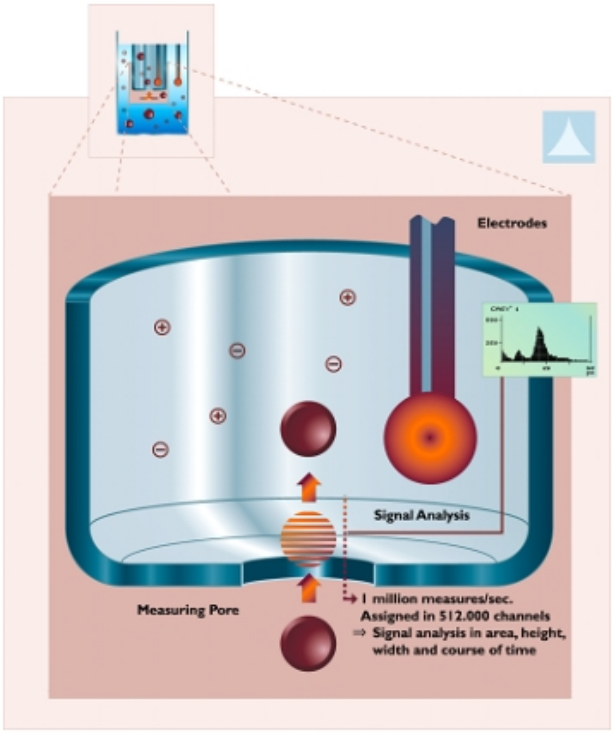

Figure 5.1: A schematic presentation of CASY cell counter working [adapted from sednascientific.com].

5.2.6 CellTiter 96® AQ_{ueous} non-radioactive cell proliferation Assay (MTS)

Cell proliferation on the films was assessed by an MTS assay. A solution of MTS (Promega UK Ltd) and phenazine methosulfate (PMS) (Sigma Aldrich, UK) was used to determine the number of viable cells on the films.

5.2.7 Alkaline phosphatase (ALP)

ALP assay was prepared by dissolving 2 × 15 mg tablets of *p*-nitrophenyl phosphate in 8.36ml of distal water in addition to 6µl $MgCl_2$ (2M) and 2.35ml of alkaline buffer solution (1.5 M) (Sigma, A9226).

5.3 METHODS

5.3.1 Film fabrication

The films were fabricated as described in detail in section 2.3.1. That is the PLA was dissolved in chloroform and once fully dissolved the nHA was added to give PLA-nHA composite films containing 10 wt % nHA (PLA-nHA10), 40 wt % nHA (PLA-nHA40) and 70 wt % nHA (PLA-nHA70). The suspension was further stirred and then the films were cast. The films were cut into 12mm circular samples and were sterilized by ultraviolet (UV) irradiation.

5.3.2 Nano-hydroxyapatite synthesis

An Ethanol-based sol–gel method was used for the synthesis of nHA as reported by Feng et al. [2005].

Calcium nitrate tetrahydrate [Ca $(NO_3)_2.4H_2O$] (0.083M) in ethanol and amonium hydrogen phosphate [$(NH_4)_2HPO_4$] (0.05M) in water were mixed and the ratio of calcium and phosphate precursors was maintained at 1.66. $Ca(NO_3)_2.4H_2O$ was mixed in 50ml of ethanol and the solution was stirred and heated upto 85°C. On reaching 85°C, $(NH_4)_2HPO_4$ dissolved in 50 ml of water was added drop by drop by means of a glass-dropping funnel. Amonium hydroxide (NH_4OH) was added into the solution to maintain the pH value above pH 10. The solution was stirred for 5-6 hrs as gel formation occurred (Equation 5.1). The final gel was then aged in an oven for 24 hrs at 40°C.

The sample was then heat treated in a Carbolite furnance (Sheffield, UK) in air. The temperature was increased at the rate of 10°C min^{-1} and on reaching 700°C the sample was held for 60 minutes and then cooled down to 20°C at the same rate. The powder was then ball milled for 12 hrs.

$$10Ca\,(NO_3)_2\,4H_2O + 6(NH_4)_2HPO_4 + 8NH_4OH \rightarrow Ca_{10}\,(PO_4)_6(OH)_2 + 20NH_4NO_3 + 6H_2O$$

Equation: 5.1

5.3.3 Films and nHA characterisation

5.3.3.1 FTIR

FTIR spectra of the PLA and PLA-nHA composite films were collected using a Thermo-Electron Nicolet 8700 FTIR spectrometer. The spectra were obtained at 8cm^{-1} resolution and a total of 256 scans were collected.

5.3.3.2 SEM

The morphology and the size of synthesised n-HA particles and the films were characterised by SEM (FEI Inspect F, EFI Company, The Netherlands) using the field emission technique. For nHA samples 20kV was used and for PLA and nHA-PLA composite films 5kV was used.

5.3.3.3 XRD

The nHA powder produced was characterized using XRD, to find chemical composition, crystal state and the crystalline content. A Simens/Bruker D5000 Diffractometer, with monochromatic Cu Ka radiation (k = 0.15418 nm) was used to obtain the nHA powder XRD. Scans were obtained in the 2θ range = 20–60, with a step size of 0.02 s^{-1}. Commercial nHA (Sigma, UK) was scanned to provide a comparative XRD pattern.

5.3.4 Cell culture

To evaluate osteoblast proliferation on different films, cells were seeded on PLA films and 10, 40, 70 wt % PLA-nHA composite films. Osteoblasts of 7-9th passage were used for the tests. 90% confluent cells were trypsinized and cell density was adjusted to 3×10^4 cells/ml. UV sterilised films were transferred into 24 well plates, a small dot of silicon was used to stick the films to the base of the wells. The films were seeded with 3×10^4 cells/ml / well for 1, 2, 4, 7, 10 and 14 days in triplicates. Wells with no films were used as controls.

For experiments in which platelet derived growth factor was added, the cell density was decreased to 1×10^4 cells/ml/well and the medium was

supplemented with 1% fetal calf serum instead of 10% fetal calf serum. The well plates were placed in a humidified incubator at 37°C with 5% CO_2. Cell proliferation was analyzed at day three.

PDL cell proliferation was analysed on 10 and 70 wt % PLA-nHA composite films. PDL cells of 11-13th passage number were used. For cell seeding on films the same protocol was used for PDL cells as was used for osteoblasts.

5.3.5 PDGF addition

The effect of PDGF added to the films on the proliferation of cells was evaluated. To pre-adsorb PDGF to films for testing, 100ng recombinant rat platelet-derived growth factor – BB (PDGF-BB) (Sigma) in 100 µl phosphate buffered saline (PBS) was added to the surface of specimens placed in 24 well plates. The films were then incubated for three hrs at 37°C. After three hrs the PBS solution was carefully removed from the surface of the films and cells at density 1×10^4 cell ml^{-1} were seeded on to the films.

In a second set of films, rather than adding PDGF directly on the films, PDGF was added to the medium in solution at the same time as adding the cells as above. The final concentration of PDGF in the medium was 100ng ml^{-1} so that the same total amount of PDGF was added to the well as when films were pre-adsorbed with PDGF. 1ml of PDGF containing medium was then added to each film placed in 24 well plates. Cells in medium without PDGF with 1 and 10% FCS supplement were used as negative and positive controls respectively.

5.3.6 CASY cell counting protocol

In order to measure the cells on the films, films were removed from the medium at days 1, 2, and 5 and were placed in new 24 well plates. The films were then washed with PBS, after which 500µl trypsin was added to each well and the plates were placed in the incubator for 10 minutes. After that 1.5ml of cell medium was added to each well and mixed with trypsin containing cells. From this cell containing medium/trypsin solution 500µl was removed and added into 4.5ml of CASY diluting solution. The cell numbers were then analysed using CASY counter.

5.3.7 MTS Assay protocol

MTS changes colour on reacting with cells. The amount of colour change is directly proportional to the number of living cells. In order to measure cell proliferation films were taken from the medium at day 1, 2, 4, 7, 10 and 14 and were placed in new 24 well plates. PMS and MTS solution were mixed at a concentration of 50µl/ml just before addition to the medium. MTS/PMS solution was then added to the medium at a concentration of 200 µl/ ml, then 500 µl of MTS/PMS solution containing medium was added to the wells containing films.

The well plates were incubated for 3 hrs, then three samples of 100µl each were taken out from each of the wells and transferred to 96 well plates. The colorimetric measurement was then performed using a spectrophotometer at 490 nm (FLUOstar Optima, BMG Labtech).

5.3.8 ALP activity

ALP activity of cells was evaluated by adding 500µl ALP solution to each film in 24 well plates. ALP solution was added to the same films after taking out MTS solution.

The films were then incubated for at 37°C for one hour. After one hour three samples of 100µl each were taken from each film and absorbance was measured at 405nm in a photospectrometer.

5.3.9 Cell morphology

SEM was used for morphological analysis of cells. At the 14^{th} day of incubation the films containing cells were washed with PBS twice before fixing the cells in 4 % formaldehyde for 15 minutes. The cells were then dehydrated by suspending in successive 50, 70, 80, 90 and 100% ethanol solutions for 5 minutes each. The films containing cells were finally transferred to hexamethyldisilazane and were allowed to dry at room temperature. The films samples were then gold coated and analyzed under SEM at 5kV.

5.3.10 Data Analysis

Statistical analyses of cell culture data were calculated by 1- way ANOVA with Bonferroni's post-test with $P < 0.05$. Analysis was carried out using GraphPad Prism software.

5.4 RESULTS

5.4.1 nHA characterisation

5.4.1.1 SEM

Figure 5.2 shows the morphology and size of nHA synthesized. The particles were agglomerates of spherical nodules with the nodules being 40-60nm across and the agglomerates being 0.5 – 1mm across. High temperature during synthesis, low temperature during ageing and then an increase in temperature during heat treatment causes variations in the size of the particles.

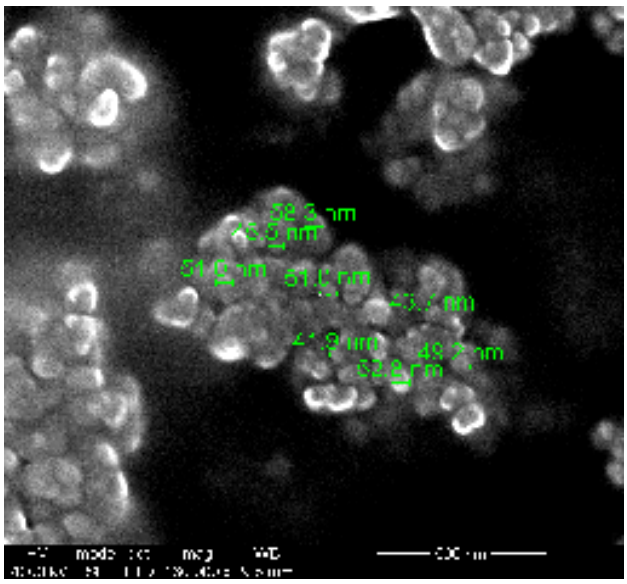

Figure 5.2 SEM of nHA showing individual nodule size and morphology within the agglomerated granules (scale bar= 500nm).

5.4.1.2 FTIR

FTIR spectrum of nHA powder is shown in Figure 5.3. The peaks at 3571 cm^{-1} and 631cm^{-1} represent OH group. The peaks at 1040, 603 and 569 cm^{-1} represent the P-O absorption band. CO_3 group is represented by the peak at 1473 cm^{-1}.

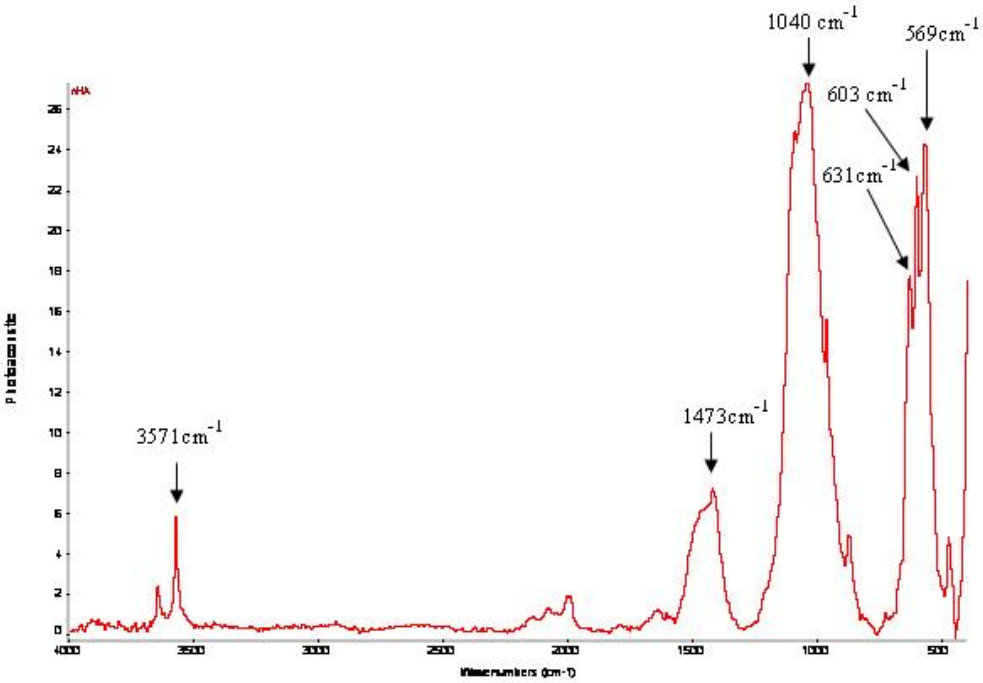

Figure 5.3: FTIR spectrum of synthesized nHA powder.

5.4.1.3 X-ray Diffraction

X-ray diffraction (XRD) of commercial (Plasma Biotal, UK) and experimental nHA are shown in Figure 5.4. A strong diffraction peak at 31.9° with lesser peaks at 32.2, 32.9 and 25.9 and 39.8, 46.7 and 49.5 confirm the presence of hydroxyapatite. The diffraction patterns correspond to hydroxyapatite and confirmed the phase purity and high crystallinity of the materials produced. The slight broadening of the peaks shows that the nHA has slightly lower crystallinity than the commercial HA.

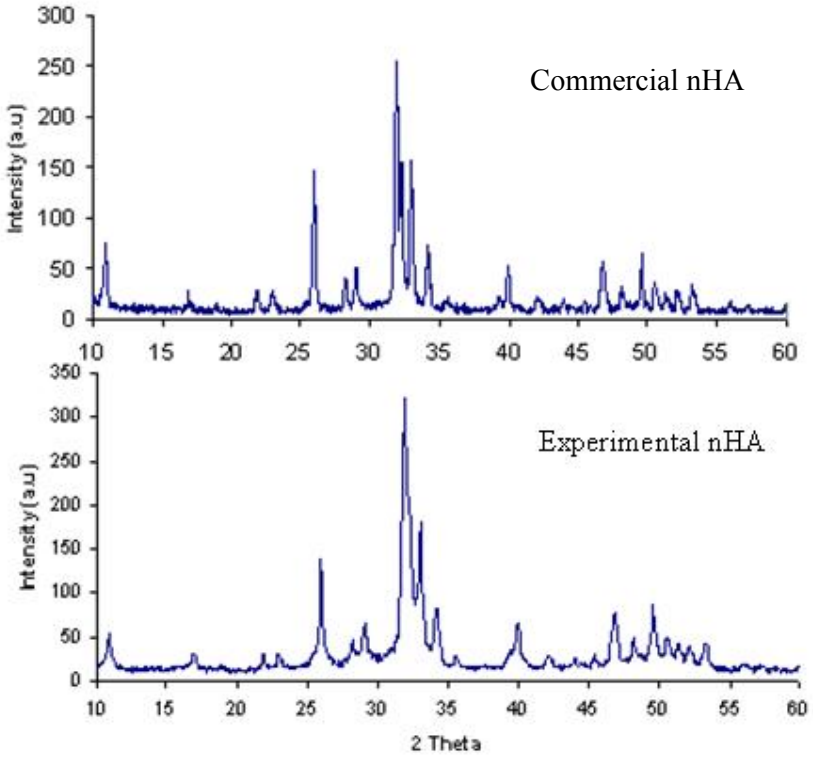

Figure 5.4 XRD pattern of commercial and experimental nHA

5.4.2 Film characterisation

5.4.2.1 SEM

Figures 5.5, 5.6 and 5.7 respectively show the morphology of 10, 40 and 70 wt % PLA-nHA composite films. The surface of PLA-nHA70 film showed more nHA on the surface as compared to PLA-nHA10 and PLA-nHA40 composite films. The surface of PLA-nHA10 film appears smooth, whereas the surface of PLA-nHA70 film is rougher, irregular and shows micropores due to presence of nHA. It is interesting to see that at 10 wt %, a few nHA agglomerates can be seen and that these are all covered in a visible PLA layer. However as the nHA content increases, the amount of visible nHA increases and at 70 wt % nHA substantial areas of the film surface appear nHA exposed from the PLA matrix. It is likely that a very thin layer of PLA is covering these particles but that the layer is too thin and thus too electron-lucent to be visible on the SEM image. All these images are of the "top" surface that is the air contacting surface as the films dried.

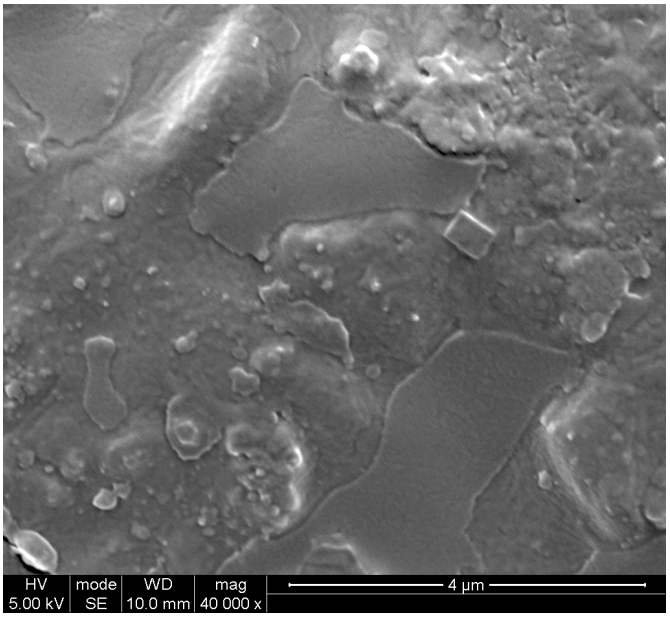

Figure 5.5: SEM image of PLA-nHA10 film (scale bar 4 µm).

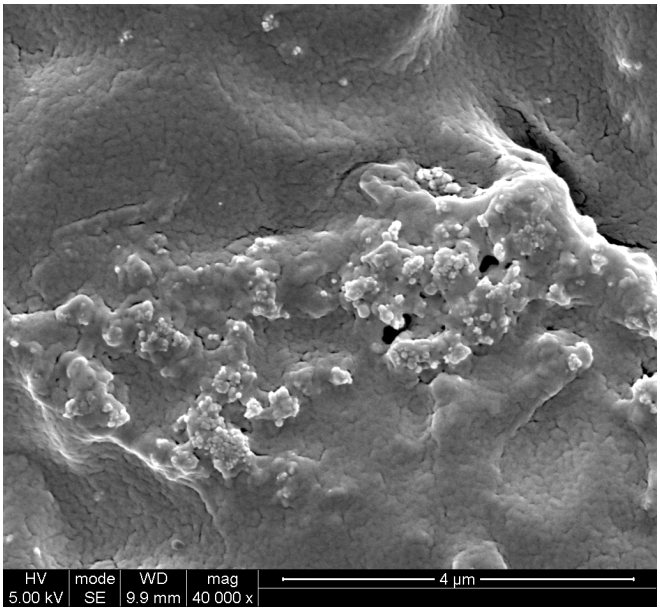

Figure 5.6 SEM image of PLA-nHA40 film (scale bar 4 µm).

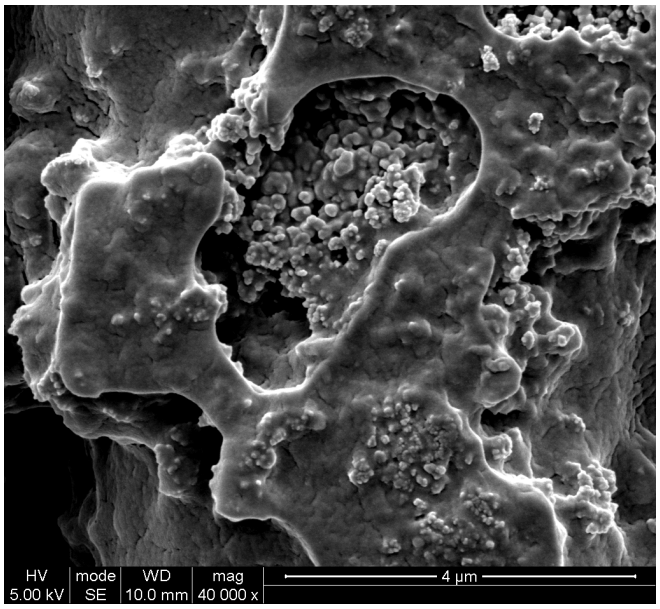

Figure 5.7 SEM image of PLA-nHA70 film (scale bar 4 µm).

5.4.2.2 FTIR

FTIR spectra of PLA film and PLA-nHA10, PLA-nHA40 and PLA-nHA70 composite films are shown in Figure 5.8. The peak at 1760cm^{-1} represents the carbonyl group of PLA which is present in all films and showed no drift even in PLA-nHA70 films. HA peak at 3571cm^{-1} is more pronounced in PLA-nHA composite film, whereas it decreases as the nHA content decreases in PLA-nHA40 and PLA-nHA10 films. The peaks between 538cm^{-1} and 638cm^{-1} represent bending peaks of phosphate from the nHA in PLA-nHA composite films.

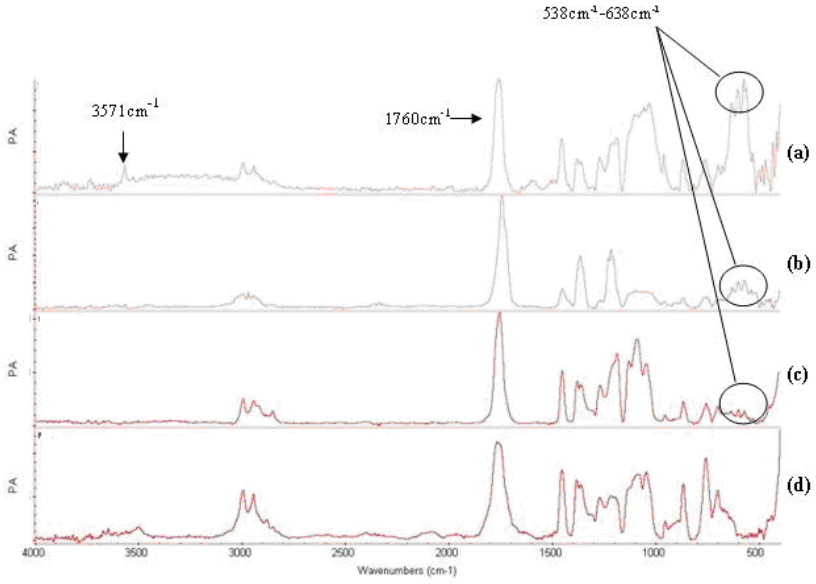

Figure 5.8 FTIR spectra of (a) PLA-nHA70 film (b) PLA-nHA40 film (c) PLA-nHA10 and (d) PLA film.

5.4.3 Cell proliferation assessed by CASY cell counter

Figure 5.9 shows the number of cells on PLA film, PLA-nHA10 and PLA-nHA70 composite films at day 1, 2 and 5 after culture. Although the cell numbers were greater at day 5 than at day 1 and 2, the cell number on different films showed no specific trend with high variations.

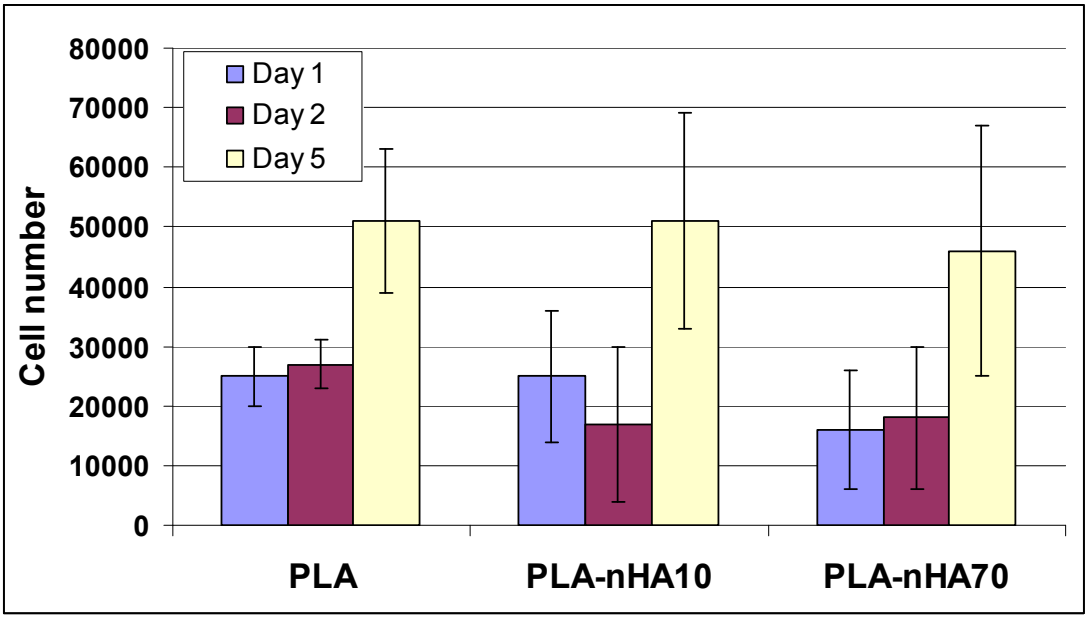

Figure 5.9: Osteoblast cell numbers on different films at day 1, 2 and 5 (n=3 per material and time).

5.4.4 Cell proliferation assessed by MTS assay

5.4.4.1 Osteoblast proliferation on PLA and PLA-nHA films

Osteoblasts cell proliferation on different films is shown in Figure 5.10. Among the films, cells showed highest proliferation on PLA-nHA10 films. The rate of proliferation of cells decreased with the increase of nHA content in the films. Cells reached confluence at 10 days on PLA and PLA-nHA10 films, whereas the cells were still proliferating on PLA-nHA40 and PLA-nHA70 composite films at day 14. PLA-nHA70 films showed less cell growth when compared to the other films. The experiment was repeated three times with similar results.

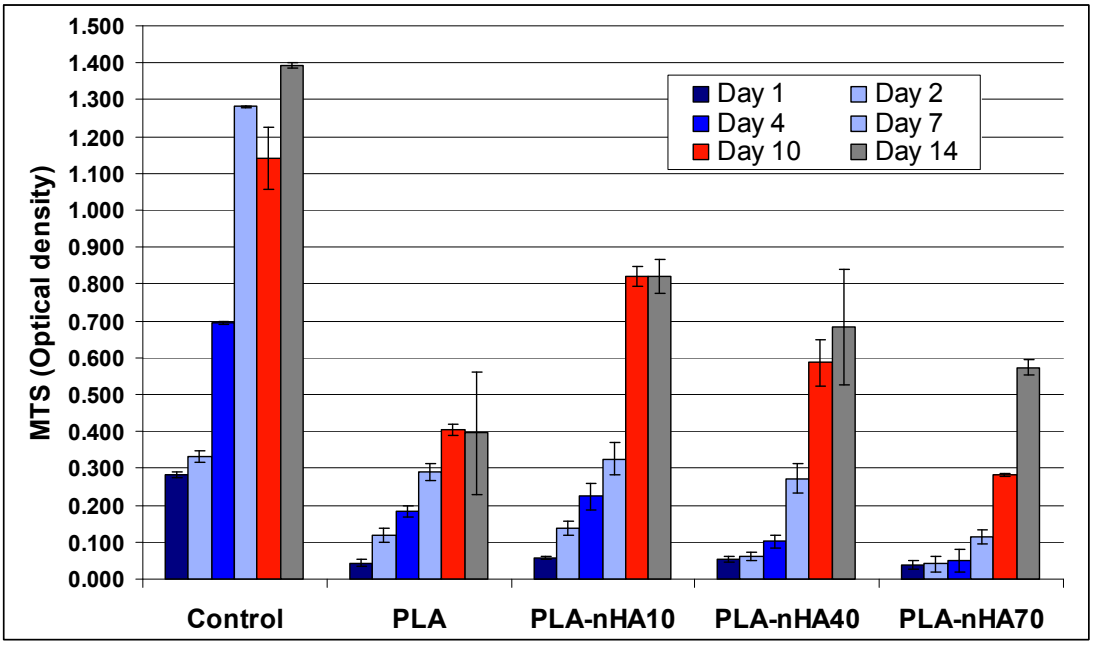

Figure 5.10: Proliferation of osteoblasts on PLA and PLA-nHA films containing different amount of nHA (n=3 per material and time)

5.4.4.2 PDL cells proliferation on PLA-nHA films

PDL cells showed similar responses on films with different nHA content. Cells proliferated less on films with higher HA content. Figure 5.11 shows more cell proliferation on PLA-nHA10 composite film than on PLA-nHA70 composite film. The experiment was repeated three times with similar results.

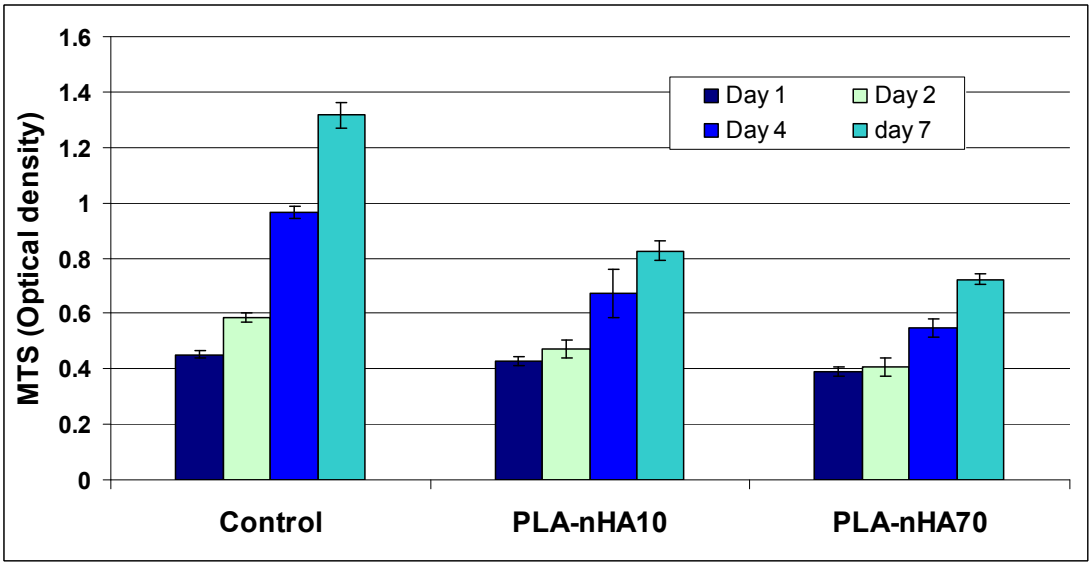

Figure 5.11: Proliferation of PDL cells on films containing different amount of nHA compared to tissue culture plastic as the control (n=3 per material and time)

5.4.4.3 Osteoblast proliferation with PDGF added on the films and in the medium

Figure 5.12 shows the proliferation of cells at day 3 on different films loaded with PDGF and on films in which PDGF was added in the cell medium. The films on which PDGF was directly added showed more cell proliferation compared to films in which PDGF was added to the cell medium. There was no difference between cell proliferation on positive control films with 10% FCS and films with PDGF in the medium, whereas PDGF adsorbed to films caused the greatest proliferation. The lowest cell proliferation was seen on negative control films with 1% FCS and no PDGF added. The experiment was repeated three times with similar results.

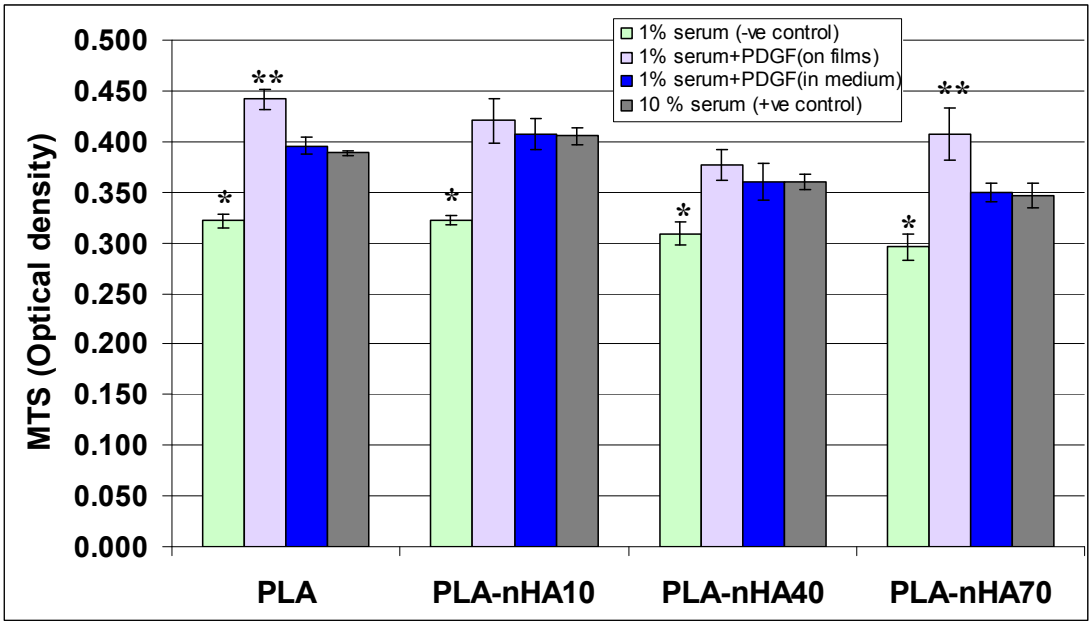

Figure 5.12: Osteoblast cell proliferation in response to PDGF adsorbed to films or in solution in the medium. Mean ± SD n=3 per material and serum condition. *Significantly less than other groups. **Significantly greater than other groups, p<0.05 1–way ANOVA and Bonferroni Post test.

5.4.4.4 Alkaline phosphatase activity

Figure 5.13 shows alkaline phosphatase activity of osteoblasts cells at the 14th day after culturing on different films. The data was normalized by cell number. The cells on PLA-nHA films containing 70 wt % nHA showed the highest alkaline activity, whereas the lowest cell activity was observed on control and PLA films.

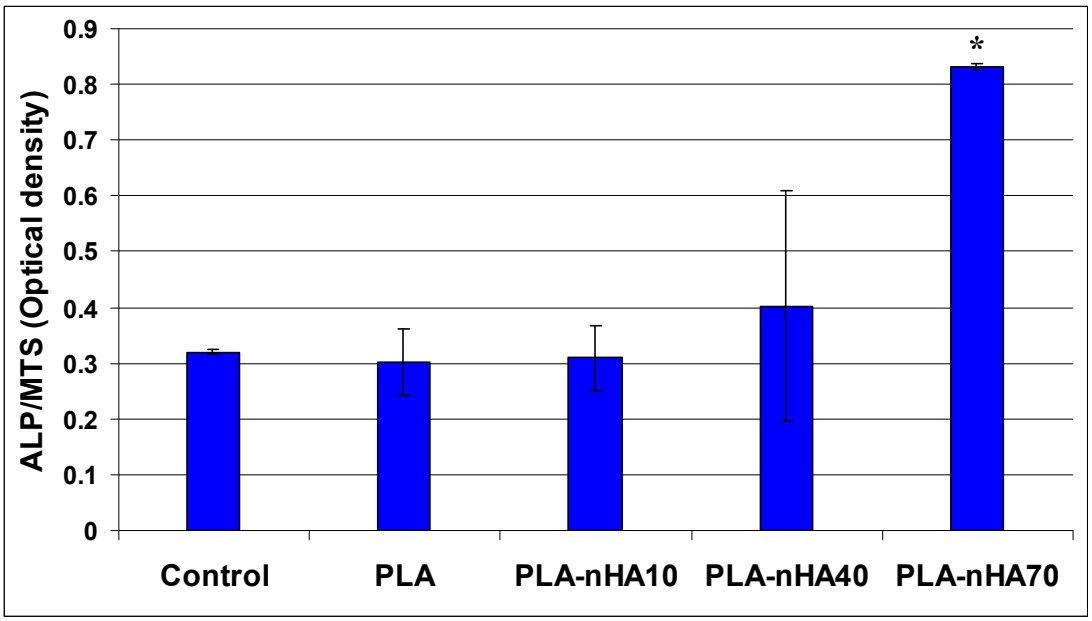

Figure 5.13: ALP activity of osteoblasts cells seeded on different films. The data was normalized by cell numbers. (n=3 per material). Mean ± SD. *Significantly greater than other groups, p<0.05 1–way ANOVA and Bonferroni Post test.

5.4.4.5 Cell morphology

SEM images of cells at day 14 after culturing on PLA, PLA-nHA10, PLA-nHA40 and PLA-nHA70 composite films are shown in Figure 5.14. The cells on the films are well spread and fully cover the films. The cells on PLA and PLA-nHA10 films are densely packed and forming layers. On the films containing 40 and 70 wt % nHA the cells are bridging over the surface depressions and pores formed by the nHA particles.

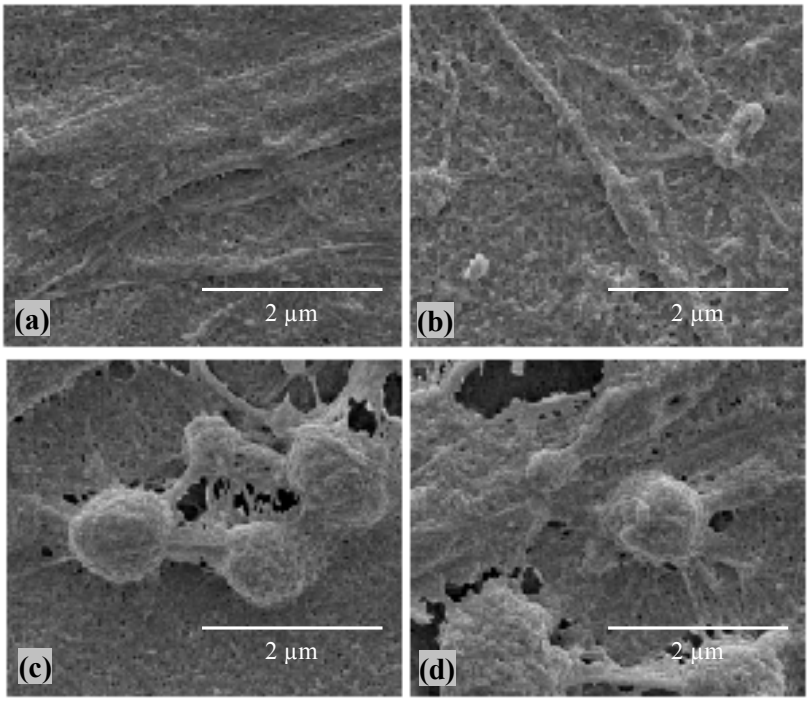

Figure 5.14: SEM images of cells cultures at day 14 on (a) PLA (b) PLA-nHA10, (c) PLA-nHA40 and (d) PLA-nHA70 composite films (All scale bars= 2μm).

5.5 DISCUSSION

Different materials are currently being used as barrier membranes for guided tissue regeneration (GTR), however with limited regeneration potential. Consequently there is considerable interest in further developments in regenerative techniques to improve outcomes and predictability. One possible development is to use growth factors incorporated in the membranes for their release at the site to enhance tissue growth.

In this study nHA-PLA composite films have been analyzed as potential materials for GTR membranes. In order to assess biocompatibility, the effect of these films on growth of osteoblasts and PDL cells was tested. The aim was to develop a membrane which can enhance regeneration by combining the properties of resorbable PLA and bioactive nHA and also has the ability to deliver bioactive proteins such as growth factors at the defect site, thus further enhancing regeneration.

Hydroxyapatite is a known biocompatible and osteoconductive material and has the ability to absorb and release proteins [Matsumoto et al., 2004]. nHA with particle size between 40-60 nm was produced and the SEM image (Figure 5.2) of nHA shows the nano and spherical structure of the particles. Nano and spherical structured HA is advantageous, as it provides more surface area and binding sites for both, cell attachment and protein absorption. The crystallinity and purity of nHA was confirmed by XRD which only showed the reflection peaks associated with HA and no peaks related to tricalcium phosphate or calcium oxide were present. Similarly, the nHA FTIR spectra showed the typical characteristics of HA [Khan et al., 2008].

SEM images of films with different nHA content showed that as the nHA content increases, the surface of film becomes rougher which could provide more surface area for cell attachment [Teng et al., 2009]. In FTIR spectra of films, there was no shift of PLA carbonyl group peak at 1760cm^{-1}, which shows that the mixing of PLA and nHA is physical and no chemical reaction took place. Bending peaks of phosphate from HA between 538cm^{-1} and 638cm^{-1} become more pronounced as the nHA content increases from 10 to 70 wt %. The OH group peak at 3571cm^{-1} is only visible in PLA-nHA containing 70 wt % nHA.

The effect of nHA-PLA films on proliferation and differentiation of osteoblasts were tested. Both cell proliferation and differentiation were assessed on the same sample so that the results can be correlated. It is known that the initial cell adhesion to a material is important, because it greatly influences the succeeding processes of cell proliferation and differentiation [Dalby et al., 2002; Verrier et al., 2004].

CASY cell counter results showed that cell number increased at 5 day compared to 1 and 3 days. However, the results did not show any specific pattern of cells growth on different films or the effect of different films on the cells proliferation. This high variation can be either due to ineffectiveness of trysinisation to completely remove cells from films or due to CASY counter reading errors resulting from the presence of nHA particles in the solution. Longer than usual incubation after trysinisation and cleaning of CASY counter (cleaning was done with running a cycle of CASY solution) after every reading

was tried to overcome this problem, but with little success. Thus the CASY technique was rejected in this application.

The MTS assay showed less variable results and a constant pattern of cell growth on different film, so after initial tests all the experiments were carried out using the MTS assay. Both osteoblasts and PDL cells showed high proliferation on films with lower nHA content and low proliferation on films with high nHA content. PDL cells showed more proliferation on films containing 10 wt % nHA than films which contained 70 wt % nHA. Similar results were shown by osteoblasts, with the highest cell proliferation being shown by cells on films containing 10 wt % nHA followed by films containing 40 and 70 wt % nHA respectively. There was minimal difference between the number of cells on PLA and PLA-nHA10 films at day 10 and 14; this may be because the cells had already reached confluence on these films at day 10, whereas the cells on PLA-nHA40 and PLA-nHA70 films were still proliferating at days 10 and 14 and showed an increase in number between days 10 and 14.

ALP levels can be attributed to the degree of cell differentiation [Matsuyama et al., 1990]. In this study, high ALP expression showing differentiation of osteoblasts cells on films containing high concentrations of nHA may explain the low number of proliferating cells on PLA-nHA40 and PLA-nHA70 film, and high number of cells on PLA and PLA-nHA10 films. The highest ALP activity was seen in the cells on PLA-nHA70 films, which is probably due to the differentiation promoting effect of nHA on cells. Low levels of ALP in cells on PLA and PLA-nHA10 films suggest no or low differentiation of these cells. Theses results are in support of various studies that nHA encourage bone cells to differentiate [Hott et al., 1997; Matsumura et al., 2004; Zhang et al., 2008].

PDGF is a heparin-binding polypeptide and has mitogenic, proliferative and chemotactic effects on connective tissue cells [Nevins et al., 2003]. PDGF adsorption in the composite films and its subsequent effect on the proliferation of osteoblasts was analyzed. The cells which were treated with PDGF, either by adding PDGF in the serum or by absorption in the films, showed more proliferation on day 3 as compared to 1% serum control samples. Cell proliferation on samples where soluble PDGF was added to the medium and on control samples containing 10% serum in the medium were similar. However the

highest cell proliferation was seen on films where PDGF had been pre-adsorbed. This result shows that the effect of PDGF on cells was highest where a carrier was used and also establishes that these films can be used as a carrier for growth factor delivery.

5.6 CONCLUSIONS

The highest proliferation of PDL cells and osteoblasts was achieved on PLA-nHA10 films, whereas highest ALP activity was shown by cells cultured on composite films containing 70 wt % nHA. PDGF enhanced the proliferation of osteoblasts. The highest proliferation was shown by cells on films pre-adsorbed with PDGF which shows the suitability of these composites as a carrier system for growth factor delivery. A composite material containing high concentration of nHA may be a very useful material for application as a GTR membrane.

CHAPTER 6: DETERMINATION OF THE FLEXURAL STRENGTH OF POLYLACTIC ACID-HYDROXYAPATITE COMPOSITE MEMBRANES

6.1 INTRODUCTION

Collapse of GTR membranes is one of the major causes of their failure which results in compromised clinical outcomes. An ideal membrane should be stiff enough to withstand overlying tissue and masticatory pressure. This requirement is more important when the GTR membrane is used without graft to cover a large bone defect. Although a stiff membrane will be able to withstand the occlusal forces, it may not be easy to adapt a stiff membrane over the bone defects and may require substantial chair side preparation. Additionally a stiff membrane may also damage the soft tissue.

The strength and stiffness of a membrane can be improved by using a fibre reinforced composite material, also the limitations of using a stiff membrane can be avoided by using a prefabricated membrane. This prefabrication can minimize the chair side preparation and will also improve membrane adaptation. As has been investigated in chapter 8, few membranes shapes can fit most of the alveolar bone defects it may be possible to use prefabricated membranes with adequate strength and stiffness to withstand the occlusal pressures.

The aim of study reported in this section is to investigate the effect of fibre orientation on the flexural strength of the proposed PLA-HA-PLA fibre composite membrane.

6.2 MATERIALS

6.2.1 PLA

The PLA used as the matrix polymer was obtained from PURAC Biochem (The Netherlands) and is described in section 2.2.1.

6.2.2 PLA fibres

Drawn PLLA fibres were obtained from Degradable Solutions Ltd, Switzerland. They had mean fibre diameter of 50 – 80 μm.

6.2.3 HA

Sintered HA (sHA) was used as filler in the composite and is described in section 2.2.3.

6.3 METHODS

6.3.1 Prepregging

PLA-HA-PLA fibre composite sheets were prepared using a prepregging machine. To prepare the prepreg, PLA fibres were pulled through a PLA-HA matrix solution and then collected on a rotating drum as shown in Figure 6.1.

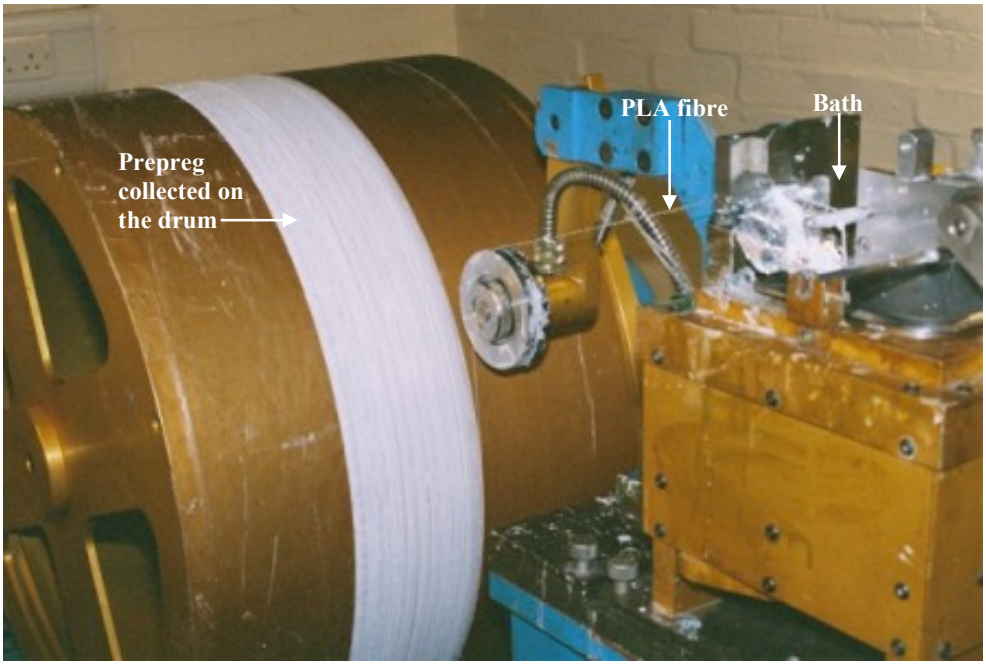

Figure 6.1: PLA fibre being collected on a drum after passing through PLA-HA matrix (image from Prof Liz Tanner).

The PLA-HA matrix solution was prepared by dissolving PLA in acetone, in which sHA was added to obtain a final 70 % wt concentration. 10 g PLA was added to 500 ml acetone in a flask and stirred for 6 hours at room temperature. Once the PLA was completely dissolved, 7 g sHA was added to the solution and stirred for a further 72 hours to ensure a homogenous mix. The matrix solution was then transferred into the bath on the prepregging machine. Next two fibre spools were mounted at the opposite side of the collection drum and the fibres were unwounded and passed through the matrix bath and wounded onto the drum which was covered with a wax paper. The machine was started to rotate the drum which also moved transversely. After the rotating drum was covered with a layer of prepreg the machine was stopped. The prepreg was left on the drum to dry overnight. Once completely dried the sheet was cut off from the drum and heat treated. For heat treatment, the prepreg was cut into smaller pieces (Figure 6.2) which were then pressed between two metal plates and placed in the oven at 70 °C for 1 hour. After one hour the oven was turned off and the specimens were allowed to cool gradually over night. An optical microscope image of the prepreg sheet is shown in Figure 6.3.

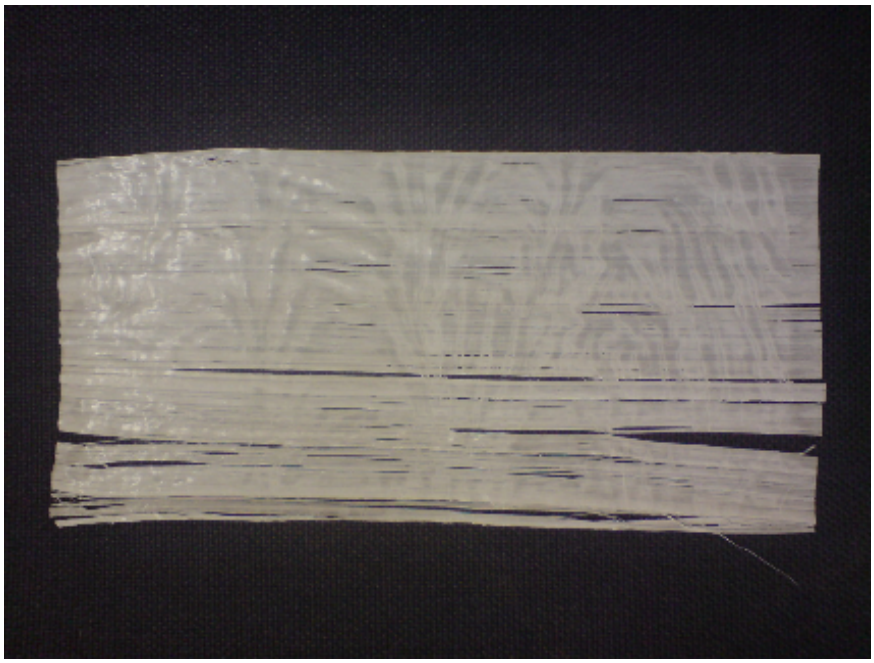

Figure 6.2: Prepreg containing PLA fibres in a PLA-HA matrix.

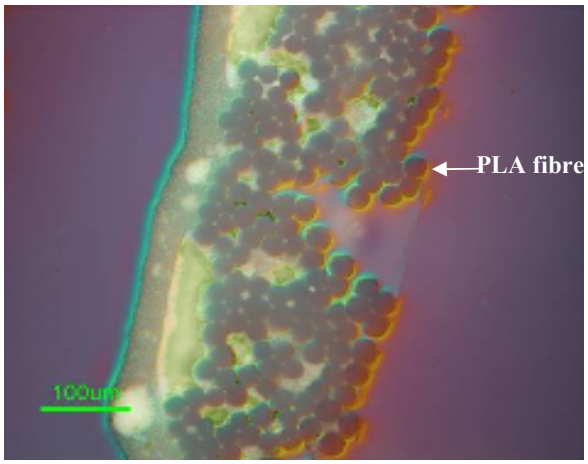

Figure 6.3: An optical microscope image of prepreg sheet showing PLA fibres embedded in the PLA-HA matrix. (Image from Dr Wojciech Chrzanowski)

6.3.2 PLA-HA-PLA fibre composite membrane fabrication

PLA-HA-PLA fibre composite membranes were fabrication by hot pressing 7 layers of prepreg in a stainless steel mould with three different lay ups. The prepreg lay up used were 0°/0°/0°/90°/0°/0°/0°, 0°/0°/90°/0°/90°/0°/0° and 0°/90°/0°/90°/0°/90°/0° as shown in Figure 6.4 (a) Group 1, (b) Group 2 and (c) Group 3 respectively.

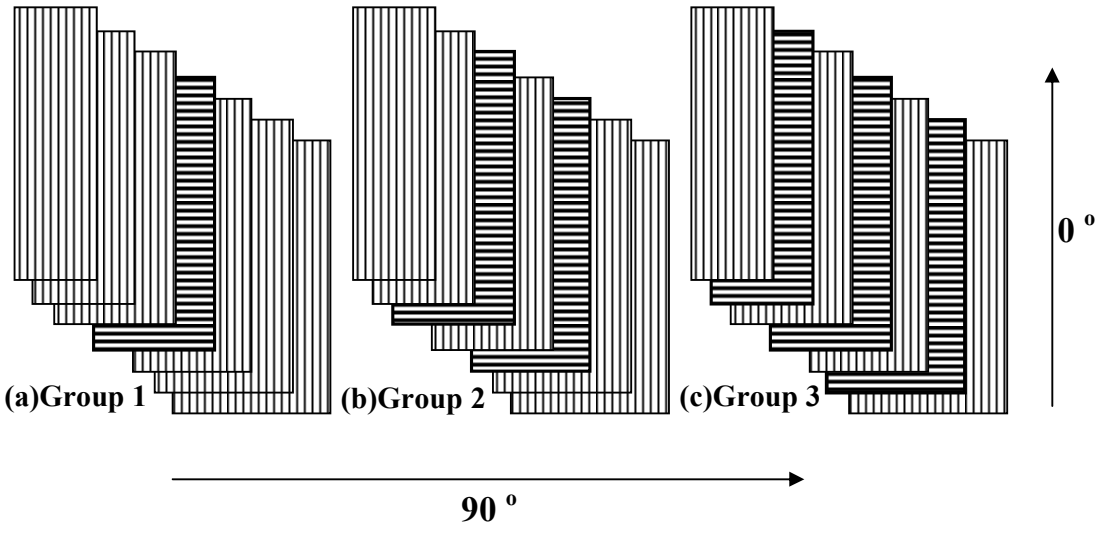

Figure 6.4: Prepreg lay up used for membranes fabrication (a) 0°/0°/0°/90°/0°/0°/0°, (b) 0°/0°/90°/0°/90°/0°/0° and (c) 0°/90°/0°/90°/0°/90°/0°.

The mould was placed in the hot press (Mackey Bowley, Kent, UK) and the pressure was applied. The temperature was gradually increased to a maximum of 140 °C. The pressure was increased with increase in the temperature, thus final pressure at 140 °C was 10 MPa. On reaching 140°C the mould was kept at this temperature for 3 minutes before the heating was turned off and the mould was allowed to cool under pressure. Once the temperature dropped to 40°C the mould was removed from the hot press and the membrane was taken out (Figure 6.5). The thickness of all the membranes produced was nominally 0.9mm. The samples were then cut parallel to long axis of the mould to get the fibre orientation shown in Figure 6.4.

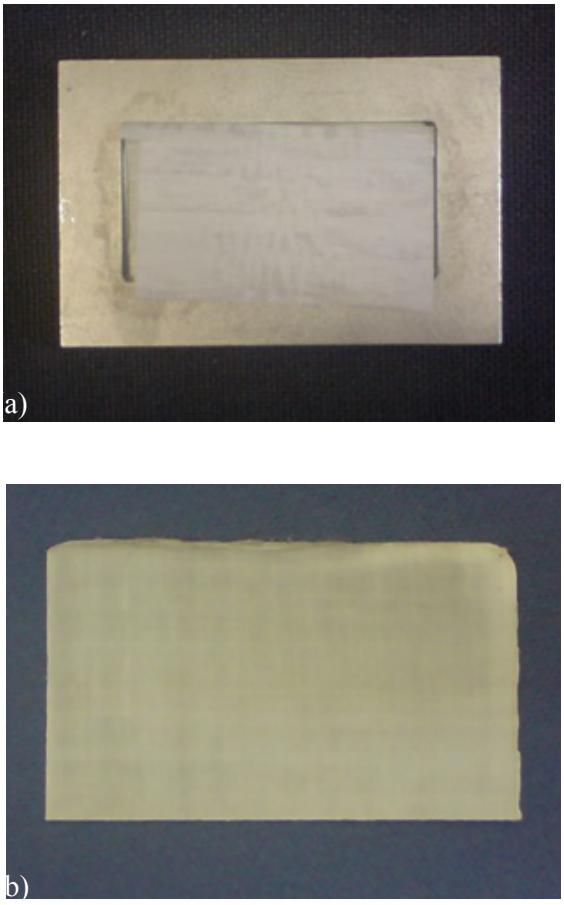

Figure 6.5: (a) Mould used to hot press the prepreg, and (b) a seven layer PLA-HA-PLA fibre composite membrane produced using the prepreg.

Additionally the membranes of Group 1,2 and 3 were cut across the long axis, which gave the samples having fibre orientation 90°/90°/90°/0°/90°/90°/90°, 0°/90°/0°/90°/0°/90°/90°and 90°/0°/90°/0°/90°/0°/90° respectively and are shown in Figure 6.6 (a) Group 4, (b) Group 5 and (c) Group 6.

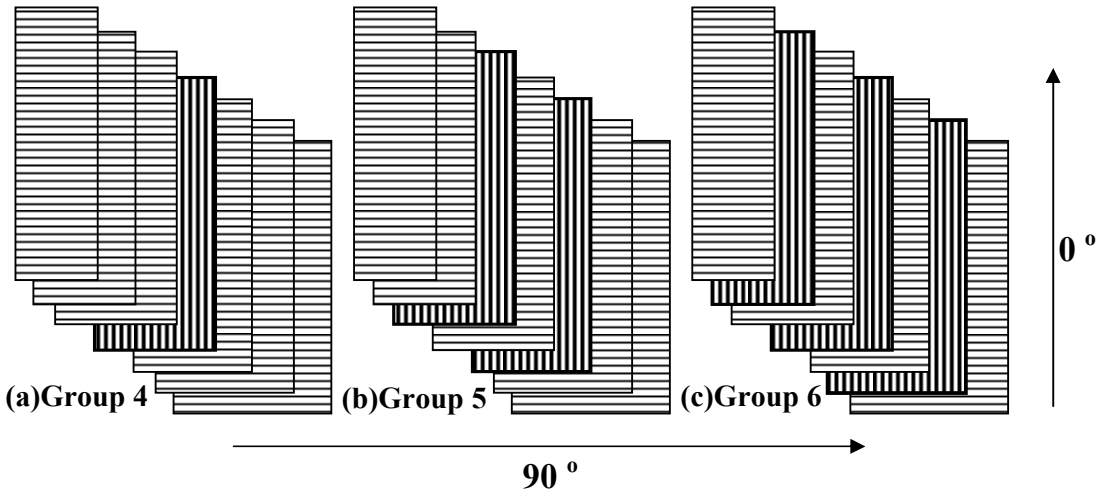

Figure 6.6: Membranes of Group 1, 2 and 3 were cut across and resulted in samples with fibre orientations (a) Group 4, 90°/90°/90°/0°/90°/90°/90°, (b) Group 5, 90°/90°/0°/90°/0°/90°/90° and (c) Group 6, 90°/0°/90°/0°/90°/0°/90° respectively.

6.3.3 Four point bending test

The tests were carried out using a MTS machine (858 MiniBionix® II). Figure 6.7 (a) shows sample setup for four point bending test and (b) a sample being tested under the applied displacement.

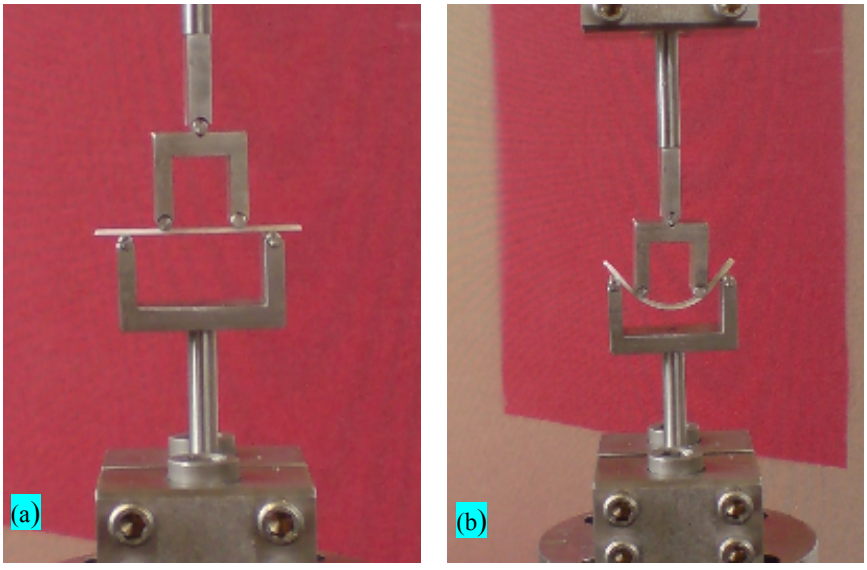

Figure 6.7: (a) Sample setup for four point test and (b) a sample being tested.

A force displacement curve was recorded for each sample. From the curve maximum force and displacement were extracted for calculating flexural strength and flexural modulus using equation 6.1 and 6.2 respectively.

$$\sigma = \frac{3FL}{4bd^2}$$ **Equation 6.1**

$$E_f = \frac{L^3 m}{4bd^3}$$ **Equation 6.2**

where **σ** is the flexural strength, **F** is the load (force) at any given point, **L** is the length of the support span, **b** is the sample width, **d** is the sample thickness and **m** is the slope.

The load was applied at the rate of 5 mm.min^{-1}. The length and width of each samples were measured and an average of three readings was obtained. Five samples were tested from each group for a maximum displacement of 8 mm.

6.3.4 Data Analysis

Statistical analyses were done by 1- way ANOVA with Bonferroni's post-test with $P < 0.05$.

6.4 RESULTS

Figure 6.8 show a force displacement curve used to calculate flexural strength and flexural modulus.

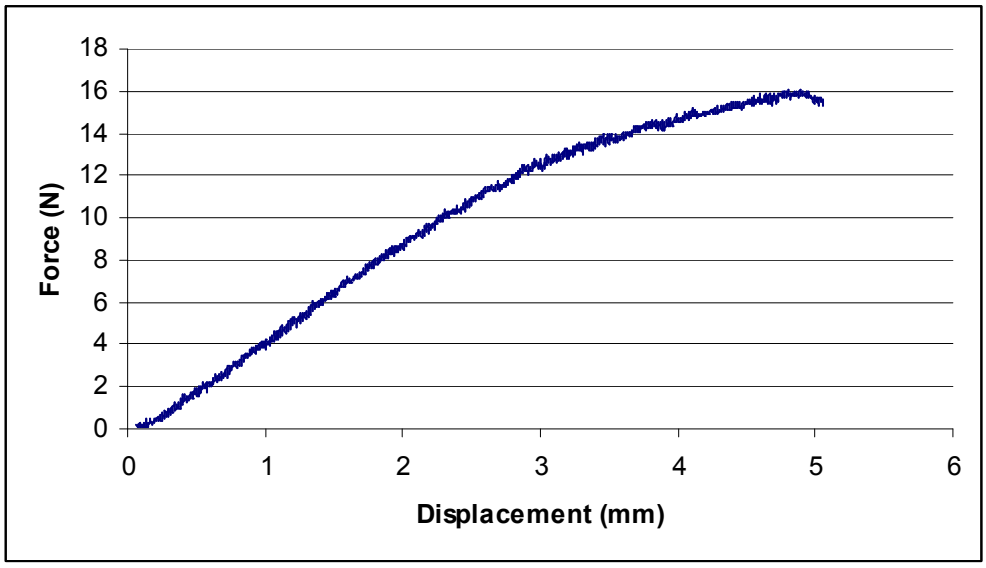

Figure 6.8: A force displacement curve used to calculate maximum force and displacement.

Figure 6.9 show the flexural strength of the membranes with different prepreg lay ups. The graph shows the mean value and standard deviation of 5 samples from each group. The highest flexural strength was shown by membranes of groups 2 which had the maximum numbers of prepreg sheets laid at 0°, although the difference was not significant from the membranes other groups, except the membranes of group 4 and 5. The membranes of group 4 and 5 which had the maximum numbers of prepreg sheets laid at 90° showed significantly low flexural strength.

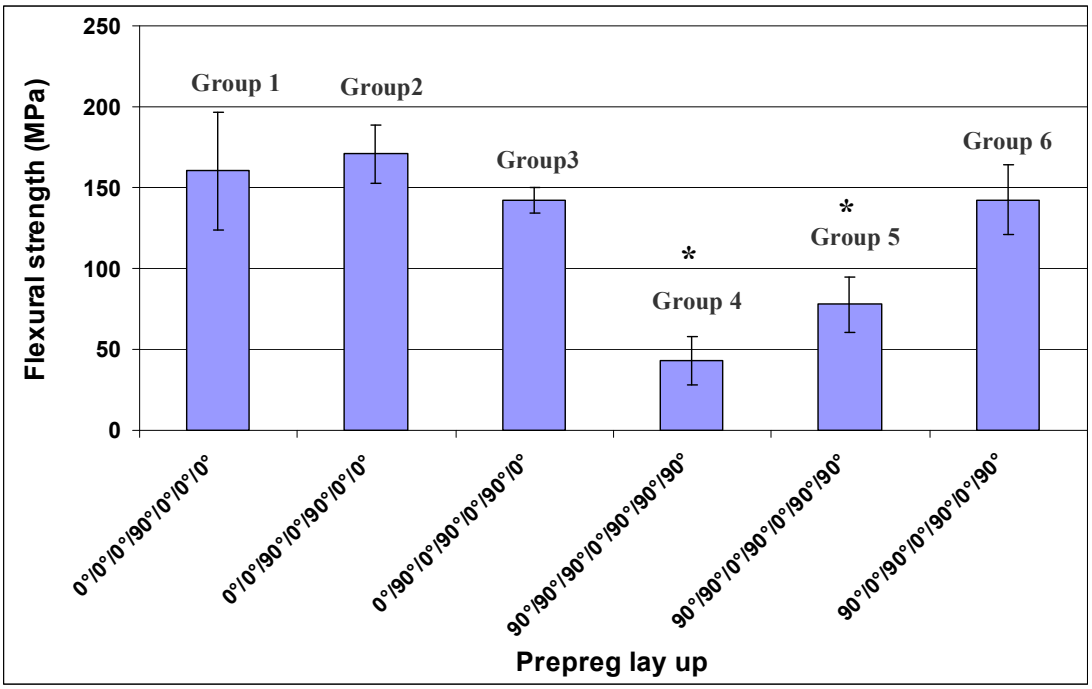

Figure 6.9: Flexural strength of PLA-HA-PLA fibre membranes having different prepreg lay ups. Mean ± SD n=5 per group. * Significantly less than other groups, p<0.05, one way ANOVA and Bonferroni post test.

Figure 6.10 show the flexural moduli of the membranes with different prepreg lay ups. The graph shows the mean value and standard deviation of 5 samples from each group. The membranes of group 4 which had the maximum numbers of prepreg sheets laid at 90° showed significantly lower flexural modulus than membranes of all other groups except from the membranes of group 5. Whereas, the highest flexural modulus was shown by membranes of groups 2 which had 5 prepreg sheets laid at 0°, however it was not significantly higher than membranes of group 1 and 3.

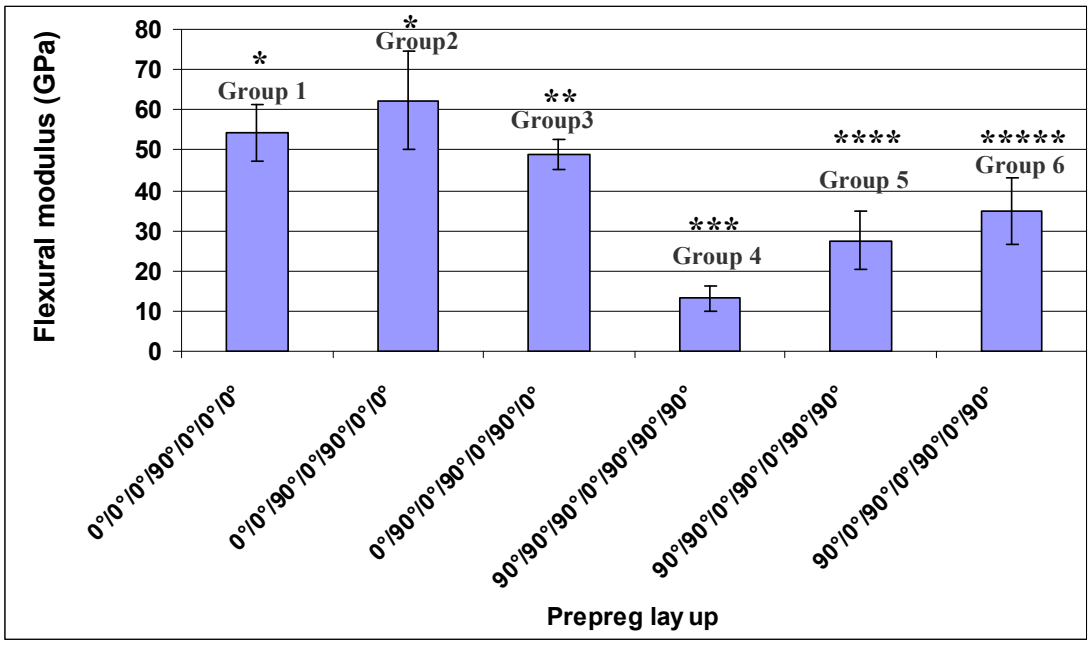

Figure 6.10: Flexural modulus of PLA-HA-PLA fibre membranes having different prepreg lay ups. Mean ± SD n=5 per group. * Significantly different than group 4, 5 and 6, ** significantly different than group 4 and 5, * significantly different than group 1, 2, 3 and 6, **** significantly different than group 1, 2 and 3, ***** significantly different than group 1,2 and 4, p<0.05, one way ANOVA and Bonferroni post test.**

6.5 DISCUSSION

In an attempt to produce a periodontal membrane with improved physical and biological properties we have investigated PLA-HA-PLA fibre composites as potential membrane materials. The use of fibres has been established to increase the properties of the material. Additionally the use of the fibres of same material as matrix results in a chemical bonding between the fibres and matrix which eliminate the possibility of a weak interface between the fibre and the matrix.

The mechanical properties of a fibre reinforced composite depends on number of factors which includes [Behr et al., 2000]:

- *orientation of fibres:*
  Unidirectional fibres= produce anisotropic mechanical properties
  Multidirectional fibres= produce orthotropic mechanical properties

- *adhesion of fibres to the matrix polymer:*
  Proper adhesion between fibres and the matrix is important for the transfer of load from matrix to the fibres. Additionally proper adhesion between the fibre and the matrix reduces the chances of voids and cracks.

In this pilot study flexural strength and flexural modulus of the PLA-HA-PLA fibre membranes were analyzed by a four point bending test.

As shown in Figure 6.9 and 6.10 the flexural strength and the flexural modulus of the PLA-HA-PLA fibre composite membranes were affected by the fibre orientation in the prepreg lay up. The highest flexural strength and modulus was shown by membranes of Group 2 which had the maximum number of prepreg layers laid at 0° reinforced transversally with two prepreg layers laid at 90°. The possible explanation for this pattern of high flexural strength for membranes having more prepreg laid up at 0° if the force is applied perpendicular to the long axis of the fibres then the fibres contribute to the resistance against the force and provide strength to the material. Whereas if the force applied is parallel to the fibre long axis, it results in the production of the failure at the matrix-fibre interface and the fibres do not contribute to the resistance against the force applied [Dyer et al., 2004]. The membranes of group 4 which had the maximum numbers of prepregs laid at 90° showed the lowest flexural strength and modulus. This result can be because the positions of maximum numbers of fibre present in these membranes were parallel to the applied force, which can result in more chances of a material failure at the fibre-matrix interface.

6.6 CONCLUSIONS

This study showed that the flexural strength of a PLA-HA-PLA fibre composite membranes depend on the orientation of fibres in the prepreg. Hence the strength of the membrane can be optimised by laying up most of the prepreg at 0° reinforced transversally by one or two layers laid at 90°.

CHAPTER 7: RELEASE OF PROTEIN FROM POLYLACTIC ACID-HYDROXYAPATITE COMPOSITE MEMBRANES.

7.1 INTRODUCTION

The ideal membrane for GTR is resorbable and has sufficient mechanical stiffness to prevent intrusion of the soft tissues into the defect, yet be sufficiently flexible for the dental surgeon to be able to fit around the defect. However, the additional potential benefits of secondary biological activities of membranes including osteoconduction and the potential to release bioactive proteins to accelerate the healing process remain to be investigated. In these cases, release of bone bioactive proteins might ideally be directed in a unidirectional manner, resulting in release to the bone contacting surface, with limited release towards the gingival contacting surface.

In this study the interaction of proteins with PLA-HA composite membrane material has been investigated. Specifically, the aims of the study are to investigate the protein release kinetics of the material, its permeability and the effects of alterations in membrane composition on these properties. As this was a release study only three layers of pre-preg was used in each specimen.

7.2 MATERIALS

7.2.1 PLA-HA Composite Membranes

Composite sheets consisting of PLA fibres in a PLA matrix with and without hydroxyapatite were used. The PLA drawn fibres had an L: D ratio of 96:4 (wt %) and a diameter between 70 to 90μm (supplied by Tampere University of Technology Finland). Matrix PLA had an L: D, L ratio of 70:30 (wt %) (Boehringer Ingelheim, Germany).

For the HA reinforced sheets the PLA matrix solution contained HA (Mean particle size=2.99, Specific surface areas 16.3 m^2g^{-1}) (Plasma Biotal Ltd, Tideswell, UK) giving PLA-HA-PLA fibres composite. Thus in the HA-PLA-PLA fibre composite the PLA fibres were held in an HA-PLA matrix while in the PLA-PLA fibre composite the PLA fibres were in an unfilled PLA matrix. In the HA-PLA-PLA fibre composite the HA content was 20 wt % of the whole specimen.

7.2.2 PLA-nHA Composite Films

For the production of PLA-nHA composite films, PLA and nHA were used as described in detail in sections 5.2.1 and 5.2.2 respectively.

7.2.3 Other materials

Bovine serum albumin, minimum 98% (Sigma, batch # 025K0598) was used to evaluate the protein release pattern of the membranes.

Bio-Rad protein assay reagents A and B (Catalog # 500113 and 500114) were used to determine the quantity of protein released.

FLUOstar Optima (BMG Labtech) microplate reader was used to read the protein concentrations.

7.3 METHODS

7.3.1 PLA-HA-PLA fibre composite membrane fabrication

The trilayer membranes were produced using a hand lay-up procedure in a stainless steel mould using a hot press (Palamine, Haverhill, UK) (Figure 7.1). The PLA fibres of the top and bottom layers were parallel, while the fibres of the middle layer were perpendicular to the other two layers (0/90/0). The membranes were produced at different pressures and temperatures. The temperatures used were 140 °C and 150 °C while the pressures used were 2.72 MPa and 3.14 MPa which gave membrane thickness of 0.25mm and 0.2mm respectively.

Figure 7.1 Hot press [Palamine, Haverhill, UK]

7.3.2 Film fabrication

The PLA and PLA-nHA composite films were fabricated as described in detail in section 2.3.1. The films were then cut into 6mm circular samples.

7.3.3 Measurement of Protein Concentrations

Protein concentrations of solutions were measured using the BioRad protein assay based on the method of Bradford [Bradford, 1976]. BioRad reagent was added to solutions as described below and optical density measured by spectrophotometery at 595 nm wavelength. Optical density readings were converted to true protein concentrations from a standard curve constructed using a series of albumin concentrations from 0 μg ml^{-1} to 500 μg ml^{-1}.

7.3.4 Measurement of Protein Release

For each experiment, PLA-HA-PLA fibres composite membrane pieces of nominally equal weight were placed in 24 well plates and 1 mg bovine serum albumin (BSA) dissolved in distilled water was added on to the surface of the membranes as a drop. Plain PLA-PLA fibre membranes were used as controls. The membranes were kept at room temperature and allowed to dry overnight. Specimens where the drop did not remain on them were discarded. Next, membranes were placed in new well plates and 1ml of PBS was added to each well. A sample solution of 50µl each was taken out at 0.25, 1, 2, 4, 24, 48, 72 and 96 hours. 50 µl Bio-Rad with an additional 50µl PBS was added to the sample solutions and the readings were obtained as before. The remaining PBS solution in the wells was completely replaced by fresh 1 ml of solution after each sampling time point. Three samples were measured for each material and each time point.

7.3.5 Permeability of films

Tests were conducted to check the permeability of PLA films and PLA-nHA composite films with different concentrations of nHA. To conduct these tests, films were placed in a 48 well micro-chemotaxis chamber (NeuroProbe Inc, CabinJohn, MD USA) (Figure 7.2). For diffusion control, films were deliberately pierced using a small gauge hypodermic needle to allow free diffusion between the upper and lower chambers. Chambers in the lower plate were filled with 26µl of solution and in the upper plate all the chambers were filled with 50µl PBS, except the positive control which was filled with 50µl albumin as shown in Table 7.1. Thus the negative control had PBS on both sides of the film and the positive control had albumin on both sides of the film, while the active chambers had PBS in the upper chamber and albumin in the lower chamber. The films tested were non-filled PLA and PLA-nHA composite films containing 25 wt % nHA (PLA-nHA25) and 75 wt % nHA (PLA-nHA75). 25µl of sample solution was obtained from the upper chambers at 0.5, 2, 4 and 24 hours. 25µl of PBS and 50µl of Bio-Rad was added to the 25µl sample solution and readings were obtained using a spectrophotometer at 595nm wavelength as before

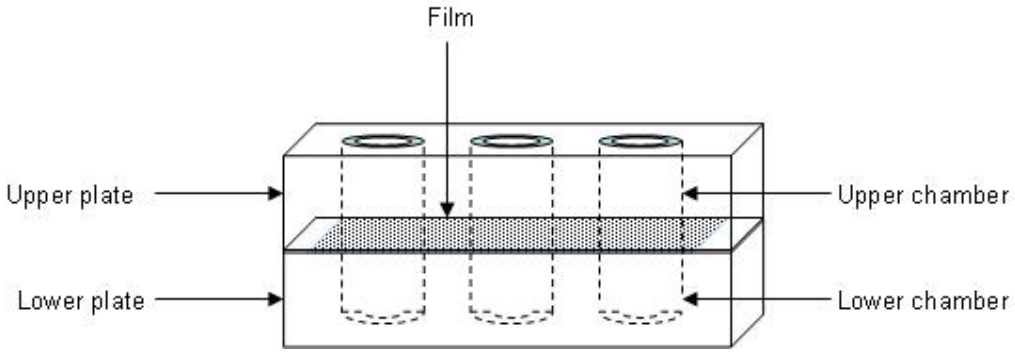

Figure 7.2: 48 well micro chemotasis chamber used to measure the permeability of PLA and PLA-nHA composite films.

Table 7.1: Set-ups for PLA-nHA composite film permeability test (n = 3 for each group) showng solutions placed in upper and lower chambers of test kit.

	Lower Chamber	Upper Chamber
-ve control	PBS	PBS
Test	BSA	PBS
Diff control*	BSA	PBS
+ve control	BSA	BSA

* Pierced Membrane

7.3.6 Statistical analysis

Where appropriate, protein concentrations were calculated from optical density readings using standard curves of known concentrations of BSA. Means and standard deviations were calculated, and statistical differences were tested by 1-way ANOVA with Bonferroni's post test. Statistical significance was assumed if the P-value was less than or equal to $P < 0.01$

7.4 RESULTS

7.4.1 Optical density values for different BSA concentrations

Figure 7.3 shows the optical density values obtained with different concentrations of BSA. This standard curve was used to convert the optical density readings obtained in the experiments into protein concentration values.

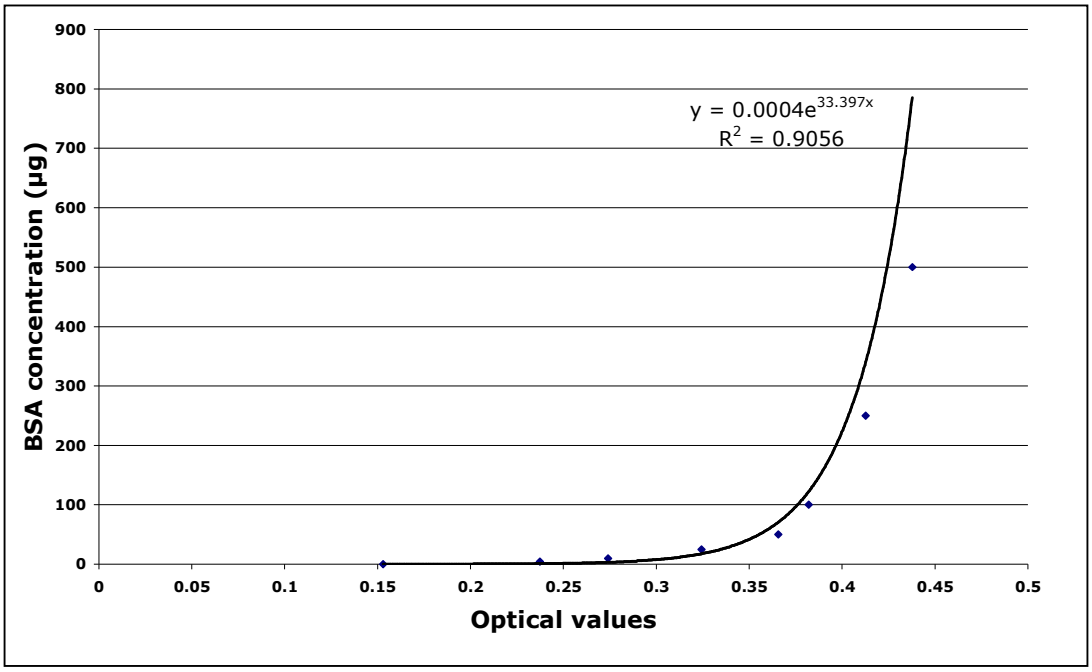

Figure 7.3 Measurement of different proteins concentrations

7.4.2 Protein release from the membranes

During the first hour the PLA-PLA fibre composite membrane released more BSA than the PLA-HA-PLA fibre composite membranes (Figure 7.4). The PLA-PLA fibre membrane released most of the BSA during the first two hours and the release reduced subsequently, by the end of 24 hours the release was negligible. However release from PLA-HA-PLA fibres composite membrane was gradual and persistent with small amounts released even at 96 hours.

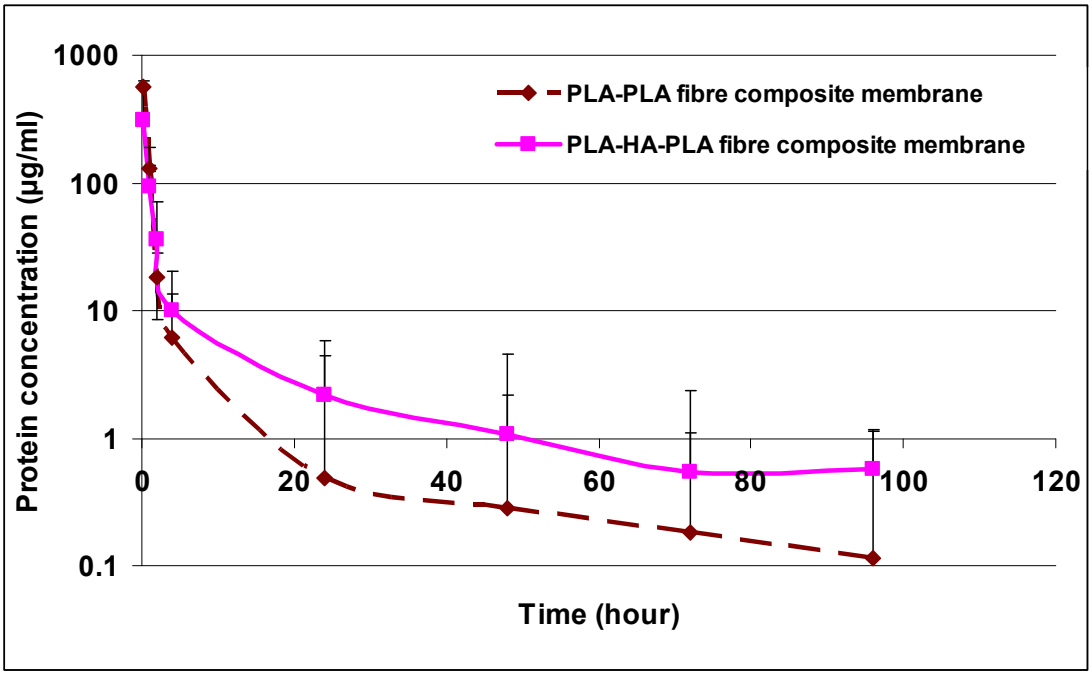

Figure 7.4 Amount of BSA released from PLA-PLA fibre and HA-PLA-PLA fibres composite membrane in 96 hours showing means and standard deviations. n=3

7.4.3 Protein release from PLA-HA-PLA fibre composite membranes produced at different temperatures and pressures

Different patterns of BSA release were observed from the PLA-HA-PLA fibres composite membranes produced at different temperatures and pressures (Figure 7.5). During the first hour the membranes produced at higher temperature and pressure i.e. 150 °C and 3.14 MPa showed greater BSA release than the membranes produced at lower temperatures and pressures i.e. 140 °C and 2.72 MPa. However, the release of BSA from the membranes produced at higher temperatures and pressures decreased to negligible amounts after four hours. In contrast release from the membranes produced at low temperatures and pressures were initially lower, and their release was more prolonged and was still detectable at 48 hours.

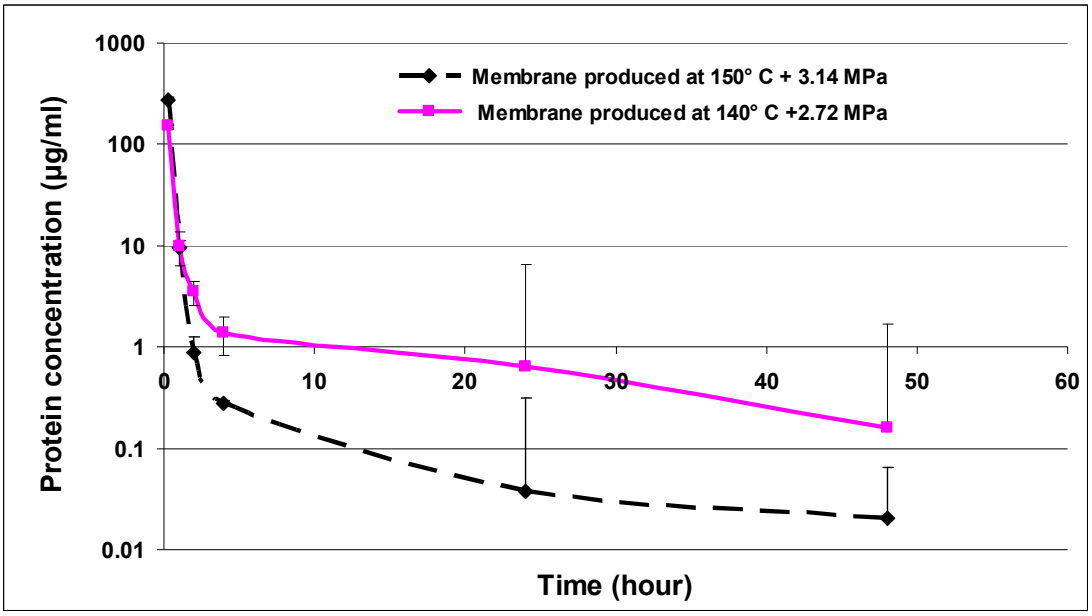

Figure 7.5 Release of BSA from PLA-HA-PLA fibres composite membranes produced at 150°C and 3.14 MPa or 140°C and 2.72 MPa upto 48 hours showing means and standard deviations. n=3

7.4.4 Permeability of membranes with different concentrations of HA

Figure 7.6(a) shows the permeability of PLA films. The diffusion through PLA film was negligible even at the end of 24 hours. Figure 7.6 (b) shows the permeability of films containing 25 and 75 wt % nHA. During the initial four hours the diffusion of protein from the two membranes was low and did not differ greatly. However at the end of 24 hours the diffusion through the PLA-nHA75 film was substantially higher than through the PLA-nHA25 film. Figure 7.6 (c) shows the results of control experiments when albumin was added to both upper and lower chambers. Albumin concentration for PLA-nHA25 film at half an hour was very high when compared to PLA-nHA75 film. Albumin concentration for PLA-nHA25 film decreased subsequently with time, whereas for PLA-nHA75 film the concentration remained low throughout. Figure 7.6 (d) shows the results of "diffusion control" experiments where albumin was placed in the lower chamber and the membrane was deliberately pierced to allow free diffusion. In these experiments, the albumin concentration for the PLA-nHA75 film was higher than PLA-nHA25 film at 0.5, 2 and 4 hours, whereas at 24 hours the albumin concentration for both the films was similar.

(a)

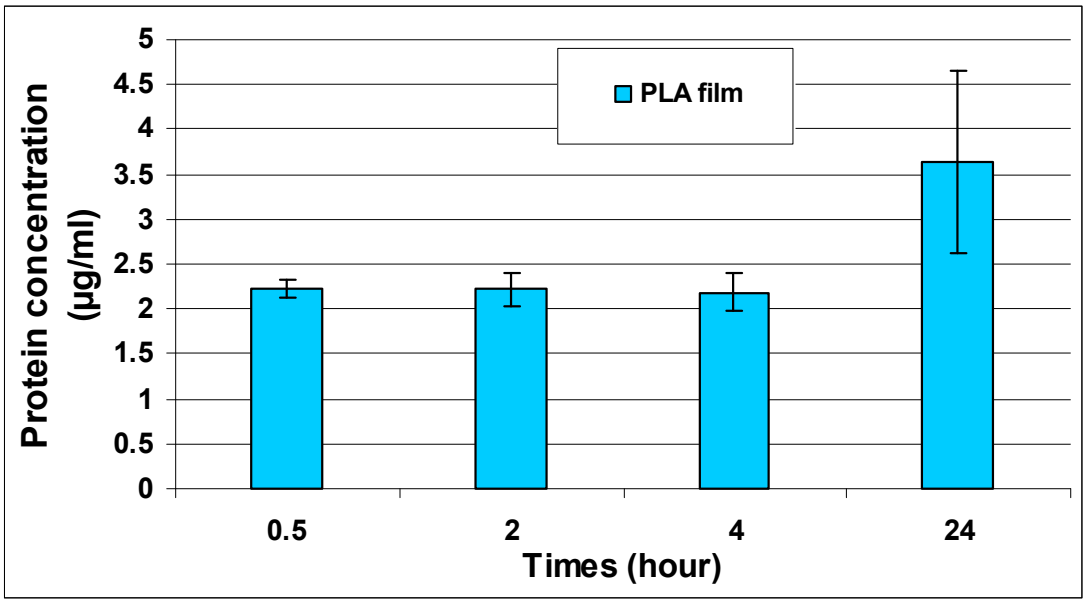
Protein concentration (µg/ml)
5
4.5
4
3.5
3
2.5
2
1.5
1
0.5
0
PLA film
0.5
2
4
24
Times (hour)

(b)

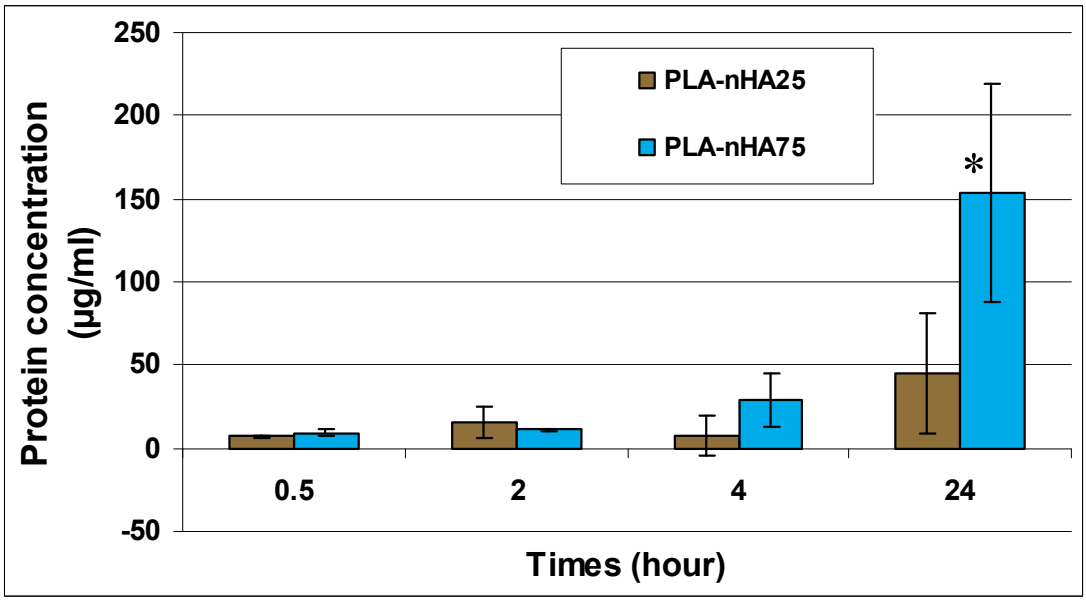
Protein concentration (µg/ml)
250
200
150
100
50
0
-50
PLA-nHA25
PLA-nHA75
*
0.5
2
4
24
Times (hour)

(c)

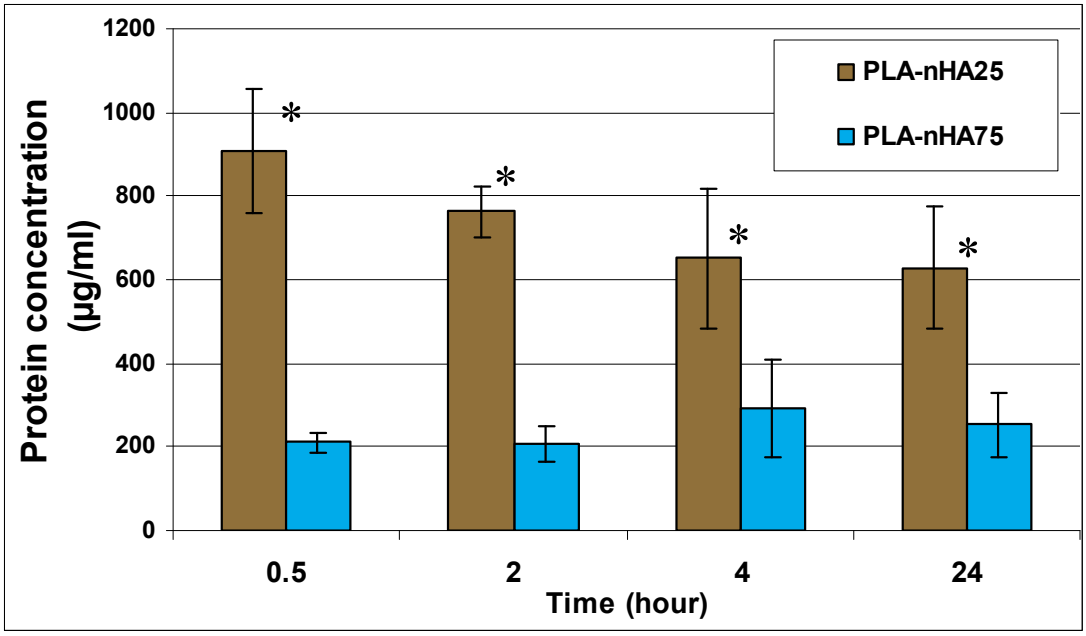

(d)

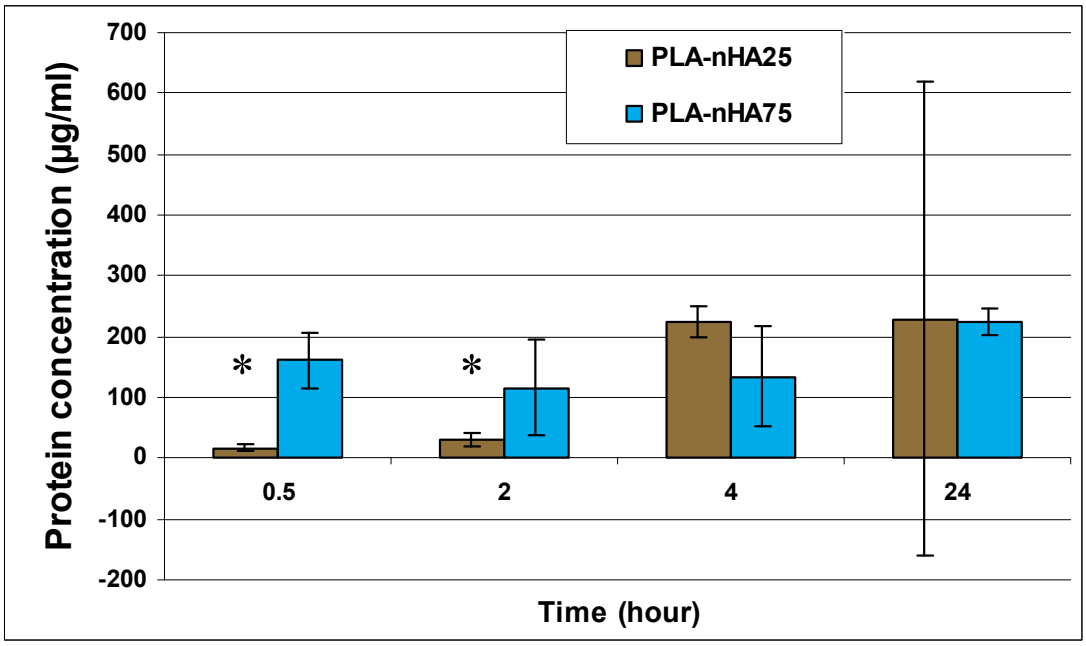

Figure 7.6: Permeability tests:
(a) Amount of protein diffused through PLA film up to 24 hours, (b) Amount of protein diffused through PLA-nHA25 and PLA-nHA75 composite films up to 24 hours, (c) Positive control. Readings obtained at different time points for PLA-nHA25 and PLA-nHA75 composite films when albumin was added to both upper and lower chambers of the micro-chemotaxis chamber and (d) Diffusion

control. Readings obtained at different time points for PLA-nHA25 and PLA-nHA75 composite films when films were deliberately pierced. Mean ± SD n = 3 replicate samples at each time point. * indicates significantly different between tests at specified time point ($P < 0.01$) by 1-way ANOVA and Bonferroni post test.

7.5 DISCUSSION

As noted previously, although a range of different materials have been used for GTR procedures, none of these have ideal properties. The construction of composite membranes using HA-filled PLA-PLA fibre laminar structures is a novel approach to this problem, which may have advantages over current materials. The material is expected to have superior mechanical properties compared to conventional membranes due to the presence of PLA fibres [Yair, 2006] even in thin sections, whilst retaining its resorbable properties. Whilst a full characterisation of the mechanical properties of these membranes is planned for further investigations, empirically these composite membranes are both stiff and strong.

Protein release patterns from PLA-HA-PLA fibre composite membranes were more sustained than protein release from PLA-PLA fibre membranes. Both membrane types released high levels of BSA during the first hour, which may be the result of the release of BSA present on the surface of the membranes and which occurred quickly. However for PLA-PLA fibre membranes there was minimal sustained protein release, whereas release from PLA-HA-PLA fibres composite membranes was more sustained with measurable release still being detectable after 48 hours. Mizushima et al. [2006] have reported the sustained release of the drug interferon alpha from porous hydroxyapatite particles, which would support these observations.

Similarly, PLA-HA-PLA fibres composite membranes produced at lower temperatures and pressures had more sustained protein release kinetics than membranes produced at comparatively higher pressures and temperatures. Membranes produced at lower temperature and pressure showed the same pattern of more sustained release for longer times, whereas for membranes produced at high temperature and pressure most of the total BSA was released

during the initial few hours. This difference is probably due to greater compaction of the membrane produced at higher temperature and pressure, allowing less space for the ingress of BSA inside the membrane. This results in the BSA being absorbed or adsorbed only onto the surface of the membrane and subsequently released quickly.

It appears that when there is space either between the pre-peg sheets or between the HA particles and the PLA matrix within a membrane or film, they are able to absorb more protein and subsequently release the protein more slowly.

PLA-nHA composite films showed much greater permeability for protein when compared to PLA films. The permeability of films increased with the increase of nHA content in the films. These results suggest that permeability is related to porosity due to nHA incorporation. PLA films without nHA were essentially non permeable.

In these experiments, a “positive control” was used to validate the assay process, whereby equal concentrations of the protein were placed in the upper chamber of the diffusion test apparatus. This experiment was carried out to determine if there were changes in protein concentration with time, due to absorption of protein to the film and the diffusion chamber. Data from these controls showed a decrease in albumin for PLA-nHA75 film as compared to PLA-nHA25 film at 30 minutes. This may be due to the fact that albumin is being absorbed at a greater rate with the higher concentrations of nHA in PLA-nHA75 film. In addition “diffusion control” was also used where films were deliberately pierced to allow free diffusion between chambers of the apparatus. The high albumin diffusion through PLA-nHA75 composite film seen in these tests during the initial four hours may be due to larger holes produced on piercing as that material is more highly filled, and therefore has more interfaces through which the protein can track. The results demonstrate that the incorporation of the nHA into the membrane substantially alters the diffusion of protein through the films and suggest the possibility that an unfilled PLA coating on one side of the GTR membrane could be readily used to direct protein release unidirectionally as required clinically.

Overall, the data demonstrates that the protein release kinetics of these composite materials can be controlled by a combination of altering membrane composition, and the temperature and pressures used for their production.

7.6 CONCLUSIONS

The protein release kinetics of PLA-HA-PLA fibre composite membranes demonstrate a more sustained release of protein when compared to PLA-PLA fibre membranes. Thus these composite membranes could be useful therapeutically as a delivery system for bioactive proteins. The diffusion of protein through PLA-nHA composite film increases with increased nHA content. This property may be beneficial in order to obtain directional release of proteins by differential coating of membrane surfaces with unfilled and filled PLA films.

CHAPTER 8: ANALYSIS OF ALVEOLAR BONE RESORPTION PROFILE

8.1 INTRODUCTION

Guided tissue regeneration (GTR) membranes are used for the regeneration of alveolar bone lost during periodontal diseases or resorbed after the loss of tooth.

Periodontal diseases affect the periodontium which is the supporting structure for the tooth and in severe cases of periodontal disease the supporting structure in the jaw gets destroyed which ultimately results in tooth loss. The treatment aim in such cases is not only to stop the disease process but to also regenerate the lost periodontal tissues. Different methods are being used for the treatment and regeneration of periodontal tissues (section 1.4).

Extraction of teeth which are damaged due to caries or trauma also results in the resorption of alveolar bone not only in the buccolingual direction but also in the vertical direction (Figure 8.1). In order to restore the alveolar ridge shape to be suitable for dental implants, different methods of bone regeneration are employed, including the use of GTR membranes.

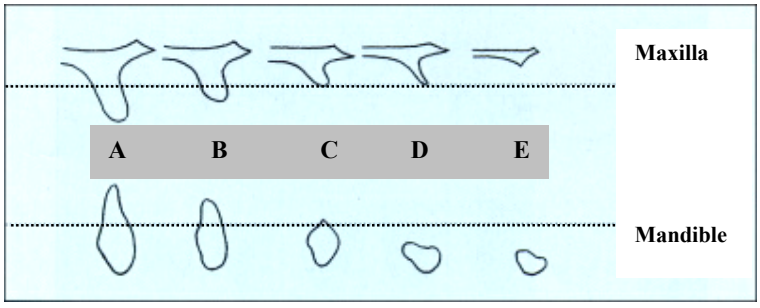

Figure 8.1: The progression of maxilla and mandible alveolar ridge resorption, from (A) shortly after extraction of tooth through to subsequent gross atrophy (E) [modified from [Floyd et al., 1999].

Different types of GTR membrane are currently used. Ease of use and adaptability are two of the major requirements of GTR membranes for successful results. However, additionally the stiffness of the GTR membrane needs to be

high enough to prevent the collapse under the soft tissue or occlusal pressure under mastication.

As a part of the study to develop a composite membrane with enhanced regeneration potential, an analysis of the alveolar bone resorption pattern was performed to define a membrane shape which is suitable for most of the cases. The PLA/PLA fibre/HA composite material described in previous chapters potentially has good mechanical properties for maintenance of space under periodontal wounds, compared to existing membranes. However existing membranes are highly flexible and can be adapted to the required shape over the bone. In contrast our PLA/ HA membranes show increased stiffness and therefore are likely to require a degree of pre-shaping during the manufacturing process. Thus it is envisaged that a clinician might select one of a number of preformed membrane shapes for each specific defect and then trim it accordingly. In order to test the feasibility of this idea it was decided to carry out a pilot study to determine the cross sectional profiles of membranes required and to determine the extent of variability of membrane profiles required.

8.2 MATERIALS AND METHODS

To determine the alveolar bone loss pattern following protocol was devised:

8.2.1 Selection of cases

To determine the profile of alveolar bone resorption seven partially and completely edentulous patients aged between 25 and 60 which were already under clinical assessment for placement of dental implants were selected. 39 computerised tomography (CT scan) slices from different edentulous areas of mandibular alveolar ridges were obtained, in collaboration with Dr Jimmy Makdissi, Consultant Radiologist, Barts and the London Dental Hospital. Figures 8.2 and 8.3 respectively show cross sectional slices of alveolar ridges of anterior and posterior mandibles of two different patients. The cross sectional scan slices

were obtained parallel to occlusal plane of the mandible. These scans were then used to draw possible shapes for GTR membranes.

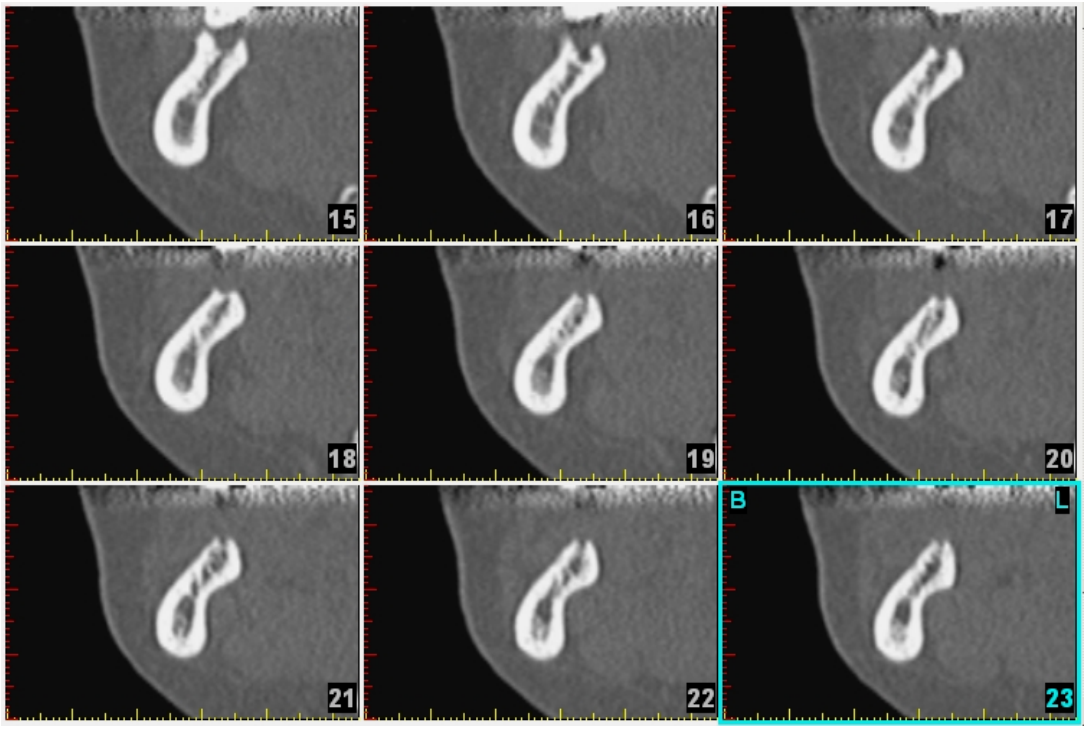

Figure 8.2: Cross sectional scan images of an anterior mandible, the distance between each scan slice was 2mm. Cortical thickness and trabeculation density can also assessed from the scan slices.

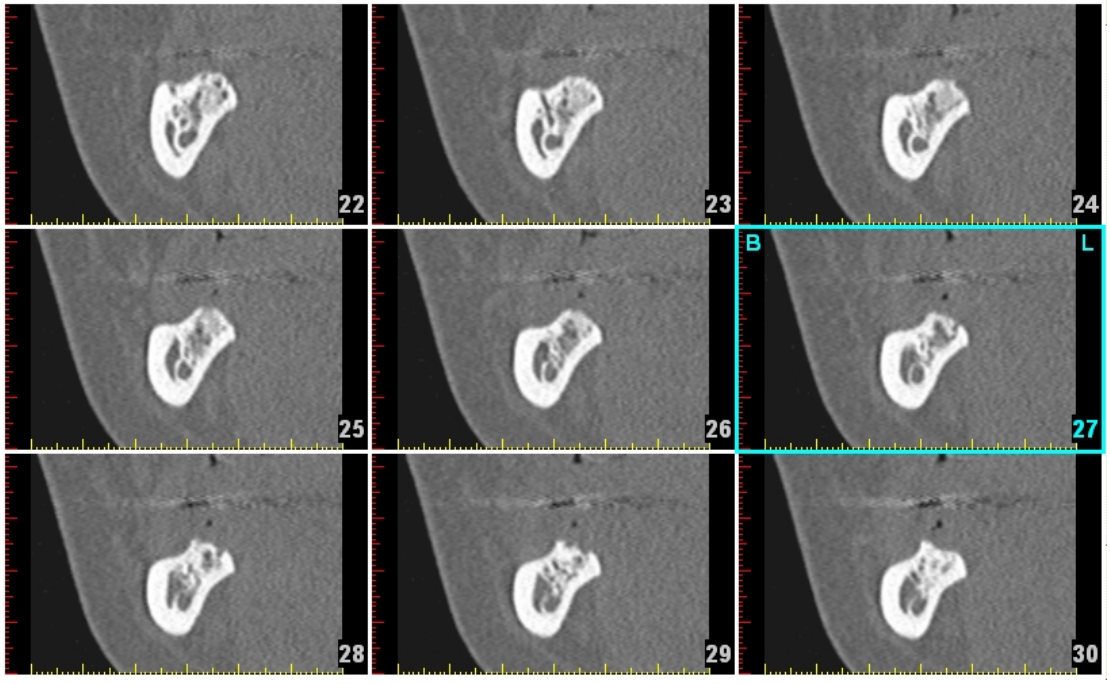

Figure 8.3: Cross sectional scan images of posterior mandible, the distance between each scan slice was 2mm. Cortical thickness and trabeculation density can also assessed from the scan slices.

8.2.2 Determination of GTR membrane shape

Cross sections of edentulous alveolar ridges obtained from CT scans were printed and a suitable GTR membrane shape was hand drawn over the alveolar ridges by an experienced periodontologist (Prof Francis Hughes). Figure 8.4 shows the profile of GTR membranes drawn over the anterior and posterior mandibular ridges of 8 different patients.

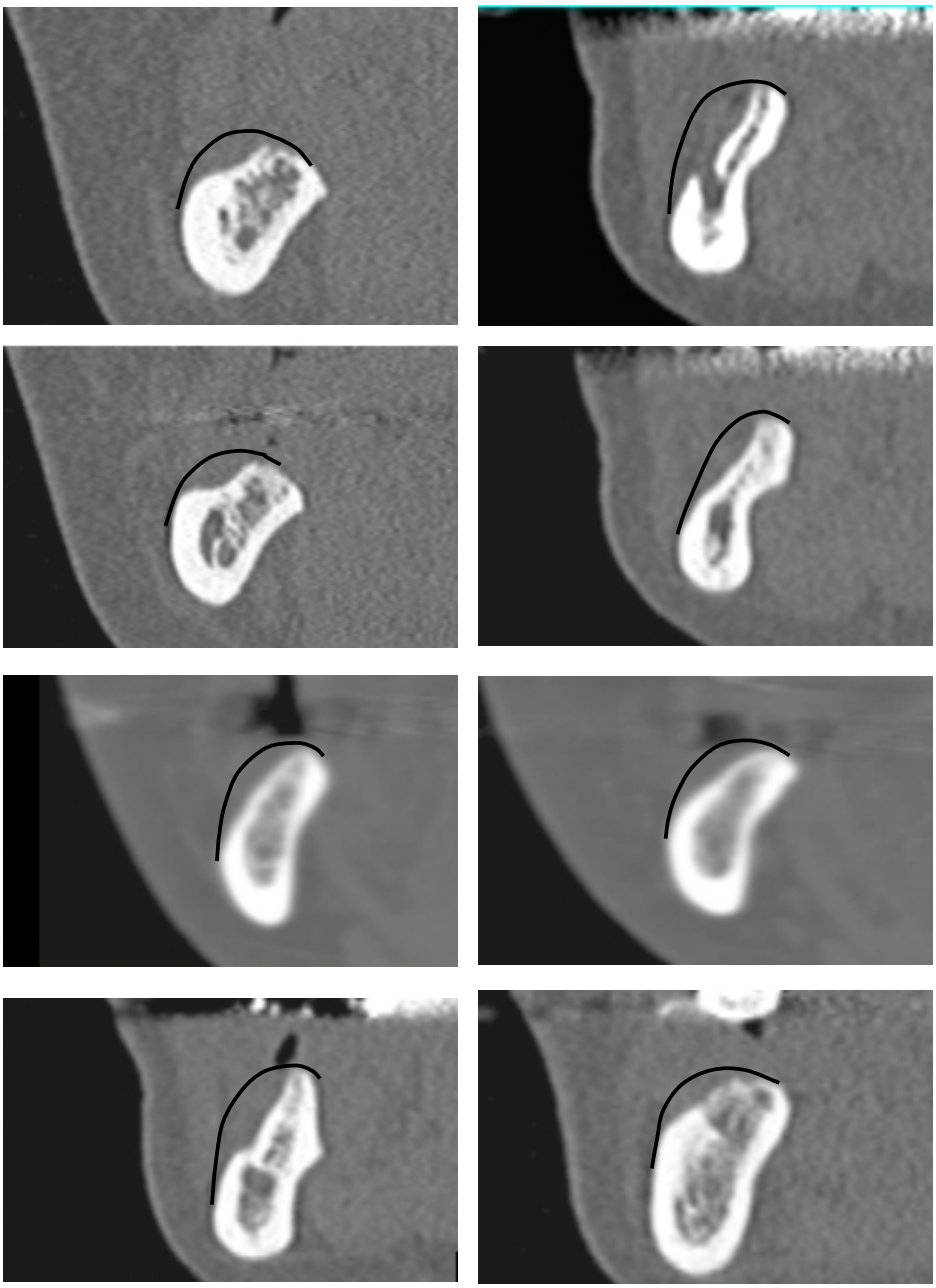

Figure 8.4: Membrane shapes, hand drawn over the alveolar ridges of anterior and posterior mandible.

8.2.3 Digitizing of membrane shapes

The hand drawn membrane contours were digitized using AccuTab digitizer (GTCO Corporation, USA) (Figure 8.5). A program was developed to convert the drawn membrane contours into mathematical XY contours. The XY contours were then exported to an Excel® spread sheet and subsequently graphs were drawn using the data obtained.

Figure 8.5: AccuTab digitizer used for digitizing membrane profiles.

8.2.4 Analysis of digitized shapes

The curves obtained by digitizing the hand drawn membrane contours were then arbitrarily aligned by hand to align them as closely as possible. Having done this the curves were analysed to describe mathematically the lines of best of fit and 95% range. This data was analysed by Pengwei Hao (Dept of computer science, QMUL) and Yanlin Geng (State Key Lab of Machine Perception, Beijing University, China) to define a suitable membrane shape.

8.3 RESULTS

Various curves were obtained from digitizing the membranes shapes which were hand drawn over the alveolar ridges scans from mandible of different patients. Some of the obtained curves are shown in Figure 8.6.

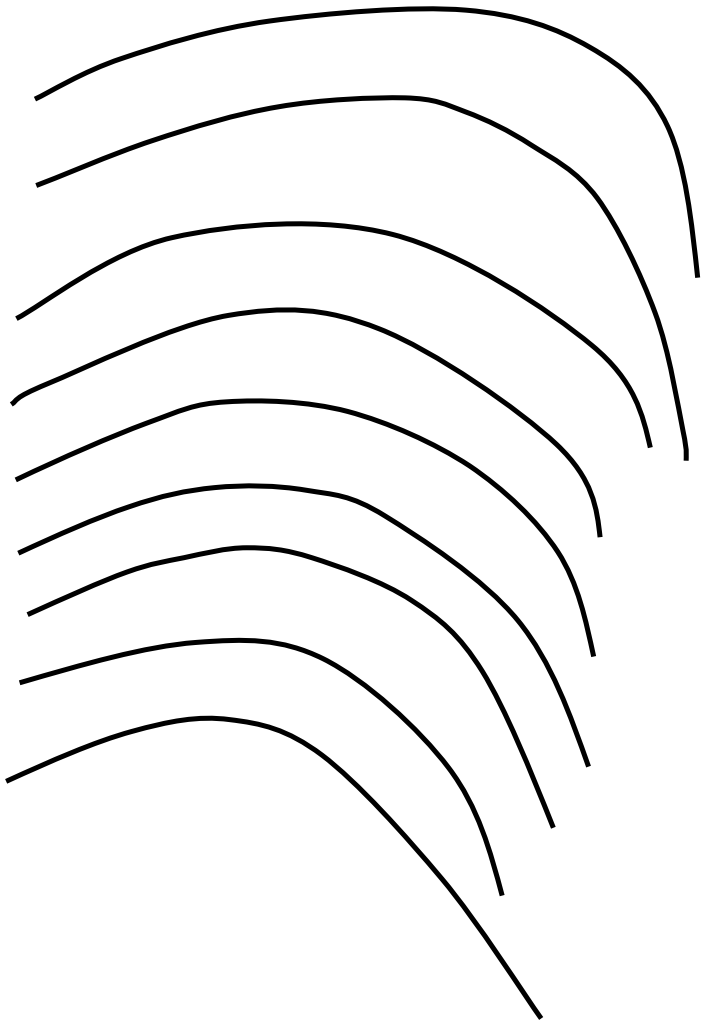

Figure 8.6: Curves obtained form digitized contours of membrane profiles hand drawn over the alveolar ridges.

The curves when superimposed were broadly divided into two main groups (A) and (B) depending on their shapes. Figure 8.7 (a) and (b) show Group A and B curves respectively and a curve which best fits most of the curves in each group was drawn and is shown by a red line. The parabolic best fit curves of two groups are represented by (a) $y=-0.1204x^2+1.8867x-0.7491$ and (b) $y=-0.1542x^2+2.0290x+0.9172$.

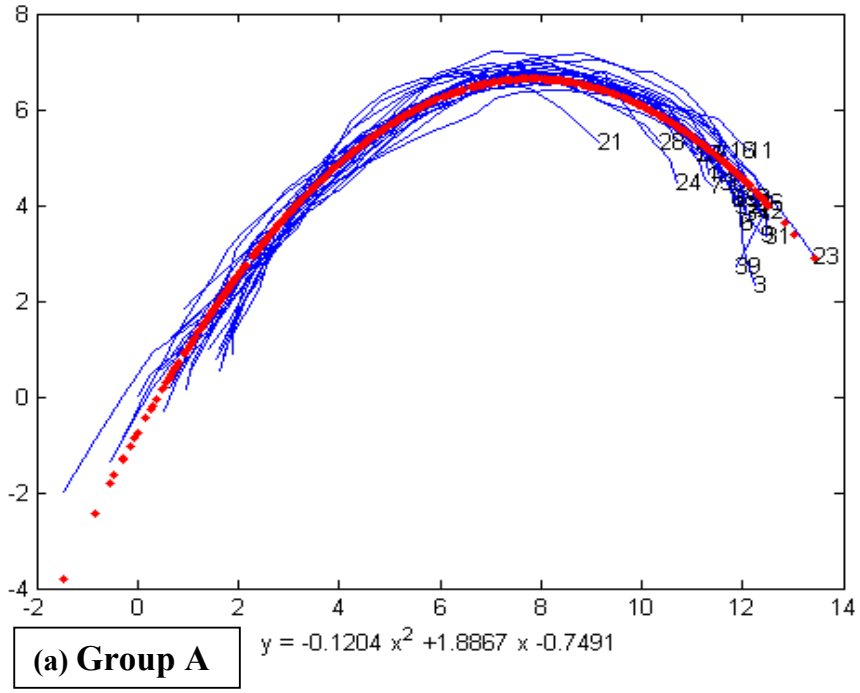

(a) Group A

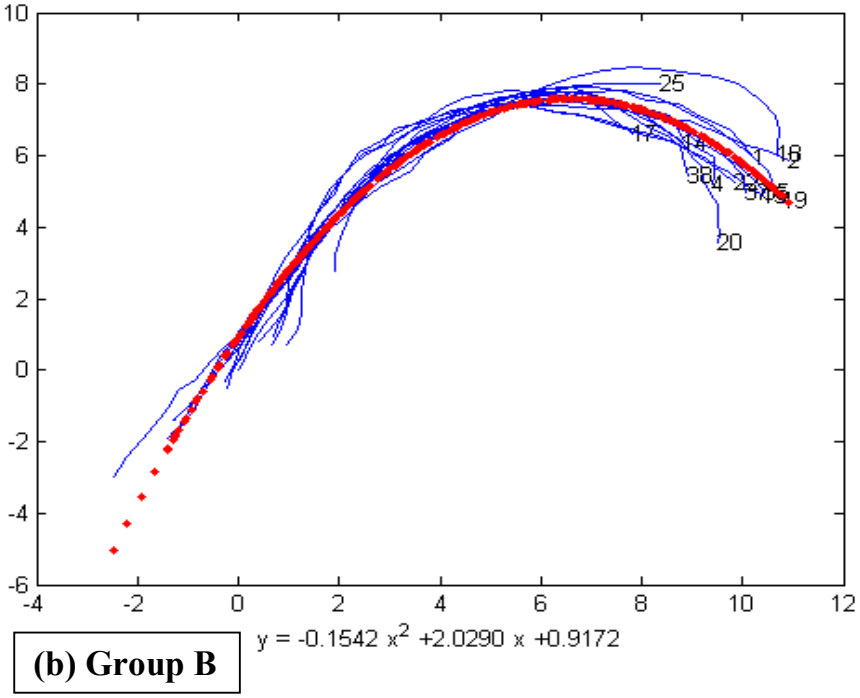

(b) Group B

Figure 8.7 (a) and (b): Two groups of superimposed curves with respective best fit curves.

As a next step inner and outer boundaries curves for the best fit curves in both the groups were drawn as shown in Figure 8.8 (a) and (b). These outer and inner boundaries curve of both best fit curves enclosed 95% of the curves in that particular group. It can be seen from the equations that the shape of the curves has not been altered it is just the offset from the zero axis that has been changed. Thus for Group A the offset is -0.7491 with the values of -0.1220 and -1.4339 for inner and outer boundaries, while for Group B the values for inner and outer boundaries are -0.1101 and + 1.9314 about the mean value of 0.9712. Thus if the curves $-0.1204\ x^2 + 1.8867x$ and $-0.1542x^2 + 2.0920x$ are used to manufacture the mould profiles they should provide an acceptably good fit to the required shape for most patient.

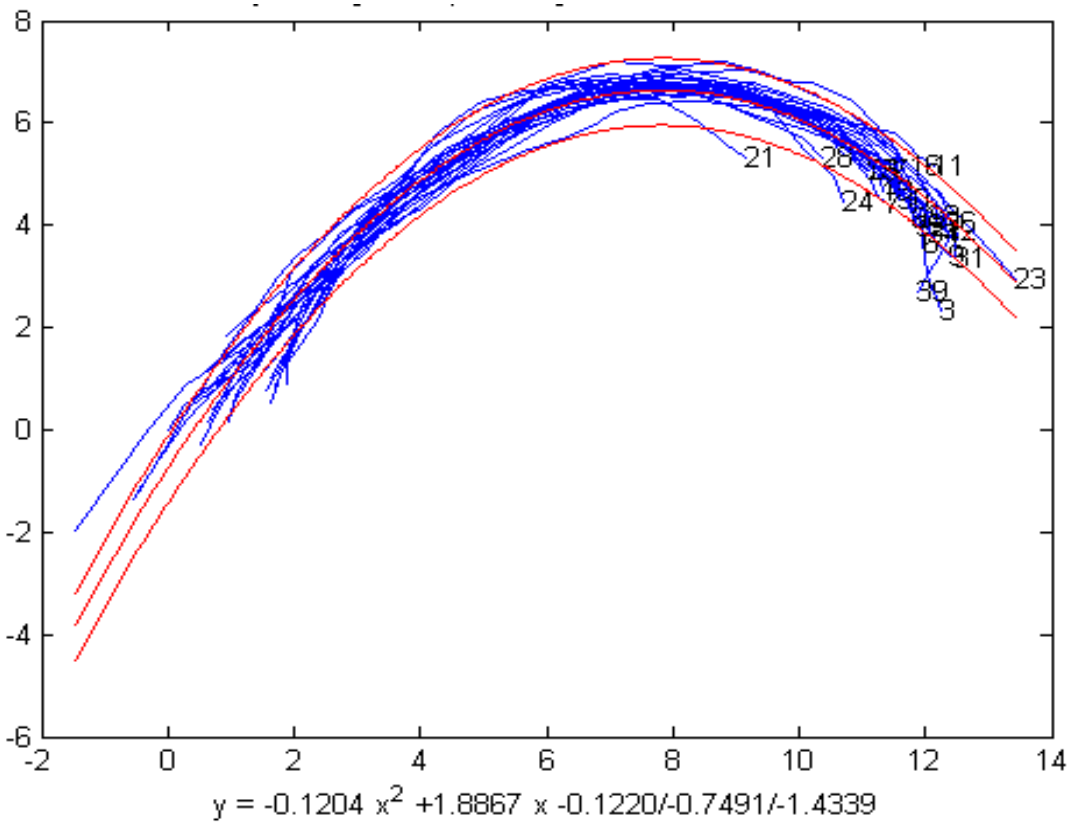

(a) Group A

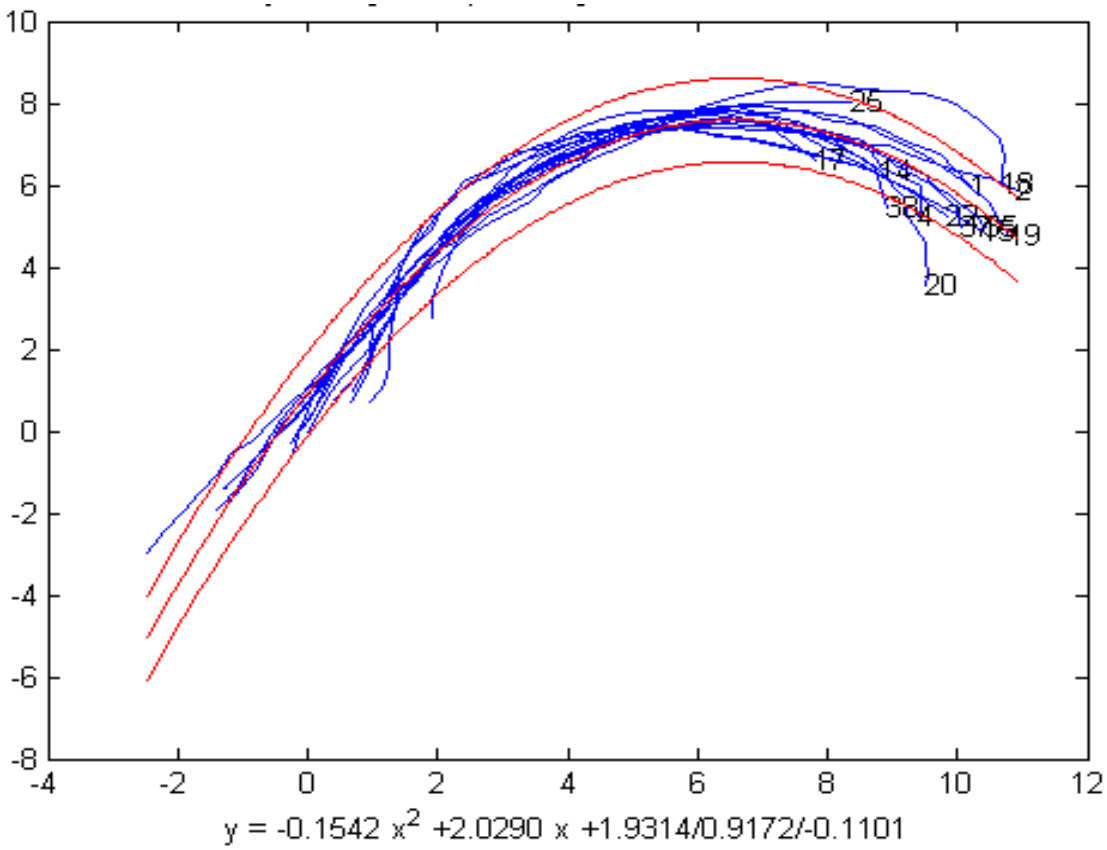

(b) Group B

Figure 8.8 (a) and (b): Best fit curves drawn with inner and outer boundaries which include most of the digitised curves in the respective group.

In a previous study which was conducted by a group member (Dr Amber Fareed, Queen Mary University of London), bone resorption profiles of alveolar ridges were analysed using ScanOra of six patients which were under assessment for dental implant placement. Figure 8.9 below shows (a) one of the ScanOra showing edentulous area of alveolar ridge used in the study (b) hand drawn alveolar bone profile on the ScanOra and (c) membrane shape hand drawn by an experienced periodontologist (Prof Francis Hughes) on the outline of the alveolar bone profile traced on a paper. Similarly membrane shapes were drawn on the alveolar bone outline of six different patients (Figure 8.10).

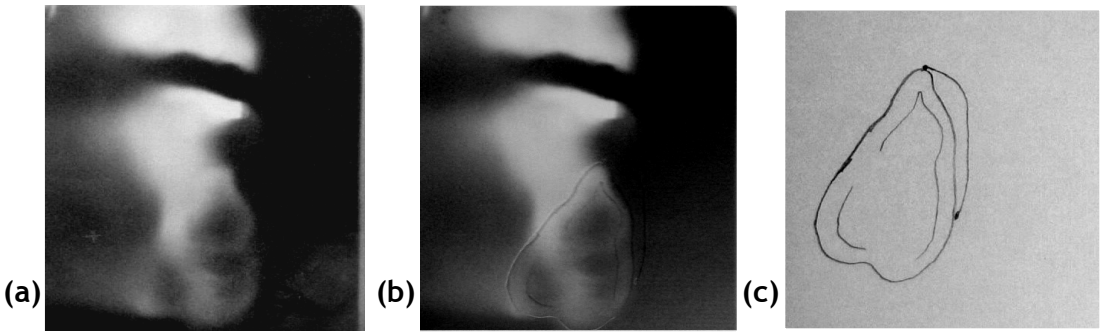

Figure 8.9: (a) ScanOra of edentulous alveolar ridges, (b) alveolar bone profile tracing on the ScanOra and (c) outline of alveolar bone profile traced on acetate paper with hand-drawn membrane shape [from Dr Amber Fareed].

Figure 8.10: Membrane shapes hand drawn on alveolar bone outline of six different patients [from Dr Amber Fareed].

The membrane shapes shown in Figure 8.10 were then digitized using the same protocol described in section 8.2.3.

Figure 8.11 (a) shows the digitized shapes of the various hand drawn membrane shapes obtained from sketching on the ScanOra of six different patients in the previous study. These membrane shapes surprisingly closely fit within the inner and outer boundaries of Group B in our study as shown in figure 8.11 (b).

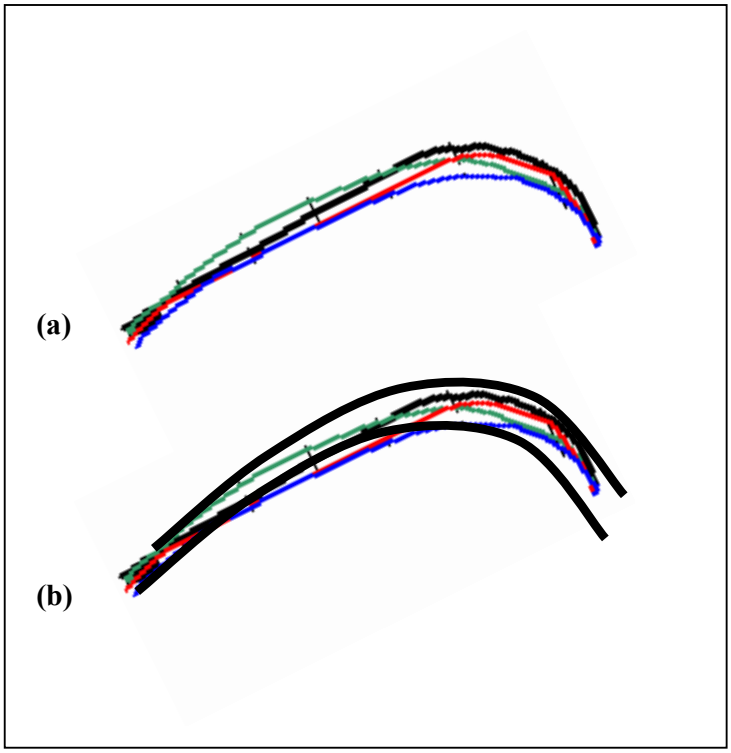

Figure 8.11: (a) Membrane shapes obtained by using ScanOra in a previous study, and (b) enclosed by thick black lines representing inner and outer boundaries of group B of the present study.

8.4 DISCUSSION

Periodontal regeneration is based on the concept of maintaining a space between soft tissue and alveolar bone by use of a GTR membrane which creates a protected environment and allows osteogenic cells to migrate to the area [Cortellini and Tonetti, 2000; Park et al., 2000a]. Different types of membranes are currently used with varying success. Some of the pre-requisites for successful periodontal bone regeneration are the ability of the GTR membranes to adapt to the bone defect, full coverage of the defected area and ability to maintain a space without collapsing under pressure by overlying flaps due to tissue tension, mastication or other physiological forces which are transmitted through the flap [Tatakis et al., 1999b; Lee et al., 2001a]. The importance of space maintenance by the GTR membrane in periodontal regeneration is well documented and had been reported in various studies. GTR membrane collapse or failure of maintaining space between the soft tissue and defect area by the membrane due

to inadequate or improper placement results in compromised periodontal regeneration [Polimeni, 2004].

The objective of this study was to analyse profiles of mandibular alveolar ridges of different patients and define a shape for GTR membranes which can be used for the vast majority of periodontal defects. A suitable sized and shaped membrane will not only reduce the time needed to complete the clinical procedure but will also enable the clinician to place the membrane properly with reduced risk of failure. This can be achieved by defining a shape of the membrane which can fit most of the defects.

CT imaging was used for the evaluation of alveolar ridges. It is one of the most commonly employed imaging tools in implant dentistry for alveolar bone assessment. Cross-sectional and 3-dimensional images can be obtained by using CT scans [Garg and Vicari, 1995]. CT scans not only provide information about the quantity of the bone available but it is also possible to asses its quality, including thickness of cortical bone and cancellous bone density. Three dimensional images of the jaw bone can be constructed and stereolithographic models can be fabricated using data obtained by CT scans [Floyd et al., 1999; BouSerhal et al., 2002].

CT scans of 7 patients were selected and 39 cross sectional slices from different areas of mandibular alveolar ridges were obtained. These cross sectional slices of alveolar ridges were then used to draw a suitable shape GTR membrane. The digitized profiles of these membrane shapes were superimposed to define a membrane shape which can fit most of the profiles. Interestingly it was found that the obtained curves can be broadly divided into two groups. To define a shape for the membrane a curve was then drawn which best fit all the curves in both the group. Further inner and outer boundaries curves for the best fit curves were drawn and it was found that the boundary curves enclosed 95% of the curves in a particular group.

In addition, when comparing the present study with an additional pilot study in our group, the total number of patients evaluated for defining the membrane shape was 13. It can be seen that most of the alveolar ridge patterns closely resemble each other.

Thus it can be considered that the alveolar ridge resorption patterns do not differ a lot from each other and that most alveolar ridge resorption defects could be treated with few pre-formed shapes of GTR membranes. As this study shows that the selected curve from each group after minimal chair side trimming should be able to fit most of the alveolar ridges in that group.

Although the CT scans analysed in this study were obtained for potential implant cases rather than periodontology involved cases, as the radiographic examination for implant assessment typically requires tomographic or CT cross sections through the jaws, it was felt that this was an appropriate compromise. Firstly because these membranes may have application for GBR in implant therapy as well as for periodontal regeneration. Secondly it is expected that buccal-lingual profiles obtained from these data are likely to be similar to those required for periodontal defects also. Further larger studies would be useful to confirm further the universality of this observation. In addition the study has so far restricted itself to analysis of mandibular profiles only, and requires to be extended to maxillary profiles in future studies.

8.5 CONCLUSIONS

Although a wider study is required to validate fully the findings of this study, it can be suggested that relatively few number of pre-moulded membranes can be employed for the regeneration of maximum number of periodontal defects.

CHAPTER 9: GENERAL DISCUSSION, FUTURE WORK AND CONCLUSIONS

9.1 GENERAL DISCUSSION

Over the last two decades GTR has evolved as a technique to treat periodontal defects [Becker and Becker, 1993; Caffesse et al., 1997]. Various studies have shown its superiority over flap debridement procedures for its ability to promote periodontal regeneration [Needleman et al., 2002; Maurizio et al., 2004]. However, the fact remains that the overall outcomes for periodontal regeneration using GTR are relatively modest [Michael and Ulf, 2001] and when compared to results obtained with other regeneration techniques such as grafts, the differences were not substantial.

Both resorbable and nonresorbable membranes are used for GTR procedures. However all the membranes used have limitations which affect the overall outcome of this technique. Resorbable membranes do not require removal with a second surgical procedure. However, most of them either lack adequate stiffness or collapse under pressure due to too early loss of strength, so the essential requirement of space maintenance is lost and the results are compromised [McAllister and Haghighat, 2007]. Non-resorbable membranes have comparatively better strength, but are generally difficult to adapt due to their stiffness and can also damage the soft tissues. To overcome the limitations of GTR membranes and to obtain better results, GTR membranes are typically used in combination with other regenerative techniques such as grafts. However, the use of graft materials may have disadvantages according to the type of graft used. For example autologus bone causes considerable donor site morbidity, and allograft or xenograft materials increase the risk of disease transfer [Sogal and Tofe, 1999].

Thus there is a need to develop a membrane with better physical and biological properties. Ideally it should have good clinical manageability, have sufficient strength to resist pressures from the overlying flap and those exerted during mastication, should not only maintain a space and act as a barrier between the defect and soft tissue, but also facilitate the regeneration of bone by virtue of

having osteoconductive properties and finally resorb without side effects. Furthermore, there may be additional advantages for a material to have the ability to carry growth factors or be seeded by autogenous stem or progenitor cells.

PLA-Ca P composites have been investigated as potential GTR membrane materials with improved physical and biological properties. The aim of the study presented here was to develop a membrane which would fulfil most if not all the requirements of an ideal membrane.

One of the major problems associated with the currently available materials which results in their failure is that they are difficult to adapt to the defect and there is a possibility that they will not properly cover the defect or collapse into the defect space. To improve the clinical manageability and to improve the adaption, it would be ideal to have high strength prefabricated membranes which will require minimum chair side preparation and still cover the defect appropriately. In a pilot study the profiles of mandibular alveolar bone has been investigated among different patients to define shapes for GTR membranes. Interestingly, it was found that a low number of different membrane shapes can fit most of the mandibular alveolar bone profiles analyzed in this study. The limitations of this study were that firstly, only the mandibular ridges were analysed and secondly, the CT images studied were of the patients under treatment for dental implants rather than for periodontal diseases. Although further investigations are required to validate these findings, it is proposed that a few shapes of prefabricated GTR membranes will be suitable to be employed for most defects. This development would enable the use of stiffer membranes with high strength. Additionally these membranes will require minimum chairside preparation. Thus the membrane material investigated will have good clinical manageability if used as pre-fabricated membranes.

Another limitation of currently used membranes is the inability to withstand occlusal pressures and their collapse into the defect area. This collapse is either due to lack of strength or too early loss of stiffness, before sufficient tissue regeneration has occurred. When collapsed, a membrane loses its barrier function of preventing migration of the faster growing epithelial and connective tissue cells to the bone defect and does not maintain a space for repopulation of

the defect area by osteogenic cells. A fibre reinforced PLA-HA composite has been investigated as a membrane material. Fibre reinforcement in addition to HA will increase the strength and stiffness and will enable the fabrication of membranes with better mechanical properties [Bleach et al., 2001]. From the study carried out to test the flexural strength of the membranes, it can be concluded that by changing the orientation of fibres in a multiple layer membrane the mechanical properties can be manipulated and further improved to optimise the membrane stiffness and strength. Additionally the use of high strength fibre reinforced composite materials for the fabrication of pre-shaped membranes will eliminate the drawbacks associated with the manageability and adaptation of the stiffer membrane materials. Although the optimal thickness of membranes and hence the number of layers within a membrane, has not been determined here, it is recognised that it is probably desirable to keep such a membrane as thin as possible and further studies on thinner membranes would be useful in future.

Tissue regeneration may be enhanced and clinical outcomes can be improved if a barrier membrane also possesses bioactive and osteoconductive properties. Tests were carried out to analyse the bioactivity and osteoconductivity of the proposed composite membrane materials. The results showed that adding HA increased the bioactivity and osteoconductivity of the material. A membrane fabricated using this composite material may thus not only act as a barrier but might also have increased bioactivity and osteoconductivity to enhance its regenerative potential.

In various studies growth factors have shown the potential to induce and enhance the regeneration of periodontal tissues [Cho et al., 1995; Nevins et al., 2003]. Therefore, there is a considerable interest in the therapeutic application of growth factors for periodontal regeneration. An ideal GTR membrane might therefore be able to carry and release growth factors in a sustained manner. In a preliminary study, albumin and serum proteins were used to analyse the kinetics of protein interactions with fibre reinforced PLA-HA composite. The results showed that the ability of these composites to absorb and release the proteins in a sustained manner were dependent on the manufacturing parameters used for the membranes. These parameters can be manipulated to optimise the potential of these composite materials as growth factor carrier. Furthermore, the ability

of PLA-HA composite films to absorb and release PDGF and its effect on the proliferation of osteoblast cells was tested. The results showed that the PDGF added to the composite materials retained its activity and enhanced the proliferation of osteoblasts when seeded onto these composite materials. Growth factors lost or released into the wrong tissue may limit their clinical effectiveness. To address this issue it is proposed to achieve a unidirectional release of growth factors by coating the two sides of the membrane with thin films of different materials. The permeability of PLA and PLA-HA composite films was tested and from the results it was concluded that the PLA films were relatively impermeable and the permeability increased with increase in the quantity of HA in the films. So the surface of the membrane towards the soft tissue could be coated with an impermeable PLA film to prevent the release of growth factors on that side, while the bone side could be composite film, thus achieving a unidirectional release of growth factor to the appropriate target. As basic protein interaction kinetics with the fibre reinforced PLA-HA composite were investigated, further studies involving growth factors (PDGF and BMPs) are needed to validate the ability of these composite materials to carry and release growth factors.

One of the issues related with early resorbable materials was their unpredictable degradation behaviour and the accumulation of their degradation products due to too rapid degradation [Bostman and Pihlajamaki, 2000]. The degradation pattern of PLA-Ca P composites was investigated. The results showed that the addition of Ca P to the polymer slowed the degradation rate of PLA. Addition of Ca P to the polymer may also neutralize the acidic aspect of PLA degradation [Niemelä, 2005]. Although this study analyzed the effect of Ca P on the degradation of PLA, it did not take into consideration the effect of fibre-matrix interfaces in the proposed multilayer fibre reinforced PLA-HA composite membrane on the degradation rate, therefore a study is needed to analyse the degradation rate of fibre reinforced membranes. The degradation rate of a fibre reinforced PLA-HA composite can be tailored to suite the application by altering the quantity of L and D isomers in the PLA and concentration of HA.

From the investigations carried out in this project it can be proposed that a fibre reinforced PLA-HA composite material will be a suitable material to develop for use as a GTR membrane and may offer significant advantages over existing

materials for this application. Although the materials investigated in this study have shown favourable properties to be used as a GTR membrane material, all the tests have been performed *in vitro*. To be sure about the properties of these materials and to ascertain how these materials will perform clinically, *in vivo* tests are required including full clinical evaluation.

9.2 FUTURE WORK

Although overall results of the studies described are very encouraging, there are a number of studies required to further develop these composite materials for possible clinical use. These include various aspects of *in vitro* testing. However, ultimately the potential application can really only be tested adequately in human clinical trials. Some specific further studies which would be valuable are considered below:

1) Work is required to improve the reliability of membrane manufacture; in particular to test the parameters which can be used to produce the membranes without any defect. Studies are required to optimise the processing of prepreg and the fabrication of fibre reinforced PLA-HA composite membranes. Use of different prepreg lay ups in the composite membrane and their effect on the mechanical properties of the membrane need to be investigated to optimise the stiffness and strength of the membranes.

2) Long term degradation studies should be carried out. Additionally, tests should be done to analyze the effects of moulding temperature and pressure on the degradation of the membranes.

3) The ability of these membranes to carry and release antibiotics and other growth factors such as BMPs needs to be investigated. Fabrication of multilayered membranes consisting of different surface layers be carried out to test the directional release of growth factors and proteins.

4) Further analysis is required of bone profiles of maxillary and mandibular alveolar ridges in both edentulous patients and patients with periodontal

diseases to broaden and validate the findings of mandibular ridge resorption profiles done in the present study.

5) Ultimately, the suitability of these membranes for GTR procedures needs to be evaluated *in vivo*. This might involve animal studies, although as these materials have all been used extensively in alternative applications in humans, this might not be necessary or particularly informative. Human clinical studies are required firstly to demonstrate safety and basic efficacy of the membranes in the first instance. In the longer term, membranes may have a variety of different applications requiring slightly different preparations, for example with supplemented growth factors, seeded stem cells and for antibiotic delivery.

9.3 CONCLUSIONS

1) PLA-Ca P composites containing three different types HAs and one TCP were produced. The production process of the films was optimised and the Ca P powders and PLA-Ca P films produced were characterised. Three different concentrations of the fillers were used for the manufacturing of PLA-Ca P films and their effect on the film's character was evaluated. Increasing the concentration of the filler increased its amount on the surface, which affected the roughness of the films.

2) The bioactivity of the PLA-Ca P composite films was dependent on the type and concentration of the HA and TCP used. The bioactivity of the composite films increased with increases in the HA or TCP concentration.

3) The degradation of PLA decreased with the addition of Ca P. The highest weight gain was shown by films containing highest HA or TCP concentrations. In addition to PLA degradation, Ca P dissolution from the composite films also added to the overall weight loss.

4) The proliferation of osteoblast and PDL cells was highest on films containing 10 wt % nHA, whereas the highest ALP activity was shown by cells on films containing 70 wt % nHA. The addition of PDGF to the films increased the proliferation of osteoblasts.

5) The fibre reinforced PLA-HA composite membranes produced at low temperature and pressure showed more sustained protein release than the membranes produced at higher temperature and pressure. Non-filled PLA films did not show any permeability, whereas the permeability of the composite films increased with increase in the nHA content.

6) Analysis of mandibular alveolar bone profiles showed that there was not much difference between them and only two specific shapes of membranes can fit most patients.

7) The flexural strength of the fibre reinforced PLA-HA composite membranes was dependent on prepreg sheet lay up. The flexural strength was highest for the membranes containing the maximum number of prepreg at 0°, although transverse fibres are needed for lateral strength.

REFERENCES

Agrawal CM, Kyriacos AA: Technique to control ph in vicinity of biodegrading pla-pga implants. Journal of Biomedical Materials Research 1997;38:105-114.

Albrektsson T, Johansson C: Osteoinduction, osteoconduction and osseointegration. European Spine Journal 2001;10:S96-S101.

Andrew JG, Hoyland JA, Freemont AJ, Marsh DR: Platelet-derived growth factor expression in normally healing human fractures. Bone 1995;16:455-460.

Antoniades HN: Human platelet-derived growth factor (pdgf): Purification of pdgf-i and pdgf-ii and separation of their reduced subunits. Proceedings of the National Academy of Sciences of the United States of America 1981;78:7314-7317.

Ara M, Watanabe M, Imai Y: Effect of blending calcium compounds on hydrolytic degradation of poly(-lactic acid-co-glycolic acid). Biomaterials 2002;23:2479-2483.

Arami H, Mohajerani M, Mazloumi M, Khalifehzadeh R, Lak A, Sadrnezhaad SK: Rapid formation of hydroxyapatite nanostrips via microwave irradiation. Journal of Alloys and Compounds 2009;469:391-394.

Armitage GC: Development of a classification system for periodontal diseases and conditions. Annals of Periodontology 1999;4:1-6.

Armitage GC: Periodontal diagnoses and classification of periodontal diseases. Periodontology 2000 2004;34:9-21.

Ashammakhi N, Peltoniemi H, Waris E, Suuronen R, Serlo W, Kellomaki M, Tormala P, Waris T: Developments in craniomaxillofacial surgery: Use of self-reinforced bioabsorbable osteofixation devices. Plast Reconstr Surg 2001;108:167-180.

Athanasiou KA, Niederauer GG, Agrawal CM: Sterilization, toxicity, biocompatibility and clinical applications of polylactic acid/ polyglycolic acid copolymers. Biomaterials 1996a;17:93-102.

Athanasiou KA, Niederauer GG, Agrawal CM: Sterilization, toxicity, biocompatibility and clinical applications of polylactic acid/polyglycolic acid copolymers. Biomaterials 1996b;17:93-102.

Aubin JE: Bone stem cells. J Cell Biochem Suppl 1998;30-31:73-82.

Ball M, Grant DM, Lo WJ, Scotchford CA: The effect of different surface morphology and roughness on osteoblast-like cells. Journal of Biomedical Materials Research Part A 2008;86A:637-647.

Barrere F, van Blitterswijk CA, de Groot K: Bone regeneration: Molecular and cellular interactions with calcium phosphate ceramics. International Journal Of Nanomedicine 2006;1:317-332.

Barton SE, Engelhard P, Conant M: Poly-l-lactic acid for treating hiv-associated facial lipoatrophy: A review of the clinical studies. Int J STD AIDS 2006;17:429-435.

Bateman J, Intini G, Margarone J, Goodloe S, Bush P, Lynch SE, Dziak R: Platelet-derived growth factor enhancement of two alloplastic bone matrices. Journal Of Periodontology 2005;76:1833-1841.

Becker W, Becker BE: Treatment of mandibular 3-wall intrabony defects by flap debridement and expanded polytetrafluoroethylene barrier membranes. Long-term evaluation of 32 treated patients. Journal of Periodontology 1993;64:1138-1144.

Becker W, Becker BE, Caffesse R, Kerry G, Ochsenbein C, Morrison E, Prichard J: A longitudinal study comparing scaling, osseous surgery, and modified widman procedures: Results after 5 years. Journal of Periodontology 2001;72:1675-1684.

Behr M, Rosentritt M, Lang R, Handel G: Flexural properties of fiber reinforced composite using a vacuum/pressure or a manual adaptation manufacturing process. Journal of Dentistry 2000;28:509-514.

Bell LC, Posner AM, Quirk JP: Surface charge characteristics of hydroxyapatite and fluorapatite. Nature 1972;239:515-&.

Bergsma JE, de Bruijn WC, Rozema FR, Bos RRM, Boering G: Late degradation tissue response to poly(-lactide) bone plates and screws. Biomaterials 1995;16:25-31.

Bezzi G, Celotti G, Landi E, La Torretta TMG, Sopyan I, Tampieri A: A novel sol-gel technique for hydroxyapatite preparation. Materials Chemistry and Physics 2003;78:816-824.

Bleach NC, Tanner KE, Kellomaki M, Tormala P: Effect of filler type on the mechanical properties of self-reinforced polylactide-calcium phosphate composites. Journal of Materials Science 2001;12:911-915.

Boden SD: The abcs of bmps. Orthopaedic nursing / National Association of Orthopaedic Nurses 2005;24:49-52; quiz 53-44.

Bogle G, Garrett S, Stoller NH, Swanbom DD, Fulfs JC, Rodgers PW, Whitman S, Dunn RL, Southard GL, Polson AM: Periodontal regeneration in naturally occurring class ii furcation defects in beagle dogs after guided tissue regeneration with bioabsorbable barriers. Journal of Periodontology 1997;68:536-544.

Bohner M, Lemaitre J: Can bioactivity be tested in vitro with sbf solution? Biomaterials 2009;30:2175-2179.

Bolander ME: Regulation of fracture repair by growth factors. Proceedings of the Society for Experimental Biology and Medicine Society for Experimental Biology and Medicine (New York, NY 1992;200:165-170.

Bonfield W, Grynpas MD, Tully AE, Bowman J, Abram J: Hydroxyapatite reinforced polyethylene -- a mechanically compatible implant material for bone replacement. Biomaterials 1981;2:185-186.

Bosshardt DD: Are cementoblasts a subpopulation of osteoblasts or a unique phenotype? Journal of Dental research 2005;84:390-406.

Bostman O, Pihlajamaki H: Clinical biocompatibility of biodegradable orthopaedic implants for internal fixation: A review. Biomaterials 2000;21:2615-2621.

BouSerhal C, Jacobs R, Quirynen M, van Steenberghe D: Imaging technique selection for the preoperative planning of oral implants: A review of the literature. Clin Implant Dent Relat Res 2002;4:156-172.

Boyne PJ, Marx RE, Nevins M, Triplett G, Lazaro E, Lilly LC, Alder M, Nummikoski P: A feasibility study evaluating rhbmp-2/absorbable collagen sponge for maxillary sinus floor augmentation. Int J Periodontics Restor Dent 1997;17:10-25.

Bradford MM: A rapid and sensitive method for the quantitation of microgram quantities of protein utilizing the principle of protein-dye binding. Analytical Biochemistry 1976;72:248-254.

Bremm LL, Sallum AW, Casati MZ, Nociti FH, Sallum EA: Guided tissue regeneration in class ii furcation defects using a resorbable polylactic acid barrier. Am J Dent 2004;17:443-446.

Bunyaratavej P, Wang H-L: Collagen membranes: A review. Journal Of Periodontology 2001;72:215-229.

Burgess CM: Treatment of facial asymmetry with poly-l-lactic acid: A case study. Aesthetic Plastic Surgery 2008;32:552-554.

Caffesse RG, Mota LF, Quinones CR, Morrison EC: Clinical comparison of resorbable and non-resorbable barriers for guided periodontal tissue regeneration. Journal of Clinical Periodontology 1997;24:747-752.

Caffesse RG, Quinones CR: Polypeptide growth factors and attachment proteins in periodontal wound healing and regeneration. Periodontology 2000 1993;1:69-79.

Cao JM, Feng J, Deng SG, Chang X, Wang J, Liu JS, Lu P, Lu HX, Zheng MB, Zhang F, Tao J: Microwave-assisted solid-state synthesis of hydroxyapatite nanorods at room temperature. Journal Of Materials Science 2005;40:6311-6313.

Cao W, Hench LL: Bioactive materials. Ceramics International 1996;22:493-507.

Carnio J, Miller PD: Increasing the amount of attached gingiva using a modified apically repositioned flap. Journal Of Periodontology 1999;70:1110-1117.

Carraro JJ, Sznajder N, Alonso CA: Intraoral cancellous bone autografts in the treatment of infrabony pockets. J Clin Periodontol 1976;3:104-109.

Caton J, Nyman S, Zander H: Histometric evaluation of periodontal surgery. Ii. Connective tissue attachment levels after four regenerative procedures. J Clin Periodontol 1980;7:224-231.

Chen F-m, Zhao Y-m, Wu H, Deng Z-h, Wang Q-t, Zhou W, Liu Q, Dong G-y, Li K, Wu Z-f, Jin Y: Enhancement of periodontal tissue regeneration by locally controlled delivery of insulin-like growth factor-i from dextran-co-gelatin microspheres. Journal of Controlled Release 2006;114:209-222.

Cho MI, Lin WL, Genco RJ: Platelet-derived growth factor-modulated guided tissue regenerative therapy. Journal Of Periodontology 1995;66:522-530.

Chong CH, Carnes DL, Moritz AJ, Oates T, Ryu OH, Simmer J, Cochran DL: Human periodontal fibroblast response to enamel matrix derivative, amelogenin, and platelet-derived growth factor-bb. Journal Of Periodontology 2006;77:1242-1252.

Christner P, Robinson P, Clark CC: A preliminary characterization of human cementum collagen. Calcified Tissue Research 1977;23:147-150.

Conn RE, Kolstad JJ, Borzelleca JF, Dixler DS, Filer LJ, Jr., LaDu BN, Jr., Pariza MW: Safety assessment of polylactide (pla) for use as a food-contact polymer. Food Chem Toxicol 1995;33:273-283.

Cooke JW, Sarment DP, Whitesman LA, Miller SE, Jin Q, Lynch SE, Giannobile WV: Effect of rhpdgf-bb delivery on mediators of periodontal wound repair. Tissue Engineering 2006;12:1441-1450.

Cortellini P, Tonetti MS: Focus on intrabony defects: Guided tissue regeneration. Periodontology 2000 2000;22:104-132.

Dalby MJ, Di Silvio L, Harper EJ, Bonfield W: In vitro adhesion and biocompatability of osteoblast-like cells to poly(methylmethacrylate) and poly(ethylmethacrylate) bone cements. Journal Of Materials Science 2002;13:311-314.

Damien CJ, Parsons JR: Bone-graft and bone-graft substitutes - a review of current technology and applications. J Appl Biomater 1991;2:187-208.

Davidson JM, Klagsbrun M, Hill KE, Buckley A, Sullivan R, Brewer PS, Woodward SC: Accelerated wound repair, cell proliferation, and collagen accumulation are produced by a cartilage-derived growth factor. The Journal of Cell Biology 1985;100:1219-1227.

de Aza PN, Guitian F, Santos C, de Aza S, Cusco R, Artus L: Vibrational properties of calcium phosphate compounds. 2. Comparison between hydroxyapatite and î²-tricalcium phosphate. Chemistry of Materials 1997;9:916-922.

de Oliveira Costa F, Diniz Ferreira S, de Miranda Cota LO, da Costa JE, Aguiar MA: Prevalence, severity, and risk variables associated with gingival overgrowth in renal transplant subjects treated under tacrolimus or cyclosporin regimens. Journal Of Periodontology 2006;77:969-975.

Deptula A, Lada W, Olczak T, Borello A, Alvani C, Dibartolomeo A: Preparation of spherical powders of hydroxyapatite by sol-gel process. Journal of Non-Crystalline Solids 1992;147:537-541.

Dereka XE, Markopoulou CE, Mamalis A, Pepelassi E, Vrotsos IA: Time- and dose-dependent mitogenic effect of basic fibroblast growth factor combined with different bone graft materials: An in vitro study. Clinical Oral Implants Research 2006;17:554-559.

Di Silvio L, Dalby MJ, Bonfield W: Osteoblast behaviour on ha/pe composite surfaces with different ha volumes. Biomaterials 2002;23:101-107.

dos Santos EA, Farina M, Soares GA, Anselme K: Surface energy of hydroxyapatite and beta-tricalcium phosphate ceramics driving serum protein adsorption and osteoblast adhesion. Journal Of Materials Science 2008;19:2307-2316.

Duan YR, Zhang ZR, Wang CY, Chen JY, Zhang XD: Dynamic study of calcium phosphate formation on porous ha/tcp ceramics. J Mater Sci-Mater Med 2004;15:1205-1211.

Dubok VA: Bioceramics - yesterday, today, tomorrow. Powder Metall Met Ceram 2000;39:381-394.

Ducheyne P, Radin S, King L: The effect of calcium-phosphate ceramic composition and structure on invitro behavior .1. Dissolution. Journal Of Biomedical Materials Research 1993;27:25-34.

Dupoirieux L, Pourquier D, Picot MC, Neves M: Comparative study of three different membranes for guided bone regeneration of rat cranial defects. International Journal Of Oral And Maxillofacial Surgery 2001;30:58-62.

Dyer SR, Lassila LVJ, Jokinen M, Vallittu PK: Effect of fiber position and orientation on fracture load of fiber-reinforced composite. Dental Materials 2004;20:947-955.

Eaton KA, Kieser JB, Davies RM: The removal of root surface deposits. Journal of Clinical Periodontology 1985;12:141-152.

Eley B.M. and Manson J.D. Periodontics.Butterworth-Heinemann, 2004. Edinburgh; New York.

Enislidis G, Lagogiannis G, Wittwer G, Glaser C, Ewers R: Fixation of zygomatic fractures with a biodegradable copolymer osteosynthesis system: Short- and long-term results. International Journal Of Oral And Maxillofacial Surgery 2005;34:19-26.

Feng W, Mu-sen L, Yu-peng L, Yong-xin Q: A simple sol-gel technique for preparing hydroxyapatite nanopowders. Materials Letters 2005;59:916-919.

Floyd P, Palmer P, Palmer R: Dental implants: Radiographic technique. Br Dent J 1999;187:359-365.

Frame JW: Hydroxyapatite as a biomaterial for alveolar ridge augmentation. International Journal Of Oral And Maxillofacial Surgery 1987;16:642-655.

Fujii H, Kitazawa R, Maeda S, Mizuno K, Kitazawa S: Expression of platelet-derived growth factor proteins and their receptor alpha and beta mrnas during fracture healing in the normal mouse. Histochemistry And Cell Biology 1999;112:131-138.

Furuzono T, Walsh D, Sato K, Sonoda K, Tanaka J: Effect of reaction temperature on the morphology and size of hydroxyapatite nanoparticles in an emulsion system. Journal of Materials Science Letters 2001;20:111-114.

Gadi T, Yoram Z, Shuanhu Z, Pam K, Ioannis KM, Yogendra PK, Luis EB, Frederick JB, Barry SK, Peter VNB, Dan G: Systemically administered rhbmp-2 promotes msc activity and reverses bone and cartilage loss in osteopenic mice. Journal of Cellular Biochemistry 2002;86:461-474.

Garg AK, Vicari A: Radiographic modalities for diagnosis and treatment planning in implant dentistry. Implant Soc 1995;5:7-11.

Garlotta D: A literature review of poly(lactic acid). J Polym Environ 2001;9:63-84.

Georgiou G, Mathieu L, Pioletti DP, Bourban PE, Manson JA, Knowles JC, Nazhat SN: Polylactic acid-phosphate glass composite foams as scaffolds for bone tissue engineering. Journal Of Biomedical Materials Research 2007;80:322-331.

Gestrelius S, Andersson C, Lidstrom D, Hammarstrom L, Somerman M: In vitro studies on periodontal ligament cells and enamel matrix derivative. Journal of Clinical Periodontology 1997;24:685-692.

Giannobile WV: Periodontal tissue engineering by growth factors. Bone 1996;19:S23-S37.

Ginebra MP, Driessens FC, Planell JA: Effect of the particle size on the micro and nanostructural features of a calcium phosphate cement: A kinetic analysis. Biomaterials 2004;25:3453-3462.

Polimeni G, Koo KT, Qahash M, Xiropaidis AV, Albandar JM, Wikesjo UME: Prognostic factors for alveolar regeneration: Effect of tissue occlusion on alveolar bone regeneration with guided tissue regeneration. Journal of Clinical Periodontology 2004;31:730-735.

Gorski JP: Is all bone the same? Distinctive distributions and properties of non-collagenous matrix proteins in lamellar vs. Woven bone imply the existence of different underlying osteogenic mechanisms. Critical Reviews in Oral Biology & Medicine 1998;9:201-223.

Gottlow J, Nyman S, Karring T, Lindhe J: New attachment formation as the result of controlled tissue regeneration. J Clin Periodontol 1984;11:494-503.

Granjeiro JM, Oliveira RC, Bustos-Valenzuela JC, Sogayar MC, Taga R: Bone morphogenetic proteins: From structure to clinical use. Brazilian Journal Of Medical And Biological Research = Revista brasileira de pesquisas medicas e biologicas / Sociedade Brasileira de Biofisica [et al 2005;38:1463-1473.

Grizzi I, Garreau H, Li S, Vert M: Hydrolytic degradation of devices based on poly(-lactic acid) size-dependence. Biomaterials 1995;16:305-311.

Gu YW, Khor KA, Cheang P: Bone-like apatite layer formation on hydroxyapatite prepared by spark plasma sintering (sps). Biomaterials 2004;25:4127-4134.

Guillemin MR, Mellonig JT, Brunsvold MA: Healing in periodontal defects treated by decalcified freeze-dried bone allografts in combination with eptfe membranes (i). Clinical and scanning electron microscope analysis. J Clin Periodontol 1993;20:528-536.

Gupta B, Revagade N, Hilborn J: Poly(lactic acid) fiber: An overview. Prog Polym Sci 2007;32:455-482.

Hammarstrom L: Enamel matrix, cementum development and regeneration. Journal of Clinical Periodontology 1997;24:658-668.

Hammarstrom L, Alatli I, Fong CD: Origins of cementum. Oral Dis 1996;2:63-69.

Hammarström L HL, Gestrelius S: Periodontal regeneration in a buccal dehiscence model in monkeys after application of enamel matrix proteins. Journal of Clinical Periodontology 1997;24:669-677.

Han Y, Li S, Wang X, Chen X: Synthesis and sintering of nanocrystalline hydroxyapatite powders by citric acid sol-gel combustion method. Materials Research Bulletin 2004;39:25-32.

Hasegawa M, Yamato M, Kikuchi A, Okano T, Ishikawa I: Human periodontal ligament cell sheets can regenerate periodontal ligament tissue in an athymic rat model. Tissue Engineering 2005;11:469-478.

Heidemann W, Jeschkeit S, Ruffieux K, Fischer JH, Wagner M, Krüger G, Wintermantel E, Gerlach KL: Degradation of poly(,)lactide implants with or without addition of calciumphosphates in vivo. Biomaterials 2001;22:2371-2381.

Heldin C-H, Westermark B: Mechanism of action and in vivo role of platelet-derived growth factor. Physiol Rev 1999;79:1283-1316

Hench LL: Bioactive ceramics: Theory and clinical applications. Bioceramics, Vol 7 1994:3-14.

Hiatt WH, Schallhorn RG: Intraoral transplants of cancellous bone and marrow in periodontal lesions. Journal Of Periodontology 1973;44:194-208.

Hiatt WH, Schallhorn RG, Aaronian AJ: The induction of new bone and cementum formation. Iv. Microscopic examination of the periodontium following human bone and marrow allograft, autograft and nongraft periodontal regenerative procedures. Journal Of Periodontology 1978;49:495-512.

Hock JM, Centrella M, Canalis E: Insulin-like growth factor i has independent effects on bone matrix formation and cell replication. Endocrinology 1988;122:254-260.

Holmstrup P: Non-plaque-induced gingival lesions. Annals of periodontology / the American Academy of Periodontology 1999;4:20-31.

Honda T, Domon H, Okui T, Kajita K, Amanuma R, Yamazaki K: Balance of inflammatory response in stable gingivitis and progressive periodontitis lesions. Clinical And Experimental Immunology 2006;144:35-40.

Hosoya A, Ninomiya T, Hiraga T, Zhao C, Yoshiba K, Yoshiba N, Takahashi M, Okabe T, Wakitani S, Yamada H, Kasahara E, Ozawa H, Nakamura H: Alveolar bone regeneration of subcutaneously transplanted rat molar. Bone 2008;42:350-357.

Hott M, Noel B, Bernache-Assolant D, Rey C, Marie PJ: Proliferation and differentiation of human trabecular osteoblastic cells on hydroxyapatite. J Biomed Mater Res 1997;37:508-516.

Howell TH, Fiorellini JP, Paquette DW, Offenbacher S, Giannobile WV, Lynch SE: A phase i/ii clinical trial to evaluate a combination of recombinant human platelet-derived growth factor-bb and recombinant human insulin-like growth factor-i in patients with periodontal disease. Journal Of Periodontology 1997;68:1186-1193.

Hsieh SC, Graves DT: Pulse application of platelet-derived growth factor enhances formation of a mineralizing matrix while continuous application is inhibitory. J Cell Biochem 1998;69:169-180.

Huang J, Lin YW, Fu XW, Best SM, Brooks RA, Rushton N, Bonfield W: Development of nano-sized hydroxyapatite reinforced composites for tissue engineering scaffolds. J Mater Sci-Mater Med 2007;18:2151-2157.

Huang YX, Ren J, Chen C, Ren TB, Zhou XY: Preparation and properties of poly(lactide-co-glycolide) (plga)/ nano-hydroxyapatite (nha) scaffolds by thermally induced phase separation and rabbit mscs culture on scaffolds. Journal Of Biomaterials Applications 2008;22:409-432.

Hughes FJ, Turner W, Belibasakis G, Martuscelli G: Effects of growth factors and cytokines on osteoblast differentiation. Periodontology 2000 2006;41:48-72.

Hurzeler MB, Quinones CR, Caffesse RG, Schupbach P, Morrison EC: Guided periodontal tissue regeneration in interproximal intrabony defects

following treatment with a synthetic bioabsorbable barrier. Journal Of Periodontology 1997;68:489-497.

Ignatius AA, Augat P, Claes LE: Degradation behavior of composite pins made of tricalcium phosphate and poly(l,dl-lactide). J Biomater Sci-Polym Ed 2001;12:185-194.

Ignjatovic N, Savic V, Najman S, Plavsic M, Uskokovic D: A study of hap/plla composite as a substitute for bone powder, using ft-ir spectroscopy. Biomaterials 2001;22:571-575.

Iizuka T, Lindqvist C, Hallikainen D, Mikkonen P, Paukku P: Severe bone-resorption and osteoarthrosis after miniplate fixation of high condylar fractures - a clinical and radiologic study of 13 patients. Oral Surg Oral Med Oral Pathol Oral Radiol Endod 1991;72:400-407.

Imai Y, Fukuzawa A, Watanabe M: Effect of blending tricalcium phosphate on hydrolytic degradation of a block polyester containing poly(l-lactic acid) segment. Journal of Biomaterials Science, Polymer Edition 1999;10:773-786.

Ioannis V, Elena A, Antonis K: Guided tissue regeneration in intrabony periodontal defects following treatment with two bioabsorbable membranes in combination with bovine bone mineral graft. Journal Of Clinical Periodontology 2004;31:908-917.

Ishii S, Tamura J, Furukawa T, Nakamura T, Matsusue Y, Shikinami Y, Okuno M: Long-term study of high-strength hydroxyapatite/poly(l-lactide) composite rods for the internal fixation of bone fractures: A 2-4-year follow-up study in rabbits. Journal Of Biomedical Materials Research 2003;66:539-547.

Jaakkola T, Rich J, Tirri T, Narhi T, Jokinen M, Seppala J, Yli-Urpo A: In vitro ca-p precipitation on biodegradable thermoplastic composite of poly(epsilon-caprolactone-co-dl-lactide) and bioactive glass (s53p4). Biomaterials 2004;25:575-581.

Jarcho M: Calcium-phosphate ceramics as hard tissue prosthetics. Clin Orthop Rel Res 1981:259-278.

Jeong SI, Ko EK, Yum J, Jung CH, Lee YM, Shin H: Nanofibrous poly(lactic acid)/hydroxyapatite composite scaffolds for guided tissue regeneration. Macromolecular Bioscience 2008;8:328-338.

Jepsen S, Heinz B, Kermanie MA, Jepsen K: Evaluation of a new bioabsorbable barrier for recession therapy: A feasibility study. Journal Of Periodontology 2000;71:1433-1440.

Jergesen HE, Chua J, Kao RT, Kaban LB: Age effects on bone induction by demineralized bone powder. Clin Orthop Relat Res 1991:253-259.

Jillavenkatesa A, Condrate RA: Sol-gel processing of hydroxyapatite. Journal Of Materials Science 1998;33:4111-4119.

Junqueira LCU, Carneiro J: Basic histology : Text & atlas, ed 11th ed. / Luiz Carlos Junqueira, José Carneiro. New York ; London, McGraw-Hill, 2005.

Kennady MC, Tucker MR, Lester GE, Buckley MJ: Histomorphometric evaluation of stress shielding in mandibular continuity defects treated with rigid fixation plates and bone grafts. International Journal Of Oral And Maxillofacial Surgery 1989;18:170-174.

Kent JN, Finger IM, Quinn JH, Guerra LR: Hydroxylapatite alveolar ridge reconstruction - clinical-experiences, complications, and technical modifications. Journal of Oral and Maxillofacial Surgery 1986;44:37-49.

Khan AS, Ahmed Z, Edirisinghe MJ, Wong FS, Rehman IU: Preparation and characterization of a novel bioactive restorative composite based on covalently coupled polyurethane-nanohydroxyapatite fibres. Acta biomaterialia 2008;4:1275-1287.

Khor KA, Li H, Cheang P, Boey SY: In vitro behavior of hvof sprayed calcium phosphate splats and coatings. Biomaterials 2003;24:723-735.

Kim HM, Himeno T, Kokubo T, Nakamura T: Process and kinetics of bonelike apatite formation on sintered hydroxyapatite in a simulated body fluid. Biomaterials 2005;26:4366-4373.

Kim SS, Sun Park M, Jeon O, Yong Choi C, Kim BS: Poly(lactide-co-glycolide)/hydroxyapatite composite scaffolds for bone tissue engineering. Biomaterials 2006;27:1399-1409.

Kinane DF: Periodontitis modified by systemic factors. Annals of periodontology / the American Academy of Periodontology 1999;4:54-64.

King GN: The importance of drug delivery to optimize the effects of bone morphogenetic proteins during periodontal regeneration. Current Pharmaceutical Biotechnology 2001;2:131-142.

King GN, Cochrant DL: Factors that modulate the effects of bone morphogenetic protein-induced periodontal regeneration: A critical review. Journal Of Periodontology 2002;73:925-936.

King GN, Hughes FJ: Bone morphogenetic protein-2 stimulates cell recruitment and cementogenesis during early wound healing. Journal of Clinical Periodontology 2001;28:465-475.

King GN, King N, Hughes FJ: Effect of two delivery systems for recombinant human bone morphogenetic protein-2 on periodontal regeneration in vivo. Journal Of Periodontal Research 1998;33:226-236.

Kitsugi T, Yamamuro T, Nakamura T, Kokubo T, Takagi M, Shibuya T, Takeuchi H, Ono M: Bonding behavior between 2 bioactive ceramics invivo. Journal Of Biomedical Materials Research 1987;21:1109-1123.

Klein C, Driessen AA, Degroot K, Vandenhooff A: Biodegradation behavior of various calcium-phosphate materials in bone tissue. Journal Of Biomedical Materials Research 1983;17:769-784.

Kokubo T: Apatite formation on surfaces of ceramics, metals and polymers in body environment. Acta Materialia 1998;46:2519-2527.

Kokubo T, Kushitani H, Sakka S, Kitsugi T, Yamamuro T: Solutions able to reproduce in vivo surface-structure changes in bioactive glass-ceramic a-w. J Biomed Mater Res 1990;24:721-734.

Kokubo T, Takadama H: How useful is sbf in predicting in vivo bone bioactivity? Biomaterials 2006;27:2907-2915.

Koutsopoulos S: Synthesis and characterization of hydroxyapatite crystals: A review study on the analytical methods. J Biomed Mater Res 2002;62:600-612.

Koyama Y, Kikuchi M, Yamada T, Kanaya T, Matsumoto HN, Takakuda K, Miyairi H, Tanaka J: Guided bone regeneration with novel bioabsorbable

membranes. JSME International Journal Series C Mechanical Systems, Machine Elements and Manufacturing 2003;46:1409-1416.

Kulkarni RK, Moore EG, Hegyeli AF, Leonard F: Biodegradable poly(lactic acid) polymers. J Biomed Mater Res 1971;5:169-181.

Kurashina K, Kurita H, Takeuchi H, Hirano M, Klein CP, de Groot K: Osteogenesis in muscle with composite graft of hydroxyapatite and autogenous calvarial periosteum: A preliminary report. Biomaterials 1995;16:119-123.

Kwon S-H, Jun Y-K, Hong S-H, Kim H-E: Synthesis and dissolution behavior of [beta]-tcp and ha/[beta]-tcp composite powders. Journal of the European Ceramic Society 2003;23:1039-1045.

Landes CA, Ballon A, Roth C: Maxillary and mandibular osteosyntheses with plga and p(l/dl)la implants: A 5-year inpatient biocompatibility and degradation experience. Plast Reconstr Surg 2006;117:2347-2360.

Lang N, Bartold PM, Cullinan M, Jeffcoat M, Mombelli A, Murakami S, Page R, Papapanou P, Tonetti M, Dyke TV: Consensus report: Aggressive periodontitis. Annals of Periodontology 1999;4:53-53.

Lanyon LE: Functional strain in bone tissue as an objective, and controlling stimulus for adaptive bone remodelling. Journal Of Biomechanics 1987;20:1083-1093.

Larry LH: Bioceramics. Journal of the American Ceramic Society 1998;81:1705-1728.

Lee SJ, Park YJ, Park SN, Lee YM, Seol YJ, Ku Y, Chung CP: Molded porous poly (l-lactide) membranes for guided bone regeneration with enhanced effects by controlled growth factor release. Journal Of Biomedical Materials Research 2001a;55:295-303.

Lee SJ, Park YJ, Park SN, Lee YM, Seol YJ, Ku Y, Chung CP: Molded porous poly (l-lactide) membranes for guided bone regeneration with enhanced effects by controlled growth factor release. J Biomed Mater Res 2001b;55:295-303.

Lee Y-M, Park Y-J, Lee S-J, Ku Y, Han S-B, Klokkevold PR, Chung C-P: The bone regenerative effect of platelet-derived growth factor-bb delivered with a

chitosan/tricalcium phosphate sponge carrier; in, 2000, vol 71, pp. 418-424.

LeGeros RZ: Biodegradation and bioresorption of calcium phosphate ceramics. Clinical Materials 1993;14:65-88.

LeGeros RZ, Parsons JR, Daculsi G, Driessens F, Lee D, Liu ST, Metsger S, Peterson D, Walker M: Significance of the porosity and physical chemistry of calcium phosphate ceramics. Biodegradation-bioresorption. Ann N Y Acad Sci 1988;523:268-271.

Lerner E, Sarig S, Azoury R: Enhanced maturation of hydroxyapatite from aqueous-solutions using microwave irradiation. J Mater Sci-Mater Med 1991;2:138-141.

Li S: Hydrolytic degradation characteristics of aliphatic polyesters derived from lactic and glycolic acids. J Biomed Mater Res 1999;48:342-353.

Liao S, Wang W, Uo M, Ohkawa S, Akasaka T, Tamura K, Cui F, Watari F: A three-layered nano-carbonated hydroxyapatite/collagen/plga composite membrane for guided tissue regeneration. Biomaterials 2005;26:7564-7571.

Liao SS, Cui FZ: In vitro and in vivo degradation of mineralized collagen-based composite scaffold: Nanohydroxyapatite/collagen/poly(l-lactide). Tissue Engineering 2004;10:73-80.

Lin KL, Chang J, Cheng RM, Ruan ML: Hydrothermal microemulsion synthesis of stoichiometric single crystal hydroxyapatite nanorods with mono-dispersion and narrow-size distribution. Materials Letters 2007;61:1683-1687.

Lindhe J, Ranney R, Lamster I, Charles A, Chung C-P, Flemmig T, Kinane D, Listgarten M, Loe H, Schoor R, Seymour G, Somerman M: Consensus report: Chronic periodontitis. Annals of Periodontology 1999;4:38-38.

Liu HN, Slamovich EB, Webster TJ: Increased osteoblast functions on nanophase titania dispersed in poly-lactic-co-glycolic acid composites. Nanotechnology 2005;16:S601-S608.

Livage J, Barboux P, Vandenborre MT, Schmutz C, Taulelle F: Sol-gel synthesis of phosphates. Journal of Non-Crystalline Solids 1992;147-148:18-23.

Lossdorfer S, Sun M, Gotz W, Dard M, Jager A: Enamel matrix derivative promotes human periodontal ligament cell differentiation and osteoprotegerin production in vitro. Journal Of Dental Research 2007;86:980-985.

Lu HH, El-Amin SF, Scott KD, Laurencin CT: Three-dimensional, bioactive, biodegradable, polymer-bioactive glass composite scaffolds with improved mechanical properties support collagen synthesis and mineralization of human osteoblast-like cells in vitro; in: 28th Annual Meeting of the Society-for-Biomaterials. Wiley-Liss, 2002, pp. 465-474.

Lunt J: Large-scale production, properties and commercial applications of polylactic acid polymers. Polymer Degradation and Stability 1998;59:145-152.

Lyngstadaas SP, Lundberg E, Ekdahl H, Andersson C, Gestrelius S: Autocrine growth factors in human periodontal ligament cells cultured on enamel matrix derivative. Journal of Clinical Periodontology 2001;28:181-188.

Machtei EE: The effect of membrane exposure on the outcome of regenerative procedures in humans: A meta-analysis. Journal Of Periodontology 2001;72:512-516.

Maquet V, Boccaccini AR, Pravata L, Notingher I, Jerome R: Preparation, characterization, and in vitro degradation of bioresorbable and bioactive composites based on bioglass-filled polylactide foams. J Biomed Mater Res A 2003;66:335-346.

Mariotti A: Dental plaque-induced gingival diseases. Annals of periodontology / the American Academy of Periodontology 1999;4:7-19.

Marra KG, Szem JW, Kumta PN, DiMilla PA, Weiss LE: In vitro analysis of biodegradable polymer blend/hydroxyapatite composites for bone tissue engineering. Journal Of Biomedical Materials Research 1999;47:324-335.

Martin TJO: Advances in understanding the molecular basis of bone remodelling: Past, present and future. Bone 2009;44:S18-S18.

Martinez-Lage JF, Poza M, Sola J, Tortosa JG, Brown P, Cervenakova L, Esteban JA, Mendoza A: Accidental transmission of creutzfeldt-jakob disease by dural cadaveric grafts. Journal Of Neurology, Neurosurgery, And Psychiatry 1994;57:1091-1094.

Massague J: Tgfbeta signaling: Receptors, transducers, and mad proteins. Cell 1996;85:947-950.

Massague J: Tgf-b signal transduction. Annual Review of Biochemistry 1998;67:753-791.

Matsumoto T, Okazaki M, Inoue M, Yamaguchi S, Kusunose T, Toyonaga T, Hamada Y, Takahashi J: Hydroxyapatite particles as a controlled release carrier of protein. Biomaterials 2004a;25:3807-3812.

Matsumoto T, Okazaki M, Inoue M, Yamaguchi S, Kusunose T, Toyonaga T, Hamada Y, Takahashi J: Hydroxyapatite particles as a controlled release carrier of protein. Biomaterials 2004b;25:3807-3812.

Matsumura K, Hyon SHS-H, Nakajima N, Iwata H, Watazu A, Tsutsumi S: Surface modification of poly(ethylene-co-vinyl alcohol): Hydroxyapatite immobilization and control of periodontal ligament cells differentiation. Biomaterials 2004;25:4817-4824.

Matsuyama T, Lau KHW, Wergedal JE: Monolayer-cultures of normal human bone-cells contain multiple subpopulations of alkaline-phosphatase positive cells. Calcified Tissue International 1990;47:276-283.

Mattson JS, Gallagher SJ, Jabro MH: The use of 2 bioabsorbable barrier membranes in the treatment of interproximal intrabony periodontal defects. Journal Of Periodontology 1999;70:510-517.

Maurizio ST, Pierpaolo C, Niklaus PL, Jean ES, Patrick A, Dominik D, Alberto F, Ioannis F, Giulio R, Roberto R, Maurizio S, Heinz T, Beat W, Michael Z: Clinical outcomes following treatment of human intrabony defects with gtr/bone replacement material or access flap alone. Journal Of Clinical Periodontology 2004;31:770-776.

Mavrogiannis M, Ellis JS, Thomason JM, Seymour RA: The management of drug-induced gingival overgrowth. Journal of Clinical Periodontology 2006;33:434-439.

Mayfield L, Nobreus N, Attstrom R, Linde A: Guided bone regeneration in dental implant treatment using a bioabsorbable membrane. Clin Oral Implants Res 1997;8:10-17.

McAllister BS, Haghighat K: Bone augmentation techniques. Journal Of Periodontology 2007;78:377-396.

Me YT, Liu XY, Chu PK, Ding CX: Nucleation and growth of calcium-phosphate on ca-implanted titanium surface. Surface Science 2006;600:651-656.

Mehta R, Kumar V, Bhunia H, Upadhyay SN: Synthesis of poly(lactic acid): A review. J Macromol Sci-Polym Rev 2005;C45:325-349.

Meinel L, Zoidis E, Zapf J, Hassa P, Hottiger MO, Auer JA, Schneider R, Gander B, Luginbuehl V, Bettschart-Wolfisberger R, Illi OE, Merkle HP, von Rechenberg B: Localized insulin-like growth factor i delivery to enhance new bone formation. Bone 2003;33:660-672.

Melcher AH: On the repair potential of periodontal tissues. Journal Of Periodontology 1976;47:256-260.

Mellonig JT: Autogenous and allogeneic bone grafts in periodontal therapy. Crit Rev Oral Biol Med 1992;3:333-352.

Michael JDM, Ulf MEW: Gingival recession defects and guided tissue regeneration: A review. Journal Of Periodontal Research 2001;36:341-354.

Middleton JC, Tipton AJ: Synthetic biodegradable polymers as orthopedic devices. Biomaterials 2000;21:2335-2346.

Moe KS, Weisman RA: Resorbable fixation in facial plastic and head and neck reconstructive surgery: An initial report on polylactic acid implants. Laryngoscope 2001;111:1697-1701.

Mostafa NY: Characterization, thermal stability and sintering of hydroxyapatite powders prepared by different routes. Materials Chemistry and Physics 2005;94:333-341.

Mumford JH, Carnes DL, Cochran DL, Oates TW: The effects of platelet-derived growth factor-bb on periodontal cells in an in vitro wound model. Journal Of Periodontology 2001;72:331-340.

Murakami N, Saito N, Horiuchi H, Okada T, Nozaki K, Takaoka K: Repair of segmental defects in rabbit humeri with titanium fiber mesh cylinders containing recombinant human bone morphogenetic protein-2 (rhbmp-2) and a synthetic polymer. J Biomed Mater Res 2002;62:169-174.

Murakami S, Takayama S, Kitamura M, Shimabukuro Y, Yanagi K, Ikezawa K, Saho T, Nozaki T, Okada H: Recombinant human basic fibroblast growth factor (bfgf) stimulates periodontal regeneration in class ii furcation defects created in beagle dogs. Journal Of Periodontal Research 2003;38:97-103.

Murphy KG, Gunsolley JC: Guided tissue regeneration for the treatment of periodontal intrabony and furcation defects.A systematic review. Annals of Periodontology 2003;8:266-302.

Murugan R, Ramakrishna S: Development of nanocomposites for bone grafting. Composites Science and Technology 2005;65:2385-2406.

Nakamura M, Sekijima Y, Nakamura S, Kobayashi T, Niwa K, Yamashita K: Role of blood coagulation components as intermediators of high osteoconductivity of electrically polarized hydroxyapatite. J Biomed Mater Res A 2006;79:627-634.

Nanci A, Ten Cate AROh: Ten cate's oral histology : Development, structure, and function, ed 6th ed. / Antonio Nanci. St. Louis, Mo. ; [London], Mosby, 2003.

Narasaraju TSB, Phebe DE: Some physico-chemical aspects of hydroxylapatite. Journal Of Materials Science 1996;31:1-21.

Nazhat SN, Kellomaki M, Tormala P, Tanner KE, Bonfield W: Dynamic mechanical characterization of biodegradable composites of hydroxyapatite and polylactides. J Biomed Mater Res 2001;58:335-343.

Needleman I, Tucker R, Giedrys-Leeper E, Worthington H: A systematic review of guided tissue regeneration for periodontal infrabony defects. Journal Of Periodontal Research 2002;37:380-388.

Needleman IG, Worthington HV, Giedrys-Leeper E, Tucker RJ: Guided tissue regeneration for periodontal infra-bony defects. Cochrane Database Of Systematic Reviews (Online) 2006:CD001724.

Neo N, Nakamura T, Ohtsuki C, Kokubo T, Yamamuro T: Apatite formation on three kinds of bioactive material at an early stage in vivo: A comparative study by transmission electron microscopy. Journal Of Biomedical Materials Research 1993;27:999-1006.

Nevins M, Camelo M, Nevins ML, Schenk RK, Lynch SE: Periodontal regeneration in humans using recombinant human platelet- derived growth factor-bb (rhpdgf-bb) and allogenic bone. Journal Of Periodontology 2003;74:1282-1292.

Niemelä T: Effect of [beta]-tricalcium phosphate addition on the in vitro degradation of self-reinforced poly-l,d-lactide. Polymer Degradation and Stability 2005;89:492-500.

Nordstrom P, Pihlajamaki H, Toivonen T, Tormala P, Rokkanen P: Tissue response to polyglycolide and polylactide pins in cancellous bone. Archives Of Orthopaedic And Trauma Surgery 1998;117:197-204.

Nowzari H, MacDonald ES, Flynn J, London RM, Morrison JL, Slots J: The dynamics of microbial colonization of barrier membranes for guided tissue regeneration. Journal Of Periodontology 1996;67:694-702.

Nyman S, Lindhe J, Karring T, Rylander H: New attachment following surgical treatment of human periodontal disease. J Clin Periodontol 1982;9:290-296.

Ohyama M, Suzuki N, Yamaguchi Y, Maeno M, Otsuka K, Ito K: Effect of enamel matrix derivative on the differentiation of c2c12 cells. Journal Of Periodontology 2002;73:543-550.

Ono I, Tateshita T, Inoue M, Kuboki Y: In vivo strength enhancement of hydroxyapatite combined with rhbmp-2. J Bone Miner Metab 1998;16:81-87.

Park JB, Matsuura M, Han KY, Norderyd O, Lin WL, Genco RJ, Cho MI: Periodontal regeneration in class iii furcation defects of beagle dogs using guided tissue regenerative therapy with platelet-derived growth factor. Journal Of Periodontology 1995;66:462-477.

Park YJ, Lee YM, Park SN, Lee JY, Ku Y, Chung CP, Lee SJ: Enhanced guided bone regeneration by controlled tetracycline release from poly(l-lactide) barrier membranes. J Biomed Mater Res 2000a;51:391-397.

Park YJ, Lee YM, Park SN, Sheen SY, Chung CP, Lee SJ: Platelet derived growth factor releasing chitosan sponge for periodontal bone regeneration. Biomaterials 2000b;21:153-159.

Park YJ, Nam KH, Ha SJ, Pai CM, Chung CP, Lee SJ: Porous poly(-lactide) membranes for guided tissue regeneration and controlled drug delivery: Membrane fabrication and characterization. Journal of Controlled Release 1997;43:151-160.

Parkar MH, Kuru L, Giouzeli M, Olsen I: Expression of growth-factor receptors in normal and regenerating human periodontal cells. Archives Of Oral Biology 2001;46:275-284.

Partio EK, Merikanto J, Heikkila JT, Ylinen P, Makela EA, Vainio J, Tormala P, Rokkanen P: Totally absorbable screws in fixation of subtalar extra articular arthrodesis in children with spastic neuromuscular disease - preliminary-report of a randomized prospective-study of 14 arthrodeses fixed with absorbable or metallic screws. J Pediatr Orthop 1992;12:646-650.

Patrick B. Smith ALSKXYSLH: Raman characterization of orientation in poly(lactic acid) films. Macromolecular Symposia 2001;175:81-94.

Paul D, Shulamith R, Linda K: The effect of calcium phosphate ceramic composition and structure on in vitro behavior. I. Dissolution. Journal Of Biomedical Materials Research 1993;27:25-34.

Paul W, Sharma CP: Ceramic drug delivery: A perspective. Journal Of Biomaterials Applications 2003;17:253-264.

Phillips MJ, Darr JA, Luklinska ZB, Rehman I: Synthesis and characterization of nano-biomaterials with potential osteological applications. J Mater Sci-Mater Med 2003;14:875-882.

Pihlajamaki HK, Karjalainen PT, Aronen HJ, Bostman OM: Mr imaging of biodegradable polylevolactide osteosynthesis devices in the ankle. J Orthop Trauma 1997;11:559-564.

Place ES, George JH, Williams CK, Stevens MM: Synthetic polymer scaffolds for tissue engineering. Chemical Society Reviews 2009;38:1139-1151.

Pontoriero R, Lindhe J, Nyman S, Karring T, Rosenberg E, Sanavi F: Guided tissue regeneration in degree ii furcation-involved mandibular molars. A clinical study. J Clin Periodontol 1988;15:247-254.

Rasmusson L, Sennerby L, Lundgren D, Nyman S: Morphological and dimensional changes after barrier removal in bone formed beyond the skeletal borders at titanium implants. A kinetic study in the rabbit tibia. Clinical Oral Implants Research 1997;8:103-116.

Ray RD, Ward AA, Jr.: A preliminary report on studies of basic calcium phosphate in bone replacement. Surg Forum 1951:429-434.

Rey C, Shimizu M, Collins B, Glimcher MJ: Resolution-enhanced fourier transform infrared spectroscopy study of the environment of phosphate ion in the early deposits of a solid phase of calcium phosphate in bone and enamel and their evolution with age: 2. Investigations in the nu3po4 domain. Calcified tissue international 1991;49:383-388.

Rezwan K, Chen QZ, Blaker JJ, Boccaccini AR: Biodegradable and bioactive porous polymer/inorganic composite scaffolds for bone tissue engineering. Biomaterials 2006;27:3413-3431.

Richardson CR, Mellonig JT, Brunsvold MA, McDonnell HT, Cochran DL: Clinical evaluation of bio-oss®: A bovine-derived xenograft for the treatment of periodontal osseous defects in humans. Journal of Clinical Periodontology 1999;26:421-428.

Rokkanen PU, Bostman O, Hirvensalo E, Makela EA, Partio EK, Patiala H, Vainionpaa S, Vihtonen K, Tormala P: Bioabsorbable fixation in orthopaedic surgery and traumatology. Biomaterials 2000a;21:2607-2613.

Rokkanen PU, Bostman O, Hirvensalo E, Makela EA, Partio EK, Patiala H, Vainionpaa SI, Vihtonen K, Tormala P: Bioabsorbable fixation in orthopaedic surgery and traumatology. Biomaterials 2000b;21:2607-2613.

Rose LF: Periodontics : Medicine, surgery, and implants. St. Louis, Mo. ; [London], Elsevier Mosby, 2004.

Ross R, Raines EW, Bowen-Pope DF: The biology of platelet-derived growth factor. Cell 1986;46:155-169.

Rossa R: Hydroxylapatite: Reconstruction of facial bones. J Oral Implantol 1991;17:184-192.

Rothstein SS, Paris DA, Zacek MP: Use of hydroxylapatite for the augmentation of deficient alveolar ridges. Journal of Oral and Maxillofacial Surgery 1984;42:224-230.

Sakou T: Bone morphogenetic proteins: From basic studies to clinical approaches. Bone 1998;22:591-603.

Sant'Ana AC, Marques MM, Barroso TE, Passanezi E, de Rezende ML: Effects of tgf-beta1, pdgf-bb, and igf-1 on the rate of proliferation and adhesion of a periodontal ligament cell lineage in vitro. Journal Of Periodontology 2007a;78:2007-2017.

Sant'Ana ACP, Marques MM, Barroso EC, Passanezi E, de Rezende MLR: Effects of tgf-beta 1, pdgf-bb, and igf-1 on the rate of proliferation and adhesion of a periodontal ligament cell lineage in vitro. Journal Of Periodontology 2007b;78:2007-2017.

Scantlebury TV: 1982-1992: A decade of technology development for guided tissue regeneration. Journal Of Periodontology 1993;64:1129-1137.

Schallhorn RG, Hiatt WH, Boyce W: Iliac transplants in periodontal therapy. Journal Of Periodontology 1970;41:566-580.

Scheyer ET, Velasquez-Plata D, Brunsvold MA, Lasho DJ, Mellonig JT: A clinical comparison of a bovine-derived xenograft used alone and in combination with enamel matrix derivative for the treatment of periodontal osseous defects in humans. Journal Of Periodontology 2002;73:423-432.

Schmitt JM, Buck DC, Joh SP, Lynch SE, Hollinger JO: Comparison of porous bone mineral and biologically active glass in critical-sized defects. Journal Of Periodontology 1997;68:1043-1053.

Sculean A, Donos N, Blaes A, Lauermann M, Reich E, Brecx M: Comparison of enamel matrix proteins and bioabsorbable membranes in the treatment of intrabony periodontal defects. A split-mouth study. Journal Of Periodontology 1999;70:255-262.

Scully C, Monteil R, Sposto MR: Infectious and tropical diseases affecting the human mouth. Periodontology 2000 1998;18:47-70.

Seymour RA, Ellis JS, Thomason JM: Risk factors for drug-induced gingival overgrowth. J Clin Periodontol 2000;27:217-223.

Sherman PR, Hutchens LH, Jr., Jewson LG, Moriarty JM, Greco GW, McFall WT, Jr.: The effectiveness of subgingival scaling and root planning. I. Clinical detection of residual calculus. Journal Of Periodontology 1990;61:3-8.

Shikinami Y, Okuno M: Bioresorbable devices made of forged composites of hydroxyapatite (ha) particles and poly--lactide (plla): Part i. Basic characteristics. Biomaterials 1999;20:859-877.

Shinto Y, Uchida A, Korkusuz F, Araki N, Ono K: Calcium hydroxyapatite ceramic used as a delivery system for antibiotics. J Bone Joint Surg-Br Vol 1992;74:600-604.

Siddharthan A, Seshadri SK, Kumar TSS: Microwave accelerated synthesis of nanosized calcium deficient hydroxyapatite. J Mater Sci-Mater Med 2004;15:1279-1284.

Sigurdsson TJ, Fu E, Tatakis DN, Rohrer MD, Wikesjo UME: Bone morphogenetic protein-2 for peri-implant bone regeneration and osseointegration. Clinical Oral Implants Research 1997;8:367-374.

Sinha VR, Bansal K, Kaushik R, Kumria R, Trehan A: Poly-[epsilon]-caprolactone microspheres and nanospheres: An overview. International Journal of Pharmaceutics 2004;278:1-23.

Socransky SS, Haffajee AD, Goodson JM, Lindhe J: New concepts of destructive periodontal disease. Journal Of Clinical Periodontology 1984;11:21-32.

Sogal A, Tofe AJ: Risk assessment of bovine spongiform encephalopathy transmission through bone graft material derived from bovine bone used for dental applications. Journal Of Periodontology 1999;70:1053-1063.

Song AM, Shu R, Xie YF, Song ZC, Li HY, Liu XF, Zhang XL: A study of enamel matrix proteins on differentiation of porcine bone marrow stromal cells into cementoblasts. Cell Proliferation 2007;40:381-396.

Soriano I, Évora C: Formulation of calcium phosphates/poly (d,l-lactide) blends containing gentamicin for bone implantation. Journal of Controlled Release 2000;68:121-134.

Spagnoli A, Granero-Molto F, Weis J: Stem cells and fracture repair. Bone 2009;44:S23-S23.

Stoller NH, Johnson LR, Garrett S: Periodontal regeneration of a class ii furcation defect utilizing a bioabsorbable barrier in a human. A case study with histology. Journal Of Periodontology 2001;72:238-242.

Strietzel FP, Khongkhunthian P, Khattiya R, Patchanee P, Reichart PA: Healing pattern of bone defects covered by different membrane types--a histologic study in the porcine mandible. Journal Of Biomedical Materials Research 2006;78:35-46.

Suchanek WL, Shuk P, Byrappa K, Riman RE, TenHuisen KS, Janas VF: Mechanochemical-hydrothermal synthesis of carbonated apatite powders at room temperature. Biomaterials 2002;23:699-710.

Sui G, Yang X, Mei F, Hu X, Chen G, Deng X, Ryu S: Poly-l-lactic acid/hydroxyapatite hybrid membrane for bone tissue regeneration. J Biomed Mater Res A 2007;82:445-454.

Sun RX, Li MS, Lu YP, Wang AJ: Immersion behavior of hydroxyapatite (ha) powders before and after sintering. Materials Characterization 2006;56:250-254.

Sun WB, Chu CL, Wang J, Zhao HT: Comparison of periodontal ligament cells responses to dense and nanophase hydroxyapatite. J Mater Sci-Mater Med 2007;18:677-683.

Suwanprateeb J, Tanner KE, Turner S, Bonfield W: Influence of ringer's solution on creep resistance of hydroxyapatite reinforced polyethylene composites. Journal Of Materials Science 1997;8:469-472.

Seitz TL, Noonan KD, Hench LL, Noonan NE: Effect of fibronectin on the adhesion of an established cell-line to a surface reactive biomaterial. Journal Of Biomedical Materials Research 1982;16:195-207.

Taddei P, Monti P, Simoni R: Vibrational and thermal study on the in vitro and in vivo degradation of a poly(lactic acid)-based bioabsorbable periodontal membrane. Journal Of Materials Science 2002;13:469-475.

Takayama S, Murakami S, Miki Y, Ikezawa K, Tasaka S, Terashima A, Asano T, Okada H: Effects of basic fibroblast growth factor on human periodontal ligament cells. Journal Of Periodontal Research 1997;32:667-675.

Takayama T, Todo M, Takano A: The effect of bimodal distribution on the mechanical properties of hydroxyapatite particle filled poly(l-lactide) composites. Journal of the Mechanical Behavior of Biomedical Materials 2009;2:105-112.

Tatakis DN, Promsudthi A, Wikesjo UM: Devices for periodontal regeneration. Periodontology 2000 1999a;19:59-73.

Tatakis DN, Promsudthi A, Wikesjo UME: Devices for periodontal regeneration. Periodontology 2000 1999b;19:59-73.

Tegnander A, Engebretsen L, Bergh K, Eide E, Holen KJ, Iversen OJ: Activation of the complement-system and adverse-effects of biodegradable pins of polylactic acid (biofix(r)) in osteochondritis-dissecans. Acta Orthop Scand 1994;65:472-475.

Tempro PJ, Nalbandian J: Colonization of retrieved polytetrafluoroethylene membranes: Morphological and microbiological observations. Journal Of Periodontology 1993;64:162-168.

Teng SH, Lee EJ, Yoon BH, Shin DS, Kim HE, Oh JS: Chitosan/nanohydroxyapatite composite membranes via dynamic filtration for guided bone regeneration. Journal of Biomedical Materials Research Part A 2009;88A:569-580.

Teoreanu I, Preda M, Melinescu A: Synthesis and characterization of hydroxyapatite by microwave heating using caso4 center dot 2h(2)o and ca(oh)(2) as calcium source. J Mater Sci-Mater Med 2008;19:517-523.

Triffitt JT, Owen M: Studies on bone matrix glycoproteins. Incorporation of (1-14c)glucosamine and plasma (14c)glycoprotein into rabbit cortical bone. The Biochemical Journal 1973;136:125-134.

Uchida A, Shinto Y, Araki N, Ono K: Slow release of anticancer drugs from porous calcium hydroxyapatite ceramic. Journal of Orthopaedic Research 1992;10:440-445.

Ueyama Y, Ishikawa K, Mano T, Koyama T, Nagatsuka H, Suzuki K, Ryoke K: Usefulness as guided bone regeneration membrane of the alginate membrane. Biomaterials 2002;23:2027–2033.

Ural E, Kesenci K, Fambri L, Migliaresi C, Piskin E: Poly(,-cactide/[var epsilon]-caprolactone)/hydroxyapatite composites. Biomaterials 2000;21:2147-2154.

Urist MR: Bone: Formation by autoinduction. Science (New York, NY 1965;150:893-899.

Urist MR, Huo YK, Brownell AG, Hohl WM, Buyske J, Lietze A, Tempst P, Hunkapiller M, DeLange RJ: Purification of bovine bone morphogenetic protein by hydroxyapatite chromatography. Proceedings of the National Academy of Sciences of the United States of America 1984;81:371-375.

Vasanthan N, Ly O: Effect of microstructure on hydrolytic degradation studies of poly (l-lactic acid) by ftir spectroscopy and differential scanning calorimetry. Polymer Degradation and Stability;In Press, Corrected Proof.

Velayudhan S, Ramesh P, Varma HK, Friedrich K: Dynamic mechanical properties of hydroxyapatite-ethylene vinyl acetate copolymer composites. Materials Chemistry and Physics 2005;89:454-460.

Vert M, Li S, Garreau H: New insights on the degradation of bioresorbable polymeric devices based on lactic and glycolic acids. Clinical Materials 1992;10:3-8.

Verrier S, Blaker JJ, Maquet V, Hench LL, Boccaccini AR: Pdlla/bioglass® composites for soft-tissue and hard-tissue engineering: An in vitro cell biology assessment. Biomaterials 2004;25:3013-3021.

Vlachos N, Skopelitis Y, Psaroudaki M, Konstantinidou V, Chatzilazarou A, Tegou E: Applications of fourier transform-infrared spectroscopy to edible oils. Analytica Chimica Acta 2006;573-574:459-465.

Wan-Ju L, Keith GD, Peter GA, Rocky ST: Biological response of chondrocytes cultured in three-dimensional nanofibrous poly(ε-caprolactone) scaffolds. Journal of Biomedical Materials Research Part A 2003;67A:1105-1114.

Wang YJ, Lin FH, Sun JS, Huang YC, Chueh SC, Hsu FY: Collagen-hydroxyapatite microspheres as carriers for bone morphogenic protein-4. Artificial Organs 2003;27:162-168.

Waris E, Ashammakhi N, Kaarela O, Raatikainen T, Vasenius J: Use of bioabsorbable osteofixation devices in the hand. Journal of Hand Surgery-British and European Volume 2004;29B:590-598.

Webster TJ, Ergun C, Doremus RH, Siegel RW, Bizios R: Enhanced functions of osteoblasts on nanophase ceramics. Biomaterials 2000;21:1803-1810.

Weiss L: Cell and tissue biology : A textbook of histology, ed 6th ed., Urban & Schwarzenberg, 1988.

Wozney JM, Rosen V, Celeste AJ, Mitsock LM, Whitters MJ, Kriz RW, Hewick RM, Wang EA: Novel regulators of bone formation: Molecular clones and activities. Science (New York, NY 1988;242:1528-1534.

Xin RL, Leng Y, Chen JY, Zhang QY: A comparative study of calcium phosphate formation on bioceramics in vitro and in vivo. Biomaterials 2005;26:6477-6486.

Yamaguchi A, Komori T, Suda T: Regulation of osteoblast differentiation mediated by bone morphogenetic proteins, hedgehogs, and cbfa1. Endocr Rev 2000;21:393-411.

Yang Y, Zhao Y, Tang G, Li H, Yuan X, Fan Y: In vitro degradation of porous poly(l-lactide-co-glycolide)/[beta]-tricalcium phosphate (plga/[beta]-tcp) scaffolds under dynamic and static conditions. Polymer Degradation and Stability 2008;93:1838-1845.

Yair Levy MZ: Novel bioresorbabale composite fiber structures loaded with proteins for tissue regeneration applications: Microstructure and protein release. Journal of Biomedical Materials Research Part A, 2006;79A:779-787.

Yukna RA: Clinical human comparison of expanded polytetrafluoroethylene barrier membrane and freeze-dried dura mater allografts for guided tissue regeneration of lost periodontal support. I. Mandibular molar class ii furcations. Journal Of Periodontology 1992;63:431-442.

Yukna RA, Evans GH, Aichelmann-Reidy MB, Mayer ET: Clinical comparison of bioactive glass bone replacement graft material and expanded

polytetrafluoroethylene barrier membrane in treating human mandibular molar class ii furcations. Journal Of Periodontology 2001;72:125-133.

Zambonin G, Camerino C, Greco G, Patella V, Moretti B, Grano M: Hydroxyapatite coated with heaptocyte growth factor (hgf) stimulates human osteoblasts in vitro. J Bone Joint Surg Br 2000;82:457-460.

Zellin G, Gritli-linde A, Linde A: Healing of mandibular defects with different biodegradable and non-biodegradable membranes: An experimental study in rats. Biomaterials 1995;16:601-609.

Zhang CZ, Young WG, Li H, Clayden AM, Garcia-Aragon J, Waters MJ: Expression of growth hormone receptor by immunocytochemistry in rat molar root formation and alveolar bone remodeling. Calcified Tissue International 1992;50:541-546.

Zhang N, Nichols HL, Tylor S, Wen XJ: Fabrication of nanocrystalline hydroxyapatite doped degradable composite hollow fiber for guided and biomimetic bone tissue engineering; in: Symposium on Next Generation Biomaterals. Elsevier Science Bv, 2005, pp. 599-606.

Zhang Y, Tanner KE: Effect of filler surface morphology on the impact behaviour of hydroxyapatite reinforced high density polyethylene composites. J Mater Sci-Mater Med 2008;19:761-766.

Zhou Y, Hutmacher DW, Sae-Lim V, Zhou Z, Woodruff M, Lim TM: Osteogenic and adipogenic induction potential of human periodontal cells. Journal Of Periodontology 2008;79:525-534.

Zhou ZH, Ruan JM, Zou JP, Zhou ZC, Shen XJ: Bioactivity of bioresorbable composite based on bioactive glass and poly-l-lactide. Transactions of Nonferrous Metals Society of China 2007;17:394-399.

Zhu XL, Eibl O, Berthold C, Scheideler L, Geis-Gerstrofer J: Structural characterization of nanocrystalline hydroxyapatite and adhesion of pre-osteoblast cells. Nanotechnology 2006;17:2711-2721.

Zitzmann NU, Berglundh T, Lindhe J: Inflammatory lesions in the gingiva following resective/non-resective periodontal therapy. Journal of Clinical Periodontology 2005;32:139-146.

Zitzmann NU, Naef R, Scharer P: Resorbable versus nonresorbable membranes in combination with bio-oss for guided bone regeneration. The International Journal Of Oral & Maxillofacial Implants 1997;12:844-852.

PUBLICATIONS

Journal Articles

1 **Absorption and release of protein from hydroxyapatite-polylactic acid (HA-PLA) membranes.** Talal A, Waheed N, Al-Masri M, McKay IJ, Tanner KE, Hughes FJ.

Journal of Dentistry. In Press

Conference Abstracts

1 **Role of Hydroxyapatite in Regulating Protein Release Kinetics from a Novel Composite Membrane for Guided Tissue Regeneration**

Presented at European Society of Biomaterials Conference, Brighton, UK, 9th-13th September 2007.

2 **Polylactic acid-Hydroxyapatite (PLA-HA) Films as Covering for Guided Tissue Regeneration Membranes to Obtain Directional Bioactive Protein Release**

Presented at 8th World Biomaterials Congress, Amsterdam, The Netherlands, 28th May – 1st June, 2008.

3 **Growth and Differentiation of Osteoblasts on Polylactic acid-Hydroxyapatite Composite Films**

Presented at Pan European Federation of the International Association for Dental Research, London, UK, 10th – 12th September 2008.

4 **Effect of Nano and Micro Hydroxyapatite on Bioactive Potential of PLA-HA Composites**

Accepted for European Society of Biomaterials Conference, Lausanne, Switzerland, 7th - 11th September, 2009.